

1. REPORT NO. WA-RD 361.1		2. GOVERNMENT ACCESSION NO.		3. RECIPIENT'S CATALOG NO.	
4. TITLE AND SUBTITLE "Seismic Vulnerability of Strutted-Column Bridge Bents"				5. REPORT DATE December 1995	
				6. PERFORMING ORGANIZATION CODE	
7. AUTHOR(S) Glen J. Pappas and M. Lee Marsh				8. PERFORMING ORGANIZATION REPORT NO.	
9. PERFORMING ORGANIZATION NAME AND ADDRESS Washington State Transportation Center (TRAC) Civil and Environmental Engineering; Sloan Hall, Room 101 Washington State University Pullman, Washington 99164				10. WORK UNIT NO.	
				11. CONTRACT OR GRANT NO. T9234, Task 16	
12. SPONSORING AGENCY NAME AND ADDRESS Washington State Department of Transportation Transportation Building, MS 7370 Olympia, Washington 98504-7370				13. TYPE OF REPORT AND PERIOD COVERED Technical Report, 2/92-12/94	
				14. SPONSORING AGENCY CODE	
15. SUPPLEMENTARY NOTES This study was conducted in cooperation with the U.S. Department of Transportation, Federal Highway Administration.					
16. ABSTRACT Strutted-column bents represent a type of reinforced concrete bridge substructure found in some bridges built before the early 1970's. The bents were designed using steel detailing and confinement that is inappropriate for ductile behavior. These bents consist of two or more columns that are connected by horizontal beams/struts, at some location along the clear heights of the columns. The presence of the struts in these bents causes an increase in the number of locations that inelastic demands can occur, relative to the number found in typical bents. The struts also increase both the lateral stiffness and strength of the bents. These features coupled with the poor detailing and confinement cause uncertainty about the seismic performance of the strutted-column bents. The seismic vulnerability of strutted-column bents was assessed by: 1.) determining the characteristics and the construction details of the bents in an inventory of bridges with strutted-column bents, 2.) evaluating the bents to determine the anticipated inelastic demands that they might experience and their potential to meet these demands, and by 3.) experimentally testing two subassemblages that were representative of the beam-column joint regions of those bents that were determined to be the most seismically vulnerable. The subassemblages exhibited poor hysteretic behavior after they attained their respective yield displacements because of the deterioration of strut bar anchorage in their B-C joints. The information that was obtained from the three phases of work was used to appraise the seismic performance potential of the bents and the bridges. The bents and the bridges should perform satisfactorily if the displacement ductility demands in the B-C joint regions of the bents, $\mu$ , are less than four. Large values of $\mu$ could jeopardize the performance of the bents, and hence the performance of the bridges as well.					
17. KEY WORDS Key words: reinforced concrete bridges, bridge bents, inelastic response, beam-column joints, reversed cyclic loading.			18. DISTRIBUTION STATEMENT No restrictions. This document is available to the public through the National Technical Information Service, Springfield, VA 22616		
19. SECURITY CLASSIF. (of this report) None		20. SECURITY CLASSIF. (of this page) None		21. NO. OF PAGES 321	22. PRICE

**Technical Report**  
for  
Research Project T9234-16  
"Seismic Vulnerability of Strutted-Column Bridge Bents"

**SEISMIC VULNERABILITY OF  
STRUTTED-COLUMN BRIDGE BENTS**

by

Glen J. Pappas and M. Lee Marsh  
**Washington State Transportation Center (TRAC)**  
Washington State University  
101 Sloan Hall  
Pullman, Washington 99164-2910

Technical Monitor: Ed Henley  
Bridge Technology Development Engineer  
Washington State Department of Transportation

Prepared for

**Washington State Transportation Commission**  
Department of Transportation  
and in cooperation with  
**U.S. Department of Transportation**  
Federal Highway Administration

December 1995

## DISCLAIMER

The contents of this report reflect the views of the authors, who are responsible for the facts and accuracy of the data presented herein. The contents do not necessarily reflect the official views or policies of the Washington State Transportation Commission, Department of Transportation, or the Federal Highway Administration. This report does not constitute a standard, specification, or regulation.

## ACKNOWLEDGMENTS

The research report herein was conducted under agreement T9234 by Washington State University. Dr. M. Lee Marsh, Assistant Professor, Civil and Environmental Engineering, and Mr. Glen J. Pappas, Graduate Student, were the principle investigators for this work.

The contributions of the following Washington State Department of Transportation personnel to this research project are gratefully acknowledged: Mr. Ed Henley, Bridge Technology Development Engineer; and Mrs. Barbara Russo, Librarian.

## TABLE OF CONTENTS

<u>Section</u>	<u>Page</u>
1.0 SUMMARY.....	1
2.0 INTRODUCTION AND PROBLEM IDENTIFICATION.....	6
2.1 Introduction.....	6
2.2 Problem Identification.....	7
2.3 Objectives.....	9
3.0 BACKGROUND.....	11
3.1 Overview of Struted-Column Bents.....	11
3.1.1 Description.....	11
3.1.2 Expected Transverse Response.....	13
3.2 Potential Deficiencies.....	15
3.2.1 Plastic Hinge Zones.....	15
3.2.2 Member Shear.....	16
3.2.3 B-C Joints.....	17
3.2.4 Objectives.....	18
3.3 Inventory Characteristics and Construction Details.....	18
3.3.1 DRC Category.....	19
3.3.2 MRC Category.....	21
3.3.3 DCC Category.....	22
3.3.4 MCC Category.....	23
3.3.5 Summary.....	23
3.4 B-C Joint Failure Modes.....	24
3.5 Understanding B-C Joints.....	26
3.5.1 Unanswered Questions.....	26
3.5.2 Sources of Knowledge.....	27
3.6 Seismic Shear Transfer in B-C Joints.....	30
3.6.1 Seismic Shear Transfer Mechanisms.....	30
3.6.2 Quantifying the Shear Stress.....	33
3.6.3 The Effect of Member Bar Bond on Shear Transfer.....	37
3.6.4 The Effect of Joint Reinforcement on Shear Transfer.....	48
3.6.5 Other Factors That Affect Shear Transfer.....	59
3.6.6 An Empirical Method for Prediction of B-C Joint Performance.....	61
3.7 Poorly Confined Column Lap Splices.....	63
3.7.1 Flexure.....	63
3.7.2 Shear.....	66
4.0 RESEARCH APPROACH.....	90
4.1 Evaluation of the Inventory.....	90
4.1.1 Criteria.....	90
4.1.2 Evaluation of Results.....	103
4.2 Experimental Test Subassemblage Prototype Selections/Designs.....	115
4.2.1 Selection of the Prototypes.....	115
4.2.2 Design of the Prototypes.....	118
4.3 Experimental Tests.....	122
4.3.1 Specimen Designs.....	122
4.3.2 Specimen Materials.....	127
4.3.3 Specimen Construction.....	129

4.3.4	Specimen Instrumentation .....	135
4.3.5	Test Set-Up.....	138
4.3.6	Testing Procedures .....	140
5.0	EXPERIMENTAL FINDINGS .....	177
5.1	The Displacement Convention .....	177
5.2	Experimental Test Results From Unit I.....	178
5.2.1	Summary of Findings .....	178
5.2.2	B-C Joint Shear Cracking.....	180
5.2.3	Specimen Yield.....	184
5.2.4	Post-Specimen-Yield .....	189
5.3	Experimental Test Results From Unit II.....	196
5.3.1	Summary of Findings .....	197
5.3.2	B-C Joint Shear Cracking.....	198
5.3.3	Specimen Yield.....	201
5.3.4	Post-Specimen-Yield .....	204
6.0	INTERPRETATION, APPRAISAL AND APPLICATION.....	252
6.1	Interpretation of the Experimental Findings From Unit I.....	252
6.1.1	B-C Joint Shear Cracking.....	252
6.1.2	Specimen Yield.....	253
6.1.3	Post-Specimen Yield .....	254
6.2	Interpretation of the Experimental Findings From Unit II.....	258
6.2.1	Bond Deterioration in the B-C Joint .....	259
6.2.2	The Role of the Strut Mechanism .....	259
6.2.3	B-C Joint Failure.....	260
6.3	The Test Results Versus the Proposed Empirical Method.....	261
6.4	Appraisal of the Seismic Performance Potential of the Inventory .....	262
6.4.1	Appraisal of the Seismic Performance Potential of the MCC Category .....	263
6.4.2	Appraisal of the Seismic Performance Potential of the Other Categories .....	264
6.4.3	Appraisal of the Seismic Performance Potential of the Bridges.....	268
7.0	CONCLUSIONS, RECOMMENDATIONS AND IMPLEMENTATION.....	273
7.1	Review of the Characteristics and the Construction Details of the Bents .....	273
7.2	Review of the Evaluation of the Bents.....	274
7.3	Review of the Findings/Interpretation of the Findings From the Tests .....	274
7.4	Review of the Appraisals of the Bents and of the Bridges .....	275
7.5	Recommendations and Implementation.....	277
REFERENCES	.....	280
APPENDIX A: ADDITIONAL INFORMATION ON B-C JOINTS.....		286
A.1	Seismic Shear Transfer in B-C Joints .....	286
A.1.1	Seismic Shear Transfer Mechanisms .....	286
A.1.2	Quantifying the Shear Stress .....	288
A.1.3	The Effect of Member Bar Bond on Shear Transfer.....	290
A.1.4	The Effect of Joint Reinforcement on Shear Transfer .....	398
A.1.5	Other Factors That Affect Shear Transfer.....	302

## LIST OF TABLES

<b><u>Table</u></b>		<b><u>Page</u></b>
1	Characteristics; DRC Category .....	67
2	Characteristics; MRC Category .....	68
3	Characteristics; DCC Category .....	69
4	Characteristics; MCC Category .....	70
5	Evaluation results; DRC Category .....	144
6	Evaluation results; MRC Category .....	144
7	Evaluation results; DCC Category .....	145
8	Evaluation results; MCC Category .....	145
9	Material properties of Units I and II .....	146

## LIST OF FIGURES

<b>Figures</b>		<b>Page</b>
1	Strutted-column bents .....	10
2	Typical locations of strutted-column bents.....	71
3	The effect of the strut on column deformation.....	71
4	Typical bent and member cross-sections for the DRC Category .....	72
5	Strut bar termination details for the DRC Category.....	73
6	Typical bent and member cross-sections for the MRC Category.....	74
7	Typical details for the MRC Category.....	75
8	Typical bent and member cross-sections for the DCC Category .....	76
9	Typical bent and member cross-sections for the MCC Category.....	77
10	Potential failure modes of B-C joint regions.....	78
11	Mechanisms of seismic shear transfer in B-C joints.....	79
12	Shear transfer after first yield of beam bars.....	80
13	Bond forces along beam bars within a B-C joint.....	81
14	Beam shear force versus story drift curves .....	82
15	Beam shear force versus slip curves.....	83
16	Slip versus story drift curves.....	83
17	B-C joint confinement versus concrete contribution to shear strength.....	84
18	Joint shear deformation/mechanics .....	84
19	Column bar tension inside of a B-C joint.....	85
20	Development of strain in the B-C joint hoops .....	86
21	Normalized hysteresis loops.....	86
22	Bond index versus volumetric hoop ratio .....	87
23	Column bar lap splice above a B-C joint.....	88
24	Flexural strength and ductility of sections .....	89

25	Typical M- $\phi$ relations for the columns and for the struts.....	147
26	Actions on an exterior joint.....	148
27	Actions on an interior joint.....	149
28	Typical M- $\phi$ relation for the struts in the inventory.....	150
29	Finite member sizes in the EPFO and IDARC software.....	151
30	Typical model of a bent used in the EPFO and IDARC software.....	152
31	Determination of bent stiffness values.....	153
32	Determination of values of the effective moment of inertia.....	154
33	Typical flexural hinge formation sequence in the MRC Category.....	155
34	Typical flexural hinge formation sequences in the MCC Category.....	156
35	Prototype subassemblage designs.....	157
36	Unit I details.....	158
37	Unit II details.....	159
38	The orientations of the test specimens.....	160
39	Stress versus strain plots; bars in Units I and II.....	161
40	Stress versus strain plots; transverse steel in Units I and II.....	162
41	Sketch of the fixture at the free ends of the struts.....	162
42	Sketch of the fixture at lower columns.....	163
43	Sketch of the fixture used to brace the specimens.....	164
44	Sketch of the fixture used to connect the actuator to the specimens.....	164
45	The fixtures for the test specimens in place.....	165
46	The shoring and the formwork after the first concrete pour.....	166
47	The shoring and the formwork prior to the second concrete pour.....	166
48	The reinforcing steel cage for the struts of Unit I.....	167
49	The reinforcing steel cage for the struts of Unit I (sleeve region).....	167
50	The reinforcing steel cage for the lower column of Unit I.....	168

52	The reinforcing steel cages in the forms for Unit II.....	169
53	The reinforcing steel cages in the forms for Unit II (joint region) .....	169
54	The specimens following removal of all formwork.....	170
55	Instrument layout for joint distortion and member rotation .....	171
56	Instrument rigs.....	172
57	Strain gage locations.....	173
58	Unit I in the test frame with the load actuators and the fixtures .....	174
59	Displacement history used for the test specimens.....	175
60	Model for the yield displacement of the test specimens .....	176
61	The displacement convention used in the tests .....	213
62	Hysteresis loops for Unit I (through 2.54 mm).....	214
63	Cracking in Unit I (through 12.7 mm) .....	215
64	Load versus strain for hoop AJ in Unit I (early on) .....	216
65	Load versus strain for hoop JB in Unit I (early on) .....	217
66	Hysteresis loops for Unit I (through 15.24 mm) .....	218
67	Hysteresis loops for Unit I (through 15.24 mm) .....	219
68	Typical strain history; main bars in the struts in Unit I (fixed-end).....	220
69	Typical strain history; main bars in the struts in Unit I (hinge).....	221
70	Bond force versus displacement for Unit I (strut lower main bar).....	222
71	B-C joint bond-condition scenarios.....	223
72	Hysteresis loops for Unit I (through 25.4 mm).....	224
73	Bond force versus displacement for Unit I (strut upper main bar).....	225
74	Load versus strain for hoop JT in Unit I.....	226
75	Load versus strain for hoop JB in Unit I.....	227
76	Load versus strain for hoops AJ and BJ in Unit I .....	228
77	Hysteresis loops for Unit I (entire test) .....	229
78	Cracking on the front of the B-C joint of Unit I (displ. = $-1.5\Delta y$ ).....	230

79	Cracking on the back face of the B-C joint of Unit I (displ. = $-1.5\Delta y$ ).....	230
80	Cracking on the front of the B-C joint of Unit I ( $2\Delta y$ ).....	231
81	Cracking on the back face of the B-C joint of Unit I ( $2\Delta y$ ).....	231
82	Spalling on the front face of the B-C joint of Unit I (displ. = $-4\Delta y$ ).....	232
83	Spalling on the back face of the B-C joint of Unit I (displ. = $+4\Delta y$ ).....	232
84	Unit I; peak displ., extend portion, first push-over cycle.....	233
85	Unit I; front, peak displ., second push-over cycle.....	234
86	Unit I; back, peak displ., second push-over cycle.....	234
87	The front of Unit I following the removal of loose concrete.....	235
88	The back of Unit I following the removal of loose concrete.....	235
89	Unit II prior to the start of testing.....	236
90	Hysteresis loops for Unit II (through 2.54 mm).....	237
91	Cracking observed in Unit II (through 12.7 mm).....	238
92	Hysteresis loops for Unit II (through 12.7 mm).....	239
93	Bond force versus displacement for Unit II (strut lower main bar).....	240
94	Bond force versus displacement for Unit II (strut upper main bar).....	241
95	Hysteresis loops for Unit II ( $1.25\Delta y$ ).....	242
96	Cracking in Unit II; hinge region, lower column (displ. = $-1.25\Delta y$ ).....	243
97	B-C joint shear cracks in Unit II (displ. = $-1.25\Delta y$ ).....	244
98	B-C joint shear cracks in Unit II; front face (displ. = $+1.25\Delta y$ ).....	244
99	Hysteresis loops for Unit II (entire test).....	245
100	Load versus strain for hoop JT in Unit II.....	246
101	The condition of the front face of Unit II (displ. = $-2.5\Delta y$ ).....	247
102	The condition of the back face of Unit II (displ. = $-2.5\Delta y$ ).....	247
103	Spalling in the lower column of Unit II (displ. = $\pm 3\Delta y$ ).....	248
104	Damage on the back of Unit II (displ. = $+4\Delta y$ ).....	248

105	B-C joint of Unit II before and after the joint faces are pushed away .....	249
106	Unit II; peak displ., extend portion, first push-over cycle.....	250
107	Unit II; peak displ., retract-portion, second push-over cycle.....	250
108	The front of Unit II following the removal of loose concrete.....	251
109	The back of Unit II following the removal of loose concrete.....	251
110	Bond index versus volumetric hoop ratio (updated).....	272
A.1	Mechanisms of seismic shear transfer in B-C joints.....	310
A.2	Crack patterns of specimens with bonded and unbonded bars .....	311
A.3	Forces acting on beam bars across a joint core.....	312
A.4	Shear strength versus B-C joint reinforcement.....	313
A.5	Detail of B-C joint lateral reinforcement schemes.....	314
A.6	Story shear -- story drift relations.....	314
A.7	Bond forces along beam bars within B-C joints .....	315
A.8	Strains in joint ties parallel to loading direction .....	315
A.9	Strains in orthogonal B-C joint ties.....	316
A.10	Total tensile force in B-C joint ties.....	317
A.11	Specimen failure modes versus a shear stress ratio.....	318
A.12	Maximum B-C joint shear stress versus concrete strength.....	319
A.13	B-C joint shear strength versus ductility factor.....	320
A.14	Details of the specimens tested by Joh et al.....	321

## CHAPTER 1

### SUMMARY

In this work, the seismic vulnerability of bridges with strutted-column bents is assessed. The assessment is based on: 1.) a review of the characteristics and the construction details of the strutted-column bents in a 39-bridge inventory in Washington State; 2.) an evaluation of potential inelastic seismic demands on these bents, and comparison with selected seismic performance criteria; and 3.) the findings from experimental tests on two subassemblages that were scale models of two "as-built" prototype subassemblages. The prototypes were designed to include details found in those strutted-column bents determined to be the most vulnerable, and the most important, in the inventory.

In the strutted-column bents, the columns are tied together by beams/struts that have small reinforcement indices and that were cast monolithically with the columns. Typically, there is one strut located between the foundation and the superstructure. The locations of the struts vary with respect to the clear heights of the columns (i.e., they are located anywhere from grade through positions that are above the mid-points of the clear heights). Although the original purpose of these struts could not be ascertained, it is certain that they affect the transverse response of the bents: with the struts in-tact, each bent has a certain transverse stiffness and strength, and, as the struts degrade and/or fail, the stiffness and strength of the bents will decrease. Such occurrences would affect the transverse vibration characteristics of the bridge itself.

The struts could degrade or fail because they, like the columns, do not have adequate transverse reinforcement (all of the bridges in the inventory were constructed prior to 1971). Thus, when the bents respond in the transverse direction, the ends of the struts may degrade if the seismically induced demands are large enough to cause the formation of flexural plastic hinges, or if the shear in these regions becomes excessive. More

importantly, the presence of the struts and the lack of adequate transverse reinforcement throughout these bents can lead to bent degradation that could jeopardize the safety of the bridge itself.

In many of the strutted-column bents, the columns have lap-spliced longitudinal bars just above the struts. In some cases, the location of the struts is low enough to precipitate a story mechanism whereby flexural plastic hinges will form in the column lap splice regions. Just as is the case with plastic hinges in the struts, plastic hinges in the column lap splice regions, coupled with high ductility demands, could bring about degradation or failure there. In the bents where the struts are located closer to mid-height, there is the possibility that the struts can cause degradation or failure of the lightly-confined strut-column joints (i.e., by creating large bar bond and/or shear stresses in the B-C joints). If the strut-column (B-C) joints degrade or fail, the ability of the columns to carry axial load could also be jeopardized or lost.

The review of the characteristics of the inventory, coupled with the analytical evaluation that was done using selected seismic performance criteria and using the expected inelastic performance of the bents, indicated that, of the problems discussed above (strut shear and/or plastic hinge degradation, column lap-splice shear and/or plastic hinge degradation, and B-C joint degradation), B-C joint degradation was the least likely, particularly with respect to shear. The reason is that the shear stress demands on the B-C joints in these bents will be small relative to accepted limits because of the small strut reinforcement indices. However, the experimental findings from the two subassemblage tests indicated that degradation will occur even though the nominal shear stress demands were within the accepted limits.

Both of the subassemblages that were tested (Units I and II) suffered severe damage within the B-C joint region, although they were able to sustain the axial load throughout the entirety of the tests. In the case of Unit I, a test specimen with struts and columns that were of approximately the same flexural strength, bar bond and shear failure

in the B-C joint occurred at a displacement ductility ( $\mu$ ) of approximately 4.0. These failures occurred prior to the development of the maximum flexural strengths of the members. In the case of Unit II, in which the struts that approximately twice as strong as the columns, bar bond in the B-C joint was lost at a value of  $\mu$  approximately equal to 2.5, and shear failure of the B-C joint occurred at a value of  $\mu$  approximately equal to 4.0. In this second test, the theoretical nominal flexural capacity of one of the columns was developed. The deterioration of bar bond in the B-C joints of these specimens lead to the shear failures since the shear had to be carried by the concrete alone instead of by a combination of the concrete, the strut bars, and the transverse reinforcement. The deterioration of bar bond in these specimens also caused a marked decrease in the stiffness of these specimens and in the energy that they dissipated (i.e., hysteretic "pinching" occurred at the smaller displacements as bond deteriorated). The experimental findings showed that the initial evaluation of the bents was unconservative in that the B-C joint regions of the bents may have a lower threshold for damage than was expected.

In those bents where the flexural strengths of the columns are less than or equal to those of the struts, there appears to be a vulnerability for B-C joint shear failures if the value of the displacement ductility in any of the interior B-C joint regions exceeds four. This vulnerability decreases as the locations of the struts are closer to the ground. As the positions of the struts approach ground-level, flexural plastic hinges are expected to form in the columns rather than in the struts. These hinges will not likely withstand large displacement ductility demands (i.e., four or more). For those bents where the columns are significantly stronger than the struts (the struts are typically located near mid-height for this case), flexural plastic hinge degradation and/or shear failure of the struts is possible if the displacement ductility demands become large.

In the majority of the bents in the inventory, there is significant potential for strut bar bond to begin to deteriorate in the B-C joints at small values of the displacement ductility in the B-C joint regions (i.e., less than four). Such deterioration will reduce the

lateral stiffness and the energy dissipation capability of the bents, neither of which should prevent satisfactory bent performance. However, if the values of the displacement ductility in the B-C joint regions become large, then bar bond deterioration will worsen, perhaps producing undesirable behavior in the B-C joints (i.e., shear transfer via the concrete alone, and an inability on the part of the members to develop their flexural capacities) that could jeopardize the stability of a bent. Given the redundancy that these bents possess, the displacements that they will have to undergo may have to be large (i.e., interstory drifts in excess of 4%) in order for there to be large values of displacement ductility demand in any of the B-C joint regions. With these appraisals of the bent vulnerabilities, the bridges in the inventory were considered next.

The inference that can be made from this work is that the bridges in the inventory will likely perform satisfactorily in seismic events that cause small displacement ductility demands in the B-C joint regions of the strutted-column bents. Under such conditions, the damage in the bents may be limited to some deterioration of strut bar bond (i.e., the deterioration will not likely be advanced enough to precipitate anchorage failures). The effects that such bar bond deterioration will have on the bridges will probably be limited to decreasing the overall lateral stiffness of the bridges and therefore altering the force demands. Such effects may not be detrimental to the performance of the bridges, and in some cases could be beneficial. For example, if the fundamental natural period of a bridge is greater than the period at which the peak spectral velocity occurs, then a decrease in the stiffness of that bridge will cause its response to increase and the force demands on it to decrease. While a case-by-case evaluation of the bridges in the inventory is required to determine the actual scenarios and their effects, the scenario described is typically beneficial to most structures.

Also, the inference can be made that the bridges might perform poorly if the displacement ductility demands in the B-C joint regions of the bents are large. Under such conditions, the strutted-column bents have several potential vulnerabilities that could

jeopardize the integrity of the bridges. However, large displacement ductility demands in the B-C joint regions in any one bent are not likely given the redundancy that is available if several bents respond in the same direction at any given time. Issues such as redundancy in these bridges, the intensity and duration of the anticipated ground motions, the effects of soil-structure interaction, and the often-times sporadic use of strutted-column bents in the bridges, must all be considered on a case-by-case basis in order to properly appraise the seismic performance potential of these bridges.

## CHAPTER 2

### INTRODUCTION AND PROBLEM IDENTIFICATION

#### 2.1 Introduction

Recent earthquakes (e.g., Loma Prieta and Northridge) have caused extensive damage to several vital freeway structures. Damage to these lifeline bridges resulted in severe economic disruptions, and in some instances, loss of life. Most of the bridges that experienced significant damage during these earthquakes were reinforced concrete bridges that were built prior to the introduction of modern seismic design criteria. Great advances in seismic design criteria for reinforced concrete bridges have been made since the early 1970's as a result of the 62 bridges that were damaged and/or failed as a result of the 1971 San Fernando earthquake. It is reassuring that reinforced concrete bridges built since the early 1970's typically did not experience significant damage in the Loma Prieta and the Northridge earthquakes. However, the extensive damage that occurred to older reinforced concrete bridges in these earthquakes underscores the need to evaluate their deficiencies and to develop methods for strengthening these bridges to meet current safety requirements.

Before the widespread damage to bridges that was produced by the 1971 San Fernando earthquake, bridges were primarily designed for gravity loads, thermal fluctuations, vehicle braking, and static wind and seismic effects. The lateral loads considered in early bridge design codes were significantly lower in magnitude than actual earthquake loads expected or, in several instances, than actual measured earthquake loads. Moreover, attention was not given to the importance of transverse or confining reinforcement and detailing, which are now known to be vital to the safe performance of reinforced concrete structures subjected to earthquake loads. Consequently, older reinforced concrete bridges, designed without both proper transverse reinforcement and detailing, are vulnerable to extensive seismic damage.

The transverse reinforcement in older reinforced concrete bridge substructures typically consists of #3 or #4 reinforcing bars placed at approximately 305 mm on center, regardless of the member cross-sectional dimensions. The ends of such reinforcement are simply lapped in the cover concrete. Thus, the deformation capacity of a member will be limited to that corresponding to the onset of spalling in the cover concrete. This type of detailing also will not prevent longitudinal bar buckling in the members. Finally, small amounts of transverse reinforcement can result in: 1.) the members being susceptible to shear failures, this includes the joints where the members are connected (beam-column joints), and 2.) the loss of member longitudinal bar anchorage in the beam-column (B-C) joints.

There are many older reinforced concrete bridges in the Western Washington and the Puget Sound area. This is an area that has experienced seismic activity in the past, and in accordance with some current forecasts, may experience large earthquakes in the future. The seismic vulnerability of one of the types of reinforced concrete bridges in the Washington State bridge inventory was investigated in this work.

## **2.2 Problem Identification**

From the bridges located in Washington State seismic zones B and C, as listed in a recent report (George 1991) that contained recommendations on the bridge seismic retrofit program, an inventory consisting of 39 reinforced concrete bridges with strutted-column bents has been identified. Figures 1a and 1b show two of the several varieties of strutted-column bents in these bridges. The construction dates range from 1925 to 1969, and accordingly the bents typically have sparse amounts of transverse reinforcement. Also, the configurations, construction, and steel detailing vary among these bents. Finally, while in some instances the strutted-column bents serve as the substructures over the entire length of a bridge, typically such strutted-column bents are used only over portions of a bridge

length.

There are three potential problems with these bents, each of which is related to reversed cyclic loading of the bents in the direction transverse to the bridges:

- 1.) The inelastic behavior of the struts, and the effects of this behavior on the bents and on the bridges, is not well understood.
- 2.) The effects that the presence of the struts will have on the inelastic behavior of the columns is not well understood.
- 3.) The behavior of the B-C joints (i.e., the B-C joints that were created by the presence of the struts) is not well understood.

The first problem has to do with the lack of adequate transverse reinforcement in the strutted-column bents. If the struts are subjected to large inelastic demands, then shear failures or flexural plastic hinge failures may occur in the struts. Without the struts, the period of a bent (with its tributary portion of the superstructure) would be expected to increase. An increase in the period of a bent will probably increase the response of the bent, while decreasing the force demands on it. This may or may not be beneficial to the bent, or to a bridge if several bents were to experience loss of the struts.

The second problem has to do with the location of the struts in a bent. The struts in a consecutive series of these bents are typically at the same elevation. As shown in Figure 1b, this elevation does not necessarily coincide with the mid-point of the clear height of the columns (as one would expect if the struts were used in the design of the bent for purely stability reasons). In those bents where the struts are located near grade, large inelastic demands may occur in the columns just above the struts, and in most cases, the columns have lap-spliced longitudinal bars in those regions. Large inelastic demands on poorly-confined column lap splices can impose even greater limits on ductility capacity than is the case with poorly-confined members with continuous reinforcement.

The last problem has to do with the fact that the subject of cyclically loaded B-C joints is a complex one, the understanding of which is still evolving. However, it is well

accepted that damage to B-C joints can cause loss of member bar anchorage in the B-C joints, which in turn can prohibit the members from developing their flexural capacities, and also decrease the stiffness and the energy-dissipating capacity of structures. In the cases where extensive damage occurs in the B-C joints, the inability of columns to carry axial load can result.

### 2.3 Objectives

The potential vulnerabilities of the strutted-column bents are investigated in this work by:

- 1.) reviewing the characteristics and the construction details of the bents,
- 2.) analytically evaluating the bents using selected seismic performance criteria, as well as determining the expected inelastic demands on the components of the bents, and by
- 3.) conducting experimental tests on two subassemblages that are representative of the B-C joint regions of some of the bents (i.e., those B-C joint regions that were indicated by the studies done in 1.) and 2.) as having the highest possibility of experiencing poor inelastic behavior).

The information obtained from items 1.) through 3.) is integrated and appraisals are given of the seismic performance potential of the bents and of the bridges in the inventory.



(a) Three-column bents with round columns



(b) Four-column bents with round columns

Figure 1 Strutted-column bents.

## CHAPTER 3

### BACKGROUND

The first topic in this chapter is a discussion of the inventory of bridges with strutted-column bents that was considered in this work. An overview of the bents is given, the potential deficiencies of these bents are reviewed, and the characteristics and construction details of the bents are presented.

The next topic is beam-column (B-C) joints. Here, the key points are presented from the literature review of information concerning planar, reverse-cyclically loaded, cast-in-place reinforced concrete B-C joints. The following issues are included: possible failure modes, complexity of behavior, shear transfer, shear transfer mechanisms, factors that affect shear transfer, and performance prediction. APPENDIX A covers some of these issues in greater detail.

The final topic in this chapter is poorly-confined column lap-splices. The results from a literature review of this topic are presented. Attention is focused on the behavior poorly-confined column lap-splices subjected to flexure and shear.

#### 3.1 Overview of Strutted-Column Bents

Herein, a description is given of the strutted-column bents in the bridge inventory that was considered. Additionally, the expected transverse response of these bents is discussed.

##### 3.1.1 Description

The inventory considered had bridges with bents in which the columns are tied together by struts. The configurations range from two-column bents through seven-

column bents. The column shapes in the bents are rectangular or circular. More often than not, strutted-column bents comprise only a portion of the bent types used on a given bridge (in some instances most of the bents have struts, but most of the time only a few of the bents contain struts). For the bridges where only a portion of the bents contain strutted columns, those bents are typically found grouped together in the area of the bridge where the bent heights increase significantly (Fig. 2).

The struts, in many cases, are deep beams that carry no gravity load other than their own self-weight and thus have small longitudinal reinforcement indices. The purpose of the struts could not be determined with certainty. The struts in a given bent and, many times, in a consecutive series of bents, are at the same elevation. In other words, the height of a given strut above grade is typically not at the mid-point of the clear height of the columns that it connects, as one would expect if the struts were used in the design of the bents for stability reasons alone. However, the struts do reduce column slenderness in the direction transverse to the bents (Fig. 3). The only conclusion that can be made with certainty is that the struts contribute to the transverse stiffness of, and increase the lateral strength of, the bents (and of an entire bridge when enough strutted bents are used). Hence, the performance of the struts during an earthquake will affect the seismic response of the bents/bridges.

None of the components of the bents are adequately confined or detailed properly for dependable seismic performance, since the bridges were constructed prior to the inception of rigorous code provisions for seismic loading (i.e., the early 1970's). Additionally, lap-splices of the column bars occur in many of the bents in potential high moment zones. Namely at the foundations and/or above the B-C joints.

### 3.1.2 Expected Transverse Response

#### Inelastic Response of Strutted-Column Bents

In an earthquake, the transverse response of the bridges in the inventory may require the strutted-column bents to behave in an inelastic manner. In general, post-earthquake reconnaissance has shown that older structures can undergo inelastic response without collapse (many remain serviceable). However, recent earthquakes have shown that bridge substructures can be vulnerable to severe damage and/or collapse when they respond inelastically. The reasons being that:

- 1.) recent earthquakes have caused relatively severe ground motions in locations with many older bridges, and
- 2.) while bridge substructures may have the overstrength that has usually been a factor in the satisfactory seismic performance seen in older structures, they do not possess the redundancy that also contributes to the success of older structures. The lack of redundancy in bridge substructures has meant that much of the inelastic response has been concentrated in regions that have detailing that has proven to perform poorly in moderate to severe earthquakes.

#### Flexural Plastic Hinging in Indeterminate Structures

In indeterminate structures, such as these strutted-column bents, inelastic response usually requires the redistribution of moments as flexural plastic hinges (hinges) are formed. However, a hinge can form at a given section of a member only if the member is adequately designed and detailed such that shear failure does not occur prior to hinge formation. Redistribution of moments can occur only if the ductility of the sections where hinges have formed is sufficient to allow redistribution of moments as the lateral load on

the structure is increased. The ductility capacity of a section is reflected mainly by the moment-curvature relationship of that section. A section is considered ductile only if moments near the ultimate value can be sustained as the curvature increases. However, the curvature in sections that have sparse transverse reinforcement is usually limited to the curvature at which concrete spalling occurs.

Assuming that member sections can develop hinges without shear failure, and that even with limited ductility, enough sections form and sustain hinges, the ultimate capacity of the structure can be attained. This is referred to as "a mechanism". When the structure has formed a mechanism it is unstable and subject to collapse if the force level is maintained. However, under reversed cyclic loading conditions, like those in an earthquake, a mechanism condition might not cause collapse. One reason being that the mechanism condition might only exist for one direction of loading. Thus, if the loading reverses itself before the structure collapses then the structure is still viable. Another reason that collapse might not occur is that the force level that caused the mechanism might decrease. Thus, even under circumstances where mechanisms have formed in all loading directions, changes in the level of force can prevent collapse. However, bridges with substructures that form mechanisms are particularly vulnerable to collapse due to the concentration of mass at the top of these structures (i.e.,  $P-\Delta$  effects and/or high overturning moments can occur).

### Types of Mechanisms

In most bridge substructures when a mechanism occurs it is in the form of a column sidesway mechanism. However, with strutted-column bents, as with most indeterminate frames, there are two potential mechanism categories: column sidesway or beam sidesway. The former occurs when the flexural capacities of the columns at a joint are less than those of the framing beams that joint ("weak column-strong beam"). The opposite is true of

beam sidesway-type mechanisms ("strong column-weak beam"). Due to the potential for loss of vertical load-carrying capacity and/or for instability, the weak column-strong beam mechanism is undesirable.

### **3.2 Potential Deficiencies**

There are three topics related to the seismic response of strutted-column bents that should be considered when determining potential deficiencies: the performance of plastic hinge zones, member shear, and the performance of B-C joints. These topics will be discussed in what follows.

#### **3.2.1 Plastic Hinge Zones**

There are three possible locations for hinges to form in strutted-column bents, depending on the type of mechanism that occurs: in the columns at the superstructure soffit, in the columns at the foundations, and/or in the members at the B-C joints.

##### Column Hinging at the Superstructure and at the Foundation

The topic of column sidesway mechanisms for bridge substructures consisting of only columns has been researched. Hinging of columns at the superstructure and at the foundation have been the focal points of these research efforts. Thus, these areas were not considered in this work, other than recognition that hinges will form in these locations during the mechanism formation sequence of some of the strutted-column bents in the bridge inventory that was considered. Obviously, the potentially poor ductility due to the detailing of these regions was taken into account as well.

### Member Hinging at the B-C Joints

There are three areas of concern related to this topic: hinging in the struts, hinging in the columns, and the effects of member hinges on the B-C joints. Optimally, the strong column-weak beam mechanism will occur and hinges will form in the struts at the B-C joints. This assumes that the struts are able to develop the required shear strength (Sec. 3.2.2). Also, the assumption is made that the B-C joints will allow the formation and sustainment of hinges (Sec. 3.2.3). Under this scenario, regardless of the ductility capacity of the struts, the process of formation of hinges in the struts will dissipate some of the energy from the ground motion (i.e., they will act as "fuses"). However, if a weak column-strong beam mechanism occurs, hinges will form in the columns. As previously mentioned, this could jeopardize both the capacity of the bents to carry vertical load and/or the stability of the bents. Additionally, lap-splices of the column bars above the B-C joints occur in many of the bents. While discussion on general column hinging and the related effects is deferred to other research, Sections 3.7.1 - .2 cover the detrimental effects of column hinging in sections that have poorly-confined lap-splices.

#### **3.2.2 Member Shear**

In the previous section, a scenario was presented in which hinges formed in the struts at the B-C joints without shear failures occurring in the struts. However, given that many of the struts can be classified as "deep", the shears that they will attract as a result of hinges forming in them at the B-C joints might be significant. Moreover, the small amount of transverse reinforcement in the struts means that the contribution of the steel to shear resistance will be small. Thus, the ability of the struts to form plastic hinges is questionable. If the struts fail in shear prior to hinge formation, then the response of the bridge may be significantly altered.

Shear failures can also occur in short columns that do not have adequate amounts of transverse reinforcement. Additionally, shear failures can occur in columns as a result of their flexural strength being underestimated when they were designed. Although, column heights tend to be large enough such that the amounts of flexure govern the behavior of columns. However, high shears in the sections of columns that have lap-splices and have hinged does present the potential for problems to occur. This subject is discussed further in Section 3.7.2.

### **3.2.3 B-C Joints**

The formation of hinges in members at B-C joints can be detrimental to the performance of the joints (Sec. 3.4). Poor performance in the joint region can jeopardize the capacity of a bent to carry vertical load, and it can reduce the hysteretic energy dissipation capacity of the bent. The latter problem may result in increased response of the bridge in an earthquake. In general, flexure in members at a B-C joint results in shear having to be transferred through the joint, and if the shear capacity of joint is not sufficient, or if the joint does not provide enough length to anchor the member bars that pass through, then hinges can not form in the members prior to degradation of the joint (Sec. 3.6). The behavior of B-C joints is a complex subject (Sec. 3.5) that has received a great deal of attention recently due to the poor seismic performance of some of the joints in various types of older structures and the catastrophic effects that this has had on those structures.

### **3.2.4 Objectives**

The objectives of this work were:

- 1.) To identify the characteristics and the construction details of strutted-column bents typically used in the State of Washington.
- 2.) To identify those configurations that have the highest potential for experiencing one or more of the following possible failure modes: increased dynamic response of the bent, joint degradation leading to reduced column axial load capacity, or column lap splice degradation leading to reduced column shear capacity.
- 3.) To identify potential inelastic demands near the column-strut regions.
- 4.) To subject reduced-scale models of representative as-built strut-column joints to quasi-static reversed cyclic loading.
- 5.) To use the information obtained in objectives "1.)" through "4.)" to assess the seismic performance potential of strutted-column bents, and of the bridges with strutted-column bents.

### **3.3 Inventory Characteristics and Construction Details**

The characteristics and the details of construction for the bridge inventory are best described by dividing the inventory into four categories: double-column bents with rectangular columns (DRC), multiple-column bents with rectangular columns (MRC), double-column bents with circular columns (DCC), and multiple-column bents with circular columns (MCC). In what follows, the characteristics and the details of construction are given for each of the categories. Note that in the figures that illustrate the various categories of bents, the superstructures are shown as portions of the bents.

### 3.3.1 DRC Category

There are six bridges with strutted-column bents that have double rectangular columns. Figure 4a is a sketch of a DRC-type bent, and Figures 4b and 4c show the cross-sections of a column and a strut that are typical for these bents. Transverse reinforcement is not shown in Figures 4b and 4c for clarity.

There are two types of superstructure construction that are used: 1.) reinforced concrete slab-with-longitudinal girders, and 2.) box-girders. In half of the bridges the foundations used for the bents are spread footings. Two of the other bridges use combined pile foundations. Combined spread footings are used in the remaining bridge. The taller bents in one of the bridges have two struts; in each instance the additional strut is located at, or below, grade.

The other characteristics of these bents are listed in Table 1. The bent "height" is taken from the top of the column footing to the superstructure soffit. The "strut length" represents the clear distance between the faces of the columns. The "strut location" is with respect to grade. Therefore, "mid-height" implies that a strut is half-way between grade and the superstructure soffit.

The column dimensions vary greatly but the orientation of the column dimensions and of the column bar locations, with respect to the orientation of the connecting struts, are consistent. With the exception of one bridge, the strut always frames into the widest column dimension ( $b_c$ ), and it is along this direction that most of the column bars are located. Accordingly, the narrow dimension of the column,  $d_c$ , typically represents the width of the joints (where the height and width dimensions would be used to describe a joint shown in a two-dimensional representation of a frame). Some of the bents feature columns that are battered from the location of the framing strut up to the superstructure. There are also some bents that have columns with tapered cross-sections. In all cases, the column transverse reinforcement consists of hoops, with lapped ends, spaced at large

### 3.3.1 DRC Category

There are six bridges with strutted-column bents that have double rectangular columns. Figure 4a is a sketch of a DRC-type bent, and Figures 4b and 4c show the cross-sections of a column and a strut that are typical for these bents. Transverse reinforcement is not shown in Figures 4b and 4c for clarity.

There are two types of superstructure construction that are used: 1.) reinforced concrete slab-with-longitudinal girders, and 2.) box-girders. In half of the bridges the foundations used for the bents are spread footings. Two of the other bridges use combined pile foundations. Combined spread footings are used in the remaining bridge. The taller bents in one of the bridges have two struts; in each instance the additional strut is located at, or below, grade.

The other characteristics of these bents are listed in Table 1. The bent "height" is taken from the top of the column footing to the superstructure soffit. The "strut length" represents the clear distance between the faces of the columns. The "strut location" is with respect to grade. Therefore, "mid-height" implies that a strut is half-way between grade and the superstructure soffit.

The column dimensions vary greatly but the orientation of the column dimensions and of the column bar locations, with respect to the orientation of the connecting struts, are consistent. With the exception of one bridge, the strut always frames into the widest column dimension ( $b_c$ ), and it is along this direction that most of the column bars are located. Accordingly, the narrow dimension of the column,  $d_c$ , typically represents the width of the joints (where the height and width dimensions would be used to describe a joint shown in a two-dimensional representation of a frame). Some of the bents feature columns that are battered from the location of the framing strut up to the superstructure. There are also some bents that have columns with tapered cross-sections. In all cases, the column transverse reinforcement consists of hoops, with lapped ends, spaced at large

intervals. Such detailing has long been recognized as a poor one for seismic loading conditions (Park 1975a). However, the structural drawings specify continuation of the column hoops through the joints at the same spacing used in the columns. In some cases the column cross-sections were large enough to warrant more than one hoop. For example, "#5 @ 457" in Table 1 is actually three-#5 hoops every 457 mm. In that case, there is one hoop that confines the entire cross-section and each of the two additional hoops confine bars in the middle third of opposite column sides. Construction joints are used at the tops of the B-C joints, and it is at this point that the column bars are lap-spliced. In Sections 3.7.1 and 3.7.2 the potential problems with poorly confined lap splices are discussed.

With respect to the strut dimensions,  $b_b$  is the width of the struts, and  $h_b$  is the height. The strut main bars terminate in the columns in various manners (Fig. 5). In most cases, the strut main bars terminate without hooks at the back faces of the columns (Fig. 5a). All of the details shown differ from the detail that has been acknowledged as being preferable - - a 90° hook at the back face of the column with a tail that extends out of the joint region into the column (Park 1975c) (Fig. 5b). The detail shown in Figure 5b was used in but a few of the bridges. However, the detail actually used had a short tail that ended inside of the joint region. In some cases the strut intermediate bars (Fig. 4c) terminate at the column faces. However, these bars usually extend into the column and terminate without hooks. The widely-spaced strut stirrups are closed. However, instead of being hooked into the concrete core (Park 1975b), the ends of the stirrups are merely lapped in the cover concrete. Some of the struts have legged ties along with stirrups (e.g., "#5 @ 140" in Table 1 is actually a #5 stirrup and a #5 tie every 140 mm).

Filletts at the strut ends are typical (Fig. 7). They are usually unreinforced with approximate dimensions of 150 mm wide x 150 mm high. The strut dimensions listed in Table 2 are for the struts only (the fillet dimensions are not included). Figure 5c depicts how most of the strut bars terminate in exterior columns, while Figure 5a shows the detail typically used in the remainder of the bridges. As mentioned earlier, Figures 5a and 5c are undesirable for good seismic performance. Furthermore, in some instances where the detail shown in Figure 5c is used, the structural drawings specify that the hooks occur near the mid-depth of the column (versus the preferred location at the back face of the column inside of the column bars). If the strut bars do not extend through the joint, problems can arise with force transfer in the joint. The strut stirrups are closed, widely spaced, and they have lapped ends.

### 3.3.3 DCC Category

The bents with double circular columns all come from the same bridge, which is part of the US interstate highway system. Figure 8a is a sketch of one of these bents, and Figures 8b and 8c show typical column and strut cross-sections. Transverse reinforcement is not shown in Figures 8b and 8c for clarity. The taller bents typically have a second strut that ties the tops of the shafts together at grade. The superstructure is a reinforced concrete slab that is thickened at the bent locations. The foundations are cast-in-drilled-hole reinforced concrete shafts.

The other characteristics of DCC-type bents are listed in Table 3. The bent "height", the "strut length", and the "strut height" are as previously defined. The column transverse reinforcement consists of widely-spaced hoops, with lapped ends, that are specified in the structural drawings to continue through the B-C joints at the same spacing used in the columns. Construction joints are used at the tops of the B-C joints, and the column bars are lap-spliced at these locations. The column axial loads listed in Table 3

represent an average value for the interior columns of the six strutted-column bents in the bridge. From the first to the last strutted-column bent, the deck progressively widens as the bridge splits into two ramps. Thus, the column axial loads vary.

The strut main and intermediate bars terminate in the columns as depicted in Figures 5b (without adequate tail lengths) and 5a, respectively. The strut stirrups are closed and the spacing between them is large. However, the structural drawings specify that the stirrup ends shall be hooked into the concrete core.

#### **3.3.4 MCC Category**

The bents with multiple circular columns (Fig. 9) are three- or four-column bents from two bridges; one of the bridges has three-column bents and the other has four-column bents. The ranges of characteristics for the bents are listed in Table 4. Confinement reinforcement is not shown in Figures 9b and 9c for clarity. These bridges are US interstate bridges. Thus, the bents are similar to those in the DCC category. For comments regarding the characteristics and construction details of MCC-type bents refer to Section 3.3.3.

#### **3.3.5 Summary**

Two of the key points made in the discussions in Sections 3.1 through 3.3 were:

- 1.) The members and the B-C joints in the strutted-column bents may not have adequate amounts of transverse reinforcement, nor adequate detailing, to respond to large inelastic demands in a ductile manner.
- 2.) There are two features that set strutted-column bents apart from other types of bridge substructures: additional B-C joints and additional column lap-splices created by the

presence of the struts. These features will play critical roles if the strutted-column bents have to respond inelastically.

Because of the importance of the poorly confined and detailed B-C joints and column lap-splices to the inelastic response potential of the strutted-column bents, it is worthwhile to review some information concerning these topics. Sections 3.4 through 3.6 consider planar, reverse-cyclically loaded, monolithic reinforced concrete B-C joints. Section 3.7 considers column lap-splices

### 3.4 B-C Joint Failure Modes

There are five different types of possible failure modes for a B-C joint (Meinheit et al. 1981): beam hinging, column hinging, column crushing, loss of bar anchorage, and joint shear (Fig. 10). The most desirable of the failure modes is ductile flexural failure of the beam ends at the joint (Fig. 10a). Plastic hinges in the beams at the faces of the joint allow for absorption of energy as a frame undergoes large inelastic deformations without losing strength. However if beam hinging penetrates into the joint, one or all of the other (undesirable) failure modes may be precipitated.

Hinging of columns at the top and bottom of the joint (Fig. 10b) are potential failure modes that also allow for energy absorption, however the potential for frame instability will exist. Additionally, column hinging will cause residual sway deflection in a frame that will, in turn, lead to repair difficulties.

Column crushing (Fig. 10c) may result from the loss of the joint core cover, and can hamper the ability of a column to carry axial load. The inability, or reduction in ability, of a column to carry axial load is certainly an undesirable failure mode.

Loss of member bar anchorage in exterior joints (Fig. 10d) is considered as a failure mode because, under this condition, lateral forces can not be transmitted by a frame. The loss of energy absorbing ability by the frame results when lateral shear can no longer

be transmitted. In the case of interior joints, loss of member bar anchorage is also a failure mode. However lateral shear can still be transmitted, as long as bars remain anchored in the exterior joints, albeit under conditions of lower frame energy absorbing ability.

The last possible failure mode, failure of the joint in shear (Fig. 10e), has the same consequences that loss of member bar anchorage in exterior joints does, and may also lead to loss of the axial capacity in the column.

In order to prevent the occurrence of the last four of the five failure modes, Meinheit et al. (1981) claim that preventing inelastic behavior in the joint is required. Inelastic behavior in the joint will not only result in severe damage (via one or more of the undesirable failure modes), it will also result in large ductility and energy dissipation demands placed on a region that is usually not suited to accommodate such demands. Elastic joint behavior is ensured when frame deformations come from elastic deformations in the members. When inelastic deformations are required they should be accommodated only by inelastic beam rotations. In this manner, the joint retains shear strength and stiffness, and the required ductile behavior is provided by the beams via flexural hinging of a beam cross-section near the joint face (Meinheit et al. 1981 and Hanson et al. 1972).

While flexural hinging of beams near the joint face is the desirable vehicle for accommodating inelastic deformations, researchers have found that when the hinging penetrates into the joint the response of the specimens is poor. Ehsani et al. (1985) concluded that the hysteretic behavior of the specimens that they tested was much more stable when flexural hinging penetration into the joint did not occur. To preclude the occurrence of beam hinge penetration into the joint, Kitayama et al. (1991) and Otani (1991) maintain that a joint face should not be the planned location of a beam hinge. Instead, beam hinges should be designed to occur some distance away from the joint face.

Over the last thirty years there have been many experimental tests done on B-C joint subassemblies, beginning with the benchmark tests conducted by Hanson and Connor in the early 1960's (Ehsani et al. 1985). The results from many of these tests (Hanson et al.

1972 and Leon et al. 1986) show that there are certain requirements that must be met if B-C joints are to remain essentially elastic, and if frames/subassemblages are to have both stable hysteretic performance and adequate energy absorption: large member bar anchorage lengths ( $l_d$ ), substantial column/beam flexural capacity ratios ( $\sum M_{nc}/\sum M_{nb}$ ), low joint shear stress ( $v_{jt}$ ), and ample joint confinement. However, despite all of the research, there is disagreement about the relative importance and the degree of interaction of these requirements.

### 3.5 Understanding B-C Joints

Herein, some insight will be given as to why B-C joint behavior is a complex subject, and to why the body of knowledge on the subject has fallen short of providing complete understanding.

#### 3.5.1 Unanswered Questions

The behavior of joints in frames that undergo reversed cyclic loading (such as that caused by an earthquake) is not fully understood. Pantazopoulou et al. (1992) attempted to describe the factors contributing to the knowledge gap. The reason for the uncertainty surrounding joint behavior is the interaction of shear, bar bond, cyclic damage and confinement phenomena. Taken independently these issues are not completely understood. Furthermore, much of the knowledge regarding B-C joints comes from experimental testing, an area that has its own set of uncertainties (Sec. 3.5.2). Experimental research results also typically suggest that B-C joints are the weak links in frames, while post-earthquake reconnaissance has shown that this is often not the case. The definition of satisfactory B-C joint performance is still debated; should joint performance be based on frame drift or ductility ratios, or on the ability of the joint to accommodate beam flexural

hinging? Questions exist regarding the design of joints for horizontal and vertical shear and regarding the function and appropriate amounts of joint reinforcement. The effect on joints from varying degrees of bond deterioration is also uncertain.

Another source of the uncertainty involved in the understanding of the seismic behavior of joints is the fact that there is little information on joint performance in actual indeterminate frames. For instance, redistribution of forces occurs in inelastically loaded indeterminate frames and, as a result, horizontal joint restraint/confinement could be developed in the plane of a frame as members exhibit inelastic growth. Joints that have such horizontal restraint are considered to be stronger than joints that do not (ACI 318M-89 1989) because horizontal restraint prevents large joint dilation.

### **3.5.2 Sources of Knowledge**

Analytical studies, post-earthquake reconnaissance, and experimental studies have each provided knowledge about B-C joint behavior. Each source, however, has demonstrated an inability, to one degree or another, to answer the questions regarding B-C joints.

The reason for the limited success of analytical studies in predicting actual B-C joint behavior is that techniques for accurately modeling shear, bar bond, cyclic damage and confinement individually are still being developed. The ability to model the interaction of these phenomena is required in order to accurately model B-C joint behavior.

Post-earthquake reconnaissance has been extremely useful in the development of building code provisions for the design of B-C joints subjected to seismic loading; certain details have proven effective and certain ones have not. Proper performance, or lack thereof, of existing frames has served to either validate existing code provisions or establish the need for new provisions for design of B-C joints. However, because of all of the interacting phenomena involved in B-C joint behavior, insights from reconnaissance

studies into understanding B-C joint behavior have been limited. Moreover, reconnaissance studies provide little information on the forces and the deformation that joints have experienced.

The majority of knowledge about B-C joints and about the associated phenomena comes from experimental research. The ability to both isolate the various phenomena in a given test matrix, and instrument specimens according to the variables being examined, has allowed researchers to build on previous test results in pursuit of providing answers to the many existing questions. However, discrepancies between B-C joint behavior noted in post-earthquake reconnaissance studies and the results from experimental research exist. Additionally, there are other concerns regarding the validity/applicability of experimental research results. Some of these concerns will be addressed in what follows.

#### Drawing Conclusions from Experimental Research Results

The complexities associated with understanding the cyclic behavior of B-C joints make test result interpretation difficult. In addition, experimental tests tend to be performed on simple subassemblages, thereby omitting the effects of the surrounding frame (Pantazopoulou et al. 1992). This produces a simplified and potentially incomplete view of the problem. The determinate nature of most test subassemblages does not account for redistribution of forces that may occur in indeterminate frames. Moreover, some tests are intended to clarify the mechanics of the problem and some are intended to aid the improvement of design provisions. Often the language and objectives of the "mechanics" and "design" pursuits get mixed, and this adds to the uncertainties of test result interpretation. The loading rate and the displacement or loading history (depending on whether a test is run under displacement-controlled or load-controlled conditions, respectively) represent two additional areas that can affect experimental test results, and as such, they can affect the interpretation of the results of the research.

*Rate of Loading and Interpretation of Test Results.* Most subassemblages tend to be loaded in a quasi-static manner. However, the rate of this type of loading is well below that which would occur in an actual seismic event. Chung and Shah (1989) examined bond deterioration in small-scale, exterior-joint subassemblages that were loaded at different rates (1.0 Hz, fast, and 2.5E-03 Hz, slow). The tests results showed that faster rates of loading improved member bar bond behavior and that the improved bar bond behavior lead to cracking that was more localized. This is in contrast to the results obtained at slower rates of loading, where the cracking in the specimens was distributed. The concentrated cracking in the specimens loaded at the higher rates resulted in sharper drops in strength following changes in the direction of loading, whereas the distributed cracking seen in the "slower-rate" specimens resulted in less-sudden strength drops. The same research also showed that the localized damage that occurs at faster rates of loading can lead to fewer and wider cracks near the column face. The wider cracks cause loss of aggregate interlock and thus the shear strength in a section can decrease earlier. This implies that brittle failure modes are possible where more ductile ones may have been anticipated. The improvement of bar bond under faster loading rates may result in the concentration of bar strains, which then may cause premature fracture of the bars. The authors also speculate that larger beams might experience shear cracking at smaller displacement ductility ( $\mu$ ) values under faster rates of loading than smaller beams. Thus, the influence of scale-related effects is another area of experimental research that needs consideration.

*Displacement/Loading History and Interpretation of Test Results.* Bonnaci et al. (1993), who conducted a database study of joint subassemblage tests, state that the displacement histories used in experimental tests play a large role in the manner in which a given specimen fails and in the manner in which the various parameters involved in the behavior of a given specimen interact with each other. Failure in any of the components of a specimen, or limitations of the applied load actuators, usually are the causes of termination of testing. In most cases, test termination occurs after specimens have been

cycled to unreasonably high story drifts (e.g., in excess of 4%). In cases where subassemblages have been tested under load-controlled conditions, variability in the applied loading histories, at the slower loading rates typically used, also may cause difficulties in the evaluation of different research results (Meinheit et al. 1981, Ehsani et al. 1990, Fuji et al. 1991).

The aspect of seismically loaded B-C joints that sets them apart from most other types of B-C joints is shear transfer. Most of the factors that account for the complexity and the lack of understanding of B-C joint behavior come to bear when joints that are cyclically loaded transfer shear. The approach that will be used in this work to examine shear transfer in seismically loaded B-C joints is in accord with the approach typically used, whereby an attempt is made to consider the key elements involved individually. However, complete execution of this approach is difficult since the key elements involved in B-C joint shear transfer actually occur in a complex interactive manner.

### **3.6 Seismic Shear Transfer in B-C Joints**

The next six sections focus on the subject of seismic shear transfer in B-C joints. The ways in which shear is believed to be transferred (the "mechanisms"), the factors that affect shear transfer (shear stress, bar bond, joint confinement, amongst others), and the evaluation of the ability of joints to transfer shear (empirical prediction of joint performance) are all considered. Herein, "shear" is understood to mean "seismic shear" (or the shear that occurs as a result of reversed-cyclic loading). Also, since interior B-C joints (i.e., two columns and two beams per joint) are unique to the strutted-column bents, interior B-C joints are the focus of attention herein.

### 3.6.1 Seismic Shear Transfer Mechanisms

There is a consensus on the two mechanisms through which joint shear is transferred: the diagonal compressive concrete strut ("strut") mechanism and the truss mechanism. There also seems to be a consensus that joint shear is transferred via a combination of the mechanisms during different portions of the loading/displacement history (depending primarily on the detailing of a given joint and on the partiality of a given researcher toward one or the other of the two mechanisms). However, there does not seem to be a consensus on either the make-up of the two mechanisms, or the relative contributions of the two mechanisms to the transfer of joint shear at any given point in time.

#### The Mechanisms

Figure 11 depicts the commonly accepted versions of the strut and truss mechanisms (Leon 1990). Each mechanism represents an extreme in behavior. The strut mechanism shown in Figure 11a consists of a large compressive concrete strut that is formed between opposite corners of the joint by the compressive stress blocks in the members. This mechanism depends solely on the ability of this strut to transfer forces across the joint, and as such is limited by the crushing strength of the concrete in the strut. The truss mechanism shown in Figure 11b is comprised of the member bars passing through the joint, the hoops in the joint, and many small concrete struts. The truss mechanism is formed, according Paulay (1986), by:

- 1.) the transfer of bond forces from the member bars into the joint core,
- 2.) the compression resistance of uniform diagonal concrete struts in the joint core, and 3.) the resistance of the tension members in the "truss" (the hoops and the vertical joint reinforcement). Column interior bars typically serve as vertical joint reinforcement. These bars, along with the hoops, are usually required for the development of normal forces at the

panel boundaries that are necessary to sustain the diagonal concrete struts of the truss mechanism (Sec. 3.6.4, "The Functions of Joint Reinforcement").

Sustaining the truss mechanism requires a significant number of hoops as well as long member bar development lengths, in order for bond stress transfer along bars to be maintained (Kitayama et al. 1991).

### The Relative Contributions of the Mechanisms

Regardless of which mechanisms are accepted, it is clear that when bond of the member bars in a joint is lost (joint anchorage failure) the truss mechanism ceases to function and the strut mechanism becomes predominant (Leon 1990). However, what is not clear is the amounts of joint shear that are carried by the two mechanisms prior to and following the onset of first yield of the member bars ("first yield" is typically the point in time when bond deterioration begins). In Section 3.6.3, the relationships between bar yield, bar bond, and the shear transfer mechanisms are studied further. The literature review indicated that sides of the argument about the relative amounts of participation of the mechanisms in transferring joint shear are chosen based primarily on the results of the respective research efforts. The research efforts are, in turn, limited to a large extent on factors such as the goals of the research (Sec. 3.6.2, "Shear Stress Capacity") and the geometry and detailing of the joint(s) studied.

*"Strut" Versus "Truss" - Prior to First Yield.* While the joint stress is small and while bond conditions are good, the forces acting on a joint are probably carried by the action of an elastic continuum, rather than by either of the mechanisms. Before the bars in the members yield, the bond of the bars in the joint is usually good. Thus, the conditions necessary for the "truss" exist. However, according to Paulay (1986), the "truss" is formed only after the shear stress in a joint core is so large that diagonal cracks form. With the formation of diagonal cracks, the strains in the tension members of the "truss" grow,

thereby activating force transfer in these members (Leon 1990). As far as the "strut" is concerned, it will probably not be participating yet because it is considered to develop after the "truss" develops or during the degradation of the "truss". The suspected non-participation of either mechanism early on might explain why there is not much in the literature concerning the relative amounts of joint shear carried by the two mechanisms prior to first yield. Moreover, the literature is primarily focused on B-C joint behavior after first yield, as this usually represents the threshold for joint degradation.

*"Strut" Versus "Truss" - After First Yield.* Once first yield of the member bars has occurred, the question of which of the two mechanisms is carrying more of the joint shear still exists. Figure 12 (Leon 1990) shows two possibilities. After first yield has occurred, the strut mechanism will be the only source of shear transfer if member bar bond conditions have deteriorated (Fig. 12a). On the other hand, if bond conditions are good and the faces of the beams are fully separated from the joint faces, then the truss mechanism will be predominant (Fig. 12b). Due to the complexity of the subject of "bar bond", further discussion about its effect on shear transfer is reserved until Section 3.6.3.

In this section the ways in which a B-C joint transfers shear have been shown to depend primarily on the shear applied to the joint region, the bond conditions of the bars in the joint, and on the joint reinforcement. All three of these issues will be discussed at length in the next three sections.

### **3.6.2 Quantifying the Shear Stress**

#### Applied Shear Stress

The term "shear stresses", when used in the context of B-C joints, is a simplification. The forces that actually occur in a joint are transmitted from the surrounding frame by shear, bar bond, and by direct compression (Leon 1991). Typically, the applied

(demand) horizontal shear stress in a joint,  $v_{jt}$ , is reported in a normalized fashion as follows:

$$v_{jt} = \frac{V_{jt}}{A_{jt}} = \gamma \sqrt{f'_c} \quad \text{(Equation 1)}$$

where:

- $V_{jt}$  = the applied shear force
- $A_{jt}$  = the effective area of the joint (see below)
- $\gamma$  = a constant =  $V_{jt}/(A_{jt}\sqrt{f'_c})$
- $f'_c$  = the compressive strength of the concrete

The values used for  $A_{jt}$  in most experimental research (particularly where the research was not involved with/tailored after building code provisions) is the gross cross-sectional area of the column ( $A_g$ ) (Bonnaci et al. 1993, Ehsani et al. 1989, Wong et al. 1990). Values of  $V_{jt}$  are typically obtained by expressions derived from force or moment equilibrium at a joint. For example, Joh et al. (1991a) used the following in their experimental research:

$$V_{jt} = \frac{(M_{b1} + M_{b2})}{j_b} - V_{col} \quad \text{(Equation 2)}$$

where:

- $M_{b1}$  &  $M_{b2}$  = the applied beam moments at the joint faces
- $V_{col}$  = the applied column shear force
- $j_b$  =  $(7/8)d_{bm}$ , where  $d_{bm}$  = the beam effective depth

all other terms are as previously defined.

Equation I was noted to apply to horizontal shear stress. Determination of vertical shear stress is not commonly done (this Sec., "Shear Stress Capacity"). According to Paulay et al (1992), it is usually appropriate to estimate the vertical shear stress as a percentage (defined by the ratio of the height of the beam to  $d_c$ ) of  $v_{jt}$ .

#### Limits on Applied Shear Stress

Many researchers have suggested limits on values of  $v_{jt}$  which should provide for adequate seismic performance. For example, Leon et al. (1986) suggest that  $v_{jt} \leq 1 - 1.5\sqrt{f'_c}$  ( $f'_c$  in MPa) in order for joints to behave elastically and for frames/subassemblages to behave with stable hysteretic performance. ACI Committee 318 (ACI 318M-89) limits  $v_{jt}$  by restricting the nominal value of joint shear strength to  $\leq 1.25\sqrt{f'_c}A_{jt}$ . Kitayama et al. studied results from 58 B-C joint tests and claim that when  $v_{jt}$  exceeded  $1.25\sqrt{f'_c}$ , regardless of the amount of joint reinforcement used, the specimens failed in joint shear whether or not flexural yielding in the beams occurred. In the database study of joint subassemblage tests by Bonnaci et al. (1993), the range over which the primary cause of failure was joint shear was  $0.75\sqrt{f'_c} \leq v_{jt} \leq 1.5\sqrt{f'_c}$ , and  $1.17\sqrt{f'_c}$  was the average value of  $v_{jt}$ . The scatter in the various joint shear stress limits is probably due to the fact that the research studied in each case differed with respect to confinement, member bar anchorage lengths ( $l_d$ ), and member flexural strength ratios ( $\Sigma M_{nc}/\Sigma M_{nb}$ ). Thus in order to have a rational frame of reference for a limiting value of  $v_{jt}$ , the values of other variables must be defined as well. Ideally, other items previously discussed such as the displacements to which a specimen was cycled, and the loading rate that it was subjected to, would be included as well.

### Shear Stress Capacity

The countries with the most advanced building codes, with respect to seismic design of reinforced concrete structures, are the United States (US), New Zealand (NZ), and Japan. However, each of those codes approaches joint design differently, primarily with respect to the role of joint reinforcement in determining the joint shear stress capacity ( $v_{njt}$ ). Each code is biased toward the results obtained from research conducted in the respective country. Thus, in order to have a frame of reference from which to consider B-C joint research results obtained by researchers from the various countries, it is necessary to understand the basis behind the calculation of  $v_{njt}$  in each code. Empirical expressions are used to determine  $v_{njt}$  in each of the codes.

In the US, provisions established by ACI 318M-89 simply state that  $v_{njt} \leq \gamma\sqrt{f'_c}$ , where  $\gamma$  is the constant defined in Equation 1 and is assigned a value based on the number of beams that frame into a given joint. The provisions are based on experimental research results that indicate that the joint shear strength is not sensitive to joint reinforcement (Paulay 1984). The role of joint reinforcement in the transfer joint shear is merely implied in ACI 318M-89, as is consideration of vertical shear and vertical joint reinforcement.

NZ code provisions are based on a rational behavioral model for the mechanisms of joint shear transfer, and so the NZ code emphasizes joint reinforcement (horizontally and vertically). Accordingly, in the provisions of the NZ code (NZS-3101, 1982), both the horizontal and vertical expressions for  $v_{njt}$  contain a term that accounts for joint reinforcement. Under certain conditions, the contribution of concrete in the  $v_{njt}$  expressions is taken as zero.

The Japanese code, AIJ 1975, also has a term in the  $v_{njt}$  expression that accounts for joint reinforcement. However, this code places more emphasis on the role of concrete in the transfer of joint shear (Otonari 1991). Additionally, AIJ does not directly consider either vertical joint shear or vertical reinforcement.

While the value of  $v_{jt}$  is a major factor in determining the performance of seismically loaded B-C joints, it is not a good predictor, by itself, of damage or of joint behavior (Leon 1990). The bond of member bars, in and around a joint, also plays an important role in the transfer of joint shear and in determining the performance of joints.

### 3.6.3 The Effect of Member Bar Bond on Shear Transfer

#### Bond in B-C Joints

*Bond Stress in B-C Joints.* The findings of ACI Committee 408 (1991) provides a background for the study of bond under cyclic loading. Portions of the committee's findings are related to B-C joints. In all reinforced concrete structures bond is measured in terms of "bond stress". Bond stress results from the transfer of load ( $F_{b,t}$  and  $F_{b,b}$ ) between bars and the surrounding concrete (Fig 13). The type of bond stress that is pertinent in the discussion of seismically loaded B-C joints, as depicted in the figure, arises from anchorage of bars in a joint (versus flexural bond, that comes from the change in force along bars due to changes in bending moment along the member). Under the seismic conditions of "low-cycle" (i.e., the load history contains less than 100 cycles), "stress reversal" loading, the bond stress ranges are typically large. The primary component of bond transfer is mechanical anchorage due to local bearing between concrete and the bar lugs. If the bond stress is too high, failure will occur in the form of either bar slip (local-type of bond failure), direct bar pull/push-out (global-type of bond failure implying loss of anchorage) and/or cover splitting. Accordingly, the tensile strength of the concrete ( $f'_t$ ), bar deformation patterns, bar cover and spacing, as well as the amount of hoops, are critical in defining appropriate bond stress levels.

*Quantifying Bond Stress and Bond Force.* The average bond stress,  $u_b$ , that results from compression in a bar on one side of the joint and tension in the same bar on the other side of the joint is determined as follows:

$$u_b = \frac{(f_{s-} + f_{s+})A_b}{\pi d_b d_c} \quad \text{(Equation 3)}$$

where,

- $f_{s-}$  &  $f_{s+}$  = the stresses in a bar at opposite joint faces
- $A_b$  = the area of a bar
- $d_b$  = the diameter of a bar
- $d_c$  = the depth of the column

To determine the maximum value of  $u_b$ , a factor is applied to the numerator to account for the possibility of bar strain hardening and/or over-strength. Leon (1991) notes that  $u_b$  is an average value; local bond stresses in the joint can be significantly greater. He also states that across large shear cracks in the joint  $u_b$  is zero. Therefore, local bond stresses must be much higher than the average stress,  $u_b$ .

The total bond force,  $F_b$ , transferred by a given bar is (Fig. 13):

$$F_b = T + C \quad \text{(Equation 4)}$$

where:

- $T$  =  $f_{s+}(A_b)$
- $C$  =  $f_{s-}(A_b)$

It is important to recognize that both  $u_b$  and  $F_b$  decrease when the magnitudes of  $f_{s-}$  and  $C$  decrease. The complete loss of bond in a joint, which results in loss of anchorage ("pull/push"-type failure), occurs when  $f_{s-}$  and  $C$  become tensile and equal in magnitude to

$f_{st}$  and  $T$ . It is very difficult to prevent high  $u_b$  and  $F_b$  values. Hence, bond deterioration is difficult to prevent without large anchorage lengths ( $l_d$ ) relative to the value of  $d_b$  of the bar being developed (Leon 1991).

*Bond Conditions.* Usually, the value of  $l_d$  is limited to the column depth ( $d_c$ ). In most cases  $d_c$  does not provide an adequate value of  $l_d$  for the bars passing through the joint because these bars must usually be developed in tension and compression (Fig. 13), and this leads to unfavorable bond conditions. Proof that the bond conditions in B-C joints are unfavorable, as well as descriptions of the typical progression of bond deterioration, can be found in a number of experimental studies (Filippou et al. 1986 and Soroushian et al. 1989). To begin, joint shear cracking occurs relatively quickly because the tensile capacity of the concrete is small. As the joint cracks, and typically after bars have yielded, bond deteriorates. Bar slip occurs as the bond deteriorates, and this slippage causes the cracks that formed earlier to widen. The growth and opening of cracks, in general, is a major source of inelastic deformation in reinforced concrete members and, as mentioned in Section 3.4, inelastic deformations in a joint are undesirable. As cyclic load reversals continue, bond conditions are further worsened, and increasing bar slip occurs along with large concentrated rotations at cracked sections of the members near the joint. The cracks may extend throughout the entire member depth; this causes bars anchored in the joint to be subjected to a cyclic "pull" from one side of the joint and a cyclic "push" from the other side, thereby inducing further bond deterioration and, possibly, complete loss of anchorage within the joint ("pull/push"-type failure).

#### The Effect of Bond on the Shear Transfer Mechanisms

The mechanism by which shear is transferred through a joint at any given time is determined by the bond conditions in the joint. According to Kaku et al. (1991), it is well known that without any bond, anchorage is lost, and a change in the joint shear transfer

mechanism from the truss to the strut mechanism occurs. However, prior to the loss of anchorage, bond conditions within a joint might be either "good" or "deteriorated". Depending on which of these two conditions exist in a joint at a given time, the roles played by the "truss" and "strut" in the transfer of joint shear can increase or decrease relative to one another. This issue will now be explored further.

*Joint Shear Transfer with Good Bond Conditions.* For situations where the areas of top and bottom bars in beams are equal, as beams undergo flexure it is likely that flexural cracks will close upon reversal of the moments. Hence, the compression regions of the beams will be available some of the time to provide confinement of the joint. Thus, the differences between the roles of the mechanisms in the transfer of shear will probably not be as great as they are in situations where the areas of top and bottom bars are not equal (Fig. 12b) and the "truss" is predominant (Paulay 1984, and Leon 1990).

*Joint Shear Transfer with Deteriorated Bond Conditions.* As mentioned in this section ("Bond in B-C Joints"), once first yield of the member bars occurs bond conditions can be expected to deteriorate. Paulay et al. (1984) argue that as bond conditions worsen, yield penetration of the bars is increased. Thus, the region of the joint that is able to transfer bond stress will be smaller than the depth of the column, thereby making it likely that the contribution of the truss mechanism to joint shear transfer will decrease. The reason being that there is less bar length over which to transfer bond, so the bond stress in this reduced region could approach levels where slip could occur

According to Leon (1990) and Paulay et al. (1984), if bond conditions deteriorate to the point where excessive bar slip or anchorage failure occurs, the "truss" ceases to function. With excessive bar slippage/anchorage failure the bar tension stresses can not be transferred to the joint core via bond. Therefore, the bar tension stresses must be resisted by concrete compression forces at the faces of the joint. The result is that beam bars are anchored across the joint and the size of the beam compressive stress blocks are large,

thereby providing the joint corners with better confinement, and thus allowing the strut mechanism to become predominant (Fig 12a).

Both Leon (1990) and Paulay et al. (1984) caution that associated with the strut mechanism is an increase in size of the compression stress in the main diagonal strut. The increase in size of the compression stress in the main diagonal strut, coupled with:

- 1.) the deterioration of strut concrete caused by reversed cyclic loading, and
- 2.) the reduction of the compressive strength of strut concrete caused by the increasing tensile strain perpendicular to the direction of the main diagonal strut, causes the shear capacity of the main diagonal strut to decrease. As a result, the main diagonal strut can eventually fail in shear compression.

Short of a joint shear failure, the strut mechanism leads to more joint cracking, and to loss of member corners, hence to more shear deformation and more loss of energy dissipation capacity.

#### The Effect of Deterioration of Bond on Seismic Response

Paulay (1986) claims that the cause for the poor performance of a large number of test subassemblages was the breakdown of bond within the joints. According to Paulay, many test specimens, as well as existing structures, were designed in accordance with building codes with provisions for elastic performance. The actual situation where plastic hinges are formed on both sides of a joint (in a "strong column-weak beam" frame/subassemblage), and where the bars connecting these hinges requires strength development, was not addressed. Moreover,  $I_d$  requirements in these older codes came from research conducted on monotonically-loaded test specimens, not reverse-cyclically loaded B-C subassemblage specimens. Even use of today's codes does not guarantee adequate performance; there is no allowance in the codes for the likelihood of poor bond performance of bars in B-C joints.

The reasons that bond deterioration of bars within a joint is detrimental is as follows:

- 1.) The hysteresis loops pinch because the ability of the member ends at the joint to dissipate energy is reduced (Tada et al. 1991, Otani 1991, Joh et al. 1991a, Kitayama et al. 1991, Kaku et al. 1991, Soleimani et al. 1979, and Filippou et al. 1986). Note that shear cracking in the joint core usually works in concert with bond deterioration to cause "pinching".
- 2.) The response during loading may increase because of the reduction in stiffness of the frame/subassemblage (Kitayama et al. 1991).
- 3.) An undesirable change in the joint shear stress transfer mechanism from the "truss" to the "strut" can occur (Kitayama et al. 1991 and Kaku et al. 1991). This also reduces the stiffness.
- 4.) Rigid end rotations of the beams can occur. This will cause increased beam deformations and, as a result, will accelerate concrete crushing at the critical section (Kitayama et al. 1991, Kaku et al. 1991, Soleimani et al. 1979, and Otani 1991).
- 5.) Yield penetration of the member bars into the joint core can occur. This will result in a further reduction of  $l_d$  (Paulay 1986, and Otani 1991).
- 6.) The moment resisting capacity of the plastic-hinge region of the adjoining members may decrease because of the loss of member cross-section that can occur (Kaku et al. 1991).
- 7.) Repair of bond deterioration is difficult (Otani 1991).

#### Factors that Influence Bond

There are four categories of factors that affect bar bond in a joint: material properties, joint design details, joint construction, and loading conditions. There tends to be an inter-relation of factors within these categories. This is one of the reasons that the issue of bond is so complex.

*The Effect of Material Properties on Bond.* The tensile and shear strengths of the concrete; the types of aggregate and cement used in the concrete; and the bar rib geometry, all affect bar bond (Leon 1991). The reasons that these properties affect bar bond can easily be deduced from the previous discussion on how bond deteriorates under reversed cyclic loading.

*The Effect of Joint Design Details on Bond.* The factors involved in the design of the specimen that affect bond are: the bar diameter ( $d_b$ ), bar yield strength ( $f_y$ ), concrete cover, spacing and anchorage length ( $l_d$ ) of the bars, and the amount and distribution of joint hoops and column intermediate bars (Leon 1991).

Clearly, the amount of cover, the spacing and the value of  $d_b$  of the bars interact in influencing the mechanics of bond deterioration. The smaller the concrete cover and bar spacing are, and the larger the value of  $d_b$  is, the less effective mechanical anchorage will be. The values of  $d_b$ ,  $f_y$ , and  $l_d$  must be considered together because the values of  $d_b$  and  $f_y$  determine the required value of  $l_d$  (under the elastic-conditions-based code provisions). Filippou et al. (1986) argue that a smaller value of  $d_b$  improves hysteretic response; a smaller value of  $d_b$ , given constant values of  $f_y$  and  $d_c$ , provides for a larger value of  $l_d$ . To achieve the same end, the value of  $f_y$  could be decreased and a larger value of the area of bottom bars (and/or the area of top bars), using the same value of  $d_b$ , could be used in the layer.

In Leon's (1991) research the influence of values of  $l_d$  and  $v_{jt}$  on bond were studied. Of the specimens tested, only those that had values of  $l_d = 24$ , or  $28d_b$  were able to develop enough bond for the beams to reach their ultimate moment capacities. Although,  $v_{jt}$  values at the time of beam yield were all about equal, regardless of the value of  $l_d$ . Therefore, Leon concluded that in order to determine whether or not a given value of  $l_d$  is adequate for inelastic structural performance, some account should be taken of the value of  $v_{jt}$ . By doing so analytically, he found that as the value of  $v_{jt}$  increased, the value of  $l_d$  required to develop and sustain plastic hinges in the beams increased.

With respect to the role of hoops, analytical research by Paulay (1989) showed that beam bar stresses at the centerline of a joint will increase with decreased amounts of hoops, thereby increasing the likelihood of bond deterioration. Through an analytical approach using first principles of shear transfer in reinforced concrete members and using equilibrium of column and beam forces in the joint, Paulay argues that when little or no hoops are provided in the joint, bar yield may penetrate to the center of the joint. His argument is based on "weak beam-strong column" behavior where plastic hinges have developed in the beams. Paulay also shows that under elastic conditions the bar stresses at the center of the joint will approach those reached at the joint faces. This occurs as a result of the bars having to offset the diagonal concrete compressive stresses in the joint ("tension-shifting" effect), regardless of bond conditions. The results of higher bar stresses inside the joint are that joint dilation may be large, that beam bars may not function in compression in regions where normally expected, and that only a small part of the bar forces can be transmitted by bond to the joint core. Bond transfer is then accomplished mostly outside of the joint in the adjacent beams. As a result, the role of the truss mechanism decreases, while that of the strut mechanism increases. Paulay's findings were corroborated by an analytical study by Ichinose (1991). Additionally, Ichinose concluded that after a certain point, there is no benefit to adding more hoops in pursuit of improved anchorage.

Experimental research by Joh et al. (1991a), Leon (1991), Soroushian et al. (1989), Yankelevsky et al. (1992), and Ehsani et al. (1985) showed that the increased joint confinement that resulted from increased amounts of hoops limited the amount and the growth of cracks in joints, thereby improving bond conditions.

*The Effect of Joint Construction on Bond.* For experimental specimens the pertinent factors related to construction that affect bond are: the casting position of the subassemblage and how it was vibrated; and the temperature and surface conditions of the subassemblage during curing (Leon 1991). The influences of the casting position of the

subassemblage and of the vibration technique used on the subassemblage concrete is based upon the issue of segregation of aggregate. Segregation of aggregate is known to be detrimental to bond. ACI 318M-89 addresses the issue for vertically-cast frames by requiring that the value of  $l_d$  must be increased for horizontal bars placed above 305 mm of fresh concrete.

With regard to the effects on bond from the temperature and from the surface conditions during curing of frames/subassemblages, shrinkage cracking is a concern. Shrinkage cracking can be detrimental to bar bond because of the possibility for concrete in the vicinity of bar lugs to be cracked, thereby detracting from bond conditions.

*The Effect of Loading Conditions on Bond.* The rate of loading and the displacement/loading history, and the amount of column axial compressive load, have an effect on bar bond.

In Section 3.5.2, "Drawing Conclusions from Experimental Test Results", the rate of subassemblage loading was shown to have an impact on experimental research results. The impact is due to the fact that bond conditions are thought to improve under realistic rates of loading, which as discussed, tend to be much higher than the loading rates used in experimental research. Faster loading rates are believed to cause increased localized damage in the concrete and in the bars near the joint region.

The effect of loading history on bond, according to Leon (1991), seems to be significant, although it is an area that has not been widely investigated. Leon believes that B-C joint test results have shown that the loading of specimens through elastic cycles affects bar bond in the joint, depending on the level of joint shear cracking in a given specimen.

Hayashi et al. (1985) showed column axial compressive load could be helpful in decreasing the beam bar "push-in" slip (versus "pull-out" slip). However, the study by Hayashi et al. was concerned with conditions prior to beam bar yield only. Kaku et al. (1991) believe that column axial compressive load is a factor that affects bond. However,

proof of this is lacking because only a few experiments have been done to investigate the phenomenon. This is probably due to the fact that the capacities of the hydraulic jacks used by most researchers are not sufficient to impart the large axial compressive loads that are required to create a wide enough spectrum of study.

#### Criteria for Bond for Seismic Performance

As has been shown, bond in reverse cyclically loaded B-C joints is a complex phenomenon due to its dependency on the interaction of many factors. Additionally, bond has been shown to play important roles in joint shear transfer and in other aspects of frame/subassembly performance. Analytical and additional experimental research results were reviewed to examine the effect of specific bond conditions on frame/subassembly performance, including various criteria proposed by several researchers regarding the bond conditions required for satisfactory frame/subassembly performance. In order to accomplish this review, a method for the determination of bond conditions was required. This method, introduced below, was applied to most of the research results and to the proposed criteria that were considered.

*Determination of Bond Conditions.* The "bond index" (BI), developed by Kitayama et al. (1991), indicates the severity of bond stress relative to the bond strength in a B-C joint. The bond stress used is  $u_b$  (Equation 3, this Sec., "Bond in B-C Joints"), while the bond strength is represented by  $\sqrt{f'_c}$  (bond strength is dependent on  $f'_t$  and  $f'_t$  is proportional to  $\sqrt{f'_c}$ ):

$$BI = \frac{u_b}{\sqrt{f'_c}} = \frac{f_y(db/dc)}{2\sqrt{f'_c}} \quad (\text{Equation 5})$$

where all terms are as previously defined.

Review of Equation 5 shows that the BI is a good measure of bond conditions: a larger BI corresponds to poorer bond conditions, and vice-versa. Also, the quantities in the equation can easily be derived and/or obtained directly from most research results. Thus, the BI is widely applicable.

*The Amount of Bond Required for Adequate Structural Performance.* It is well established that bond deterioration is difficult to prevent. Fortunately, recent research has shown that some bar slip can be tolerated without the sacrifice of overall structural performance. In an analytical dynamic analysis study by Kitayama et al. (1991), the amount of beam bar slip that should be allowed was quantified, based on consideration of the energy dissipation capacity of beam ends and on the influence of the energy dissipation capacity of beam ends on the seismic response of frames. It was determined that, for an allowable deformation level equal to a story drift of 2%, the BI should be  $\leq 1.4$  in order to ensure that the beam ends have some energy dissipation capacity.

Otani (1991) argues that some loss of bond is tolerable since it may not lead to a sudden loss of beam resistance, provided that:

- 1.) the beam is adequately confined,
  - 2.) the beam bars are anchored through the joint, and
  - 3.) the majority of the other joints in a frame maintain their resistance and stiffness.
- Otani's conclusion is based upon his study of the work done by Kitayama et al. (1991), where it was shown that the largest structural response is not very sensitive to the hysteretic energy dissipated. However, Otani contends that the number of large-amplitude oscillations will certainly increase with decay of the hysteretic energy dissipated. Finally, Otani cautions that the AIJ (1975) requires that where bars are expected to yield at both faces of the joint,  $d_c/d_b$  shall be such that slip-type hysteretic behavior under load reversals does not occur.

*Additional Research Results and Criteria.* In experimental research done by Kaku et al. (1991) the hysteresis loops from tests on three specimens, with BI values = 1.88 (A), 1.28 (N), and 0.96 (O), revealed that specimen A had pinched loops. Figure 14 shows

that specimens N and O maintained relatively large hysteresis/energy absorbing capacity. Beam bar slip was measured in the three test specimens and is shown in Figure 15, where positive slip values (i.e., "S" = + mm) represent pull-out slip and negative slip values represent push-in slip. Push-in slip and pull-out slip were evident in specimen A, while specimen N exhibited primarily pull-out slip, and specimen O experienced only pull-out slip. Figure 16 shows that pull-out slip for specimen A increases rapidly with increasing deformation, while for specimens N and O the increase is gradual. Specimens N and O exhibited such similar behavior that Kaku et al. concluded that once the BI falls below a certain value (0.96 in this case) the effect of reducing bar slip is lost. A dynamic analysis, similar to the one done by Kitayama et al. (1991), was done on specimens A, N, and O to study the effect of energy absorbing capacity. Once again it was found that no significant difference in displacement response occurred provided that the beam ends possessed some energy dissipation capacity.

Bonnaci et al. (1993) conclude that for specimens with Gr 60 beam bars and BI values  $> 1.7$ , bond failures occurred. Sugano et al. (1991), based on their experimental test results, proposed the criterion  $BI \leq 1.7$ , for beam bar bond performance in higher strength concretes ( $f'_c \geq 35$  MPa). Additionally, for joints with normal strength concrete ( $21 \leq f'_c \leq 35$ ),  $BI \leq 2$  was suggested by Sugano et al.

Having considered the joint shear stress demand ( $v_{jt}$ ) and bond, the last of the areas of complexity, and of greatest importance in B-C joint shear transfer, remains to be considered: joint reinforcement.

#### **3.6.4 The Effect of Joint Reinforcement on Shear Transfer**

As was detailed in Section 3.6.1, it is widely accepted that there are two mechanisms by which shear is transferred through a joint: the "truss" and the "strut". Theories regarding the truss and strut mechanisms were presented with respect to the make-

up of the mechanisms and with respect to the amount of joint shear carried by each mechanism at given points in time. In the current section, the debate about how shear is transferred through a joint will be considered with regard to the roles of the joint hoops. Also, in Section 3.5.1 it was mentioned that the functions (confinement and shear transfer) of vertical and horizontal joint reinforcement, and the appropriate amounts of joint reinforcement required to perform these functions, are still being debated. These issues will also be considered in the current section.

### The Role of Hoops in the Shear Transfer Mechanisms

Figure 17 is the result of the study on a database of joint subassemblage tests that was conducted by Bonnaci et al (1993). The figure was constructed to clarify whether the role of the hoops in joints is as envisioned in the "truss" (shear transfer and confinement roles) or as envisioned in the "strut" (confinement role). Definitions of the symbols used in the figure are as follows:

$\rho_{sv}$  = the volumetric hoop ratio, expressed as a percentage,

$f_y$  = the yield strength of the beam bars (ksi),

$f'_c$  = the compressive strength of the concrete (psi),

$\bar{V}_p$  = the total yield force that can be developed by joint hoops parallel to the direction of the applied load ( $= A_v f_y h$ ), divided by  $A_{jt}$ , and normalized with respect to  $\sqrt{f'_c}$ ,

$A_v$  = the total area of the joint hoops parallel to the direction of the applied load,

$\bar{V}_m$  = the maximum joint shear stress demand.

Bonnaci et al., while acknowledging that Figure 17 does not clearly settle the debate concerning the roles of hoops, claim that the figure might be interpreted as follows: as the

confinement index ( $\rho_{sv}f_{yh}/f'_c$ ) increases, the demand on the concrete core ( $V_m - V_p$ ) decreases, the relative portion of joint shear transferred by the hoops increases, and the number of joint shear failures decreases (considering the number of joint shear failures, "x", in each seven unit increment in the value of  $\rho_{sv}f_{yh}/f'_c$ ). Conversely, as the amount of confinement decreases, the demand on the concrete core increases, as does the number of joint shear failures. Perhaps the reason that the figure does not clearly settle the debate concerning the role of hoops in the transfer of joint shear is due to the lack of consideration of the role played by bond (Section 3.6.3, "The Effect of Bond on the Shear Transfer Mechanisms").

In addition to the controversy surrounding the issues related to the mechanisms of joint shear transfer in B-C joints, and to the roles played by the hoops in the mechanisms, there are also differing opinions concerning the potential of all of the types of joint reinforcement to provide shear transfer capacity and/or confinement required by the mechanisms.

#### The Functions of Joint Reinforcement

In addition to the questions regarding hoops performing shear-transfer and/or confinement functions in their roles in the joint shear transfer mechanisms, debate about the ability of the other types of joint reinforcement to perform those functions exist as well. When bond conditions are good, and when there is enough joint reinforcement, it is more than likely that the participation of the truss mechanism is significant. In the "truss", the role of the hoops, the column intermediate bars, and perhaps the beam intermediate bars, is primarily to perform as tension members that enable a "truss mechanism" to form and to transfer shear through the joint. When the bond conditions are deteriorated, the strut mechanism becomes predominant and the role of the hoops, possibly with the aid of the member intermediate bars, is primarily to perform a confinement function.

*Shear Transfer.* Paulay (1989) claims that the joint deformations that result from the applied shear can be related to that shear by consideration of the shear strains in a joint. As a result, the importance of the shear-transfer function of joint reinforcement can be explained. When the joint shear strains become large enough the tensile strength of the concrete will be reached and cracking will occur. Once joint cracking occurs diagonal tension load paths will cease to exist. However, the shear stress imposed on the joint can not be transmitted without those diagonal tension load paths. Thus, reinforcement within the joint is required to carry the tensile force that was borne by the concrete prior to cracking.

Both Paulay and Leon et al. (1986) claim that orthogonally placed joint reinforcement offsets the loss of the diagonal tensile strength of elements of concrete inside the joint. Figure 18 depicts a shear-deformed diagonally-cracked concrete element. Also shown in the figure are the compressive stresses acting at the boundaries of a concrete element, and the strains from orthogonal joint reinforcement (labeled "steel forces") that allow the compressive stresses at the boundaries to occur. When these compressive stresses combine with shear stresses the development of a diagonal compression field is possible. This diagonal compression field provides the mechanism by which the element transfers shear stresses.

Jirsa et al. (1975) and Meinheit et al. (1981), based on the experimental test results from fourteen subassemblages, observed that the shear strength of the joint was relatively insensitive to the amount of hoops. Based on this observation, Meinheit et al. concluded that joints could perform satisfactorily, without large amounts of hoops, provided that  $v_{jt} \leq 1\sqrt{f'_c}$ . The method that was suggested for keeping within the threshold value of  $v_{jt}$  was to increase the values of  $f'_c$  and the joint area. Meinheit et al. also observed, as did Joh et al. (1991a), that the shear cracking strength of joints was not influenced by the amount of hoops. However, the test results from the research by Meinheit et al. showed that the

measured joint shear capacity was much greater than the first cracking strength when a nominal amount of hoops were present.

Otani (1991) believes that while a minimum amount of joint hoops are required, regardless of which of the two shear transfer mechanisms are acting, hoops over and above that minimum may increase joint shear resistance in the truss mechanism, but they will not in the strut mechanism. Moreover, Otani claims that increases in the amount of hoops will not contribute as much to shear transfer as believed by some (e.g., researchers from NZ).

Column intermediate bars have been shown to participate in the transfer of vertical shear. Experimental research by Cheung et al. (1991) indicated that the column intermediate bars could resist 40% of the resultant vertical force acting on one side of a vertical plane through the joint core. The additional amount of resultant vertical force, 60%, was carried by the concrete diagonal compression strut. In general, it was noted that the significant values of tensile strain shown by column intermediate bars in the joint indicated participation of these bars in transferring vertical joint shear.

Paulay (1986) uses first principle equilibrium equations to show that vertical joint shear reinforcement, normally consisting of column intermediate bars, is required unless the axial compression load on a column is large. With little or no axial compression load on a column the stress on column bars inside of the joint undergo a "tension shift" from the calculated values, due to the loss of joint concrete tensile capacity caused by diagonal cracking. The "tension shift" will likely result in significant amounts of tension in the column intermediate bars (Fig. 19, Fujii et al. 1991). Paulay claims that highly-stressed member bars, particularly those in members expected to develop their full strength at a plastic hinge adjacent to a joint, are ineffective as joint reinforcement. Thus, additional vertical reinforcement is usually required unless the axial compression load on a column is large. With large axial compression on a column, Paulay (1989) argues that when columns have reserve flexural strength, intermediate bars can act as vertical shear reinforcement (tension members opposing the diagonal concrete compression struts).

Beam intermediate bars have also been shown to participate as horizontal joint shear reinforcement. Fujii et al. (1991) tested specimens with beam bars arranged in two layers. Bond deterioration was not observed in the outer layer bars. However, the inner layer bars exhibited bond deterioration quickly. At locations at the joint faces that normally produced compressive stresses in the beam bars, the stresses in the inner layer bars became tensile early in the test and the value of  $u_b$  eventually became zero. The inference made by Fujii et al. was that part of the reduction in the value of  $u_b$  was due to the inner layer bars behaving as horizontal joint reinforcement. Pantazopoulou et al. (1992), based on their review of other experimental research, agree that beam intermediate bars can aid in the transfer of horizontal joint shear. Priestley (1991) contends that beam bars in the central region of the joint, properly anchored at the boundaries of the joint, may be considered effective as joint reinforcement if the beam is not expected to form a plastic hinge adjacent to the joint (i.e.,  $M_{nb} \gg M_{nc}$ ).

*Confinement.* Paulay (1986) claims that interpretation of test results, where the cause of failure is inferred to be breakdown of bond rather than shear resistance, can lead to the generally untenable claim that joint shear strength is not sensitive to joint reinforcement (because the confinement provided by the hoops is overlooked). The mechanisms and purpose of confinement are much different from those of shear transfer. The vital issue with confinement, according to Paulay, is the control of diagonal tension across the joint.

If a joint is confined with enough reinforcement, then diagonal tension will be controlled, thereby

- 1.) increasing the diagonal compressive strength of the concrete core because the principal tensile strains will be reduced (Pantazopoulou et al. 1992 and Joh et al. 1991a), and
- 2.) improving the bond conditions and decreasing the joint deformation because diagonal tension cracking will decrease.

The first point, 1.), is intuitive, and in point 2.) the relationship between joint confinement and bond has already been considered (Sec. 3.6.3, "Factors that Influence Bond").

With respect to joint deformation, some researchers (Sugano et al. 1991, Leon 1990) have found that when the relative deformation experienced by B-C joints (exclusive of bar bond deterioration and of bar slippage) exceeds 25% of the total deformation of the frame/subassemblage, joint shear failures can be expected. Pantazopoulou et al. (1992) argue that the smaller the joint deformation contribution is to the total structure deformation, the better overall structural response will be. However, they found that the dependence of joint stiffness on the stiffness contributed by the joint reinforcement is often overlooked because of the two-dimensional representations of joints that are typically used. Two-dimensional representations of joints falsely indicate that the joint core concrete stiffness contribution to the joint stiffness is independent of the confinement role of joint reinforcement because the stiffening effect of the reinforcement is only realized by consideration of the thickness of joints.

According to Pantazopoulou et al. (1992), beam intermediate bars can not act as joint confinement reinforcement. Pantazopoulou et al. claim experimental work (done by others) has proven this. The inability of beam intermediate bars to provide confinement to a joint is due to the fact that the compatibility of the bars with the core concrete depends only on bond. Bond has been shown likely to degrade under cyclic loading (Sec. 3.6.3, "Bond in B-C Joints"). Therefore any benefit from intermediate bars in the way of confinement diminishes quickly.

Column intermediate bars, on the other hand, have been shown to enhance the stiffness of the joint (Joh et al. 1991a).

In this section, issues surrounding the roles of joint reinforcement in the shear transfer mechanisms have been reviewed. In an attempt to clarify these issues, specific amounts of joint reinforcement used by several researchers is considered next.

### Specific Amounts of Joint Reinforcement

In the following, the specific amounts of joint hoops used by various researchers, and the resulting effects on the shear-transfer and confinement functions, and on the behavior of the joints, is considered.

Discussion of specific amounts of hoop used by various researchers is made easier with a common index. In many instances in the literature the hoop spacing used in the joint regions is not given but the total number of hoops in the joints is. Therefore, use of the hoop volumetric ratio,  $\rho_s$ , provides a consistent reference. For circular hoops:

$$\rho_s = \left( \frac{A_{sh}\pi d_h}{A_g h_b} \right) 100\% \quad \text{(Equation 6)}$$

where,

$A_{sh}$  = the total cross-sectional area of joint hoops in-between the top and bottom layers of the beam bars

$d_h$  = the hoop diameter

$A_g$  = the gross cross-sectional area of the column

$h_b$  = the height of the beam

and other terms are as previously defined.

For rectangular hoops:

$$\rho_s = \left( \frac{A_{sh}L}{A_g h_b} \right) 100\% \quad \text{(Equation 7)}$$

where,

$L$  = the total length of the four sides of a hoop

and other terms are as previously defined.

Experimental studies were conducted by Kitayama et al. (1991) to determine the values of  $\rho_s$  required to transfer shear, and to confine the core concrete, after bond deterioration of the beam bars occurs at high joint-shear levels. To accomplish these objectives, some specimens were designed with ties serving as the joint reinforcement, and the strains on these ties were monitored throughout the loading history. Kitayama et al. claim that the joint ties parallel to the loading direction transferred joint shear and confined the joint core concrete until bond began to deteriorate, although the beam bars had not yet yielded. The claim was also made that the ties in the parallel direction were performing as portions of the truss mechanism, until bond deteriorated. As the drifts increased beyond the point at which bond deteriorated, the strains in the "parallel" ties did not change much, perhaps indicating a change from the "truss" to the "strut". The "perpendicular" ties confined the joint core concrete normal to the loading direction, according to Kitayama et al. The strains in these ties increased markedly with drift, implying lateral expansion of the joint core concrete. For drifts larger than the point at which bond deterioration began, the contribution by the "parallel" ties toward the transfer of joint shear decayed, indicating the decay of the truss mechanism. Kitayama et al. argue that once the truss mechanism decayed the principal role of the lateral reinforcement became confinement of the cracked core concrete. The confinement function was fulfilled by the specimens until yield of the lateral reinforcement normal to the loading direction occurred. The conclusion drawn by Kitayama et al. from their tests was that a minimum value of  $\rho_s = 0.5\%$  is recommended.

The similar performance of two specimens (BCJ5 and BCJ7) tested by Leon et al. (1986) lead to their conclusion that increasing the value of  $\rho_s$  from 0.5% (BCJ5) to 2.5% (BCJ7) had little effect. However, larger beam rotations and slightly lower joint shear strains occurred in BCJ7

According to Otani (1991), the minimum value of  $\rho_s$  is the value that will accomplish the following:

- 1.) prevent diagonal tension failure of the main joint diagonal,

- 2.) improve the joint ductility by confining the cracked core concrete, and
- 3.) protect column corner bars from bond splitting failures.

Otani points out that the minimum value of  $\rho_s$  required by the AIJ is  $\geq 0.2\%$ .

Information regarding specific amounts of joint reinforcement can provide insight into the arguments surrounding the functions and the roles of joint reinforcement involved with the transfer of joint shear. However, there are other indicators that are related to joint reinforcement that warrant consideration as well.

### Behavior of Joint Reinforcement

The strains in the joint hoops and the extent and type of joint cracking can indicate the behavior and the condition of the joint.

In four subassemblage tests by Fujii et al. (1991) the strains in the hoops at peak loads during cycling were considered (Fig. 20). Fujii et al. noted that at first cracking in the joints the strain in the hoops suddenly increased (i.e.,  $P = 2$  tons). Sharp increases in joint hoop strains at first cracking have also been noticed by others (Joh et al. 1991b).

As the loads on a joint increase beyond the point at which first cracking occurs, the hoop strains can be expected to continue to increase. However, the meaning of the subsequent increases in strains with regard to the role of the hoops in joint shear transfer are the subjects of debate. Two of the viewpoints in this debate are discussed next.

Cheung et al. (1991) conducted experimental tests on subassemblages in which the joints were designed to carry shear primarily through the truss mechanism. Cheung et al. inferred that, as specimen displacements grew, increasing strains in the hoops indicated that the participation of the hoops was increasing in the transfer of joint shear (as portions of the truss mechanism), and in the confinement of the joint core.

In experimental tests on subassemblages by Leon (1990), the joints were detailed to resist shear primarily through the strut mechanism. While Leon does not mention the strain

in the hoops, he does state that he believes that most of the force transfer through the joints was accomplished via the strut mechanism. Accordingly, as the joint regions of Leon's specimens deteriorated (one specimen actually suffered a joint shear failure), it is rational to attribute the increase of strains in the hoops to the hoops' failure to confine the joint cores (because confinement is the primary role of the hoops in the strut mechanism).

Stevens et al. (1991) tested reinforced concrete panels in reversed-cyclic shear. These tests produced data on the stresses in both the panel concrete and in the reinforcement. The conclusion made by Stevens et al. was that when shear stress levels cause reinforcement yielding, the eventual failure is by concrete crushing. Stevens et al. recommend that joint hoops should be designed to remain elastic, and preferably the steel used should transition directly from elastic behavior to strain hardening (i.e., not have a yield plateau)..

Pantazopoulou et al. (1992) warn of two scenarios that can occur in B-C joints: 1.) the concrete diagonal struts can crush before the hoops yield, and 2.) the concrete diagonal struts can crush and the column intermediate bars can yield after the hoops yield.

In experimental research conducted by Sugano et. al (1991), a specimen (J4-O) with  $\rho_s = 1.1\%$ ,  $BI = 1.6$  suffered a joint shear failure and showed strains in the joint hoops that continued to increase as the specimen approached failure. However, the hoops never reached yield. Sugano et al. concluded that the hoops did not function effectively due to the failure of concrete struts in the joint.

Joh et al. (1991a), in their experimental research involving six specimens, noticed that in the specimen with the lowest  $\rho_s$  value (LH;  $\rho_s = 0.3\%$ ) only a few wide diagonal cracks existed in the joint region when the ultimate strength of the specimen was reached. Conversely, shear cracks in the specimens became smaller and more dispersed at ultimate as the value of  $\rho_s$  was increased (up to a value of about 1% in specimen HH). The values of  $\rho_s$ , and the respective crack patterns, affected the behavior of the specimens, as proven

by the shapes of the hysteresis loops. The hysteresis loops for the specimens exhibited more pinched shapes, as values of  $\rho_s$  went from high to low. Figure 21 shows the normalized hysteresis loops, one from an elastic cycle and one from the maximum-strength cycle, for the specimens HH and LH. The "maximum strength cycle" loop for specimen HH is spindle-shaped (preferred), while the same loop for specimen LH is flattened (undesirable). Since the details for both of the specimens were identical, except for the values of  $\rho_s$ , the differences in the joint crack patterns and in the shapes of the hysteresis loops must be attributed to the values of  $\rho_s$  that were used.

### 3.6.5 Other Factors That Affect Shear Transfer

The strength of the concrete used in the joint, the cross-sectional dimensions of the members, the deformation of the members, and the amount of column axial load also influence B-C joint shear transfer.

#### Joint Concrete Compressive Strength

Some researchers (Otani 1991, Sugano et al. 1991) have found that when B-C subassemblages experienced joint shear failures the joint shear strength was heavily dependent on the value of  $f'_c$ .

#### Member Cross-Sectional Dimensions

Meinheit et al. (1981) found no trends related to the variation of the joint aspect ratio (for  $0.72 \leq d_c/h_b \leq 1.0$ ) in their experimental tests. However, Otani (1991) noted that when  $d_c/h_b \leq 0.5$  the shear resistance of the joint decreases. This scenario also produces the undesirable "strong beam-weak column" behavior.

Paulay (1989) claims that the width of the beam can be greater than that of the column, as long as most of the beam bars pass through the column. On the other hand, Paulay (1984) noted that when the width of the column gets much larger than that of the beam, the interaction of the beam with the column will not be fully effective, since neither the concrete nor the bars that are far from the vertical faces of the beam will participate efficiently in resisting the beam moments. Experimental research by Leon et al. (1986) corroborates Paulay's (1984) findings.

#### Member Deformation

Experimental work done by Joh et al. (1991b) suggests that the more the joint shear capacity of a specimen exceeds the joint shear required to develop plastic hinges in the beams, the larger the ductility capacity of the specimen will be.

#### Column Axial Load

Currently there seems to be little consensus regarding the effects of column axial compressive load on B-C joint shear transfer. The lack of agreement stems from the fact that column axial compressive load may interact with other aspects of joint shear transfer (e.g., joint shear stress demand, bar bond, joint reinforcement, etc.). With one exception (Pantazopoulou et al. 1992), none of the work reviewed indicates that larger column axial compressive load is detrimental to B-C joint shear transfer. Paulay (1986, 1989) believes that if the axial load becomes too small, then there is a detrimental effect on joint shear transfer. Fujii et al. (1991), Meinheit et al. (1981), and Jirsa et al. (1975) believe that the level of axial load has no influence on the shear capacity of a joint. Bonnaci et al. (1993) found that the effect of column axial load on joint shear transfer was inconclusive. Leon et al. (1986) noticed that the difference in joint shear capacity of specimens with and without

axial load was negligible. Whether or not joint shear capacity or joint shear transfer is helped or hindered by the presence of column axial compressive load, most of the researchers agree that increased column axial load increases joint stiffness, increases the joint shear corresponding to first cracking, and decreases cracking and hoop strains. All of these effects are beneficial.

Thus far, the review of the topic of reverse-cyclically loaded B-C joints has focused primarily on the transfer of shear in B-C joints and on the ability of B-C joints to influence frame/subassemblage performance. In the last portion of this review, attention will be given the development of a semi-empirical method for the prediction of B-C joint performance.

### **3.6.6 An Empirical Method for Prediction of B-C Joint Performance**

Given the large body of B-C joint subassemblage test results available, it is common for researchers to incorporate as many of the results as possible in empirical relations. One such method is developed here: the bond index versus the joint volumetric hoop ratio (%),  $BI - \rho_s$ , graph. From the review of the literature presented in this work, it is expected that the performance of joints can largely be predicted if the values of  $BI$  and  $\rho_s$  are known for a given specimen. The accuracy of this method will be shown to be dependent on the drifts to which a given subassemblage is cycled to.

The application of the  $BI$  (Equation 5, Sec. 3.6.3, "Criteria for Bond for Seismic Performance") and  $\rho_s$  (Equation 7, Sec. 3.6.4, "Specific Amounts of Joint Reinforcement") to a large body of test results was performed by Bonnaci et al. (1993), where these parameters, along with several others, were tabulated for a battery of 86 subassemblage test results. Figure 22 is a plot of the  $BI$  and  $\rho_s$  values from many of the 86 test specimens. Additionally, pairs of values taken from other sources are plotted. In keeping within the constraints of this work, the only data used were those from research

where the specimens consisted of planar B-C subassemblages (i.e., no slabs or transverse beams), and where beam hinges were not restricted to form away from the joint faces (i.e., no "hinge-relocation" specimens). The abbreviations in the legend describe the mode of specimen failure and are defined as follows:

- S. F. — joint shear failure (detected by yielding of the joint hoops),
  - B. H. — beam hinging,
  - B. H., S. F. — beam hinge(s) developed first, then joint shear failure occurred,
  - B. H., A. F. — beam hinge(s) developed first, then anchorage failure occurred,
- the rest of the abbreviations are similar.

The graph, with a few exceptions, supports two of the limits suggested for values of BI and  $\rho_s$ . In Section 3.6.3, "Criteria for Bond for Seismic Performance", Bonacci et al. (1993) proposed the limit  $BI \leq 1.7$  for joints with Gr 60 bars. Only one specimen (the "B. H., A. F." specimen) suffered an anchorage failure despite being below the BI limit. However, the specimen had a  $BI = 1.62$ , which is just below the limit. With respect to value of  $\rho_s$ , in Section 3.6.4, "Specific Amounts of Joint Reinforcement", Kitayama et al. (1991) implied that joint shear failures could be prevented if the value of  $\rho_s \geq 0.5\%$ . Only one specimen that was in accordance with this  $\rho_s$  limit, and had a value of  $BI \leq 1.7$ , suffered solely from a joint shear failure (one of the "S. F." specimens). However, the value of  $\rho_s$  was 0.5% for this specimen, which is right at the limit. There are five "B. H., S. F." specimens that met both limits, yet still suffered joint shear failures following beam hinging. Further investigation of the five specimens indicates that they all performed to drifts in excess of 4% prior to experiencing joint shear failures. All of the rest of the plotted points that meet the BI and  $\rho_s$  limits represent subassemblages that failed in the preferable beam-hinging (B. H.) mode. Thus, use of Figure 22 with the limits  $BI \leq 1.7$  and  $\rho_s \geq 0.5\%$ , seems reasonable for the prediction of subassemblage joint performance,

with respect to ensuring the "B. H." failure mode, provided that specimens are not cycled to unreasonably large drifts.

This concludes the summary of the literature that was reviewed concerning B-C joints. As mentioned earlier, APPENDIX A contains additional detail on some of the issues that were covered here. Next, the results of a literature review on poorly confined column lap splices are presented.

### **3.7 Poorly Confined Column Lap Splices**

In what follows, the behavior of poorly confined lap splices under conditions of reversed cyclic loading is considered. First, flexural behavior is reviewed. This is followed by a discussion on the behavior with shear. It is now commonly accepted that lap splices should not be used in regions where flexural hinges are expected to form because such splices have proven to have unreliable ductility capacity. Nevertheless, lap splices in older structures occur in regions of high moment. Thus, the emphasis herein is on poorly confined lap splices in column regions subjected to inelastic demands.

#### **3.7.1 Flexure**

##### The Effect of Poor Confinement

The experimental and analytical research done by Priestley (1991), indicates that lap splices of column bars above a B-C joint can be considered "unlikely to be adequately confined" if the hoops consist of #4 bars spaced at 304.8 mm (Fig. 23). The reason being is that the amount of confinement stress afforded by such detailing will be insufficient to develop inelastic deformation capacity in, or perhaps even the yield strength of, the lap splice.

According to Priestley (1991), test results indicate that the clamping pressure provided by detailing shown in Figure 23 is usually not adequate to prevent anchorage failure of the bars. The progression of the loss of bar anchorage is as follows. First, vertical cracks develop parallel to the column bars. Then "fracture surfaces" ("Section A-A" in the fig.) develop as a result of the dilation caused by the vertical cracks. Next, concrete spalls away from the fracture surfaces and separation can occur between the column bar and the concrete that is attached to the starter bar. Under the conditions described, anchorage failures may result at less than the flexural strength of the lap splice. Even if the yield strength of the lap-spliced bars developed, the ductility can be expected to be small.

The results from the experimental research by Paulay (1982) and Lukose et al. (1982) agree with Priestley's findings with respect to the importance of hoops to the integrity of lap splices. Additionally, Lukose et al. found that if the portions of columns just outside of the plastic hinge regions are poorly confined, then the rate of bond deterioration and the propagation of deterioration will increase.

Improper detailing of the ends of the hoops can increase the possibility of anchorage failure. Once the fracture surfaces spall, the separation of the column bar from the concrete attached to the starter bar is likely unless the hoops continue to provide confinement. Priestley et al. (1984) note that hoops that have lapped ends can be expected to unwind when the cover concrete spalls. Therefore, they suggest that hoop ends be welded together or anchored into the core concrete.

With respect to detailing of the bars, Priestley et al. (1984) noted that four of the five specimens that they tested that did not experience anchorage failures had radial lap splices; the starter bars were straight and the spliced bars were bent in toward the center of the column. The specimen that suffered the anchorage failure had a circumferential lap splice where the starter bars and the spliced bars were placed side by side.

## Flexural Strength and Ductility

Priestley developed a model that he proposes describes the flexural strength and ductility of columns with lap splices (Fig. 24). Each of the four lines in the figure represents a different column (the initial stiffnesses of each of the columns are the same):

- 1.) Line 1 represents a well-confined column section without a lap splice. The response of the column is modeled in a bi-linear fashion. At a displacement ductility ( $\mu$ ) of unity, the value of the flexural strength ( $M_n$ ) is reached. At " $\mu_1$ ", the overstrength moment capacity (" $M_o$ ") is attained. Due to the good confinement and due to strain-hardening of the bars,  $M_o > M_n$ .
- 2.) Line 2 represents a poorly-confined column section without a lap splice. The value of  $M_n$  is obtained at a value of  $\mu = 1$ , but there is no overstrength and the maximum ductility occurs at " $\mu_2$ " (the ultimate value of the extreme fiber concrete compressive strain,  $\epsilon_{cu}$ , was assumed to be 0.005 in the determination of the value of  $\mu_2$ ). Values of  $\mu_2 = 3$  are typical. Once the maximum ductility is reached, just as in the case of the column section represented by line 1, the strength of the section quickly diminishes because the concrete core crushes and the bars buckle.
- 3.) Line 3 represents a column section that has a lap splice. Here, the lap splice is not designed to achieve the value of  $M_n$ . At a value of  $\mu < 1$ , the strength begins to degrade from the maximum strength (" $M_s$ ") that was achieved. The degradation continues until the residual strength (" $M_r$ ") becomes effective at a value of  $\mu = 3$ . The reason that there is residual strength is that the splice deteriorated prior to crushing of the concrete core or to buckling of the bars.
- 4.) Line 4 represents a column section that has a lap splice. However, in this situation the value of  $M_n$  is reached. At " $\mu_4$ " ( $\epsilon_{cu} = 0.002$ ), degradation begins. The degradation ceases when the value of  $M_r$  is attained.

Each value of  $M_r$  was determined by taking the product of the axial load and the lever arm between the axial load and the centroid of the compression zone of the confined column core. Priestley claims that " $M_r$ " typically occurs at values of  $\mu = 3$ .

### 3.7.2 Shear

#### The Effect of Poor Confinement

According to Priestley (1991), column sections that are expected to experience demands of  $\mu \geq 4$  will receive little if any assistance from the concrete in resisting shear. The loss of aggregate interlock with the development of wide flexural cracks will cause most of the shear force to be carried by the hoops. This condition is exacerbated if axial loads are small, thereby reducing the efficiency of compression zone shear transfer. Thus, the inference can be made that in poorly confined lap splice regions with small axial loads the degradation of shear strength will possibly begin at values of  $\mu < 4$ . Priestley argues that as a result of degradation in shear strength, the flexural ductility capacity of a section might be less than anticipated (in Sec. 3.7.1). Additionally, once the shear strength is attained, the structural response will degrade rapidly.

Lukose et al. (1982) found that if the portion of column just outside of the plastic hinge region is not well confined then failure can occur. The failure can take the form of cover splitting along the splice or the form of localized deterioration at the section just beyond the splice.

Table 1 Characteristics of double-column bents with rectangular columns  
(DRC category).

bent characteristics	
age (yr.)	1925 - 1967
height (m)	11 - 42
strut length (m)	4 - 15
strut location	grade - above mid-height
column characteristics	
dimensions (mm, $d_c \times b_c$ )	610 x 762 - 2362 x 2134
bars	8-#6 - 40-#14
hoops (spacing in mm)	#2 @ 305 - #5 @ 457
lap splice	30 - $41d_b$
axial load (MN, $f'_c$ in MPa)	0.015 - $0.085f'_cA_g$
strut characteristics	
dimensions (mm, $b_b \times h_b$ )	305 x 457 - 1219 x 3658
main bars	2-#6 - 14-#18
intermediate bars	none - 4 sets of 2-#5
stirrups (spacing in mm)	#2 @ 610 - #5 @ 140
material properties	
steel	Gr 40
concrete ( $f'_c$ in MPa)	21 - 28

Table 2 Characteristics of multiple-column bents with rectangular columns  
(MRC Category).

bent characteristics	
age (yr.)	1926 - 1969 (1945)
height (m)	6 - 17 (12)
strut length (m)	1.7 - 4 (2.5)
strut location	grade - above mid-height (mid-height)
column characteristics	
dimensions (mm, $d_c \times b_c$ )	508 x 508 - 1069 x 1069 (508 x 914)
bars	8-#7 - 28-1 $\frac{1}{4}$ in <sup>2</sup> (10-1 in <sup>2</sup> )
hoops (spacing in mm)	1 $\frac{1}{4}$ in <sup>2</sup> @ 457 - 1 $\frac{1}{2}$ in <sup>2</sup> @ 305 (#3 @ 305)
lap splice	20 - 50 $d_b$ (34)
axial load (MN, $f'_c$ in MPa)	0.02 - 0.1 $f'_c A_g$ (0.05)
strut characteristics	
dimensions (mm, $b_b \times h_b$ )	305 x 457 - 610 x 914 (381 x 762)
main bars	2-#6 - 4-#1 $\frac{1}{4}$ in <sup>2</sup> (3-1 in <sup>2</sup> )
intermediate bars	none - 4 sets of 2-#5
stirrups (spacing in mm)	#3 @ 457 - #5 @ 457 (#4 @ 305)
material properties	
steel	Gr 33 - 40 (40)
concrete ( $f'_c$ in MPa)	21 - 28 (25)

Table 3 Characteristics of double-column bents with circular columns  
(DCC Category).

<b>bent characteristics</b>	
age (yr.)	1965
height (m)	13 - 22
strut length (m)	4.5 - 8.25
strut location	below mid-height - mid-height
<hr/>	
<b>column characteristics</b>	
dimensions (mm, dia.)	1219 - 1524
bars	12-#11 - 18-#11
hoops (spacing in mm)	#4 @ 305
lap splice	42.5d <sub>b</sub>
axial load (MN, f' <sub>c</sub> in MPa)	0.01 - 0.02f' <sub>c</sub> A <sub>g</sub>
<hr/>	
<b>strut characteristics</b>	
dimensions (mm, b <sub>b</sub> x h <sub>b</sub> )	762 x 1219 - 914 x 1219
main bars	4-#10 - 5-#11
intermediate bars	2-#6
stirrups (spacing in mm)	#5 @ 457
<hr/>	
<b>material properties</b>	
steel	Gr 40
concrete (f' <sub>c</sub> in MPa)	28

Table 4 Characteristics of multiple-column bents with circular columns  
(MCC Category).

bent characteristics	
age (yr.)	1963, 1965
height (m)	4.5 - 16
strut length (m)	4 - 5
strut location	grade - above mid-height
column characteristics	
dimensions (mm, dia.)	914 - 1219
bars	8-#10 - 12-#11
hoops (spacing in mm)	#4 @ 305
lap splice	38 - 48d <sub>b</sub>
axial load (MN, f' <sub>c</sub> in MPa)	0.03 - 0.05f' <sub>c</sub> A <sub>g</sub>
strut characteristics	
dimensions (mm, b <sub>b</sub> x h <sub>b</sub> )	762 x 1219 - 762 x 1524
main bars	4-#9 - 4-#11
intermediate bars	2-#5 - 2-#6
stirrups (spacing in mm)	#5@457
material properties	
steel	Gr 40
concrete (f' <sub>c</sub> in MPa)	28

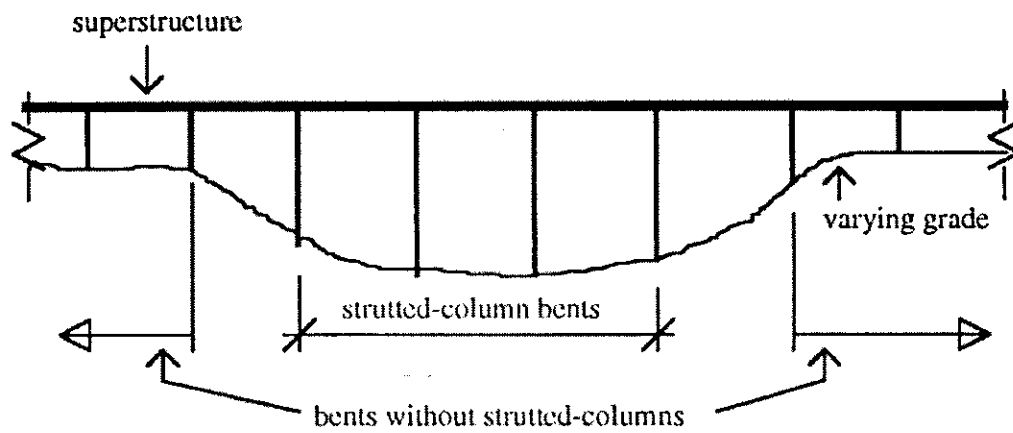


Figure 2 Typical locations of struted-column bents in a bridge with only a portion of the bents containing struts.

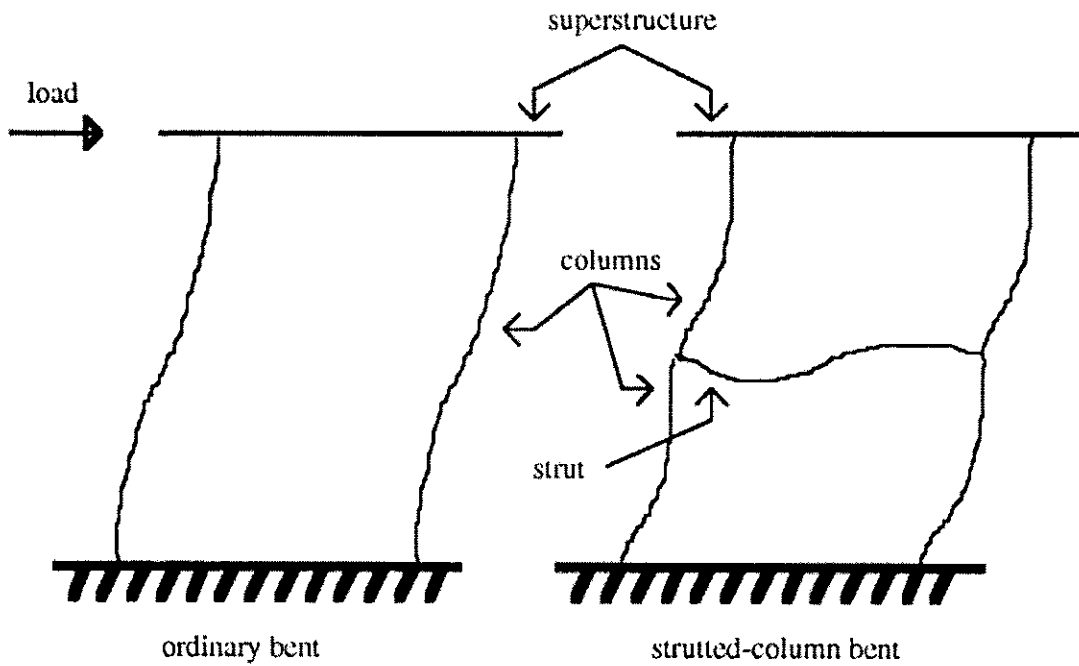
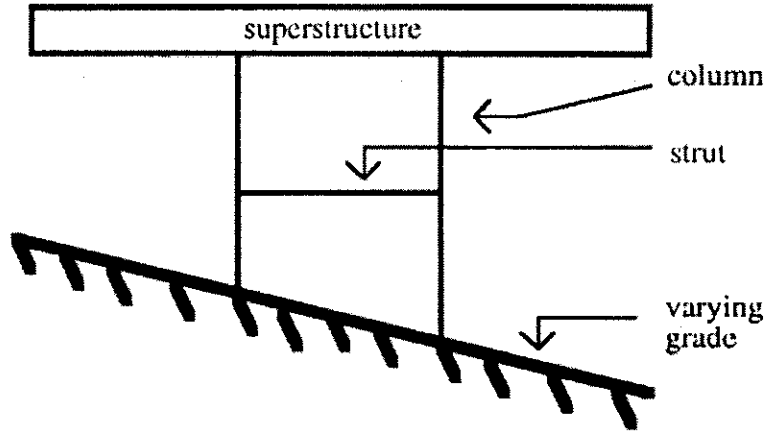
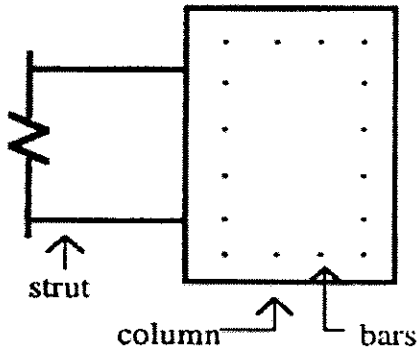


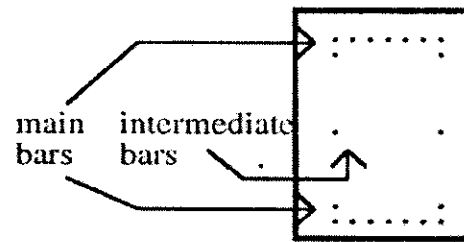
Figure 3 The effect of the strut on column deformation under transverse lateral loading.



a) Transverse bent elevation



b) Typical interior column cross-section



c) Typical Strut cross-section

Figure 4 Typical struted-column bent and member cross-sections for the double-column bents with rectangular columns.

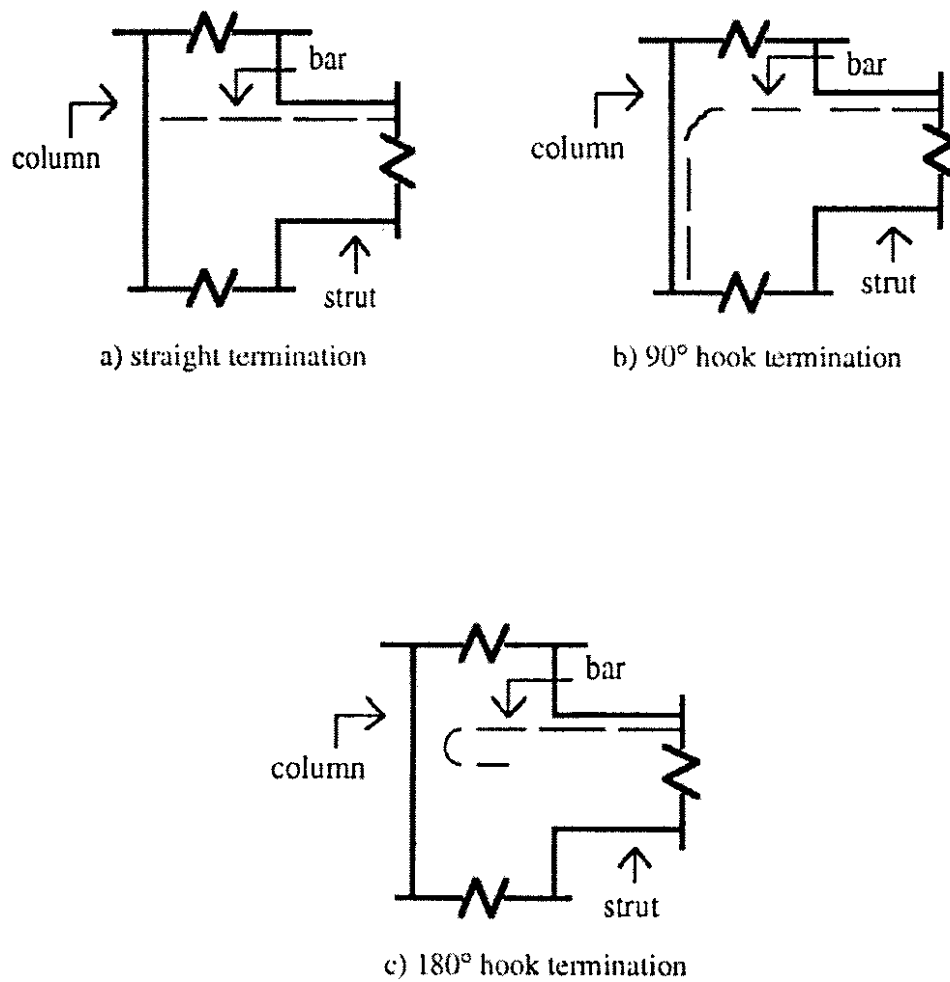
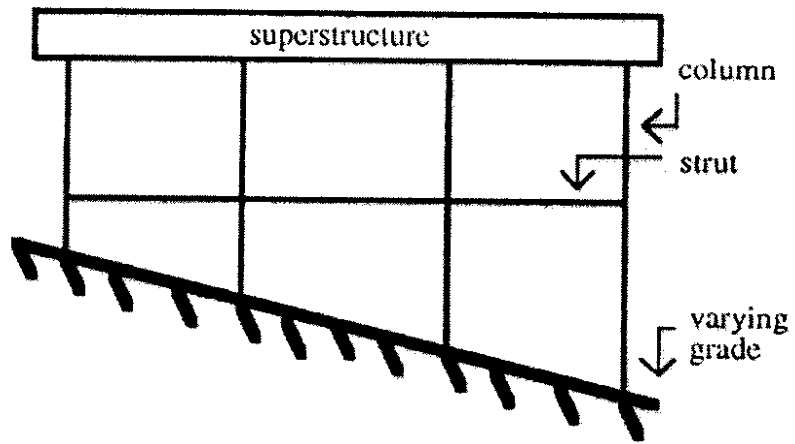
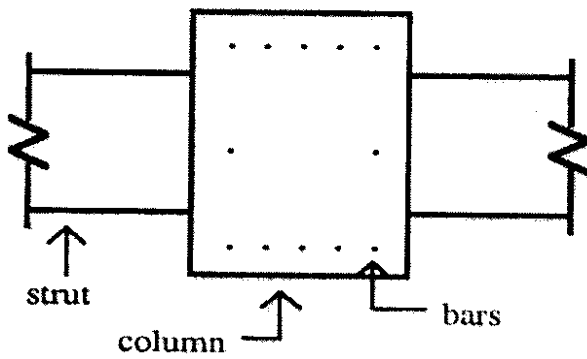


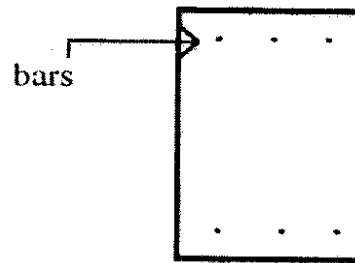
Figure 5 Strut bar termination details for the double-column bents with rectangular columns.



a) Transverse bent elevation



b) Typical interior column cross-section



c) Typical Strut cross-section

Figure 6 Typical struted-column bent and member cross-sections for the multiple-column bents with rectangular columns.

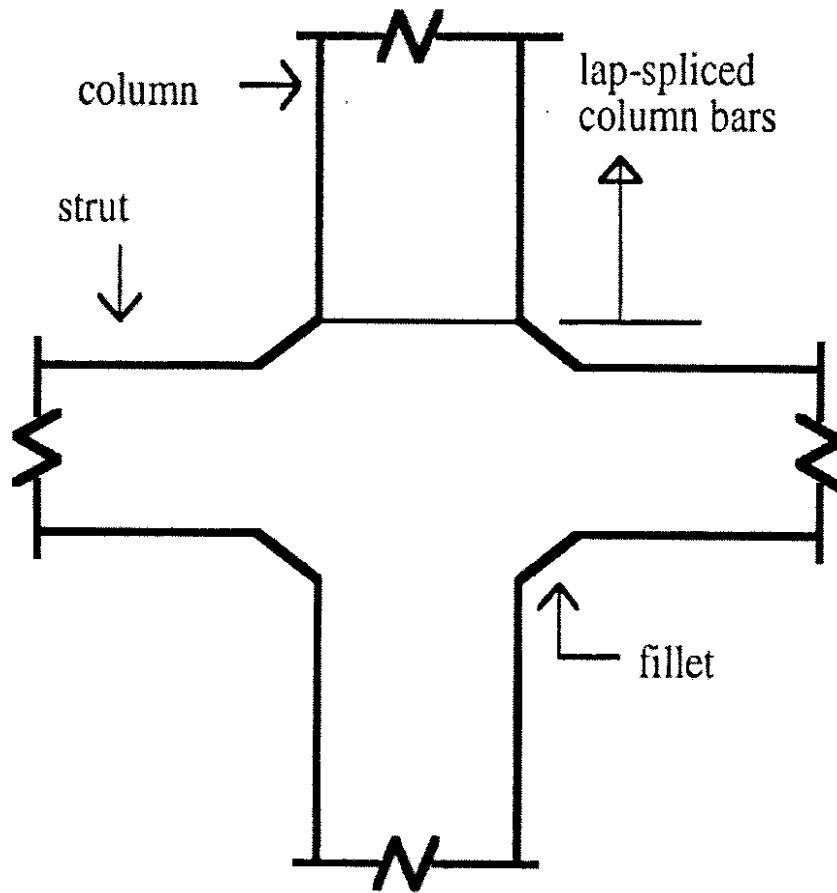
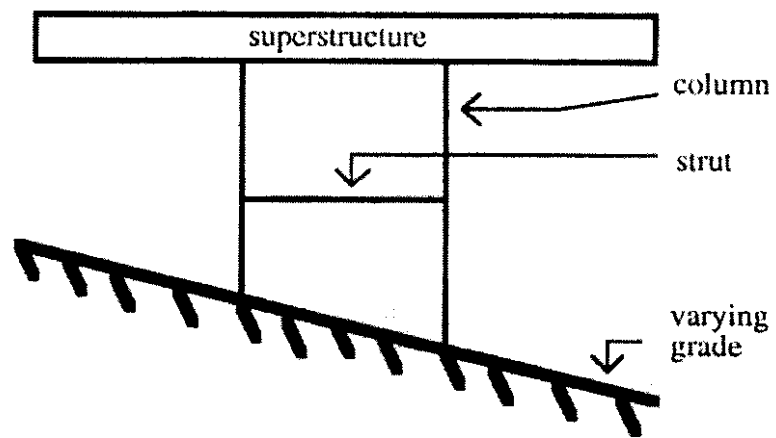
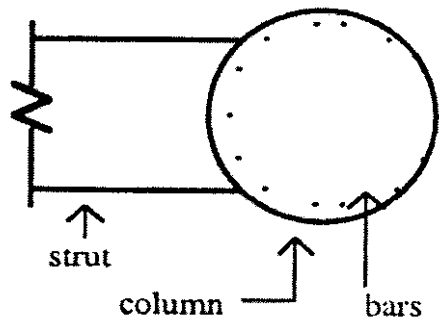


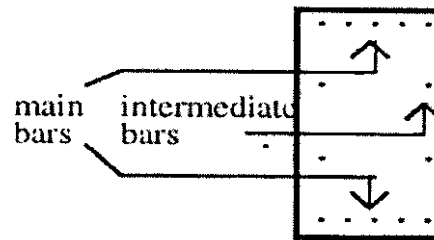
Figure 7 Typical details for the multiple-column bents with rectangular columns.



a) Transverse bent elevation

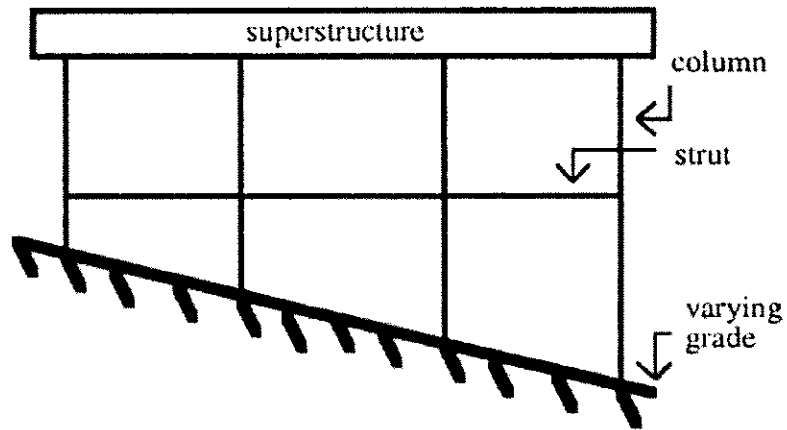


b) Typical interior column cross-section

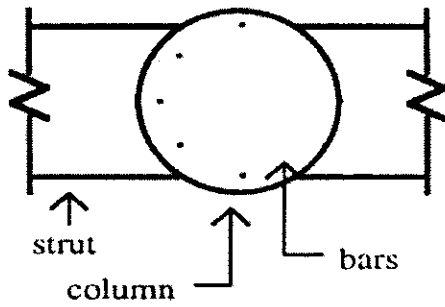


c) Typical Strut cross-section

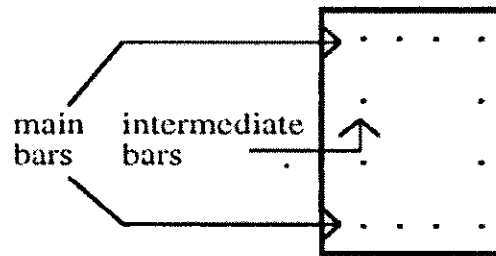
Figure 8 Typical struted-column bent and member cross-sections for the double-column bents with circular columns.



a) Transverse bent elevation



b) Typical interior column cross-section



c) Typical Strut cross-section

Figure 9 Typical strutted-column bent and member cross-sections for the multiple-column bents with circular columns.

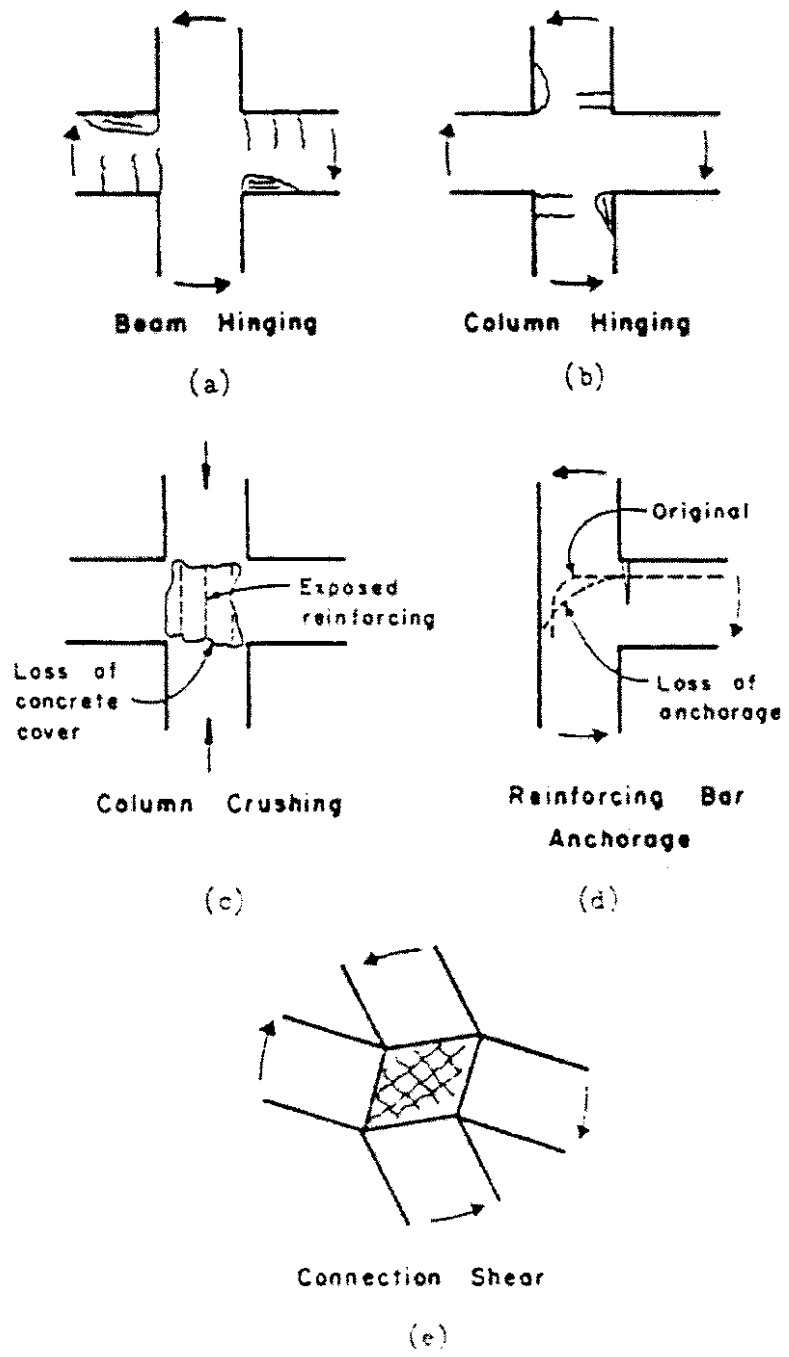


Figure 10 Potential failure modes of B-C joint regions (from Meinheit et al. 1981).

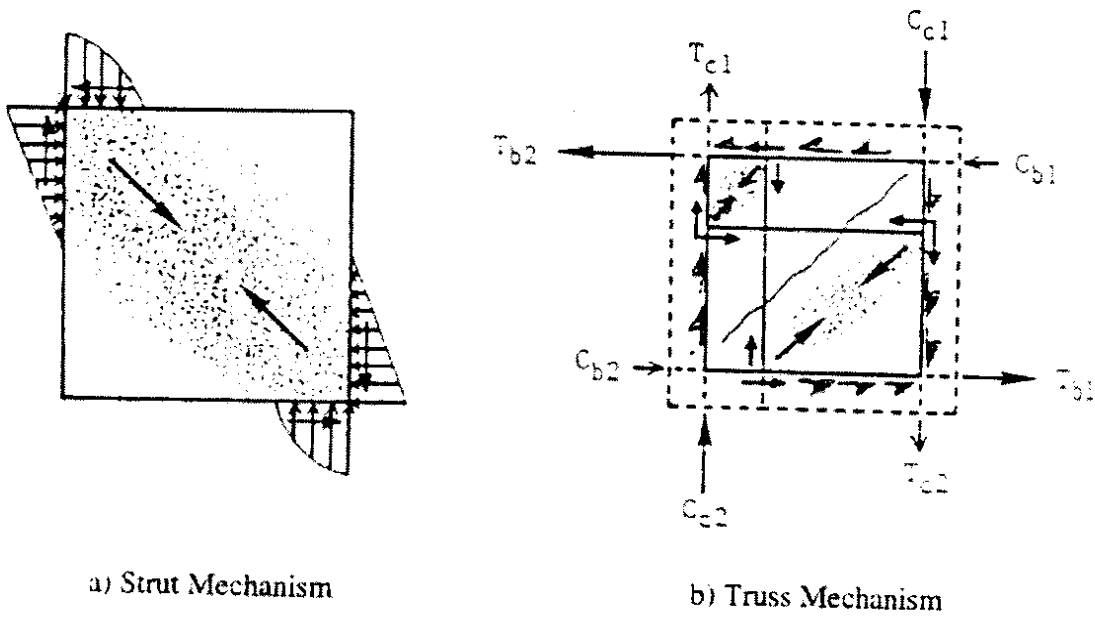
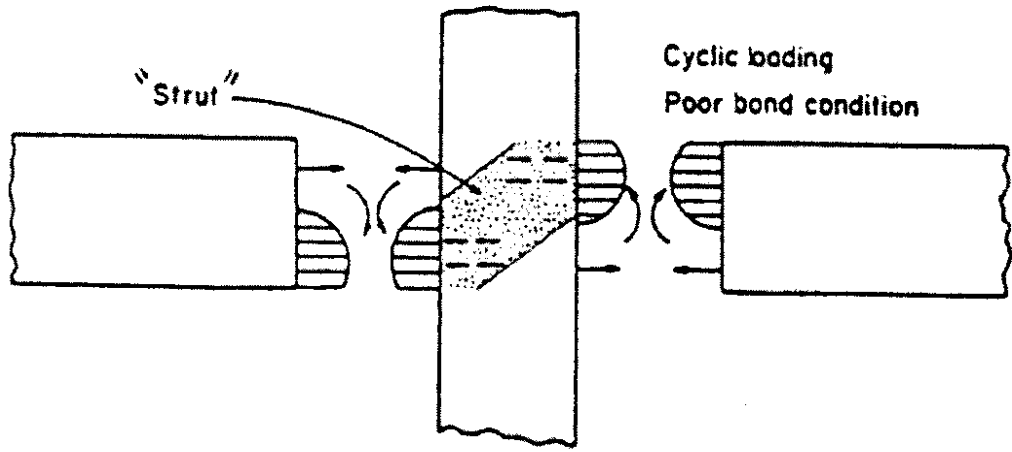
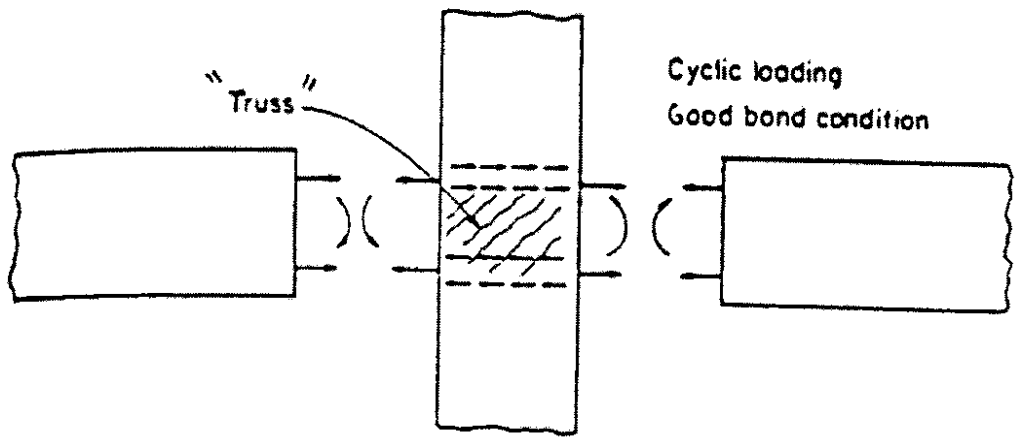


Figure 11 Mechanisms of seismic shear transfer in B-C joints (from Kitayama et al. 1991).

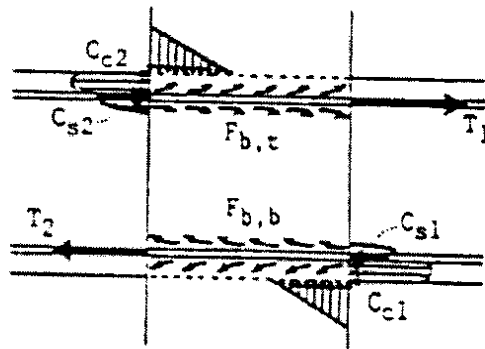


(a) Shear transfer with poor bond of beam bars



(b) Shear transfer with good bond of beam bars

Figure 12 Shear transfer after first yield of beam bars (from Leon 1990).



$$T1 = Cc1 + Csl$$

$$T2 = Cc2 + Cs2$$

$$F_{b,t} = T1 + Cs2 \text{ (Bond Force along Top Bars)}$$

$$F_{b,b} = T2 - Csl \text{ (Bond Force along Bottom Bars)}$$

Figure 13 "Bond forces along beam bars within a joint" (from Kitayama et al. 1991).

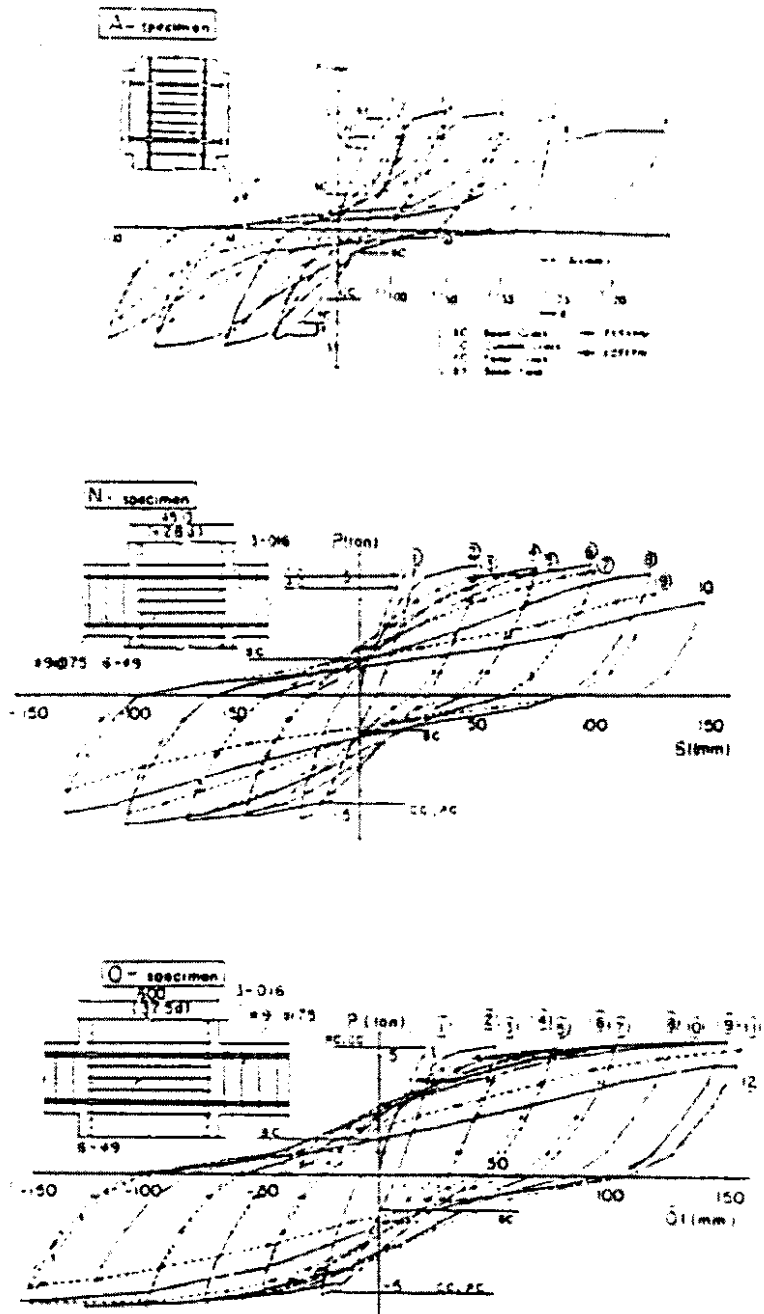


Figure 14 "Beam shear force -- story drift curves for selected specimens" (from Kaku et al. 1991).

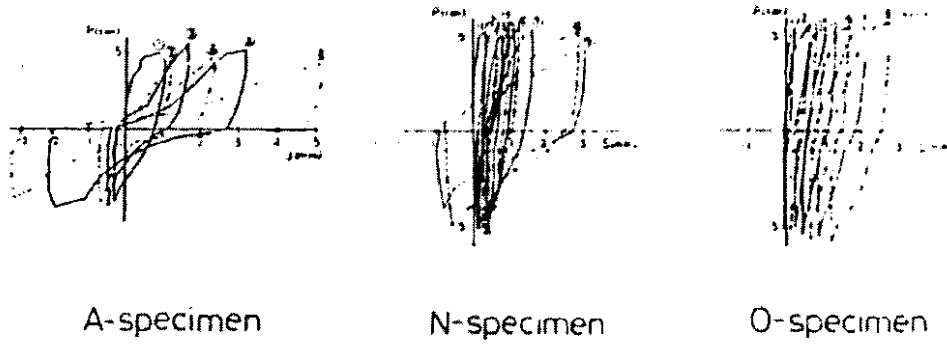


Figure 15 "Beam shear force -- slip curves for selected specimens" (from Kaku et al. 1991).

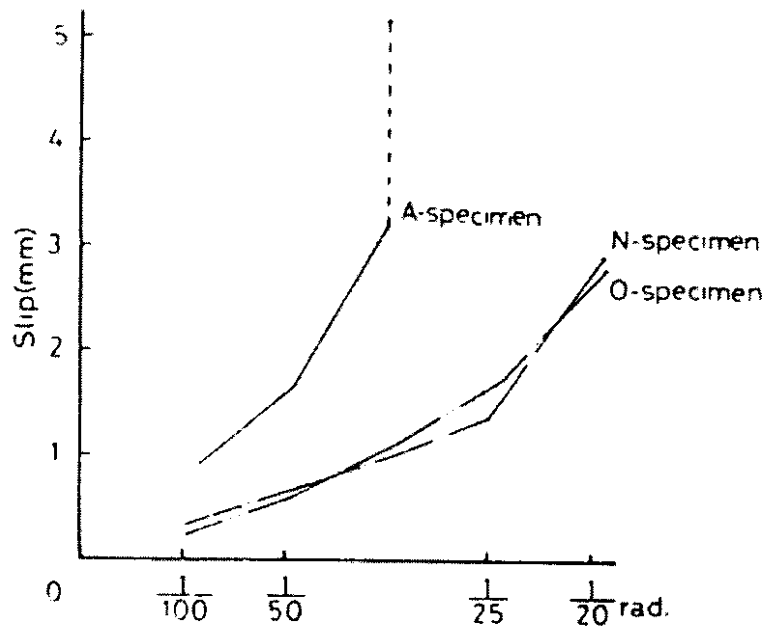


Figure 16 "Slip -- story drift curves for selected specimens" (from Kaku et al. 1991).

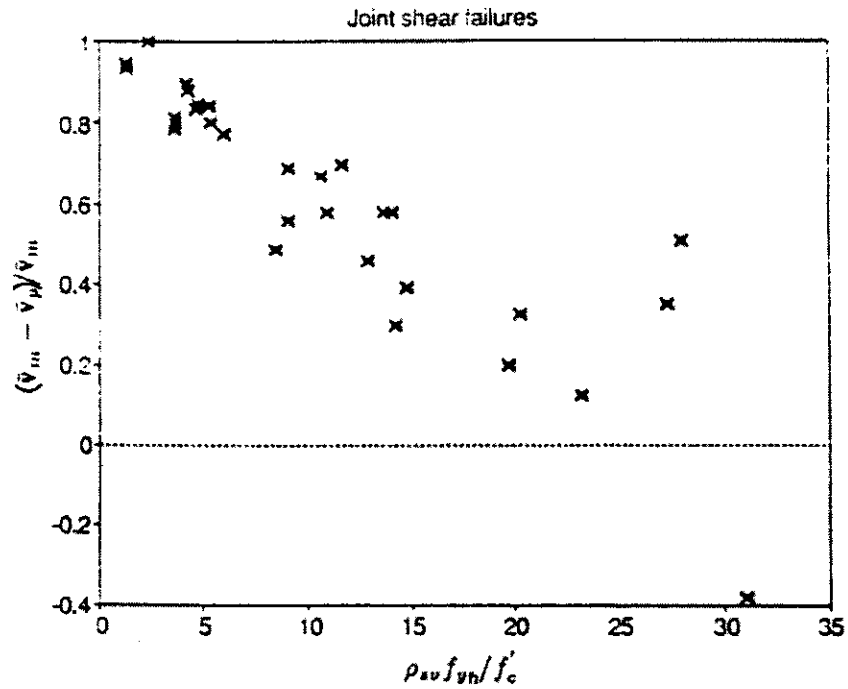


Figure 17 "Influence of confinement on contribution of concrete to overall joint shear strength" (from Bonnaci et al. 1993).

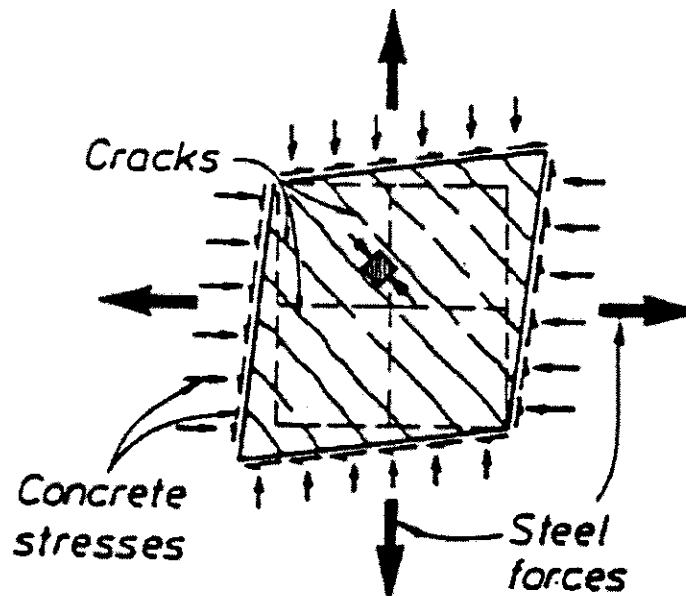


Figure 18 Joint shear deformation/mechanics (from Paulay 1989).

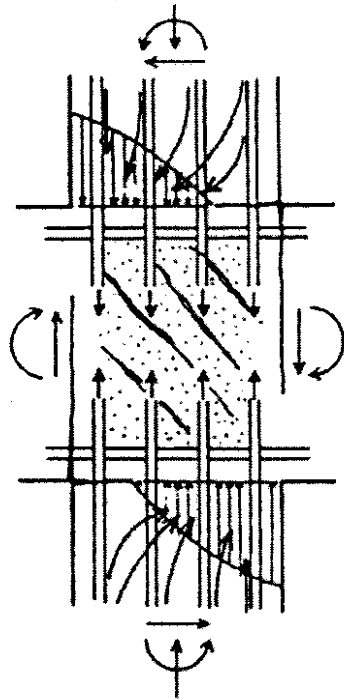


Figure 19 Column bar tension inside of a B-C joint (from Fujii et al. 1991).

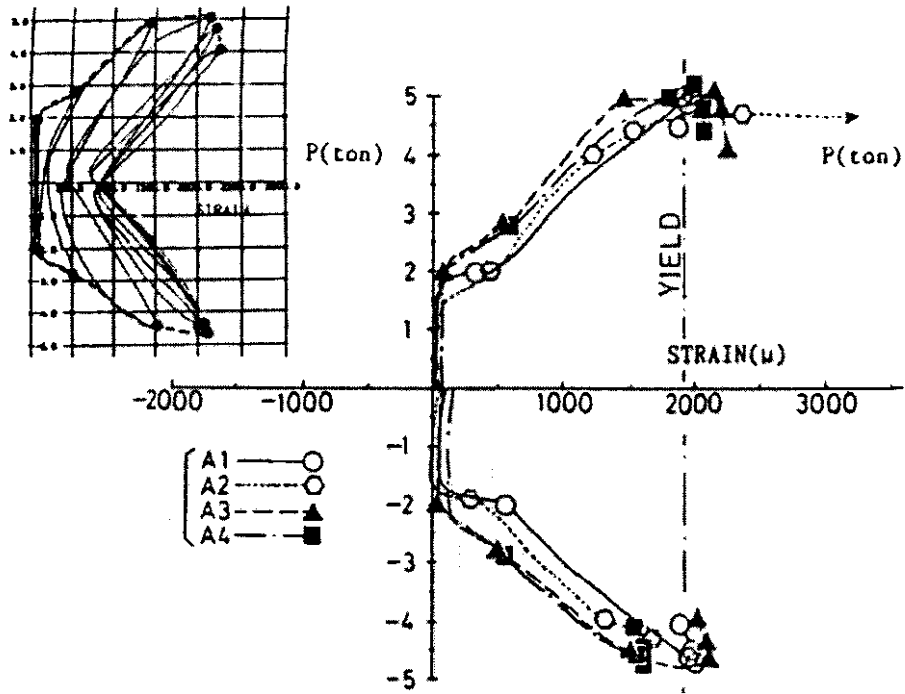


Figure 20 Development of strain in the B-C joint hoops (from Fujii et al. 1991).

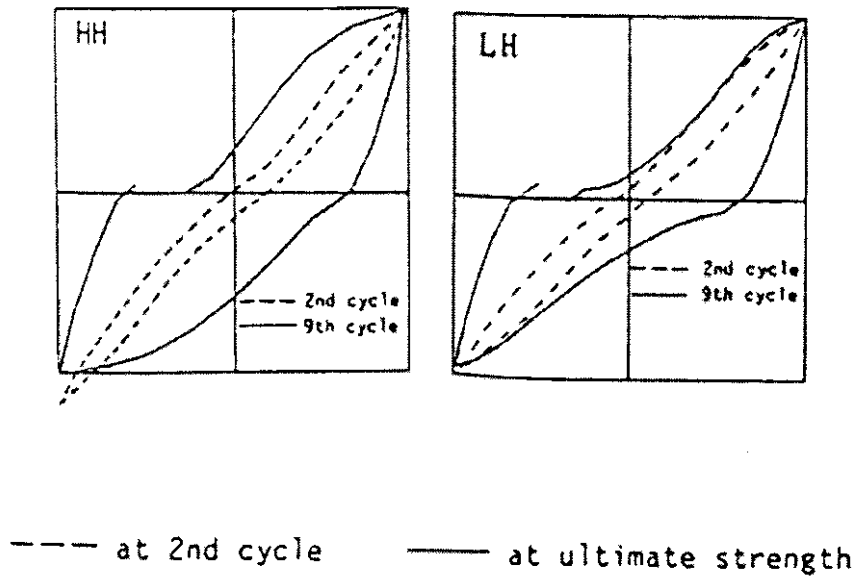


Figure 21 "Normalized hysteresis loops in the relations of column shear -- story drift angle" (from Joh et al. 1991a).

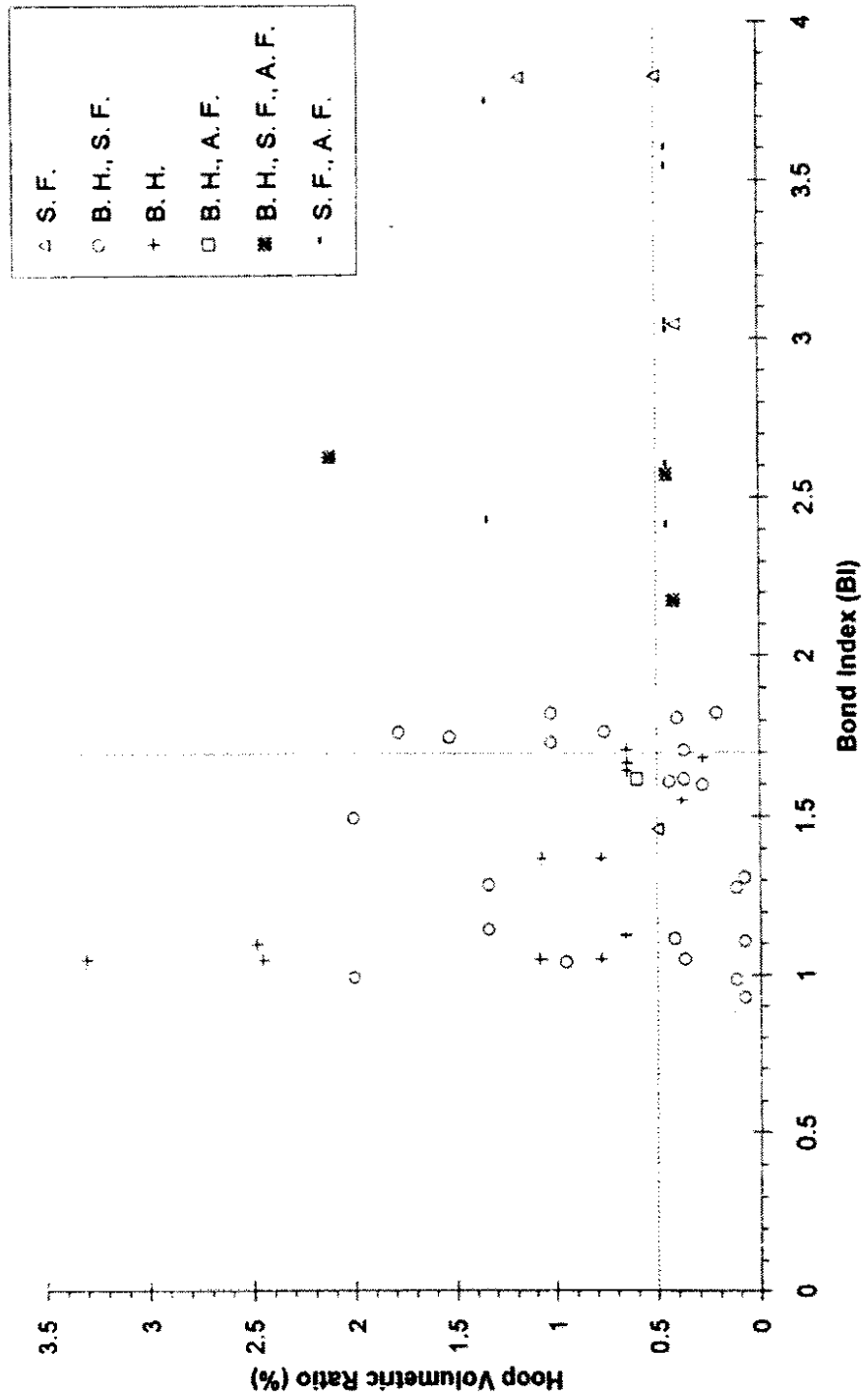
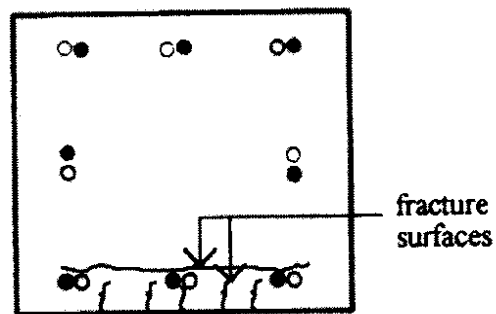
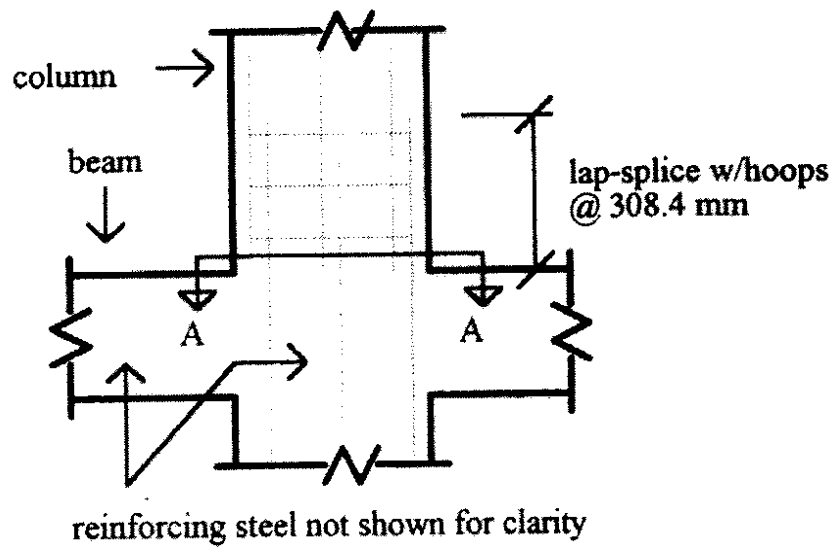


Figure 22 Bond index (BI) versus volumetric hoop ratio ( $\rho_s$ , %).



Section A-A

Figure 23 Column bar lap splice above a B-C joint.

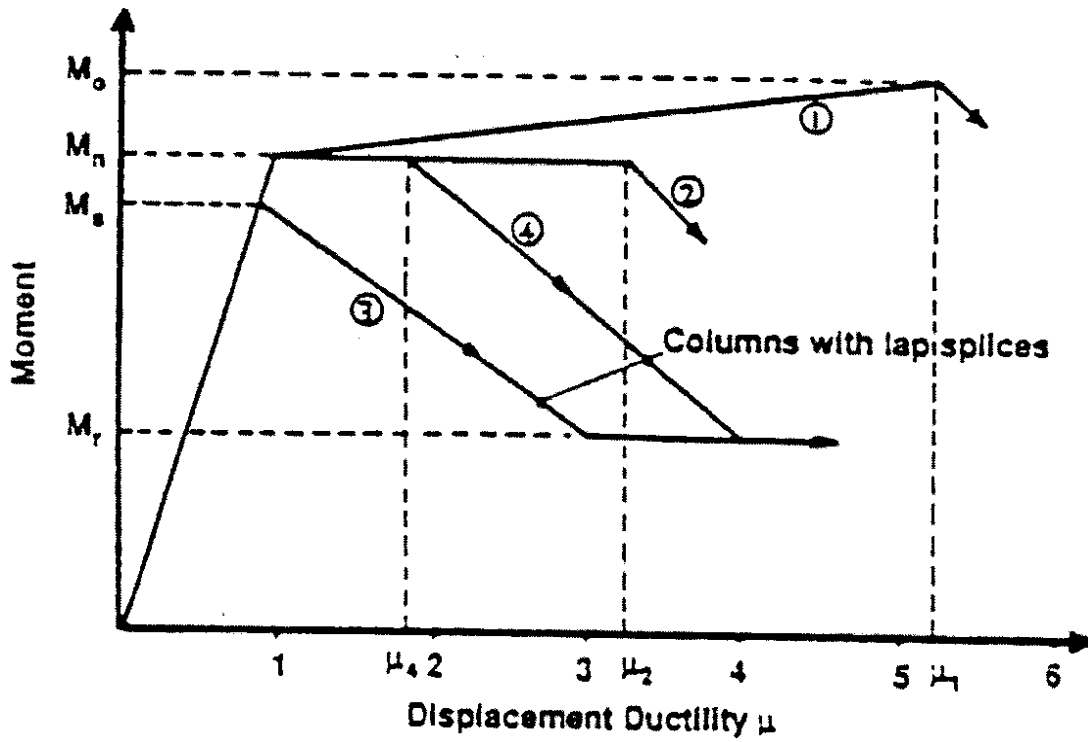


Figure 24 "Flexural strength and ductility of sections" (from Priestley 1991).

## **CHAPTER 4**

### **RESEARCH APPROACH**

In this chapter the inventory of bridges containing strutted-column bents is evaluated. The criteria used in this evaluation and the results of the evaluation are presented. Additionally, the selection and the design of the prototype subassemblages are discussed. Finally, the experimental tests are considered, including the design of the specimens, the materials used in the specimens, the construction of the specimens, the instrumentation used for the specimens, the test set-up, and the testing procedures.

#### **4.1 Evaluation of the Inventory**

In order to fulfill objectives "2.)" and "3.)" (Chap. 3, Sec. 3.2.4) it was necessary to supplement the information obtained from objective "1.)". This was done by evaluating the bridge inventory using several criteria. Herein, the criteria are reviewed and the results from the application of the criteria to each of the four bent categories (DRC, MRC, DCC, and MCC) are presented. In what follows, the tributary portion of a superstructure for a given bent shall be considered a part of the bent.

##### **4.1.1 Criteria**

The criteria that were used to evaluate the bridge inventory were chosen on the basis of the background presented in Chapter 3:

- 1.) The ratios of the column and the strut flexural strengths were determined in order to assess which type of hinging mechanism could be expected in the bents (i.e., strong column-weak beam or weak column-strong beam). These criterion would also indicate

whether the struts or the columns would place demands associated with hinge formation on the B-C joints.

- 2.) The shear stress demands on the B-C joints were determined in accordance with the forces associated with strut hinging in order to have a benchmark for how severely the joints could be loaded.
- 3.) The shear stress demands on the struts were determined in accordance with the forces associated with strut hinging in order to compare with the strut shear stress capacities.
- 4.) The member bar anchorage details were reviewed in order to determine whether or not anchorage failures could be expected.
- 5.) The sequences of hinge formation were determined in order to find out which regions of the bents will have the greatest ductility demands.
- 6.) The transverse fundamental periods ( $T_n$ ) were estimated in order to assess relative spectral demands.

In many of the criteria, the concrete strength ( $f'_c$ ) was called for. The values of  $f'_c$  that were used were those values specified in the structural drawings. However, they were increased by fifty percent to account for the strength gain of the concrete with age (Priestley 1991).

### Flexural Strength Ratios

The ratios of the column and beam flexural strength capacities ( $M_{nc}/M_{nb}$  for exterior joints and  $\sum M_{nc}/\sum M_{nb}$  for interior joints) were computed based upon ultimate concrete compressive strain ( $\epsilon_{cu}$ ) values of 0.003. This value was used in order to have consistency in the ratio; a common value of  $\epsilon_{cu}$  was required for  $M_{nc}$  and  $M_{nb}$ . The shape of the moment-curvature relations ( $M-\phi$ ) for the columns tended to peak at values of  $\epsilon_c = 0.003$ , after which the curves "roll off" quite suddenly (Fig. 25).

### Joint Shear Stress Demands

The values of the joint shear stress demands ( $v_{jt}$ ) that were calculated are the maximum expected joint shear stress demands ( $v_{jt}^*$ ). The determination of values of  $v_{jt}^*$  were based on the formation of flexural plastic hinges in the struts (Figs. 26 and 27), since the flexural capacities of the columns ( $M_{nc}$ ) typically exceeded those of the struts ( $M_{nb}$ ). The struts were assumed to be located at mid-height for those cases where the actual strut location is above grade. Symbols used in Figures 26 and 27 are defined as follows:

- $M_{nb}$  = the amount of moment required to form a plastic hinge.
- $M_c$  = the moments in the column above and below the joint.  
 $M_c$  was assumed to be equal to  $M_{nb}/2$  in Figure 26, and  
 $M_c$  was assumed to be equal to  $(M_{nb1} + M_{nb2})/2$  in Figure 27.
- $V_c$  = the shears in the column above and below the joint =  $2M_c/l_c$ , where  
 $l_c = 1/2(\text{bent height}) - h_b$ .
- $P_c$  = the applied axial compressive column load.
- $A_s'$  = the total area of bars in the top of the strut.
- $A_s$  = the total area of bars in the bottom of the strut.
- $T_b$  =  $A_s'(1.25f_y)$ , where "1.25" accounts for strain hardening and possible overstrength of the bars.
- $C_{cb}$  = the resultant force from the concrete compressive stress block.
- $C_{sb}$  = the compressive steel force.

In Figures 26 and 27 it is assumed that  $C_{cb} + C_{sb} = C_b = T_b$

The joint shear at mid-depth ( $x-x$ ) of exterior joints (Fig. 26) is determined as follows:

$$V_{jt} = T_b - V_c \quad (\text{Equation } 8)$$

The joint shear at mid-depth (x-x) of interior joints (Fig. 27) is determined as follows:

$$V_{jt} = T_{b1} + C_{b2} - V_c \quad (\text{Equation 9})$$

The value of  $v_{jt}^*$  is then calculated in accordance with Equation 1 (Chap. 3, Sec. 3.6.2, "Applied Shear Stress"). What follows is the basis used to determine values of  $v_{jt}^*$  as described.

The struts were located at mid-height in those instances where the actual strut heights were above grade because:

- 1.) There were many instances where a given bridge had bents where the strut heights varied from bent to bent due to the changing grade elevation.
- 2.) There were many instances where the strut heights changed within a given bent due to changing grade elevations across the bent.
- 3.) The degree of fixity provided by the soil at grade was unknown since the soil is usually fill material, the degree of compaction of which was not recorded.

Given the variability in the strut locations and the uncertainty surrounding the restraint provided at the varying grade locations, the mid-height location for the strut was selected in order to obtain a reference for comparing  $v_{jt}^*$  from bridge to bridge. In addition, based on the mechanics involved, the strut location that yields the greatest value of  $v_{jt}^*$  is mid-height.

In each analysis the value of  $M_{nb}$  was determined by consideration of the  $M-\phi$  relation for the respective strut (Fig. 28). The criterion used for selecting a given value of  $M_{nb}$  was as follows:  $M_{b1} < M_{nb} < M_{b2}$ , where  $M_{b1}$  and  $M_{b2}$  are the amounts of moment at  $\phi_{b1}$  and  $\phi_{b2}$ , which correspond to values of  $\epsilon_{cb} = 0.004$ , and  $= 0.006$ , respectively. The reasons for selecting  $M_{nb}$  based upon  $0.004 < \epsilon_{cb} < 0.006$  were:

- 1.) For the typical lightly-reinforced strut analyzed, the  $M-\phi$  relationship is such that the value of  $M_{nb}$  is often reached after the bars have strain-hardened and the value of  $\epsilon_{cb}$  is

quite large (i.e.,  $0.004 < \epsilon_{cb} < 0.006^+$ ). In other words, the values of  $\epsilon_{cb}$  from first yield to the onset of strain hardening are often too small to presume the occurrence of plastic hinging (i.e.,  $\epsilon_{cub}$  is not reached until post-strain hardening).

2). It is commonly accepted that poorly confined sections can obtain  $\epsilon_{cu}$  values of  $0.005^+$  (Priestley 1991).

The values used for the effective joint area ( $A_{jt}$ ) in Equation 1 consisted of the confined cross-sectional areas of the columns. The values of  $A_{jt}$  were determined in this manner because it was assumed that by the time plastic hinges had formed in the beams there would be considerable cover spalling in the columns. The relative shapes of the  $M-\phi$  curves for the columns and struts (Fig. 25), together with the results from the bent hinge formation sequence analyses (Sec. 4.1.2, "The Bent Hinge Formation Sequences"), indicates that the moments in the columns are typically well in excess of their cracking moments by the time the struts reach  $M_{nb}$ .

In those instances where the struts were located at grade,  $v_{jt}^*$  was determined in a manner similar to that which has been described (i.e., the lower column was removed from Figs. 26 and 27). Note that in these cases the hinge will likely form in the column above the strut. However, the forces input to the joints in these analyses were those that would arise from hinge formation in the struts because this represents the worst scenario. The same methodology was employed in the rare instances where the struts were above grade and were stronger than the columns.

Vertical joint shear stress demands were not evaluated (Chap. 3, Sec. 3.6.2, "Applied Shear Stress").

#### Strut Shear Stress Demands

The values of the strut shear stress demands ( $v_b$ ) that were calculated are the maximum expected strut shear stresses ( $v_b^*$ ) when hinges form at both ends of the struts. Just as was done in determining values of  $v_{jt}^*$ ,  $v_b^*$  was based on  $M_{nb}$ , beginning with:

$$V_b = \frac{2M_{nb}}{l_s} \quad \text{(Equation 10)}$$

where:

$l_s$  = the strut clear span

The equation used to determine  $v_b^*$  was as follows:

$$v_b^* = \frac{V_b}{b_b d_{bm}} = \gamma \sqrt{f'_c} \quad \text{(Equation 11)}$$

where:

$\gamma$  = a constant =  $V_b / (b_b d_{bm} \sqrt{f'_c})$

$b_b$  = the strut width

$d_{bm}$  = the strut effective depth

and the other terms are as previously defined.

The values of  $v_b^*$  were compared with the strut shear capacities ( $v_{nb}$ ), where  $v_{nb}$  is equal to  $V_{nb} / (b_b d_{bm})$ . Values of  $V_{nb}$  were computed in accordance with ACI 318M-89:

$$V_{nb} = V_c + V_s = 0.17 \sqrt{f'_c} b_b d_{bm} + \frac{A_v f_y d_{bm}}{s} \quad \text{(Equation 12)}$$

where:

$V_c$  = the shear carried by the concrete

$V_s$  = the shear carried by the stirrups

$f'_c$  = the concrete strength in MPa

$s$  = the spacing of the strut stirrups

$A_v$  = the area of the strut stirrups within  $s$

and the other terms are as previously defined.

It should be noted that in the first term of Equation 12 the "0.17" factor has proven in static monotonic tests to be unconservative when the longitudinal reinforcement ratio of a beam ( $A'_s$  or  $A_s$  divided by  $b_b d_{bm}$ ) is less than approximately 1.2% (Ferguson 1979). Tables 1 - 4 indicate that all of the struts in the inventory have longitudinal reinforcement ratios that are below 1.2%. Thus, even those struts that are evaluated as having adequate shear capacity might be susceptible to shear failures.

The shear capacity versus the shear demand in the columns was checked by inspection. Usually, the contribution of the steel (hoops) toward resisting shear in the columns is small. However, due to the typically long clear spans of the columns, the shears are small enough for the contribution of the concrete alone to resist most, if not all, of the column shear (i.e., the column cross-sections are relatively large compared to those of the struts). While shear in the columns of the bents was not considered as one of the criteria, it should be noted that in the lap splices above the joints any shear could be too much if the effects of flexure have degraded the lap splice (Chap. 3, Sec. 3.7.2).

#### Member Bar Anchorage Details

The member bar anchorage details were rated either "satisfactory" or "unsatisfactory" based on consideration of the values of development length ( $l_d$ ) of the member bars. For exterior joints, the detailing of the member bars was considered as well. Strut bar anchorage details at exterior joints were considered "satisfactory" if the bars were detailed with 90° hooks and had  $l_d$  values that were in accordance with the guidelines in ACI 318M-89, Section 21.6, "Development length of bars in tension". No attention was given to bar tail lengths because in most cases this information was not provided in the construction plans that were reviewed. However, as was noted in Chapter 3, Section 3.3,

in no case were the tails on the bars in accordance with guidelines recommended by Paulay (1975c).

Strut bar anchorage details at interior joints were considered "satisfactory" if the  $l_d$  values of these bars were in accordance with the guideline established by Leon (1990): the column width should be at least equal to  $24d_b$  (i.e.,  $b_c \geq 24d_b$ ). Leon's guideline came from experimental tests that he conducted on subassemblages with very light joint reinforcement.

Column bar anchorage details were considered "satisfactory" if the  $l_d$  values of these bars were in accordance with a similar guideline that came from the same research (Leon 1990): the height of the strut should be at least  $24d_b$  (i.e.,  $h_b \geq 24d_b$ ).

#### Bent Hinge Formation Sequences

The bent flexural plastic hinge formation sequences were determined through the use of static, monotonic, limit analyses (i.e., "push-over"). Only material non-linearity was considered. While the goal of most limit analyses is to find the collapse load of a structure, the emphasis here was on determining the sequence of hinge formation. The poor confinement and bar anchorage details used in the inventory raises questions about the ability of expected hinge locations to withstand large inelastic demands. However, as was mentioned in Chapter 3, Section 3.2.1, attention was focused on those bents where the analyses indicated that hinges could be expected to form adjacent to a B-C joint early on in the hinge formation sequence. Those bents where the analyses indicated that hinges are expected to form solely in the columns, at either the foundations or the superstructure soffits, were disregarded as candidates for further consideration in this work. The tools used to conduct the limit analyses were:

- 1.) SAP90 (Computers and Structures Inc., *SAP90* 1989): a series of computer programs for the static and dynamic finite element analysis of structures.
- 2.) EPFO (Harrison, H. B., "Automatic Elastic-Plastic Analysis of Plane Frameworks." *Computer Methods in Structural Analysis*, Prentice-Hall, Inc., Englewood Cliffs, NJ, 1973, pp. 207-234): a program for the elastic-plastic analysis of plane frames.
- 3.) IDARC (Park, Y. J., A. M. Reinhorn, and S. K. Kunnath, *IDARC: Inelastic Damage Analysis of Reinforced Concrete Frame - Shear-wall Structures*, Technical Report NCEER-87-0008, Dept. of Civil Engrg., State University of New York at Buffalo, Buffalo, NY, Jul. 1987): a program for the inelastic damage analysis of reinforced concrete frame - shear-wall structures.

*SAP90*. Limit analyses using *SAP90* requires step-by-step processing of results. After each iteration the user must: check the demand moments against the moments required for the formation of hinges ( $M_n$ ), calculate and apply the load factors, and nullify the ability to resist bending moments in the ends of those members where hinges have occurred. The user must also determine the gravity-load moments and add/subtract them to/from (as required by the sense of the moments in the limit analysis determined from a preliminary run) the  $M_n$  values of the members. However, the extra work required by the step-by-step process does have an advantage in that material properties can be changed as increasing damage is interpreted to be occurring. Examples of where this advantage can be used are:

- 1.)  $M_n$  values for columns change as the lateral loading increases due to the changes in axial loading.
- 2.) The senses of the moments can change during an analysis. This influences whether or not the gravity load moments are added (subtracted) to (from) the column  $M_n$  values.
- 3.) Values of the moment of inertia (I), and the elastic modulus (E) change as the demand moments increase beyond the cracking moments of the members.

*EPFO.* The use of EPFO to conduct limit analyses was much faster than SAP90 in that EPFO performs a complete analysis in just one application. The user must apply the gravity-load moments to the  $M_n$  values prior to the execution of the program, in accordance with the initial sense of the moments (i.e., a preliminary run is required to determine the initial sense of the moments). However, the material properties that are used initially can not be changed during a limit analysis.

*IDARC.* IDARC was the most comprehensive software used because the output from a run includes: the stiffness of the members, the cracking and yield moments of the members, and the  $T_n$  values for the model. The yield moments of the members are used by the program in the same run to determine the plastic hinge locations. However, there are several drawbacks with using IDARC:

- 1.) IDARC requires input including: the member cross-sectional dimensions; the values of  $f'_c$  and E for the members; and the bar and the hoop sizes, spacing, cover, and strength.
- 2.) IDARC determines that hinges have occurred in locations where members have reached their yield moments; the program does not consider whether or not concrete has reached the crushing strain.

The latter drawback is important for the struts in this work (this sec., "Joint Shear Stress Demands")

The centerline-to-centerline member geometry used by the three programs leads to unrealistically large deflection values. Consideration of the finite member sizes prevents the overestimation of structure deflections. The capability to account for the actual finite size of the members exists in each of the programs, directly or indirectly.

To begin with, all three programs assume the joints to be rigid. In SAP90, the user can specify values of parameters in the input that tells the program the finite sizes of the members. Specifically, the portions of the lengths of elements that are actually part of the joint region are specified by the user. The user can then specify the portions of these element lengths that are parts of the joints that are to behave as the rigid joints do (i.e., rigid

links at the ends of the members). Conversely, in EPFO and IDARC the specification of rigid links at the ends of the members is done in an indirect manner. The user must manipulate the material properties input into EPFO and IDARC. Figure 29 illustrates how the material properties input into EPFO and IDARC were manipulated in order to avoid artificial flexibility. The terms used in the figure are defined as follows:

- "rigid links" are elements for which the flexural strength ( $M_n$ ) = the moment of inertia ( $I$ ) = cross-sectional area ( $A$ ) =  $\infty$
- the links adjacent to the rigid links were assigned properties in accordance with the relative sizes of the columns and the struts. For example, in those cases where a column was much wider than a strut was deep, the link adjacent to the rigid link in the strut was also modeled as rigid, while the links adjacent to the rigid links in the columns were assigned "normal" properties (the properties used in modeling the portions of the members away from the joint region). On the other hand, if the members were of similar depths, then the links adjacent to the rigid links in all of the members framing into the joint were assigned values of  $M_n = \infty$ , and  $I = A =$  "normal".

A typical model of a bent used in the EPFO and IDARC programs is shown in Figure 30.

### Transverse Fundamental Periods

The values of the likely transverse fundamental periods ( $T_n$ ) were estimated for individual bents. The calculation of the values of  $T_n$  assumed the superstructure or deck to be rigid in the transverse direction. The calculation did not account for the stiffness that may be provided by the superstructure acting to transfer loads to the abutments, nor did it account for the location of expansion joints in the superstructure. Typically there are two or more bents located in-between expansion joints. Hence, the likelihood of a single bent responding with only the portion of the superstructure tributary to that bent is remote.

These factors would tend to produce lower  $T_n$  values than those estimated here. Moreover, only the translational flexural stiffness of the columns in a bent were considered, as the struts and the superstructure were taken as rigid. The rationale behind this assumption was:

- 1.) The clear spans of the columns are typically long enough such that their the flexural stiffness will dominate their response (i.e., shear stiffness contribution will be relatively small).
- 2.) Since many of the struts are deep beams, the stiffness of the struts will be large relative to the flexural stiffness of the columns.
- 3.) Superstructures are typically very stiff relative to columns.

These factors would tend to further decrease the  $T_n$  values estimated here.

Under all of the assumptions described, in addition to the assumption of elastic response, the likely transverse values of  $T_n$  of the bents was estimated as follows:

$$T_n = 2\pi\sqrt{\frac{m}{k}} \quad \text{(Equation 13)}$$

where:

- $m$  = the tributary portion of the superstructure for a given bent
- $k$  = the stiffness for a given bent

Values of  $k$  were determined in accordance with Figure 31. Figure 31a represents bents with struts located at grade, while Figure 31b represents bents with struts located above grade. The symbols used in Figure 31 are defined as follows:

- $v, v_1, v_2$  = unit displacements/degrees of freedom
- $f$  = the force required to impose a unit displacement for the bent

$n$  = the number of columns in the bent

Applying the following:

$$f = kv \quad \text{(Equation 14)}$$

to the bent in Figure 31a yields:

$$k = n \left( \frac{12E_{\text{eff}}}{L^3} \right) \quad \text{(Equation 15)}$$

where:

$E$  = the elastic modulus =  $5000\sqrt{f'_c}$  ( $f'_c$  in MPa, Priestley 1991)

$I_{\text{eff}}$  = the effective moment of inertia (a percentage of the gross moment of inertia,  $I_g$ )

The values of  $I_{\text{eff}}$  that were used come from a chart (Fig. 32) developed by Priestley (1991). The chart is a plot of values of the moment of inertia ratio ( $I_{\text{eff}}/I_g$ ) versus values of the axial load ratio ( $P/f'_c A_g$ ; where  $P$  is the axial load and  $A_g$  is the gross cross-sectional area of concrete) for four different longitudinal reinforcement ratios ( $A_{st}/A_g$ ; where  $A_{st}$  is the area of the bars). The chart accounts for the distributed cracking over the length of a column at the time of first yield of the bars.

In Figure 31b, treatment of  $v_1$  and  $v_2$  require the matrix form of Equation 14:

$$\begin{Bmatrix} f \\ 0 \end{Bmatrix} = 12E_{\text{eff}} \begin{bmatrix} L_1^{-3} & -L_1^{-3} \\ -L_1^{-3} & (L_1^{-3} + L_2^{-3}) \end{bmatrix} \begin{Bmatrix} v_1 \\ v_2 \end{Bmatrix} \quad \text{(Equation 16)}$$

Based on the length of  $L_2$  with respect to  $L_1$ ,  $v_2$  can be expressed in terms of  $v_1$ . In this manner,  $v_2$  can be condensed out of the equations and a single expression for  $k$  will result. It should be noted that in order to apply Equation 16 to a strutted-column bent, the right side of the equation must be multiplied by the number of columns in the bent ( $n$ ).

The assumptions made in the computation of  $T_n$  values may be reasonable if the increases in stiffness created by the assumptions described earlier are offset by the  $I_{eff}$  values that were selected for use here. The reason being that these  $I_{eff}$  values probably decrease the stiffness below the actual value. The relative shapes of the  $M-\phi$  curves for the columns and struts (Fig. 25), together with the results from the bent hinge formation sequence analyses (Sec. 4.1.2), indicates that the moments in the columns are usually below yield when the struts reach yield. Therefore, the values of  $I_{eff}$  used here are probably smaller than the actual values of  $I_{eff}$ .

#### 4.1.2 Evaluation of Results

##### DRC Category

As a reminder, there are six bridges in the category with double-column bents with rectangular columns. The ranges of results from applying the criteria (Sec. 4.1.1) to this category are as listed in Table 5 (strut and column bar anchorage detail ratings are shown as "SAD", and "CAD", respectively). The results from the bent hinge formation sequence analyses do not appear in Table 5. However, they are discussed in the following summary of all of the results.

*Flexural Strength Ratio.* One recommendation for the desirable range of values of the flexural strength ratio ( $M_{nc}/M_{nb}$ ) is 1.8 - 2.5 (Leon et al. 1986). With one exception, the values of  $M_{nc}/M_{nb}$  were near or slightly higher than the suggested criterion.

**Maximum Demand Joint Shear Stress.** ACI 318M-89 requires that the maximum demand joint shear stress ( $v_{jt}^*$ ) be less than or equal to  $1.0\sqrt{f'_c}$  ( $f'_c$  in MPa) for exterior joints, and requires  $v_{jt}^* \leq 1.25\sqrt{f'_c}$  for interior joints. AASHTO (1991) does not distinguish between interior and exterior joints, and in that specification  $v_{jt}^* \leq 12.0\sqrt{f'_c}$  ( $\leq 1.0\sqrt{f'_c}$ ;  $f'_c$  in MPa) for all joints. The values of  $v_{jt}^*$  in the DRC category, where all of the joints are exterior-type, are small compared to  $1.0\sqrt{f'_c}$ . This is due to the small values of  $M_{nb}$ , relative to the large values of the effective joint area ( $A_{jt}$ ), found in these bents.

**Maximum Strut Shear Stress Demand.** For most of these bents the large spacing of the stirrups causes  $V_s \ll V_c$  (Equation 12). However, the struts are usually deep enough such that the concrete alone can provide adequate shear capacity. In two of the bridges the shear stress capacity is less than the demand corresponding to flexural hinging in the struts (i.e.,  $v_{nb} < v_b^*$ ).

**Member Bar Anchorage Details.** Most of the unsatisfactory SAD ratings were due to the fact that the majority of these bents have strut bars that terminate in the columns without hooks (Fig. 5a). However, in many of the bridges that have this type of detail, the relatively large-sized columns provide anchorage lengths ( $l_d$ ) that are long enough to develop the bars in tension according to ACI 318M-89, Section 21.6, "Development length of bars in tension". Only one of the six bents had column bars that received an unsatisfactory CAD rating.

**Bent Hinge Formation Sequences.** The typical hinge formation sequence will be: the tops of the columns (at the superstructure soffits) will hinge first, then hinges will form in the struts at the joint faces, followed by hinge formation in the bottoms of the columns (at the tops of the foundations). The order in which the latter two sets of hinges form depends on the restraint provided by the backfill material at the lower portions of the columns. If the hinges at the ends of the struts form prior to the hinges in the bottoms of the columns, then large ductility demands may be placed on the strut ends.

*Transverse Fundamental Periods.* The estimated transverse fundamental periods ( $T_n$ ) for these bents are "long" relative to those of the bents in the other categories. The spectral demands on structures with such values of  $T_n$  (i.e., 1 - 2 s) usually cause increased response and decreased force demands.

*Conclusions.* What follows are the conclusions that were drawn based on the evaluation of the bents in the DRC category, and based on their characteristics and construction details. References made to "failure" are based on the assumption that the bents will respond well into the inelastic range (i.e., several plastic hinges will have formed).

1.) The bents will probably not experience joint shear failures due to the small expected values of  $v_{jt}^*$ . However, failure may occur in the joints in the form of loss of bar anchorage. The reasons being that the strut bars are poorly detailed where they terminate, the joints lack adequate confinement, and there is the possibility of yielding from the strut hinges penetrating into the joints.

2.) The bents may suffer failure at strut plastic hinge locations due to the possibility of large ductility demands coupled with the poor confinement in these regions.

3.) The bents could experience strut failures due to either high values of the shear stress demands or the fact that the struts may experience large ductility demands. The poor confinement of the strut hinge regions adds to the likelihood of shear failures occurring. The low longitudinal reinforcement ratios may also contribute to shear failures.

4.) The bridges could experience period elongation due to strut shear failure, and/or the degradation that may occur in the strut hinges and in the bond of the strut bars. Given that the  $T_n$  values are approximately one to two seconds, such period elongation should increase the response of these bents but decrease the force demands.

Because there is little chance of either a lap-splice failure in the columns above the joints or a joint shear failure, bents from the DRC category were not given further consideration in this work.

### MRC Category

As a reminder, there are thirty bridges in the category with multiple-column bents with rectangular columns. The ranges of results from applying the criteria to this category are as listed in Table 6 (average values are in parentheses, and subscripts "ext" and "int" imply "exterior" and "interior" joints, respectively). The results from the bent hinge formation sequence analyses do not appear in Table 6. However, they are discussed in the following summary of all of the results.

*Flexural Strength Ratio.* The typical value of  $\Sigma M_{nc}/\Sigma M_{nb}$  meets the guideline established for use here (1.8 - 2.5).

*Maximum Demand Joint Shear Stress.* The values of  $v_{jt}^*$  shown were calculated at interior columns. Values of  $v_{jt}^*$  at exterior columns did not warrant calculation, as visual inspection and the experience obtained in working with the double-column bents revealed that values of  $v_{jt}^*$  would be very small. With a few exceptions, the values of  $v_{jt}^*$  at interior joints were well below the limits specified by ACI 318-89 ( $1.25\sqrt{f'_c}$ ) and by AASHTO (1991) ( $1.0\sqrt{f'_c}$ ). This is due to the small values of  $M_{nb}$ , relative to the large values of the effective joint area ( $A_{jt}$ ), found in these bents.

*Maximum Strut Shear Stress Demand.* For half of these bents, the small contributions of the stirrups to the shear capacities (caused by the large stirrup spacing that is typical of all of the bents) resulted in their shear capacities being less than the demand shears associated with the formation of flexural hinges in the struts (i.e.,  $v_{nb} < v_b^*$ ).

*Member Bar Anchorage Details.* The average strut bar anchorage detail rating at exterior joints ( $SAD_{ext}$ ) is "unsatisfactory" because the poor details shown in Figures 5a and 5c are used. Moreover, many of the bents that received "satisfactory"  $SAD_{ext}$  ratings have square reinforcing bars. Thus, those bents also have questionable strut bar anchorage potential. While the typical bent received a "satisfactory"  $SAD_{int}$  rating, the prevalent use

of square bars renders most of the "satisfactory" ratings questionable. The same holds for the column bar anchorage detail (CAD) ratings.

*Bent Hinge Formation Sequences.* Due to the large number of bridges in this category and the broad ranges of both the characteristics and the evaluation results, limit analyses were not performed on specific bents. Instead, the values of the average characteristics (Table 2) were used to construct a model of a multiple-column bent that would best represent the hinge formation sequence of this portion of the inventory. An exception was made in the "strut height" characteristic. Although the average value of the strut height is listed in Table 2 as "mid-height", in the model bent used in these hinge formation sequence analyses the strut was placed below mid-height. This was done to determine whether large moments would result in the lap splice regions of the columns above the joints.

As a check on the accuracy of the model bent, a sensitivity analysis was done in order to determine the effects of averaging the characteristics. The parameters that were studied in the sensitivity analysis were: the strut height, the column flexural strength ( $M_{nc}$ ), the volumetric ratio of the hoops (stirrups) and the core concrete of the column (strut), the bar diameter in the columns and in the beams, the weight of the superstructure, the number of columns, and several material properties. The results from the sensitivity analysis indicated that as long as the parameters were varied no more than ten to fifteen percent, there was not much effect on the hinge formation sequence in the model bent.

The results from the limit analysis are indicated in Figure 33, which also shows the model bent and its dimensions. The dots indicate the plastic hinge locations and the numbers above/next to the dots indicate the sequence of hinge formation. Where hinging is expected to form early on, the inelastic demands may be large. The figure shows the ductility demands are expected to be relatively small in the upper columns just above the struts (lap splice regions). However, when the height of the strut is lowered in excess of fifteen percent of that height used in the model bent, the ductility demands in those regions

will be much larger. Additionally, the columns tend to be axially loaded relatively lightly. Thus, as hinges form in the splice regions, shear may become a problem (Chap. 3, Sec. 3.7.2). This is particularly true in the case of one of the two exterior columns, where the axial load will be reduced depending on the direction of motion.

*Transverse Fundamental Periods.* The average value of  $T_n$  indicates that most of these bents are considerably stiffer than the bents in the DRC category. However, structures with values of  $T_n = 0.8$  s might still experience spectral demands associated with flexible structures (i.e., increased response, and decreased force demands). The effect on the periods of the unreinforced filleted strut ends (typically found in these bents) has not been considered. The fillets will certainly decrease the values of  $T_n$  and may contribute to period elongation as they degrade.

*Conclusions.* What follows are the conclusions that were based on the evaluation of the bents in the MRC category, and based on their characteristics and construction details. References made to "failure" are based on the assumption that the bents will respond well into the inelastic range (i.e., several plastic hinges will have formed).

1.) The bents will probably not experience joint shear failures due to the small expected values of  $v_{jt}^*$ . Many of the joints in the bents may undergo bar-anchorage-type joint failures. The reasons being that the strut bars are poorly anchored/detailed, the joints lack adequate confinement, and there is a possibility of yielding from the strut hinges penetrating into the joints. Similar detrimental traits are found in the columns of some of the bents; these could also cause joint anchorage failures.

2.) The bents may experience strut hinge failures at exterior joints due to the fact that the strut ends at exterior joints may undergo several inelastic cycles, and due to the fact that the hinge regions are poorly confined.

3.) Half of the bents do not have the shear capacity required to develop plastic hinging in the struts. Additionally, high shear demands (relative to the shear capacities) are expected in many of the other half of the bents. Therefore, there is a strong likelihood for strut shear

failure in most of this portion of the inventory. Other reasons for this possibility are the likelihood of large ductility demands in some of the strut hinges and the poor confinement detailing of the struts in most of the hinge regions. The low values of the longitudinal reinforcement ratios might also contribute to shear failures.

4.) The bents with struts close to grade might experience shear or flexural hinge failure in the lap splice regions in the columns above the joints. The reasons for this are the high moment demands that may occur, the relatively small amounts of axial column loads that may be present, and the poor confinement detailing of these lap splice regions.

5.) The bridges could experience period elongation due to strut shear failures, or to degradation of the strut hinges, of the column lap splices, and of the bar anchorages. Given that the average values of  $T_n$  are approximately 0.8 s, such period elongation should increase the response of these bents but decrease the force demands.

Because of the potential for problems to occur in the lap-splice regions in the columns above the joints, multiple-column bents with rectangular columns were given further consideration in this work.

#### DCC Category

As a reminder, there is one bridge in the category with double-column bents with circular columns and there are six strutted-column bents in this bridge. The ranges of results from applying the criteria to this category are as listed in Table 7. The results from the bent hinge formation sequence analyses do not appear in Table 7. However, they are discussed in the following summary of all of the results.

*Flexural Strength Ratio.* The value of  $M_{nc}/M_{nb}$  is below the guideline established for use here (1.8 - 2.5).

*Maximum Demand Joint Shear Stress.* The value of  $v_{jt}^*$  is small relative to  $1.0\sqrt{f_c}$  (ACI 318M-89, AASHTO 1991). This is due to the small values of  $M_{nb}$ , relative to the large values of the effective joint area ( $A_{jt}$ ), found in these bents.

*Maximum Strut Shear Stress Demand.* For these bents the large spacing of the stirrups causes  $V_s \ll V_c$  (Equation 12). However, the struts are deep enough such that the concrete and the small contribution from the stirrups can provide adequate shear capacity. In all of the bents  $v_{nb} > v_b^*$ .

*Member Bar Anchorage Details.* The SAD and CAD ratings were "satisfactory" for all of the bents. It should be noted that because the rectangular struts frame into circular columns the  $l_d$  values of the strut bars vary (i.e., the corner bars have smaller  $l_d$  values than do the interior bars). Only one of the six bents had column bars that received an unsatisfactory CAD rating.

*Bent Hinge Formation Sequences.* The results from the limit analyses conducted on these bents indicates that the hinge formation sequence is expected to be as follows. Hinges will form in the struts at the joint faces relatively early, followed much later by hinge formation at the top of one of the columns (at the superstructure soffits), then hinges will form in the bottoms of the columns (at the tops of the foundations) and, finally, the last hinge will form at the other column top. The early formation of hinges expected in the struts may impose large ductility demands in these regions.

The variation that exists from one bent to the next with respect to the locations of the struts alters the hinge formation sequence slightly. As the strut height decreases toward grade, both of the column tops are expected to hinge prior to the column bottoms. However, as the strut height is lowered, the timing of the formation of the hinges changes substantially, as does the magnitude of the moments in the columns just above the joints (column bar lap splice regions). Under these conditions, the hinges in the column tops are expected to form soon after the strut hinges, and the moments in the lap-splice region of the

4.) The bents with strut heights close to grade might experience shear or flexural hinge failures in the lap splice regions in the columns above the joints. The reasons for this are the high moment demands that may occur, the relatively small amounts of axial column loads that may be present, and the poor confinement detailing of these lap splice regions.

5.) The bents will probably experience period elongation due to strut shear failures, or due to the degradation of strut hinges, column lap splices, and bar bond. Given that the values of  $T_n$  are approximately 0.4 s, and that period elongation is likely, the behavior of these bents might transition from "stiff" to "flexible".

Because of the potential for problems to occur in the lap-splice regions in the columns above the joints, coupled with the fact that this bridge is a part of the US interstate system, double-column bents with circular columns were given further consideration in this work.

#### MCC Category

As a reminder, there are two bridges in the category with multiple-column bents with circular columns. The ranges of results from applying the criteria to this category are as listed in Table 8. The results from the bent hinge formation sequence analyses do not appear in Table 8. However, they are discussed in the following summary of all of the results.

*Flexural Strength Ratio.* The values of  $\sum M_{nc}/\sum M_{nb}$  range from very low to acceptable.

*Maximum Demand Joint Shear Stress.* The values of  $v_{jt}^*$  shown were calculated at interior columns. Values of  $v_{jt}^*$  at exterior columns did not warrant calculation, as visual inspection and the experience obtained from the double-column bents revealed that  $v_{jt}^*$  would be very small. All of the strutted-column bents in these bridges had small values of  $v_{jt}^*$  at interior joints. This is due to the small values of  $M_{nb}$ , relative to the large values of the effective joint area ( $A_{jt}$ ), found in these bents.

*Maximum Strut Shear Stress Demand.* For these bents the large spacing of the stirrups causes  $V_s \ll V_c$  (Equation 12). However, the struts are deep enough such that the concrete and the small contribution from the stirrups can provide shear capacity that exceeds the maximum demand.

*Member Bar Anchorage Details.* The SAD and CAD ratings are "satisfactory".

*Bent Hinge Formation Sequences.* The results from some of the limit analyses that were conducted on the three- and four-column bents are shown in Figure 34. The dots indicate the plastic hinge locations and the numbers above/next to the dots indicate the sequence of hinge formation. In the analysis results shown, only the ends of the upper columns are expected to form hinges. In these columns, the regions just above the struts (lap splice regions) appear to be particularly susceptible to experiencing large inelastic demands; the first hinges will probably form in these locations early on in the sequence. However, while the results in Figure 34b are typical (the bents are all alike with 914 mm diameter columns joined by 762 mm x 1219 mm struts), the results in Figure 34a are not. Half of the bents in the three-column-type bents are as shown in the figure (with 914 mm diameter columns joined by 762 mm x 1524 mm struts), and the other half have struts that are located at mid-height across the width of the bent (with 1219 mm diameter columns joined by 762 x 1219 struts). The latter bents are expected to feature hinge formation at the ends of the struts, rather than in the columns.

*Transverse Fundamental Periods.* The values of  $T_n$  indicate that these bents are "stiffer" than the bents in the MRC category, but they are more "flexible" than the bents in the DCC category.

*Conclusions.* What follows are the conclusions that were drawn based on the evaluation of the bents in the MCC category, and based on their characteristics and construction details. References made to "failure" are based on the assumption that the bents will respond well into the inelastic range (i.e., several plastic hinges will have formed).

1.) The bents will probably not experience joint shear failures due to the small expected values of  $v_{jt}^*$ . The bents will probably not experience member bar anchorage failures because the anchorage lengths/detailing appear to be adequate. However, joint failures might still result due to the effect on bar anchorage from the poor joint confinement, and due to the possibility of hinge penetration from the columns and/or struts into the joints.

2.) A few of the bents will probably experience strut hinge failures because hinging in the struts is expected to be predominant. Large inelastic demands may be placed on these regions and they have poor confinement detailing.

3.) The bents will probably not experience strut shear failures because the struts have the shear capacity required to develop plastic hinging in the struts. However, large inelastic demands may be placed on the regions where hinging is expected and these regions have poor confinement detailing. This coupled with the low values of the longitudinal reinforcement ratios may lead to shear failures at a later point during the inelastic loading.

4.) The bents may experience shear or flexural hinge failure in the lap splice regions in the columns above the joints. This is due to the fact that many of the bents have single struts with strut heights close to grade, and flexural hinges are expected to form early during the response. There is a good probability of having high moment demands, high ductility demands, and relatively small amounts of axial column loads on the poorly confined lap splice regions.

5.) Given that the values of  $T_n$  are in the approximate range of 0.5 - 0.8 s, coupled with the period elongation that may occur due to the possibility of degradation of the column lap splices, the strut hinges, and the bar anchorages, the spectral demands on these bents might cause them to respond as "flexible" structures.

Because of the potential for problems to occur in the lap-splice regions in the columns above the joints, coupled with the fact that this bridge is a part of the US interstate system, multiple-column bents with circular columns were given further consideration in this work.

Having selected the MRC, DCC, and MCC categories for further consideration, the next step was to choose prototype subassemblages from these categories.

## **4.2 Experimental Test Subassemblage Prototypes**

Described herein is the selection and the design of the prototype subassemblages for the experimental testing portion of this work.

### **4.2.1 Selection of the Prototypes**

Prior to deciding which of the three categories of bents (MRC, DCC, MCC) would be selected for use as prototypes, the number of subassemblages that would be tested had to be considered.

#### **The Influence of the Test Matrix on Prototype Selection**

At the outset of this work, testing three to four subassemblages was envisioned as being feasible. Two to three subassemblage specimens, modeled after "as-built" prototype subassemblages (Chap. 3, Sec. 3.2.4, objective "4."), would be tested initially. The one or two remaining tests would be conducted on:

- 1.) retrofitted version(s) of one (two) of the "initial" specimens, and/or
- 2.) repaired version(s) of one (two) of the "initial" specimens (i.e., damage done in the "initial" tests would be repaired prior to the "additional" tests), if the findings from the "initial" tests indicated that such "retrofit/repair" tests were worthwhile.

How this concept of the test matrix influenced the selection of the prototype subassemblages will be explained in what follows.

Testing of subassemblages taken from the MRC category was ruled out for several reasons.

- 1.) Because this portion of the inventory was so large and had such broad ranges of characteristics and construction details (Table 2), it was decided that selecting just two to three "as-built" subassemblages would not lead to enough test results to enable conclusions to be drawn about the entire category.
- 2.) Due to the broad ranges of results from the evaluation of this category (Table 6), it was decided that in selecting two to three "as-built" subassemblages it would be very difficult to test for all of the potential problems that might occur in these bents.
- 3.) Given the average age of the bridges in this category (almost 40 years), and the reduced usage of most of the bridges since the advent of the US interstate system, it is doubtful that these bridges will remain in service much longer. Accordingly, focusing the experimental testing portion of this work on such bridges was questioned.

With just the DCC and MCC categories left to consider, the choice of prototype subassemblage selection became much easier because there are just three bridges in these two categories and these bridges are similar. However, in order to account for bents in both categories, a minimum of three test specimens would be required because of the three different column sizes that occur in these categories (1219 and 1524 mm - DCC, and 1219 and 914 mm - MCC). Additionally, there are many differences in the characteristics and the construction details among the bents in the two categories (exterior versus interior joints; bent heights and widths; strut sizes; numbers of member bars; member bar sizes; Tables 3 and 4, respectively). Thus, it was decided that representation of the two categories could not be achieved with only three subassemblages.

The DCC category was not considered because of the large differences in the characteristics and the construction details between this category the MCC category (i.e., the DCC category has much larger column diameters and bent heights, and it has exterior joints only).

Two prototype subassemblages were selected from the MCC category: one representative of the 1219 mm diameter columns in the three-column bents, and the other representative of the 914 mm diameter columns in the four-column bents.

#### The Configuration(s) of the Subassemblages

There were three configurations that were viewed as candidates for the prototype subassemblages, two featured exterior joints and one featured interior joints.

*"Exterior Joint" Configurations.* The first exterior joint configuration was a B-C joint subassemblage obtained by cutting an upper and a lower exterior column from a bent at the mid-height points, and by cutting the framing strut at mid-span (i.e., a "T" rotated 90°). The reason for "cutting" at mid-height of the columns and at mid-span of the strut is that elastically the points of inflection (i.e., zero moment) typically occur at these locations. Such a configuration would allow for study of both the B-C joint and column lap splice behavior.

The second exterior joint configuration was the same as the first, except the entire upper column is left in-tact. Additionally, a piece of the superstructure remains attached to the upper column. In addition to being able to study the B-C joint and column lap splice behavior, such a configuration would allow for the study of the behavior of the column where it connects to the superstructure.

The second exterior joint configuration was a strong candidate because of the versatility it offered. The evaluation of the MCC category (Sec. 4.1.2) indicated that hinge formation in the exterior columns at the superstructure in the three-column bents will likely precede hinge formation elsewhere. In the subassemblage described, load can still be applied to the B-C joint/lap splice region after the column hinges at the superstructure. Thus, while modeling the realistic sequence of events in the case of the three-column bents,

this configuration might also allow for investigation of the potential problems in the B-C joint and lap splice regions of three- and four-column bents.

However, the second exterior joint configuration was eventually discarded because the space available at the testing facility dictated the use of a specimen scale on the order of 1/3. This scale was too small (Sec. 4.3.1, "The Scale Factor").

*"Interior Joint" Configuration.* The configuration of this candidate is identical to that described in the first exterior joint configuration, except that the subassemblage would consist of an interior B-C joint (i.e., "+"). Here also, joint and lap splice behavior could be studied.

*The Final Selection.* The interior joint configuration was chosen over the first exterior joint configuration. The reason being that the interior joint configuration causes more shear to occur in a joint than does the exterior joint configuration. Thus, the prototype that was selected provided the greatest opportunity to study joint behavior, in addition to providing the opportunity to study column lap-splice behavior.

#### **4.2.2 Design of the Prototypes**

With the removal of exterior joint configurations from consideration as candidate prototypes, the next task was the design of two cruciform-shaped prototype subassemblages that were representative of the MCC category. One prototype had a 1219-mm diameter column, while the other had a 914-mm diameter column.

##### **The Location of the Strut**

The design decision that caused the most deliberation was where to locate the struts. The evaluation of the MCC category indicated that one concern might be the flexural hinging anticipated in the column lap splice regions above the joints. Additionally, the

analyses showed that the greatest ductility demands on these regions occurred when the strut was close to grade. Thus, the prototype designs that would provide the best opportunities for studying possible degradation of lap splice regions would be ones where the struts were well-below mid-height. However, another concern raised by the evaluation of the MCC category was the possibility of large inelastic demands occurring at strut hinges. In these situations the struts occurred near mid-height. With the strut at mid-height the joint shear demands are the largest, although relative to the limiting values they are small. Also, the evaluation of the MCC category indicated that when column hinging in the lap splice regions above the joints is expected to occur, the possibility of hinging exists whether the strut is at grade (highest ductility demands) or at mid-height (smallest ductility demands).

Thus, the decision was made that each of the prototypes would be designed with the struts located at mid-height, thereby providing opportunities for the study of joint-shear-related, strut-hinge-related, and of lap-splice-related problems. Additionally, as mentioned in Section 4.1.2, while the struts in the bents of the MCC category successfully met the shear capacity criterion, it was noted that the large ductility demands in the strut hinges, the poor confinement of the hinge regions, and the small longitudinal reinforcement ratios could still result in shear failures. Thus, strut-shear-related problems might be observed in the prototypes as well.

The joint-shear-, strut-hinge-, and strut-shear-related problems are most assured to occur in a "strong column-weak beam" design, while the lap-splice-related problems are most assured to occur in a "weak column-strong beam" design. In the interest of having the opportunity to study the problems related to both types of designs, the geometry of the prototype subassemblages was designed such that one prototype was a "strong column-weak beam" subassemblage and the other a "weak column-strong beam" subassemblage.

## Geometry and Other Issues Related to Prototype Design

*Member Cross-Section Geometry.* The "strong column-weak beam" prototype had the member geometry of the three-column bent-type in which strut hinging was expected (1219 mm diameter column and 762 mm x 1219 mm struts; Unit IP), and the "weak column-strong beam" prototype had the member geometry of the four-column bents in which column hinging was expected (914 mm diameter column and 762 mm x 1219 mm struts; Unit IIP).

The rest of the design decisions involved issues such as: the heights of the prototypes, the strut lengths of the prototypes, the member bar layouts and sizes, the member transverse reinforcement layouts and sizes, the column bar lap splice lengths, the axial loads, and the material properties.

*Column Heights.* The bent height range (4.5 - 16 m) was large so it was decided to use a value of 10.5 m (approximately the average clear height) for the heights of the bents from which the prototypes would be taken from. With the strut dimensions chosen, the lengths of the upper and lower columns of the prototypes were determined. The height of the strut was subtracted from 10.5 m, then 1/4 of the difference was taken to obtain the lengths of the upper and lower columns (2.32 m).

*Strut Lengths.* The strut lengths of the prototypes were based on the typical 5 m clear span of the struts in the MCC category. The actual lengths of the prototype struts were determined by dividing 5 m in half (i.e., 2.5 m).

*Member Bars and Bar Layouts.* The struts in the MCC category had bar layouts such as the one shown in Figure 9c (i.e., four bars top and bottom, with two layers of two intermediate bars). The average size of the main bars is a #10, while the typical intermediate bar size is a #6. These layouts and bar sizes were used in the prototype struts.

The layout of the eight column bars in the 914 mm diameter columns of the MCC category is as shown in Figure 9b. The layout of the column bars in the 1219 mm diameter

columns of the three-column bents is similar. However, there are twelve equally-spaced bars in these columns (i.e., a bar at each of the hours of twelve-hour clock). These layouts were used in the prototypes as well. The bar sizes used in the prototypes coincide with the bar sizes used in the MCC category: #10 and #11, for Unit IIP and Unit IP, respectively.

*Member Transverse Reinforcement.* The diameters and the spacings of the hoops and the stirrups used in the prototype members were identical to those used in the members of the MCC category: #4 hoops at 305 mm in the columns and #5 stirrups at 457 mm in the struts. Since the number of joint hoops is not specified on the structural drawings, the number that was used in the prototypes (four, with two between the top and bottom strut main bars) by invoking the 305-mm spacing beginning at the bottoms of the lower columns of the prototypes (the inflection points in the "as-built" bents).

*Column Bar Lap Splice.* The column bar lap splices above the struts in the MCC category are 1524 mm long (i.e.,  $43d_b$  for Unit IP and  $48d_b$  for Unit IIP) and this value was used in the prototypes. Circumferential lap splices were used in the prototypes.

*Column Axial Loads.* The axial load range for the interior columns in the MCC category is  $0.03 - 0.05f'_cA_g$  ( $f'_c$  in MPa). The evaluation of this category indicated that the effect of the use of one axial load or another (where the difference is about  $0.02f'_cA_g$ ) did not alter the moment capacities of the columns enough to change the sequence of hinge formation in the bents. Thus, there was flexibility in the selection of the axial loads that were to be used in the design of the prototypes. This flexibility was exploited as one axial load was selected in the design of both prototypes. The load that was chosen was 1157 kN, which equates approximately to  $0.025f'_cA_g$  for Unit IP and to  $0.043f'_cA_g$  for Unit IIP. The reason for the use of a 1157-kN axial load for both prototypes was the scale chosen for the test specimens and the repercussions of this scale on the capability of the system used for application of the axial load (Sec. 4.3.5, "Loading").

*Concrete and Steel Strengths.* The prototypes were designed with Gr 40 steel (bars and transverse reinforcement) since that is what was used for the MCC bents. However,

while  $f'_c = 28$  MPa was the specified concrete strength that was used for the MCC category,  $f'_c = 42$  MPa was used in the prototypes. The reason for increasing the concrete strength by fifty percent was to account for the strength gain with age that has occurred in the bents.

*Summary of the Designs.* The results of the design for Unit IIP are shown in Figure 35. Unit IP was designed identically, unless otherwise noted by quantities in parentheses. The roller supports at the ends of the struts and the pin support at the bottom of the lower column provide, in an approximate sense, the behavior of an actual bent. By applying the reversed cyclic lateral load and the axial load at the top of the upper column, the prototype is subjected to a loading similar to that it would see if it were integral with a bent.

With the design of the prototypes completed, the next steps involved the experimental subassembly tests.

### **4.3 Experimental Tests**

In what follows, the steps taken to obtain the test specimen subassemblies from the prototype subassemblies are discussed, the materials that were used in the specimens are reviewed, and the construction of the specimens is considered. Also, the instrumentation used and the layout of the instruments on the specimens are discussed. Finally, the test set-up is described as are the testing procedures.

#### **4.3.1 Specimen Designs**

##### The Scale Factor

One of the objectives of this work was to evaluate the performance of "as-built" construction (Chap. 3, Sec. 3.2.4, objective "4.>"). Given the size of the available testing

facility, full-scale testing of the prototype subassemblages was not possible. Thus, the scale of the test specimens needed to be as large as possible so that materials used in full-scale construction practice could be used and so that scale-related effects could be minimized. A lower bound of approximately 1/2.5-scale was therefore established.

A geometric scale factor of 1/2.5 was applied to the prototype subassemblages to obtain the test specimen subassemblages. The reasons were as follows:

- 1.) This scale factor allowed for placement of the test specimens, the supporting fixtures and the load actuators, and for the full expected response of the test specimens within the space provided by the existing test frame.
- 2.) With this scale factor the #10 bars used in the columns and struts in Unit IIP, as well as the #10 bars used in the strut of Unit IP, scaled exactly to #4 bars. Therefore, the same number and layout of the #10 bars used in the prototypes could be used in the specimens without any effect from the scaling process.
- 3.) Application of this scale factor to the prototype axial loads resulted in an axial load for the test specimens that was within the capacity of the axial-load delivery system (Sec. 4.3.5, "Loading").

### The Specimens

The result of applying the scale factor to the prototype subassemblages is depicted in Figures 36 and 37 (the prototype Unit IP became the test specimen Unit I, and Unit IIP became Unit II; all dimensions are in mm). Note that there are two hoops in-between the top and bottom layers of strut bars in the joint region of each specimen, just as was the case with the prototypes (Sec. 4.2.2, "Geometry and Other Issues Related to Prototype Design"); the lower hoop is obscured in Figures 36 and 37 by the lower intermediate strut bar.

After the scale factor was applied to the prototypes, a few design features had to be altered in the specimens: the bars in the column of Unit I, the geometry of both specimens, and the transverse reinforcement used in both specimens.

*Unit I Column Bars.* The #11 column bars of Unit IP (Fig. 36) scaled to a diameter that is approximately ten percent larger than a #4 bar, and thirteen percent smaller than a #5 bar. Therefore, since the decision was made to keep the total number of bars constant, a choice had to be made between using twelve-#5 bars or using twelve-#4 bars. The percentage differences between the scaled diameter and the diameters of #4 and of #5 bars grow disproportionately when the total area of all twelve bars is considered. Thus, #4 bars were selected for use.

The repercussion of using #4 bars was that the flexural strength ratio ( $\Sigma M_{nc}/\Sigma M_{nb}$ ) of Unit I was smaller than that of Unit IP. This reduction in the size of the ratio made it possible for the behavior of Unit I to differ from that of Unit IP. While hinging of the struts was expected in the design of Unit IP, hinging in the columns of Unit I became a possibility. The analyses conducted on Unit I with *SAP90* indicated that while first yield for the subassembly would occur in the struts, the formation of a plastic hinge might occur in either the column in the lap splice region or in one of the struts at the joint. The question regarding the location of the first plastic hinge would be determined by the actual crushing strain of the concrete in the struts. The results of the analyses indicated that if  $\epsilon_{cu}$  for the struts did not reach 0.006, then the first plastic hinge would probably form in one of the struts (Sec. 4.1.2, "Joint Shear Stress Demands"). If the strut  $\epsilon_{cu}$  value were to reach 0.006, the moment in the column would be near its maximum expected value.

*Test Specimen Geometry.* Another problem that was encountered upon scaling the prototypes was that no allowance was made in the length of the upper column of the test specimens to accommodate the finite size of the lateral load actuator (Sec. 4.3.5, "Loading"). In the analyses conducted on the prototypes with *SAP90*, the lateral load was applied as a point load at the top of the upper columns. The lateral load actuator used

change in orientation (Fig. 38a shows the "as-designed/as-built" test specimen orientation and 38b shows the "as-tested" specimen orientation). Only details considered relevant to the issue are included in the figure. Thus, Figures 36 and 37 are applicable when rotated 180° in-plane.

*Test Specimen Transverse Reinforcement.* Non-standard bar sizes resulted from the application of the scale factor to the hoops and to the stirrups of the prototypes: #2 bars for the stirrups and a size that was smaller than #2 for the hoops. While these sizes of standard deformed bars and hoops were not available, three types of wire were: D3, D5 and 9 Ga wire (Sec. 4.3.2, "steel").

Several designs were considered in which each of the types of wire was used as hoops and as a stirrups. The goal of the process was to find a design where the contribution of the wire ( $V_s$ ) toward the shear strength of the columns and the struts would match the shear strengths dictated by the scale factor. Thus, in each of the designs considered, the variables were the cross-sectional area, the value of  $f_y$ , and the spacing ( $s$ ) of the wire.

The value of  $s$  served as the measure by which the final designs were selected. An attempt was made to approximately preserve (on the low side) the scaled values of  $s$  for the stirrups and for the hoops in the prototypes. The reason being that significant increases in the values of  $s$  in the prototypes result in only a few stirrups/hoops in the shear spans of the specimens' members. The designs that were selected are shown in Figures 36 and 37, with the D3 wire serving as the hoops, and with the 9 Ga wire serving as the stirrups. Note that two 9 Ga wire stirrups were designed to act as one "stirrup". In "Section B-B" of Figure 36, a 12.7 mm gap is specified as the separation between the two 9 Ga wire stirrups. This gap was used to allow concrete to completely envelop each 9 Ga wire stirrup to ensure that the capacities of both stirrups could be fully mobilized if required.

There are two repercussions associated with the wire that was used:

1.) the value of  $f_y$  for the D3 hoops is about fifty percent larger than that of the Gr 40 steel used for the prototype hoops, and

2.) the wire is mechanically deformed with dimples (D3 wire) or indentations (9 Ga wire).

With respect to the first point, hoops with higher yield strengths are beneficial to B-C joint behavior (Chap. 3, Sec. 3.6.4, "Behavior of Joint Reinforcement"). Thus, the performance of the B-C joints in the specimens might be better than that which would actually occur. As for the second point, dimpled wire will not develop the same bond stress as conventional reinforcement (lugs are vital to mechanical anchorage as discussed in Chap. 3, Sec. 3.6.3, "Bond in B-C Joints"). This should not be a concern with the 9 Ga stirrups as the ends are hooked around the corner bar into the core concrete of the struts. However, excessive slip or complete loss of bond of the D3 hoops could allow the B-C joints of the specimens to dilate sooner and more than they actually would in the prototypes. It seems possible that concerns "1.)" and "2.)" could work to negate each other (i.e., some local slip of the D3 wire, below the value of  $f_y$ , could simulate yield of Gr 40 steel).

#### **4.3.2 Specimen Materials**

The materials used in the design and analysis of the prototype subassemblages were Gr 40 steel (bars and transverse reinforcement) and concrete with a value of  $f'_c = 42$  MPa. While the application of the scale factor to the prototype subassemblages resulted in changes in the yield strengths of some of the steel used in the specimens (i.e., the wire used as transverse reinforcement), the scale factor did not result in changes in the average value of the concrete strength used in the specimens. A summary of the materials used appears in Table 9. The bond index (BI) values listed in Table 9 for each of the specimens represents an average value (Sec. 4.1.2, "DCC Category").

## Concrete

The concrete used for both of the specimens was a 7-1/2-sack mix, with a water/cement ratio of 0.43. Type I/II Portland cement was used in the mix, along with river gravel coarse aggregate with a maximum size of 19 mm. Additionally, the mix was air-entrained, and had a water-reducer and a superplasticizer. A local ready-mix plant supplied the mix. The average value of  $f'_c$  at the time of testing was approximately 42 MPa determined using 152 mm by 305 mm test cylinders.

The values of  $f'_c$  shown in Table 9 for the columns are an average of the  $f'_c$  values for the upper and lower columns (each specimen was constructed using two concrete pours; Sec. 4.3.3, "Concrete Placement"). In Unit I the average value of  $f'_c$  for the upper column was 43.7 MPa, while that for the lower column was 38.5 MPa. In Unit II the average value of  $f'_c$  for the upper column was 46.5 MPa, while that for the lower column was 39.9 MPa.

## Steel

The bars used in the columns, as well as the "main bars" used in the struts, were #4 Gr 40 reinforcing bars with an average value of  $f_y$  of approximately 362 MPa. The "intermediate bars" in the struts were #3 Gr 40 reinforcing bars with an average value of  $f_y$  of approximately 402 MPa. The column and joint hoops consisted of D3 wire (ASTM 1985) that had an average value of  $f_y$  of approximately 538 MPa. The closed stirrups used in the struts were 9 Ga wire. The wire was annealed because the mechanical deformation process increased the value of  $f_y$ . The average value of  $f_y$  was 317 MPa, after annealing.

The average values of  $f_y$  for the #4 and #3 bars and for the D3 and D5 wire were determined by tension tests. Prior to the tests, electrical resistance strain gages (ERSG)

were mounted to the bars/wire. During the test, load values were read off of the testing machine display and strain values were read from a strain-indicating instrument. The load values were divided by the original cross-sectional areas (determined at sections of the bars/wire away from the ERSG's). Stress was then plotted against strain, and the values of  $f_y$  were determined from the plots. Figure 39 shows typical stress versus strain curves for the #4 and #3 bars. Figure 40 shows typical stress versus strain curves for the D3 wire. The average value of  $f_y$  for the 9 Ga wire was determined by tension tests. The machine used for these tests was connected to a computer that displayed load versus deformation. The load at which yield of the wire occurred was read off of the display. These loads were then divided by the original cross-sectional areas of the wire to determine  $f_y$ . A typical stress versus strain curve for the 9 Ga wire is shown in Figure 40.

#### 4.3.3 Specimen Construction

The specimens were constructed in four phases. The first phase involved the design and construction of fixtures. Then, shores and forms were built. In the third phase, the reinforcing steel cages were assembled and placed in the forms. The final phase consisted of the placement of the concrete.

##### Fixtures

In order to have the subassembly specimens behave nearly as they would in an actual bent undergoing motion transverse to a bridge, several steel fixtures were required. In addition, steel fixtures were also required to brace the specimens against out-of-plane motion, and to connect the load actuators to the specimens. Herein, all dimensions are in mm, "Ø" implies "diameter", and "x" implies "by".

*"Response" fixtures* There were three fixtures required to simulate actual response conditions: two designed to behave as "rollers" at the free ends of the struts in the specimens, and one designed to behave as a "pin" at the bottom of the lower columns in the specimens (Figs. 41 and 42).

Each of the "roller" structures consisted of:

- 1.) a 445-kN, floor-mounted swivel,
- 2.) a 64  $\text{\O}$  x 318-long standard weight steel pipe with threaded adapters at each of the ends of the pipe (the threaded adapters were welded to 25-thick steel plates that were welded to the pipe ends),
- 3.) a 445-kN load cell,
- 4.) a 45  $\text{\O}$  x 330-long, threaded rod, and
- 5.) a yoke assembly made from 152-wide x 102-long x 25-thick steel plates, 152 x 508 x 25 steel plates, 127 x 127 x 6-thick tube steel, and a 51  $\text{\O}$  x 381-long 4140 HT steel rod.

The tube steel served as the base of the yoke assembly, while the plates served as the sides. The steel rod, which was held in the specimens by the steel "sleeves" that were cast in the struts (Figs. 36 and 37; openings at the free ends of the struts), was cradled by the 152 x 508 plates. The 152 x 102 plates were bolted to the 152 x 508 plates to prevent the supported strut ends from pulling away from the fixtures. The plates were bolted together after the strut was positioned, and after the steel rod was passed through the greased "sleeve". The threaded adapters at the pipe ends were connected to the swivel and to the underside of the load cell. The threaded rod connected the top of the load cell to the base of the yoke assembly (the tube steel). Three 45  $\text{\O}$  nuts were placed on the threaded rod (one at the load cell, one underneath the tube steel, and one above the tube steel) to allow for height adjustment of the yoke assembly while the specimens were being positioning. The components of the two-force "roller" structures were designed to carry the axial load caused by the maximum expected reaction at the strut ends (determined from *SAP90* analyses of the specimens).

The "pin" structure consisted of a 222-kN floor-mounted swivel, and three 610 x 610 x 25 steel plates (Fig. 42). The bottom steel plate was bolted to the top plate of the swivel. The upper two steel plates were bolted to the bottom steel plate. These upper plates had 508  $\varnothing$  holes in their centers to accommodate the columns of the specimens. In this way, the columns were prevented from sliding off of the fixture. All connections were designed for the maximum amount of shear anticipated (determined from *SAP90* analyses). The bottom steel plate was checked for corner warping ("dishing"). The dead load of each specimen and the applied axial load were summed and these sums were checked against the swivel capacity.

*"Brace" fixtures* In order to prevent the specimens from moving out of the plane of the applied lateral load, a brace was required in-between the column and the ends of the struts in each specimen (Fig. 43). The components of each brace were:

- 1.) a steel W 8 x 18 column that was welded to a floor plate,
- 2.) two pieces of 5-thick tube steel; 76 x 76 x 508-long horizontal section and 127 x 127 x 762-long vertical section,
- 3.) eight all-thread-mounted ball casters (four per side), and
- 4.) an 16  $\varnothing$  x 1016 all-thread rod.

The horizontal section of tube steel was welded to the column flange, while the vertical section of tube steel was welded to the horizontal section. The ball caster assemblies on one side were mounted on the vertical section of tube steel, while those on the other side were mounted on the column flange. The top of the vertical section of tube steel was connected to the top of the column with the all-thread rod to strengthen that side of the brace. The specimen was held in-plane by the action of the ball caster assemblies rolling on steel plates that were epoxied to the sides of the struts. With the exception of the ball casters, the components of the "brace" structures were designed to carry loads resulting from eight percent of the maximum anticipated lateral load (i.e., the total capacity of two braces was sixteen percent). The capacity of each group of four ball caster assemblies was

about three percent of the maximum anticipated lateral load. However, to ensure against the ball casters "locking up", grease was applied to the strut-mounted plates.

*"Load actuator" fixtures* The fixtures required to attach the axial and lateral load actuators to the specimens consisted of swivels and steel plates. In the case of the axial load actuator, the actuator piston was connected to the top of a swivel. A plate that rested on top of the columns was bolted to the swivel base plate. The swivel allowed for the lateral displacement of the specimens. To prevent the plate that rested on top of the columns from sliding, steel tabs were welded on the plate in a circular pattern in accordance with the respective column diameters.

The lateral load actuator has swivels pre-attached to both ends. Thus, two 610-wide x 407-long x 25 steel plates and four 32  $\varnothing$  x 914 all-thread rods were required to hold the specimen-end of the actuator to the tops of the upper columns (Fig. 44). The plates and the rods in effect "sandwiched" the columns. To assist the flat plates in "grabbing" the circular-shaped columns, two 762 x 76 x 6, 406-long steel angles were welded on to each plate.

Figure 45 shows all of the fixtures in place (45a is a front view and 45b is a rear view).

### Shoring and Formwork

In order to duplicate "as-built" construction practice the specimens were constructed standing upright. Thus, to support the formwork and the concrete for the struts, shores were built. Figure 46 shows the shoring and the formwork after concrete from the first pour was placed (resulting in the "T"-portions of the cruciforms). The upper column forms were put in place after the first concrete pour. Figure 47 shows the upper column form for Unit I and the associated bracing prior to placement of the concrete from the second pour.

### Reinforcement Cages

The sequence of events in the construction of the reinforcing steel cages was as follows. Each bar and wire was bent, the ERSG's were mounted (Sec. 4.3.4, "Bar and Hoop Strain Measurements"), and finally the reinforcement cages were assembled.

*Bar/wire bending* All bend diameters and tail and lap lengths were as specified on the structural drawings (with account taken for the scale factor for tail and lap lengths). In those instances where specifications were not provided on the structural drawings, the building codes that were in affect at the time that the bridges were designed were consulted (Washington Standard Specifications 1963).

*Cage assembly* The cages for the struts and for the columns were assembled separately. The two strut cages (one for each specimen) were each assembled horizontally with the aid of three wooden stocks that were placed near the center and the ends of the cages. The stocks were constructed such that the main bars and the intermediate bars could be held in the proper alignment while the stirrups were positioned and tied in place.

The "stirrups" (two 9 Ga wire stirrups = a "stirrup", Figure 36) were positioned on each cage starting from a mark established at the centerline (this represented the centerlines of the columns as well). The column radius was marked off on each side of the centerline mark. Approximately 25 mm were added in each direction to account for the likelihood that in the "as-built" bents the first stirrup on each of the column sides is located some distance away from the column (the actual location of the first stirrup was not shown on the structural drawings). The first "stirrups" on each of the column sides were then tied on to the cage. The remaining "stirrups" were then tied in place in accordance with the spacing shown in Figures 36 and 37.

Once the stirrups were tied, the cages were released from the stocks. The two hoops in the joint region of each specimen were then appropriately placed and tied into the

cages. The last step in the assembly of the strut cages involved attaching the "sleeves" for the "roller" support fixtures to the cages.

The upper and lower column cages were assembled separately (to allow the lap splice to be built following the first concrete pour). The column cages were assembled upright with the aid of two plywood disc forms that were placed at points along the heights of the cages. The forms had semicircles cut at appropriate locations around their circumferences. The depths of the semicircles were approximately one-half of the diameter of a #4 bar. This allowed the #4 bars to be secured against the forms with steel bands while the hoops were being positioned and tied in place. The procedure for tying the hoops in place was similar to the procedure used for the strut stirrups, except that the two hoops at the edges of the joint region (top and bottom of joint, Figs. 36 and 37) were positioned first. As shown in Figs. 36 and 37, this resulted in the hoops being located at the design spacing, with the exception of the hoop at the bottom and the hoop at the top of the columns. Once the hoops were tied in place, the bands holding the bars against the wood forms were cut and the forms were taken out. Figures 48-51 show the finished cage for the Unit I struts, an end-on view of a "sleeve" region in the finished cage for the struts in Unit I, the finished lower column cage for Unit I, and the finished lower column cage for Unit II, respectively.

Once all of the cages were constructed, they were placed in the forms as follows. First the lower column cages were placed into the lower column forms. The tops of each lower column cage extended above the top of the strut forms by a distance equal to the lap splice length. Then, each strut cage was put into the strut forms by lowering the cage through the intersecting column bars. At this time, the two joint hoops that were attached to the strut cage were freed and tied to the column cage. Figure 52 shows the cages for the lower column and the struts inside the forms of Unit II. Figure 53 is similar to Figure 52, except that it focuses on the joint region. Prior to the second concrete pour, the upper

column cages were placed on top of the joints and tied to the lower column cages (Fig. 47, foreground).

#### Concrete Placement

The concrete was placed in two pours. The first pour consisted of the struts and the lower columns. One week later, the upper columns were poured. The upper columns were allowed to cure in the forms for one week, then all formwork was removed (Fig. 54). Vibrators were used to consolidate the concrete in both pours. The specimens then cured for an additional 2-1/2 months before Unit I was tested. Unit II was tested approximately one month later. The test cylinders for each of the specimens were tested when the specimens were tested. Additionally, each specimen received a coat of flat, white-white, interior latex paint to enhance the visibility of cracks in photographs taken during and after testing.

#### **4.3.4 Specimen Instrumentation**

Throughout the tests, measurements were made of applied loads, lateral displacements of the tops of the upper columns, joint distortions, member rotations, bar and hoop strains, and reactions at the free ends of the struts in both specimens.

#### Applied Load and Lateral Displacement Measurements

The loads from the lateral actuator were measured with a load cell that was mounted on the actuator. The configuration of the specimens made it possible to use the actuator LVDT (linear variable differential transformer) for the measurement of the displacements of the specimens (i.e., since the bottom of each specimen was pinned at one column inflection

point and the actuator was mounted at the other, the LVDT was measuring "inter-story drift").

The hydraulic pressure required to deliver the axial load of 177.9 kN for both of the test specimens was set with a pressure gage. The appropriate pressure was determined using a calibration curve for the system.

Additional comments regarding the lateral load and the axial load actuators are made in Section 4.3.5, "Loading".

#### Joint Distortion and Member Rotation Measurements

The joint distortions and the member rotations were measured with an array of potentiometers (pots.) and LVDT's (Fig. 55). The pots. that were used have a 50.8 mm stroke, while that for the LVDT's that were used is 101.6 mm. Each pot./LVDT measures the change in distance between the two fixed points (all-thread anchors) to which it is attached. Specially designed rigs were used to mount the pots./LVDT's between the anchors (Fig. 56).

Each of the LVDT rigs was composed of two self-aligning bearings, two anodized aluminum angles, and four nylon clips. The base of the bearings were attached to one end of the angles. The heads of the bearings were slid over the all-thread anchors, where they were held in place with nuts. Spacers were used on the anchors to separate the bearings as necessary to prevent interference. The free ends of the two angles were "lap spliced" using the nylon clips. The nylon clips were rigidly attached to one angle and allowed the other angle to slide freely. In each rig, the LVDT housing was mounted on one angle, while the core was mounted on the other. With the ends of the rigs free to rotate at the all-thread anchors, the slip between the angles (hence the measurements by the LVDT's) was due only to the linear displacements between the anchors. Prior to conducting the specimen

tests, the LVDT's were calibrated in the rigs to ensure that the rigs were not altering the performance of the instruments.

The pot. rigs were the same in principle as the LVDT rigs. However, the lighter weight of the pots, allowed for simpler rigs. On one end of each rig, a piece of PVC pipe connected the bearing to the pot. housing. On the other end of a rig, the pot. core threaded into an adapter that was attached to a bearing. The rigs were then positioned by placing the heads of the bearings on the all-thread anchors.

Each of the all-thread anchors was mounted into the core of the members so that the anchors would be isolated from spalling of the concrete cover. The all-thread anchors located nearest to the three reaction points were situated as shown in Figure 55 in order to prevent disturbance either during placement of the specimens in the fixtures or during the response of the specimens during the tests. The anchor at the top of the upper column was located as shown in order to be at the line of action of the lateral load actuator.

#### Bar and Hoop Strain Measurements

The strains in the bars and in the hoops were measured with bonded precision ERSG's. After mounting the ERSG's on the bars and on the hoops, the gages were coated to protect them from water and shock damage. The locations of the ERSG's are shown in Figure 57. The stirrups did not have any ERSG's. Therefore, the stirrups are omitted from Figure 57 for clarity. Additionally, Figure 57a shows the column bars radially lap-spliced for clarity. As shown in Figure 57a, two strut bars and two column bars had ERSG's. Figure 57b clarifies the locations of these bars. Note the two adjacent ERSG's in the lap splice region and the two ERSG's on each of the two hoops inside the joint. In general, the layout of the ERSG's was designed to get the most information possible by using the maximum number of ERSG's that the data acquisition system would permit. The layout also features redundancy in anticipation of gage failures.

The ERSG's located farthest from the joint region were located in the positions shown because it was expected that these locations would approximate the ends of the flexural plastic hinge regions. Two of these ERSG's were used adjacent to one another in the lap splice region in order to discern failure in the splices (i.e., inability to transfer the same forces from bending action).

The ERSG's at the perimeter of the joint region were located in the positions shown because it was expected that these locations would experience the largest moments. In addition, these ERSG's, along with the ERSG's on the bars inside the joint, would give an indication of how forces were being transferred through the joint, and of the bond conditions in the joint.

The ERSG's located on the hoops were located in the positions shown because it was expected that these locations would experience the largest stresses due to the combination of shear transfer and confinement. The use of two ERSG's on each of the hoops in the joint was for redundancy.

#### Strut End Reaction Measurements

The reactions at each of the free ends of the struts were measured using a 444.8-kN load cell (Fig. 41). Knowledge of these reactions was required to render the subassemblages determinate.

#### **4.3.5 Test Set-Up**

The "pin" and "roller" fixtures were mounted in the test frame, then the specimen was positioned on the fixtures. The lateral and axial load actuators were then mounted to the test frame and to the specimen. The following describes these features of the test set-up in greater detail.

### Test Frame

Figure 58 shows Unit I in the test frame, along with the actuators and all of the fixtures. While the struts were cast monolithically with the B-C joint region, there are light vertical lines shown in the figure where the struts meet the joints. The lines were drawn to represent the intersection of the rectangular struts and the round B-C joint. The height-adjustable beam in the test frame is a W18x119 section. The columns in the test frame are W14x90 sections. The diagonal brace on the right-hand side of the test frame is a W8x18 section.

As discussed in Section 4.3.3, "Fixtures", the fixtures were designed to allow the specimens to displace laterally in the plane of the frame only. As per Section 4.3.1, "The Specimens", the specimen as shown is rotated 180° in-plane from the position in which it was constructed (i.e., the construction joint and column bar lap splice are below the B-C joint). Thus, the distance from the line of action of the lateral load actuator to the top of the B-C joint is less than the distance from the bottom of the B-C joint to the lower pin support. Also, the length of the moment arm for the lower column (the distance from the pivot point in the "pin" support fixture to the bottom of the B-C joint) equals:

$$914 \text{ mm (Fig. 38b)} + 120.7 \text{ mm (the distance from the pivot point in the "pin" support fixture to the bottom of the lower column)} = 103.5 \text{ cm .}$$

### Loading

The load actuator systems shown in Figure 58 allowed horizontal shears (without any moment) and the constant vertical load to be applied. The following are descriptions of the lateral and vertical load actuator systems.

*Vertical load actuator system* The vertical load actuator system consisted of a hydraulically-controlled, 889.6-kN ram (152.4-cm stroke), mounted on a roller bearing trolley device attached underneath the test frame beam. The ram was connected to the specimen with a swivel. Thus, the loading system remained vertical and centered on the upper columns of the specimens regardless of the lateral displacement. Prior to conducting specimen tests with this system, the system was calibrated to determine the friction that would be developed between the "roller device" and the test frame. The tests indicated that the friction values were negligible and repeatable values, as long as the axial load did not exceed 222.4 kN. This value exceeds the 178 kN required. Once the design axial load was applied, the system ran for the duration of the tests, with only occasional minor corrections to maintain the constant axial load.

*Lateral load actuator system* The lateral load actuator system consisted of a 978.6-kN, MTS servo-controlled hydraulic actuator, with a 50.8-cm stroke. This actuator is equipped with swivels at the head and base, and with a load cell and an LVDT. The swivels allowed for the application of pure shear to the upper column tops of the specimens. The load cell and the LVDT provided continuous signals corresponding to load and displacement.

#### **4.3.6 Testing Procedures**

The testing procedures included the data acquisition process, the displacement histories that the specimens were subjected to and the method by which the tests were conducted.

### Data Acquisition

In all, 44 channels of data were collected during each of the tests on an electronic high-speed data acquisition system. All of the instruments were connected to a digital computer, which collected and recorded the incoming data. A computer-based data acquisition program also displayed the lateral load value and LVDT displacement continuously on the monitor during the tests. These load versus displacement hysteresis curves were the primary means of observing the progress of the tests, particularly with regard to determining yield of the specimens. Data from the ERSG's located on the member bars at the faces of the joint region were also monitored to aid in the determination of specimen yield.

### Displacement Histories

Each of the specimens was tested by subjecting it to quasi-static, reversed-cyclic loading, via displacement-control of the lateral load actuator. Displacement-control of the actuator was accomplished by the computer. Initially, each specimen was cycled twice to displacements of 2.54 mm (displacement from 0.0 to 2.54 to -2.54 to 0.0 mm constitutes one cycle) in order to obtain the initial stiffness of the specimens. These initial cycles were conducted to ensure that all aspects of the test were performing properly as well. Next, the specimens were cycled three times at each of seven displacements from 5.08 to 20.32 mm (where the displacements were incremented by 2.54 mm each time). Figure 59 depicts the displacement histories used during the tests.

In both specimens, yield was determined to have occurred during cycling to 20.32 mm. Thus, 20.32 mm was referred to as  $\Delta_y$ . Determination of  $\Delta_y$  was accomplished by a combination of the following:

- 1.) consideration of the envelope of the hysteresis loop peaks, and

2.) approximation of the hysteretic response as an elastic-perfectly plastic model.

Figure 60 depicts how "1.)" and "2.)" were used to determine  $\Delta_y$  for the specimens. In words,  $\Delta_y$  was presumed to have occurred when the envelope of the hysteresis loop peaks indicated that a significant change in stiffness had taken place (relative to the changes in stiffness up to that point).

Displacement cycling then proceeded at increments of 1.25, 1.5, 2, 2.5, 3, 4, 5 and  $6\Delta_y$ , with three cycles conducted at each of the displacements. Finally, a "push-over" sequence, consisting of two cycles to displacements limited by either the ram stroke, the fixture ranges, and/or the specimen capacity, was conducted via manual-control of the lateral load actuator.

### Test Conduct Methodology

Prior to conducting the tests, the design axial load was applied to the specimens with the "roller" support fixtures at the free ends of the struts released (i.e., the nuts above and below the tube steel in the yoke assemblies were loosened; Figure 41). This procedure allowed the entire structure to deflect under the action of vertical loads. Since resistance to deflection at the free ends of the struts would introduce fictitious moments at the B-C joints and would reduce the axial load in the lower column, the "roller" support fixtures were not "tightened" until the specimens were in the compressed positions.

Limit analyses with SAP90 indicated that  $\Delta_y$  for the specimens would be approximately 6.35 mm. These analyses were conducted with the actual bar and wire strengths. Because the test cylinders were not broken until after the tests were conducted,  $f'_c$  values of 42 MPa were assumed (fortuitously, the average strength of the concrete actually used was 42 MPa; Section 4.3.2, "Concrete"). Thus, after cycling twice to 2.54 mm with Unit I to obtain the initial stiffness, the test plan called for cycling three times to 5.08 and then to 7.62 mm. With this method it was anticipated that the actual value of  $\Delta_y$

for Unit I could be determined. Once  $\Delta_y$  was determined, each displacement increment was to consist of three cycles at multiples of  $\Delta_y$ , depending on how the degradation in the behavior of Unit I proceeded. Due to the fact that Unit I was much more flexible than what was predicted by SAP90,  $\Delta_y$  did not occur by the time cycling to 7.62 mm was completed. The methodology then employed was to continue to increment the displacement cycles by 2.54 mm until Unit I was determined to have yielded. Finally, at cycles to 20.32 mm,  $\Delta_y$  occurred. Unit I was then cycled three times at each of the various multiples of  $\Delta_y$  shown in Figure 59. In order to maintain uniformity in the testing procedure for both specimens, thereby enabling direct comparisons in the behavior of the two specimens to be made, it was decided to subject Unit II to all of the cycles below  $\Delta_y$  that Unit I was subjected to. As it turned out,  $\Delta_y$  for Unit II was identical to that for Unit I. Thus, the same multiples of  $\Delta_y$  were used for Unit II, post-yield, as were used for Unit I.

Due to length of time involved with the execution of each set of three cycles and due to the number of sets of three cycles, each subassembly test took several days to complete. At the end of each day, with the specimens at zero displacement (i.e., the lateral load actuator was at 0.0 mm displacement and at some force greater than 0.0 kN), the axial load was released with the strut "roller" fixtures "loosened". Then, the strut "roller" fixtures were "tightened" and the lateral load actuator was turned off. In this way, the specimens were kept in the "zero-displacement" position until the testing was resumed the next day.

**Table 5** Results from the evaluation of double-column bents with rectangular columns (DRC).

$M_{nc}/M_{nb}$	0.7 - 5.3
$v_{jt}^*$ (MPa)	$0.04 - 0.68\sqrt{f'_c}$
$v_b^*$ (MPa)	$0.06 - 0.4\sqrt{f'_c}$
SAD	unsatisfactory
CAD	satisfactory
$T_n$ (s)	1 - 2

**Table 6** Results from the evaluation of multiple-column bents with rectangular columns (MRC category).

$\Sigma M_{nc}/\Sigma M_{nb}$	0.8 - 4.0 (2.0)
$v_{jt}^*$ (MPa)	$0.08 - 0.98\sqrt{f'_c}$ (0.4)
$v_b^*$ (MPa)	$0.08 - 0.86\sqrt{f'_c}$ (0.34)
$SAD_{ext}$	unsat. - sat. (unsat.)
$SAD_{int}$	unsat. - sat. (sat.)
CAD	unsat. - sat. (sat.)
$T_n$ (s)	0.08 - 4.4 (0.80)

Table 7 Results from the evaluation of double-column bents with circular columns (DCC category).

$M_{nc}/M_{nb}$	1.6
$v_{jt}^*$ (MPa)	$0.15\sqrt{f'_c}$
$v_b^*$ (MPa)	$0.11\sqrt{f'_c}$
SAD	satisfactory
CAD	satisfactory
$T_n$ (s)	0.4

Table 8 Results from the evaluation of multiple-column bents with circular columns (MCC category).

$\Sigma M_{nc}/\Sigma M_{nb}$	0.5 - 1.9
$v_{jt}^*$ (MPa)	$0.17 - 0.47\sqrt{f'_c}$
$v_b^*$ (MPa)	$0.11 - 0.21\sqrt{f'_c}$
$SAD_{ext}$	satisfactory
$SAD_{int}$	satisfactory
CAD	satisfactory
$T_n$ (s)	0.5 - 0.8

Table 9 Material properties of Units I and II.

Specimen	Unit I	Unit II
Strut	(304.8x482.6 mm)	(304.8x482.6 mm)
$f'_c$ (MPa)	49.2	46.5
Main Bars	4-#4	4-#4
$A_s/A_s'$ (mm <sup>2</sup> )	516.1	516.1
$t$ (%)	0.37	0.37
$f_y$ (MPa)	362.8	355.1
Intermediate Bars	2-#3	2-#3
$A_u/A_l$ (mm <sup>2</sup> )	141.9	141.9
$f_y$ (MPa)	401.6	401.6
Stirrups	2-9 Ga @ 120.7	2-9 Ga @ 120.7
$w$ (%)	0.2	0.2
$f_y$ (MPa)	317.2	317.2
Column	(482.6 mm dia.)	(355.6 mm dia.)
$f'_c$ (MPa)	41.1	43.2
Total bars	12-#4	8-#4
$A_{st}$ (mm <sup>2</sup> )	1548.4	1032.2
$g$ (%)	0.9	1.0
$f_y$ (MPa)	362.4	366.4
Hoops	D3 @ 178	D3 @ 178
$w$ (%)	0.1	0.1
$f_y$ (MPa)	537.8	537.8
Axial load (kN)	177.9	177.9
Joint		
$f'_c$ (MPa)	43.7	46.5
BI	0.8	1.1
Hoops	2-D3	2-D3
$A_h$ (mm <sup>2</sup> )	39.9	39.9
$s$ (%)	0.1	0.1
$f_y$ (MPa)	537.8	537.8

Note:  $A_s/A_s'$  = area of bottom/top bars,  
 $t$  = tension reinforcement ratio for bottom/top bars,  
 $w$  (%) = web reinforcement ratio (ratio of volume of steel to volume of confined core),  
 $A_u/A_l$  = area of upper/lower layer of intermediate bars,  
 $A_{st}$  = total area of column bars,  
 $g$  = gross reinforcement ratio,  
 $A_h$  = total area of hoops placed between the top & bottom beam bars in the joint,  
 $s$  = volumetric hoop ratio defined by Equation 6 (Chap. 3),  
 $f_y$  = steel yield strength,  
 $f'_c$  = concrete compressive strength,  
BI = bond index defined by Equation 9.

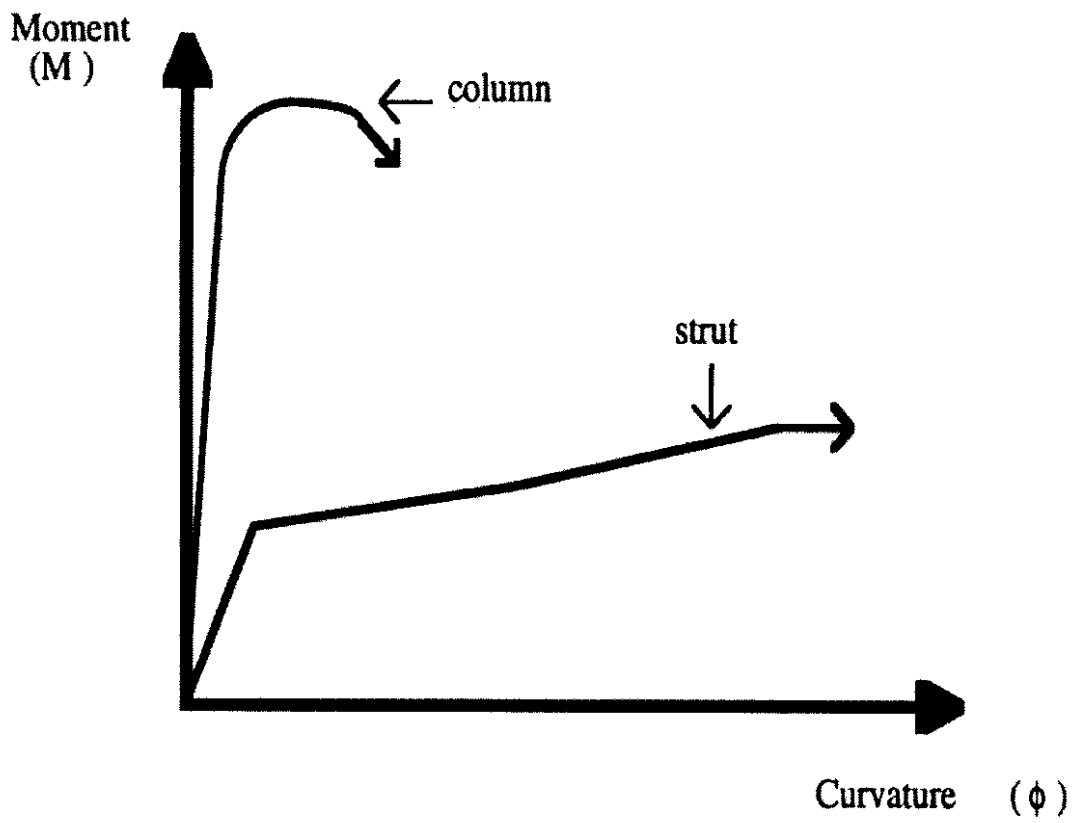


Figure 25 Typical M- $\phi$  relations for the columns and for the struts in the inventory.



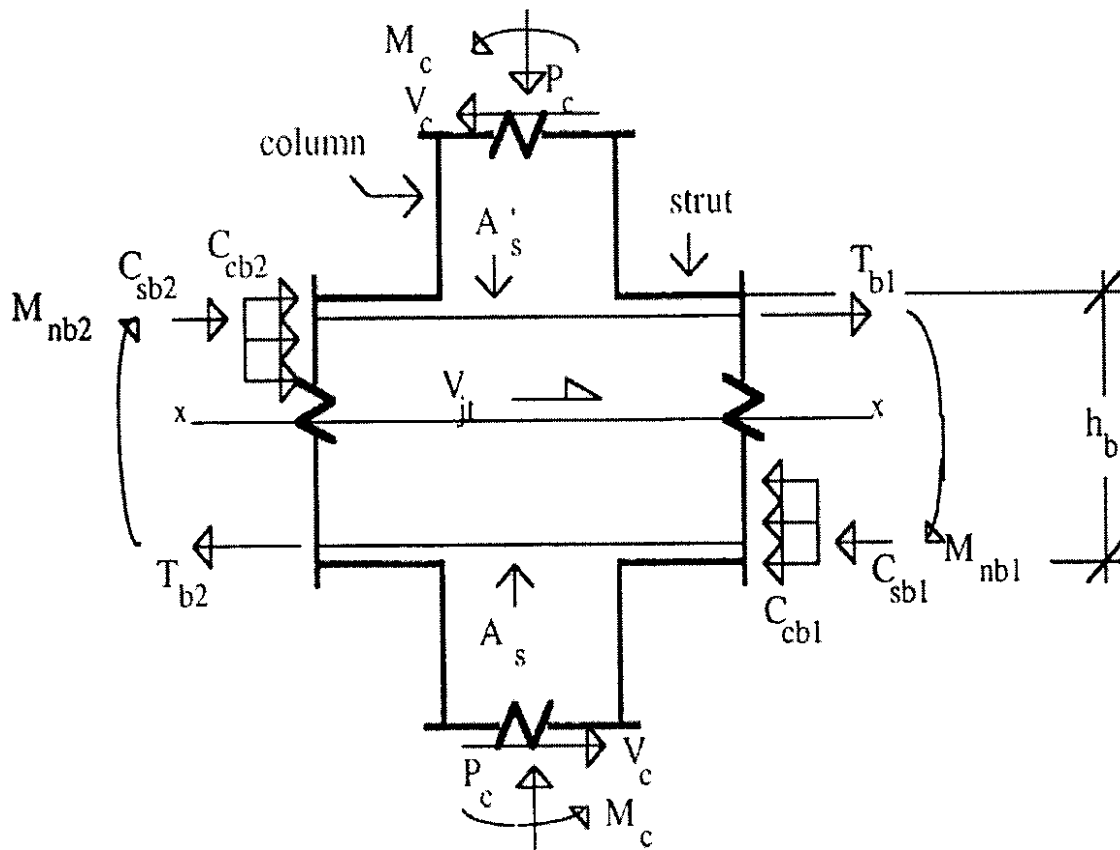


Figure 27 Actions on an interior joint that determine  $v_{jt}^*$ .

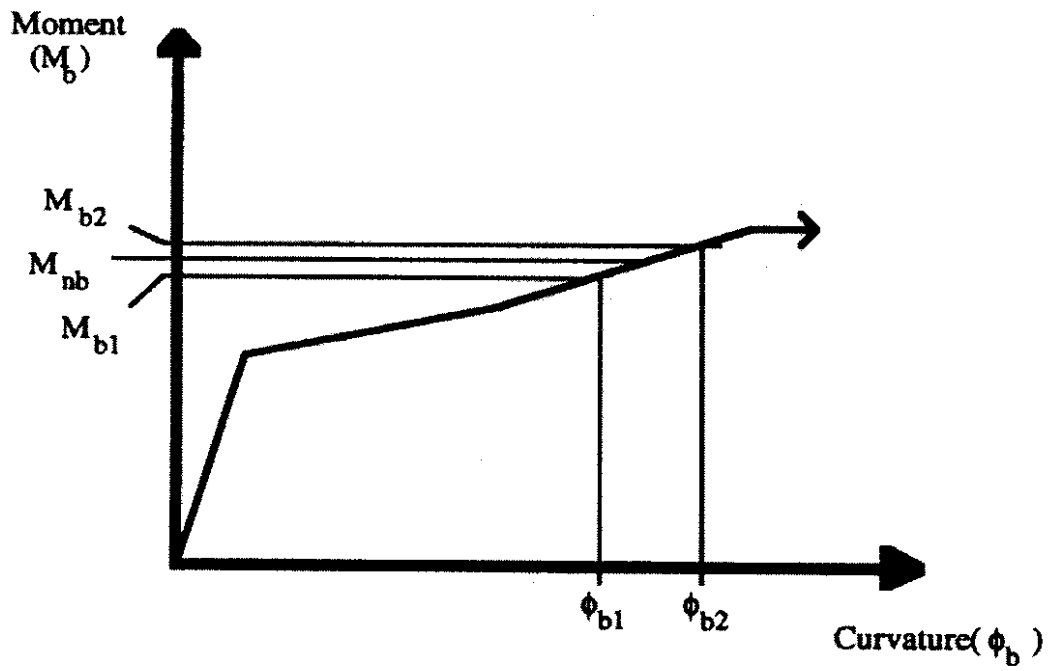


Figure 28 Typical  $M-\phi$  relation for the struts in the inventory.

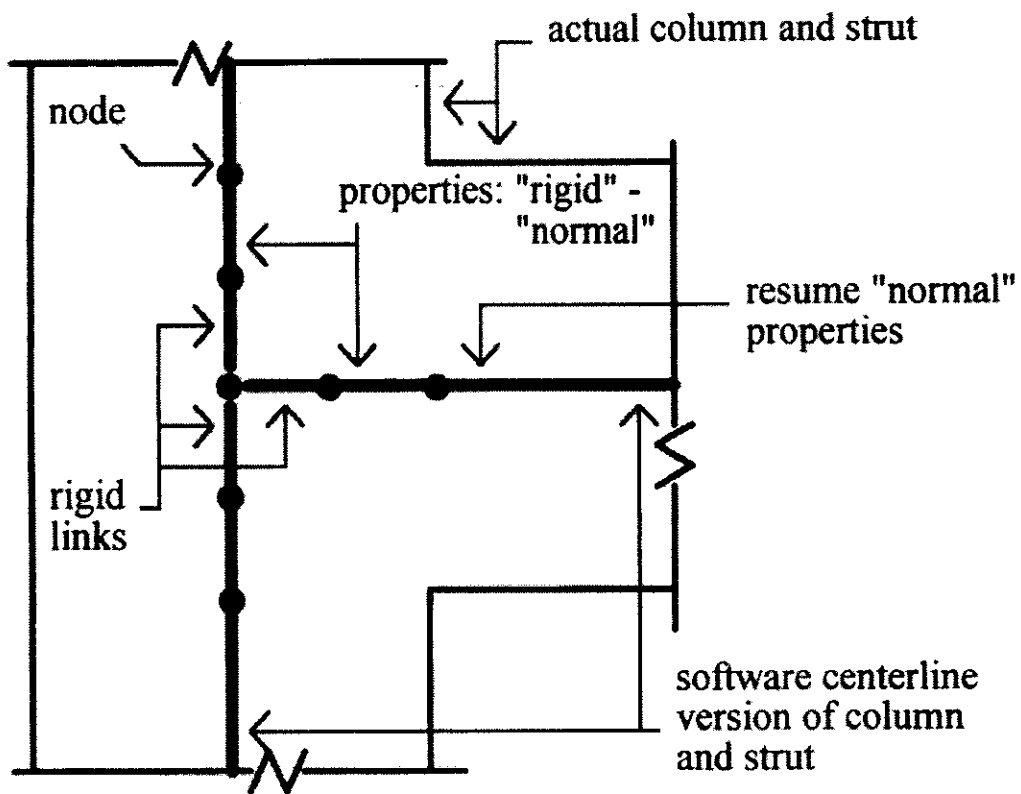


Figure 29 Actual finite member sizes at a joint and the centerline-to-centerline geometry used by the *EPFO* and the *IDARC* software.

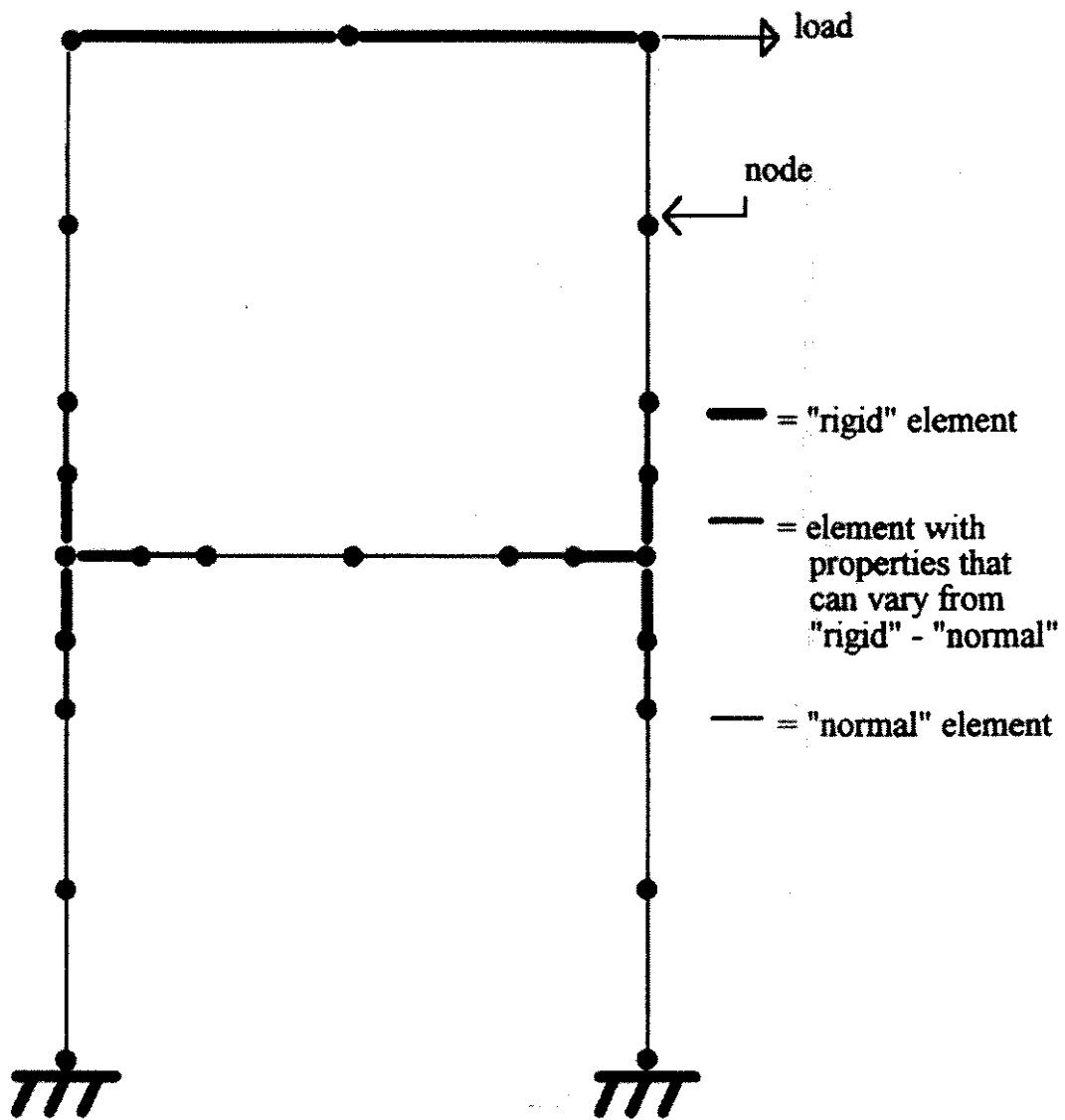
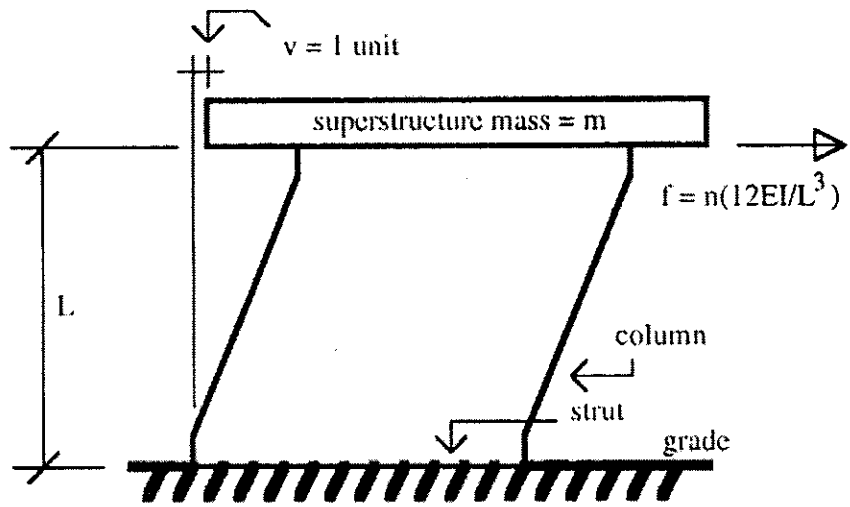
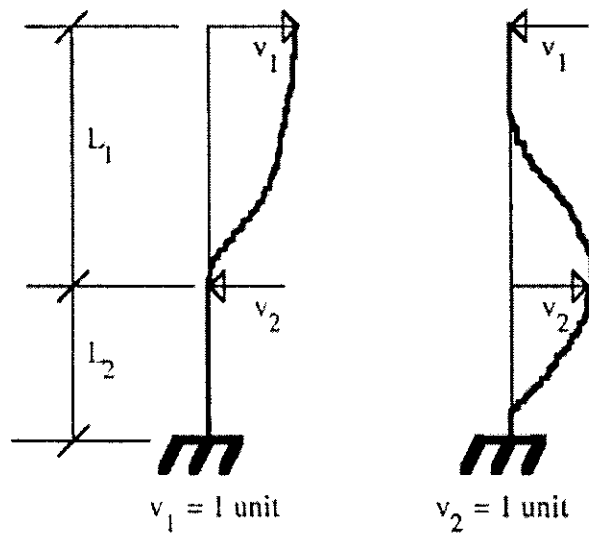


Figure 30 Typical model of a bent used for limit analyses in the *EPFO* and the *IDARC* software.

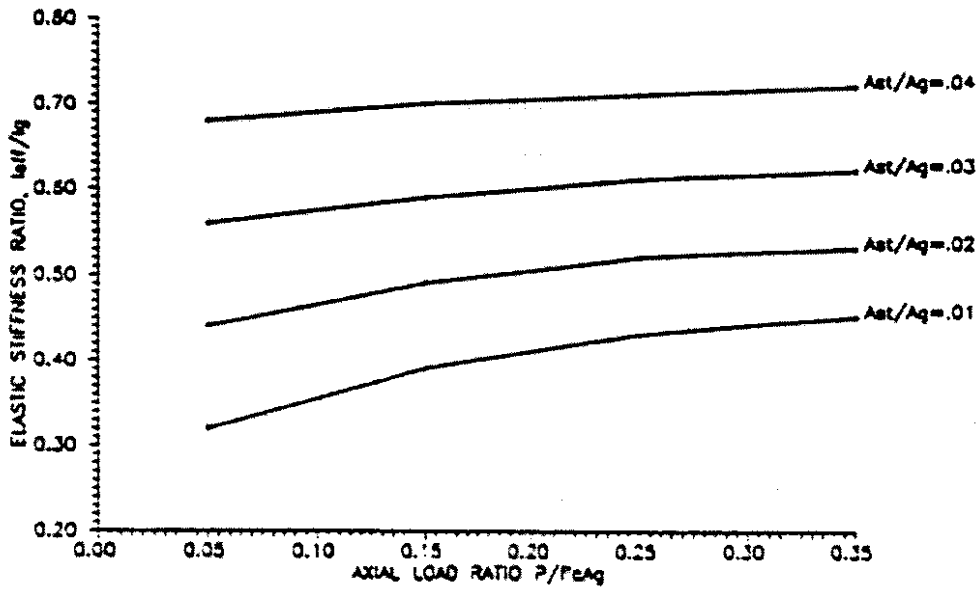


a) Bents with struts at grade

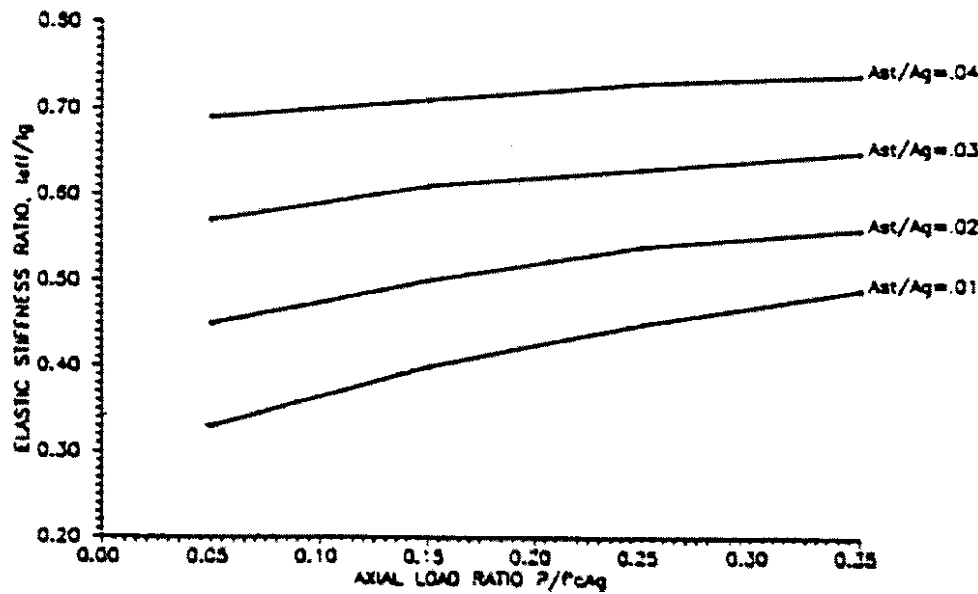


b) Degrees of freedom used to derive matrix  $k$  in bents with struts above grade

Figure 31 Determination of bent stiffness ( $k$ ) values for computation of  $T_n$  values.



(a) Circular Sections



(b) Rectangular Sections

Figure 32 Determination of values of the effective moment of inertia ( $I_{eff}$ ). (from Priestley 1991)

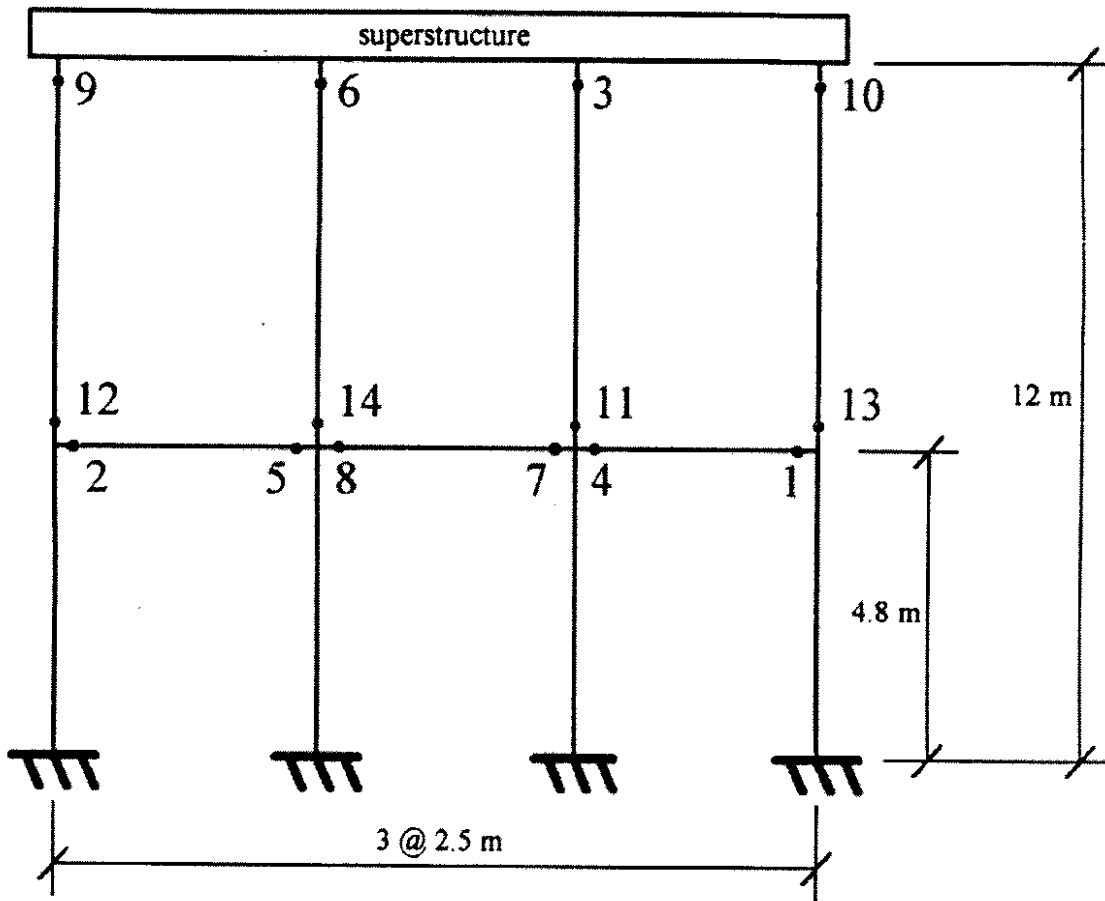
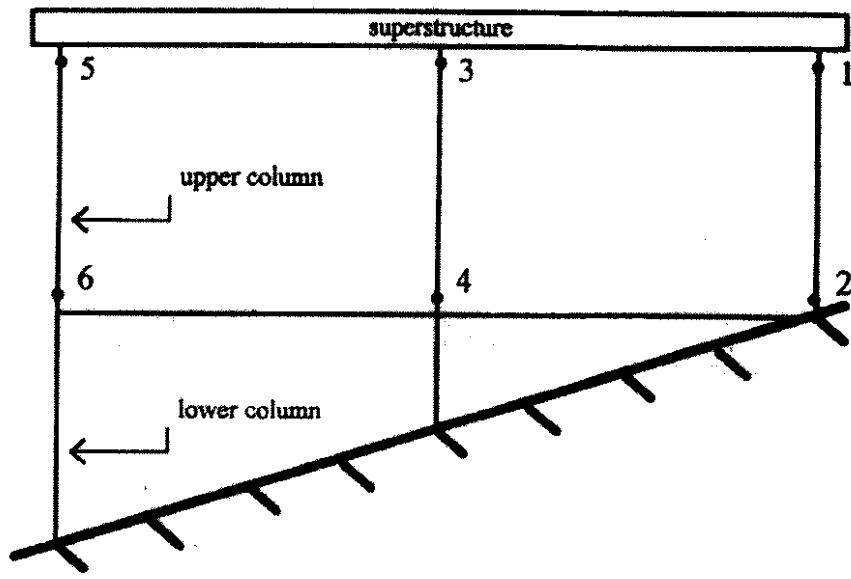
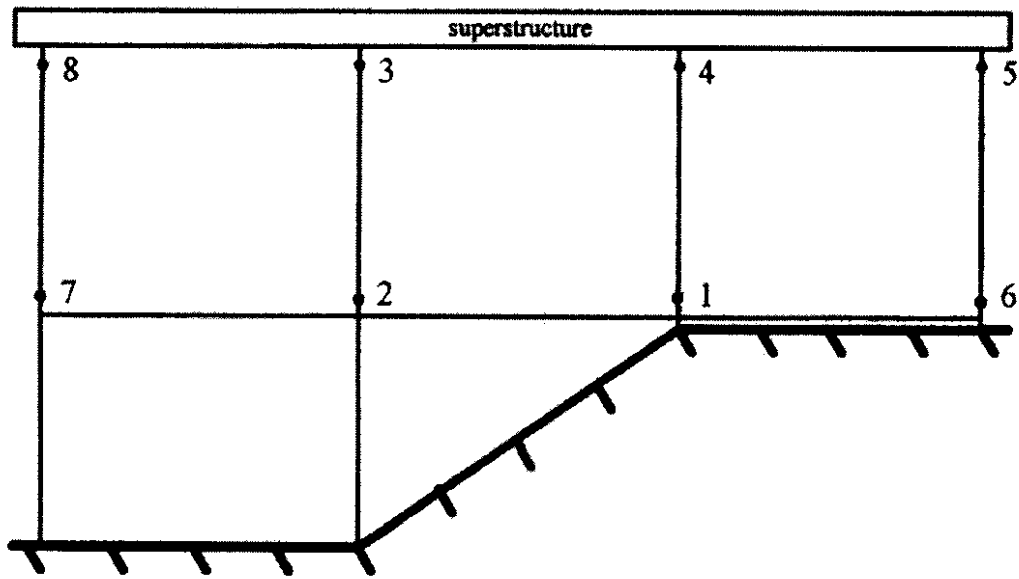


Figure 33 Model bent used to represent the flexural hinge formation sequence in multiple-column bents with rectangular columns.

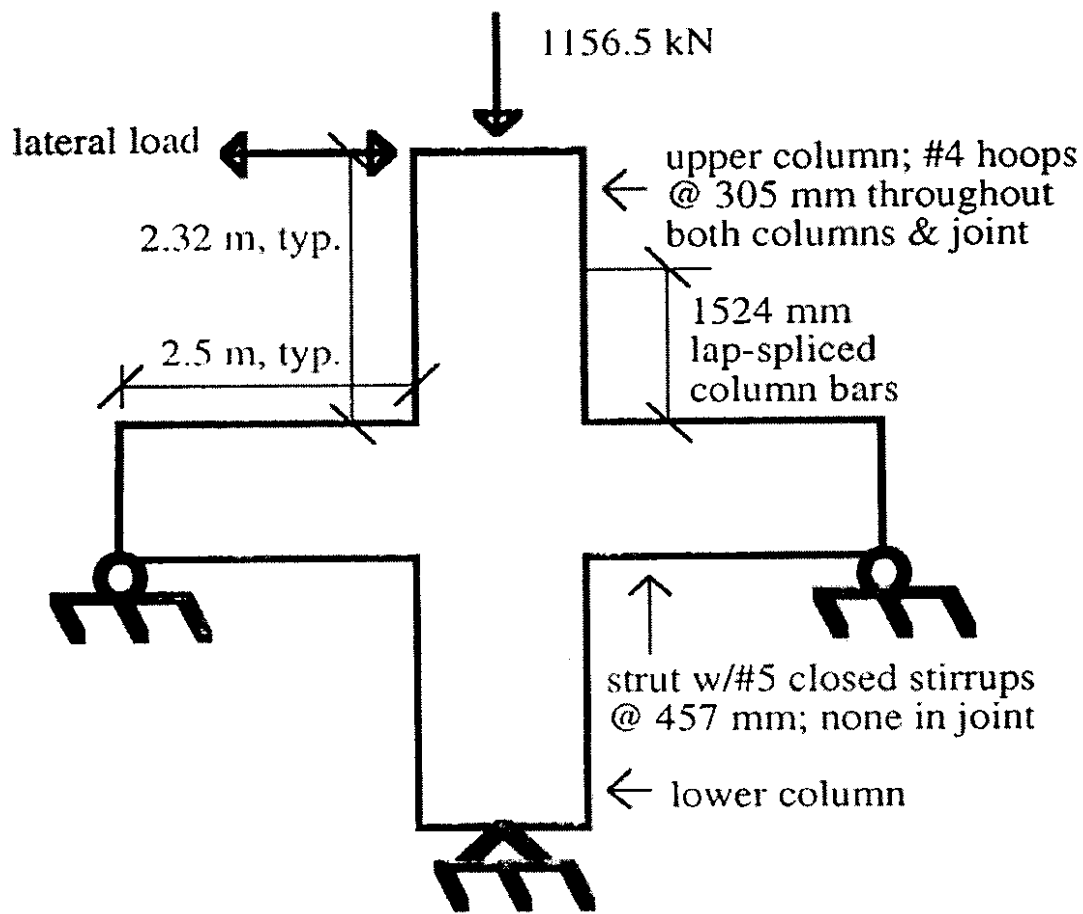


a) A hinge formation sequence in a three-column bent

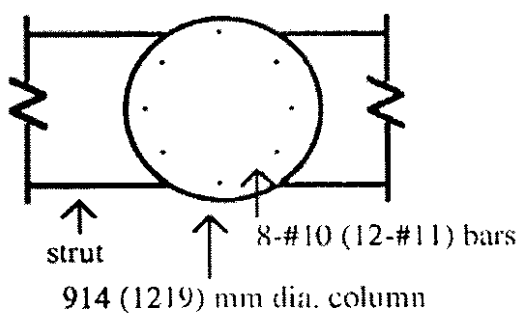


b) Typical hinge formation sequence in a four-column bent

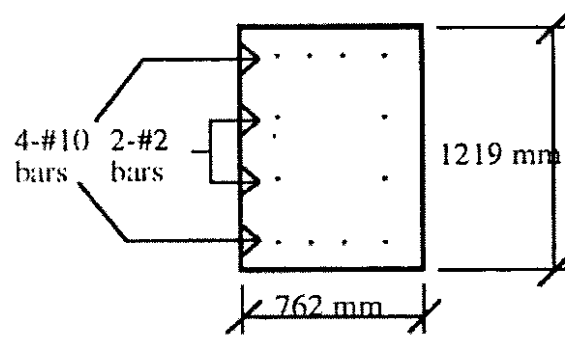
Figure 34 Some of the results from the flexural hinge formation sequence analyses for multiple-column bents with circular columns.



a) Elevation

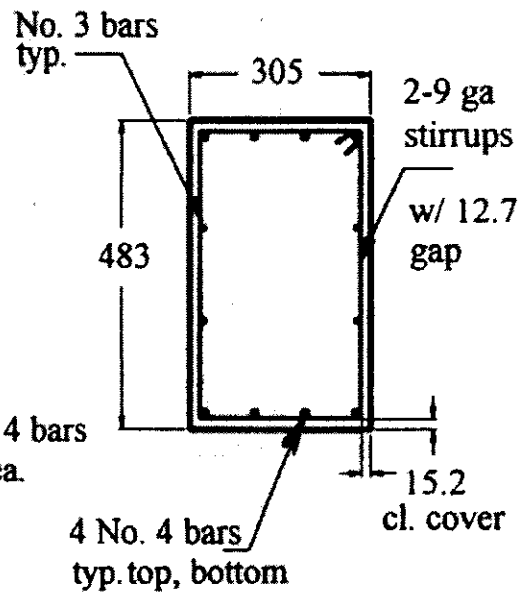
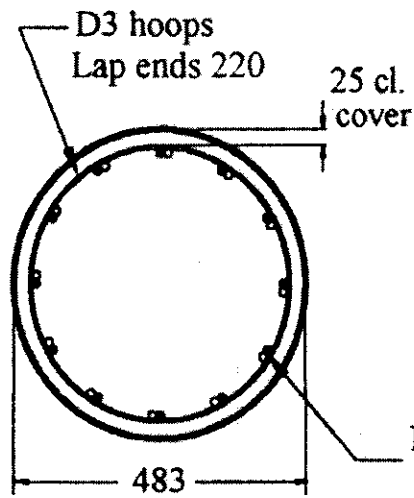
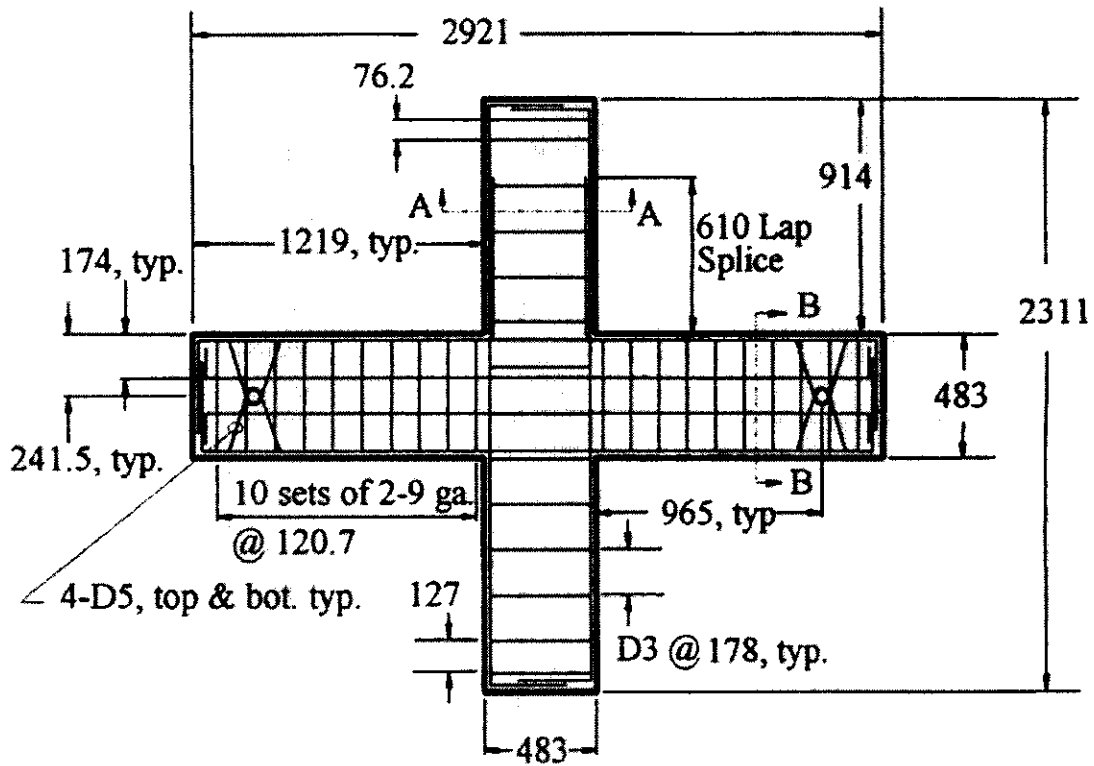


b) Typical column cross-section



c) Typical Strut cross-section

Figure 35 Prototype subassembly designs.

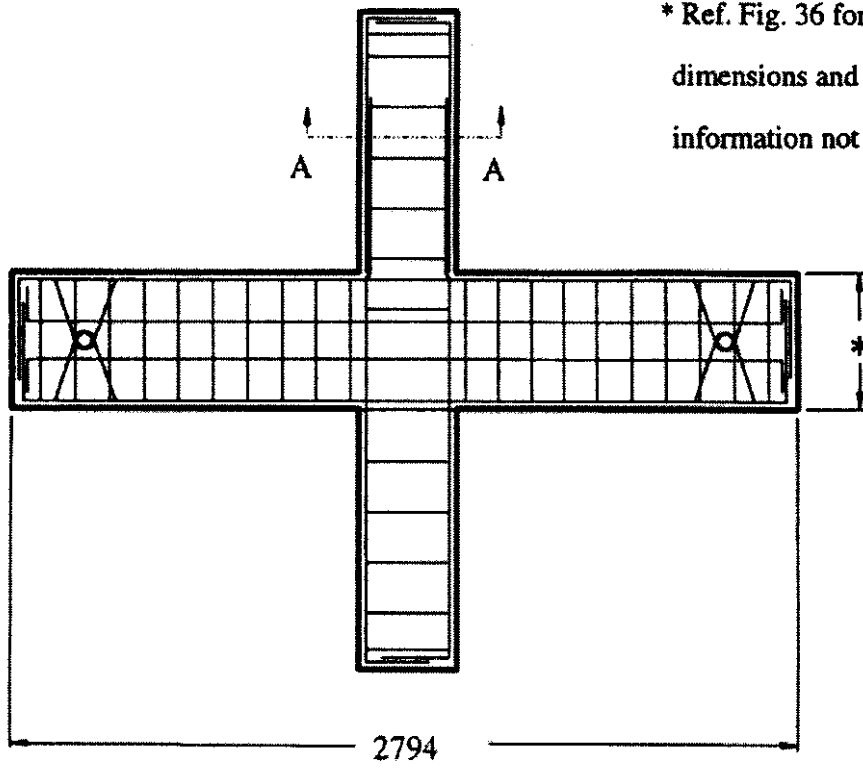


- = Original bar
- = Splice bar (upper col.)

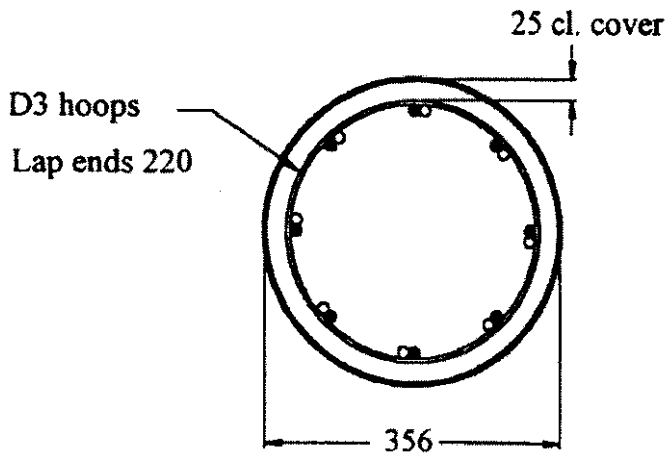
**Section A- A**

**Section B- B**

**Figure 36 Unit I details.**

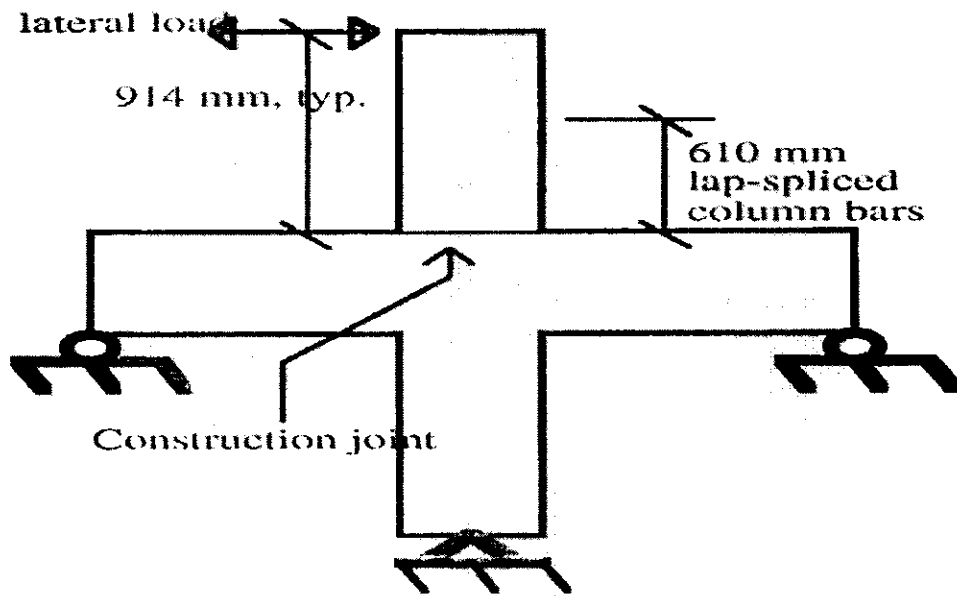


\* Ref. Fig. 36 for all dimensions and information not shown

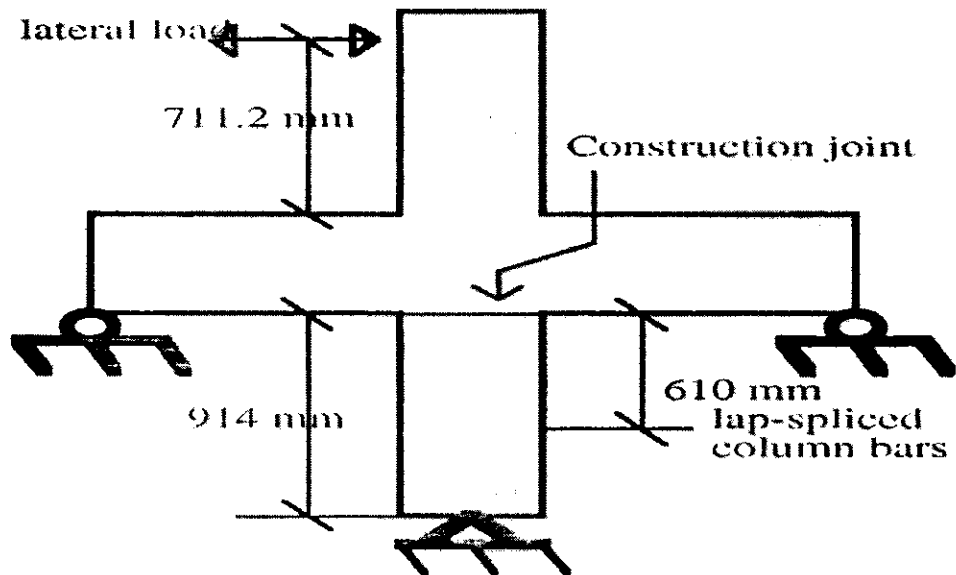


Section A- A

Figure 37 Unit II details.



a) The "as-designed/as-built" specimen orientation



b) The "as-tested" specimen orientation

Figure 38 The orientations of the test specimens.

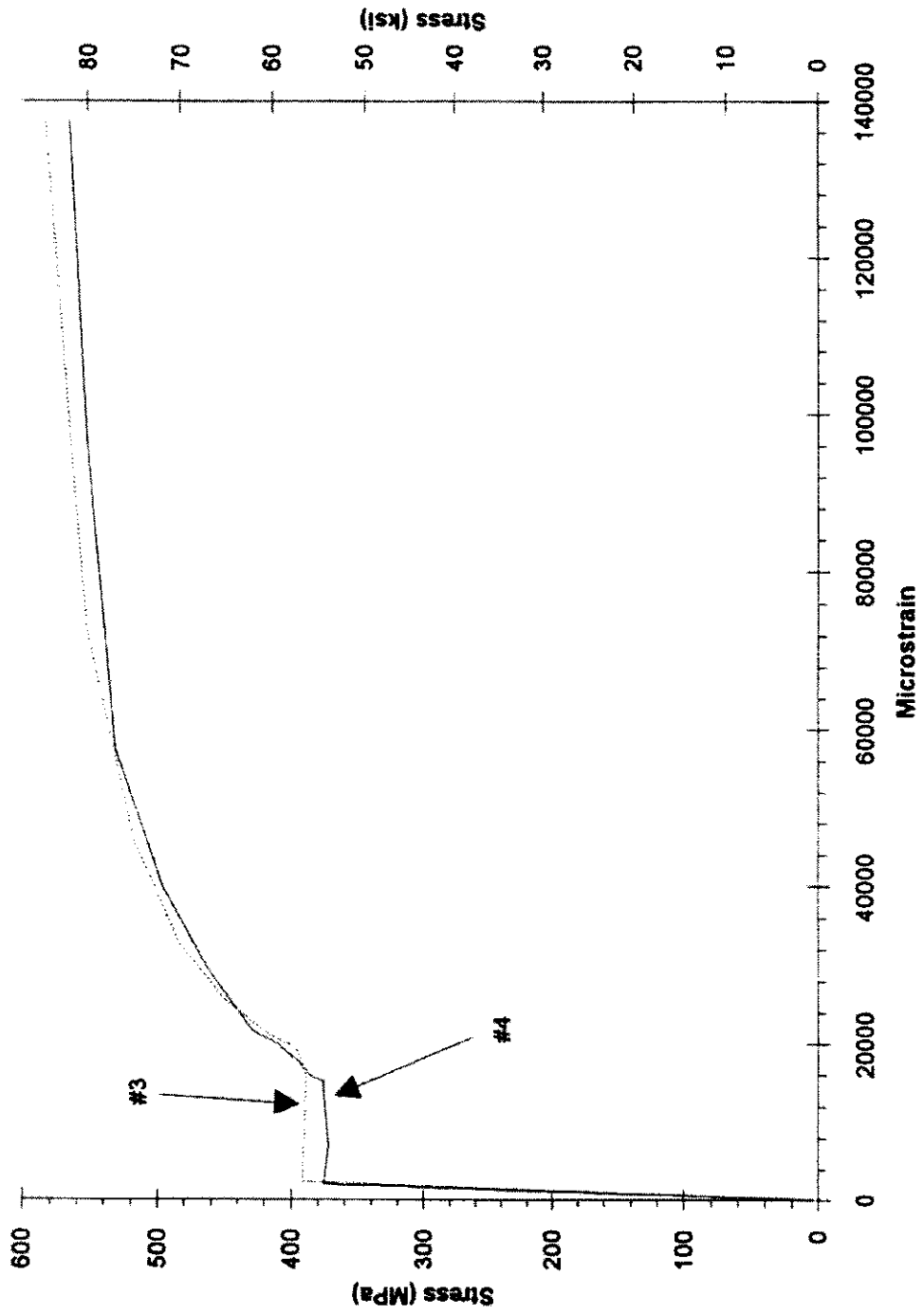


Figure 39 Typical stress versus strain plots for the #4 and #3 bars used in Units I and II.

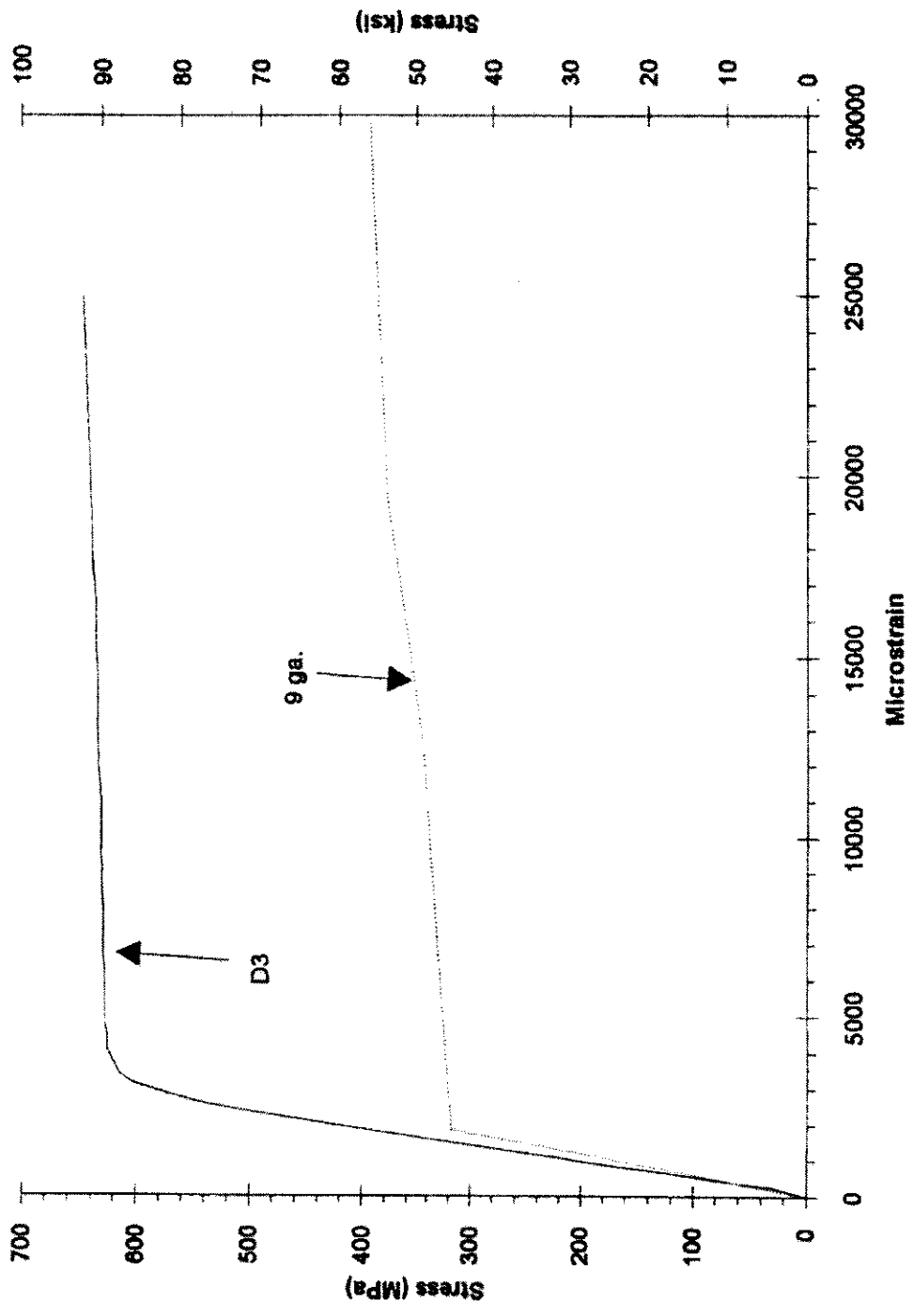


Figure 40 Typical stress versus strain plots for the D3 and 9 Ga wire used in Units I and II.

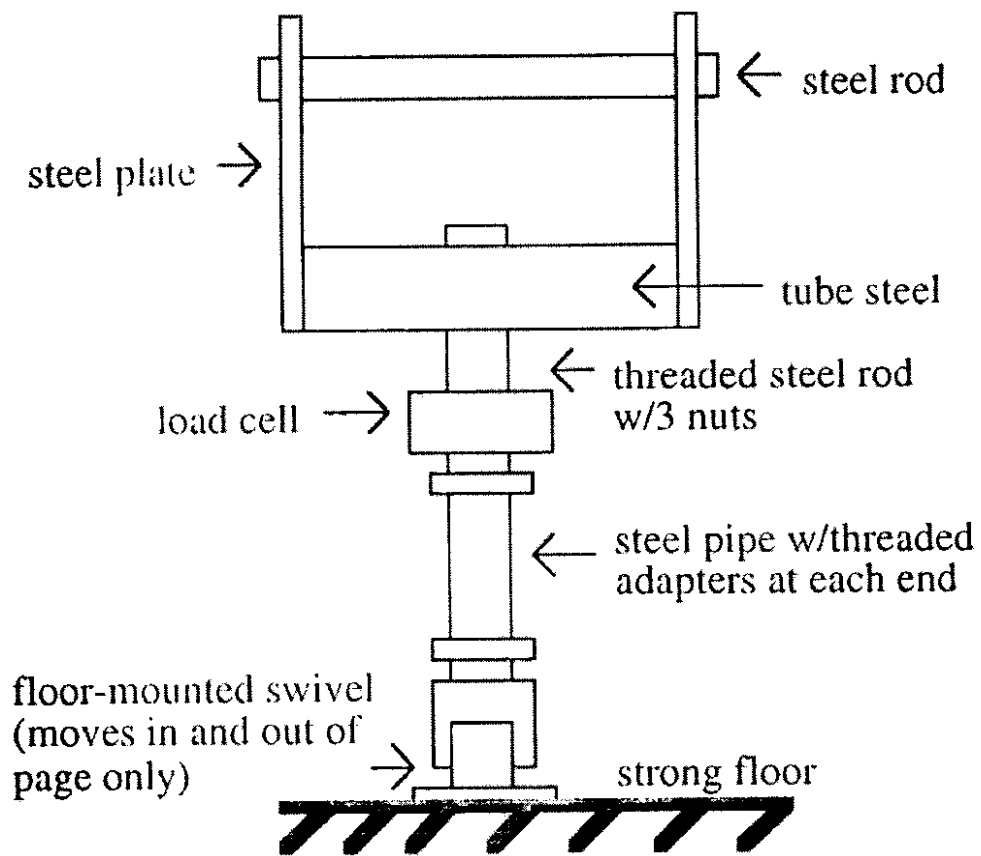


Figure 41 Sketch of the structure used as a "roller" support fixture at the free ends of the struts in the specimens.

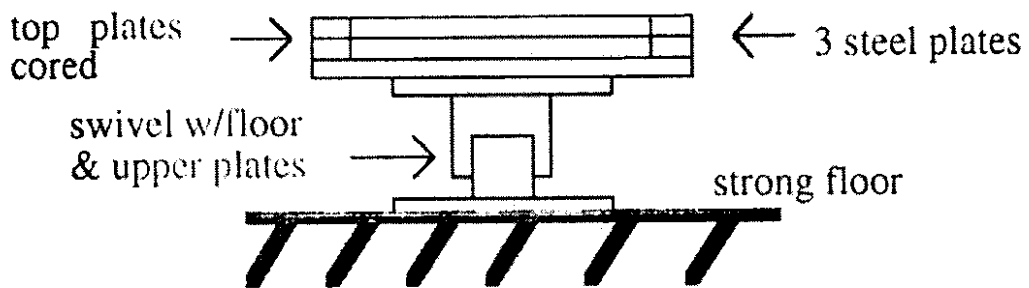


Figure 42 Sketch of the structure used as a "pin" support fixture at the lower columns of the specimens.

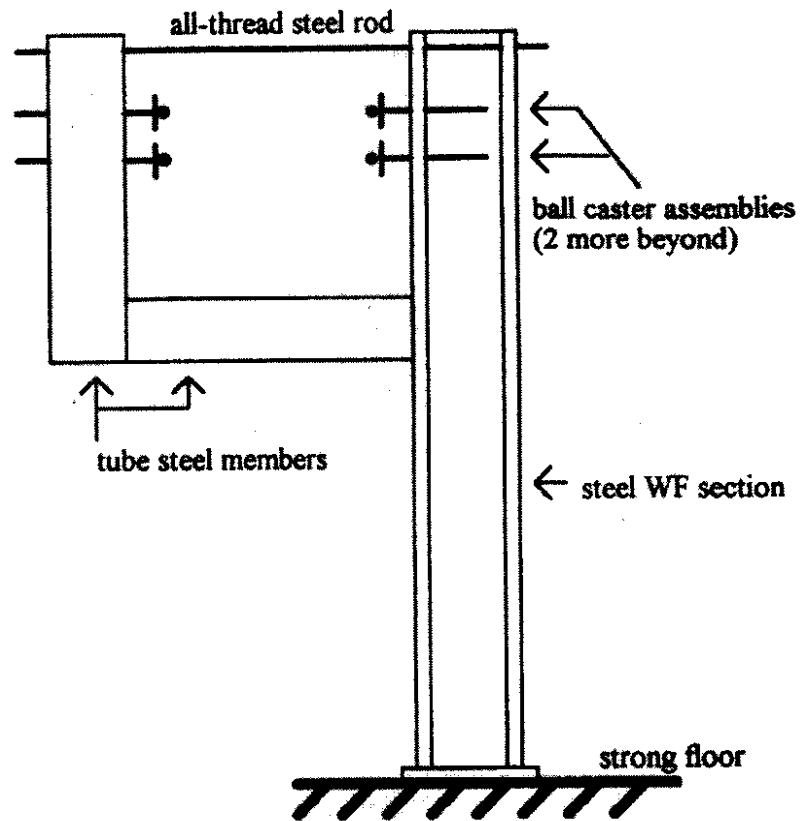


Figure 43 Sketch of the fixture used to brace the specimens against out of plane motion.

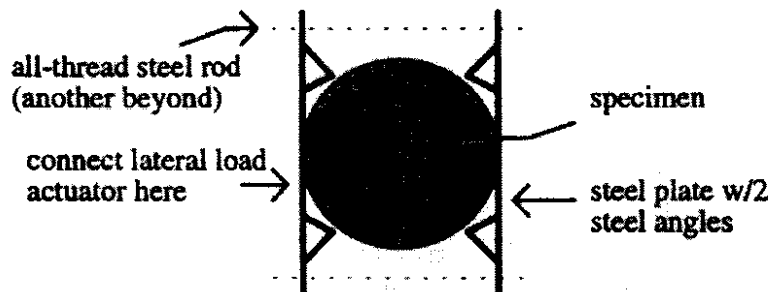


Figure 44 Sketch of the fixture used to connect the lateral load actuator to the specimens.

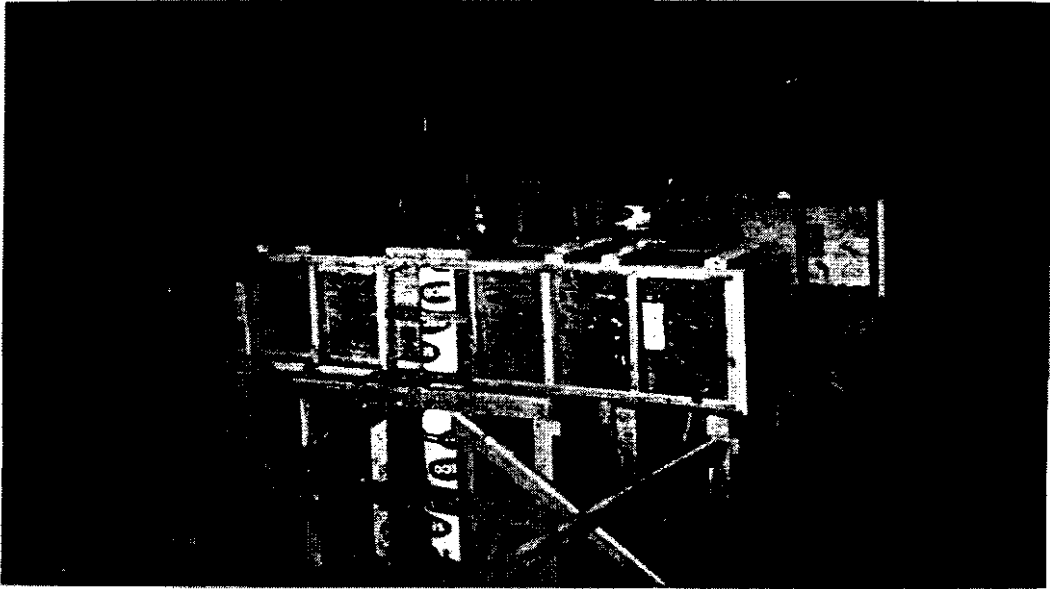


Figure 46 The shoring and the formwork after the first concrete pour.

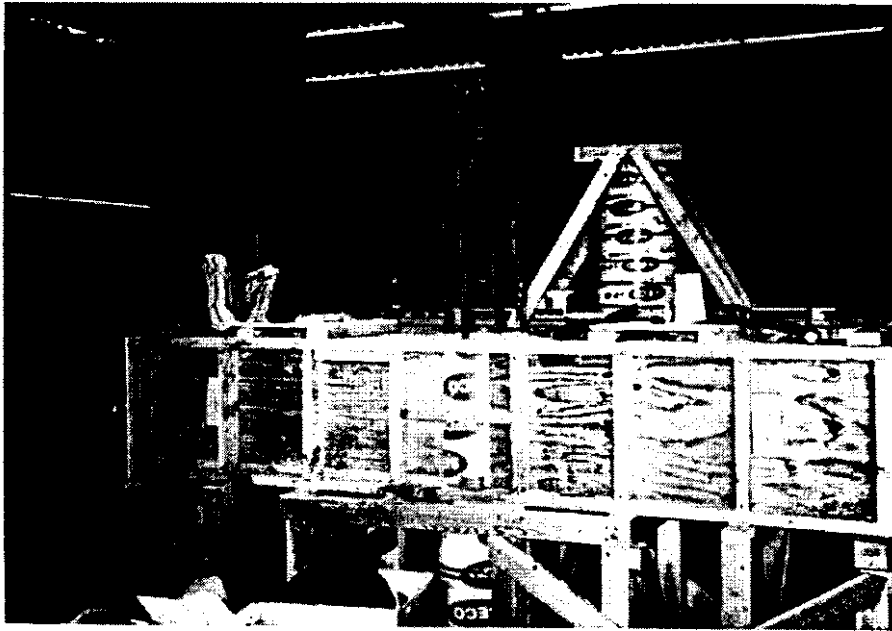


Figure 47 The shoring and the formwork prior to the second concrete pour (upper column of Unit I).

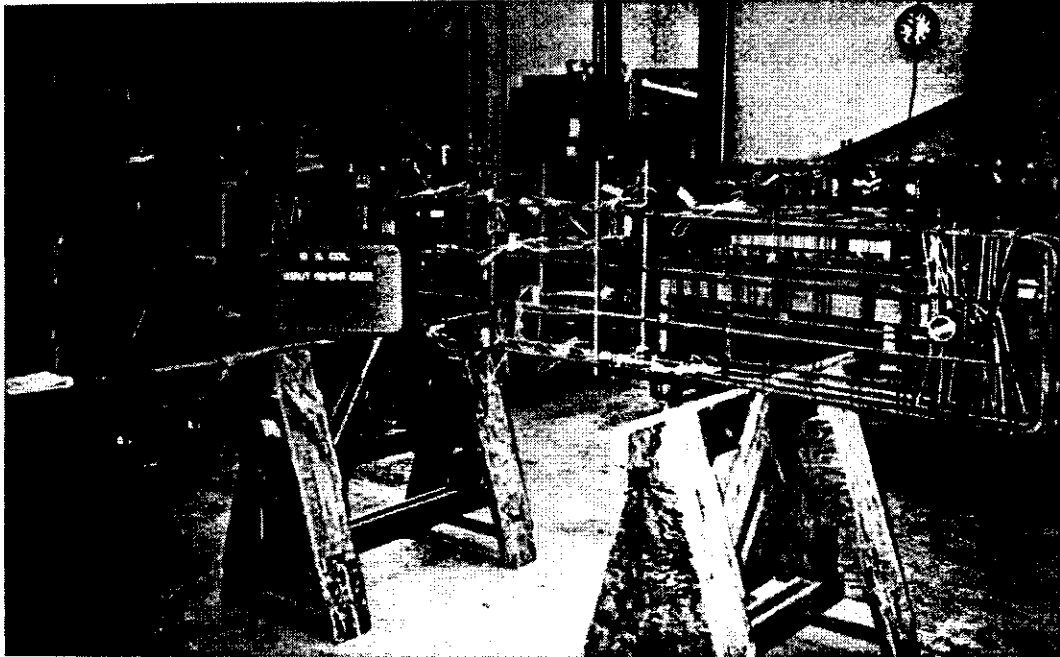


Figure 48 The reinforcing steel cage for the struts of Unit I.

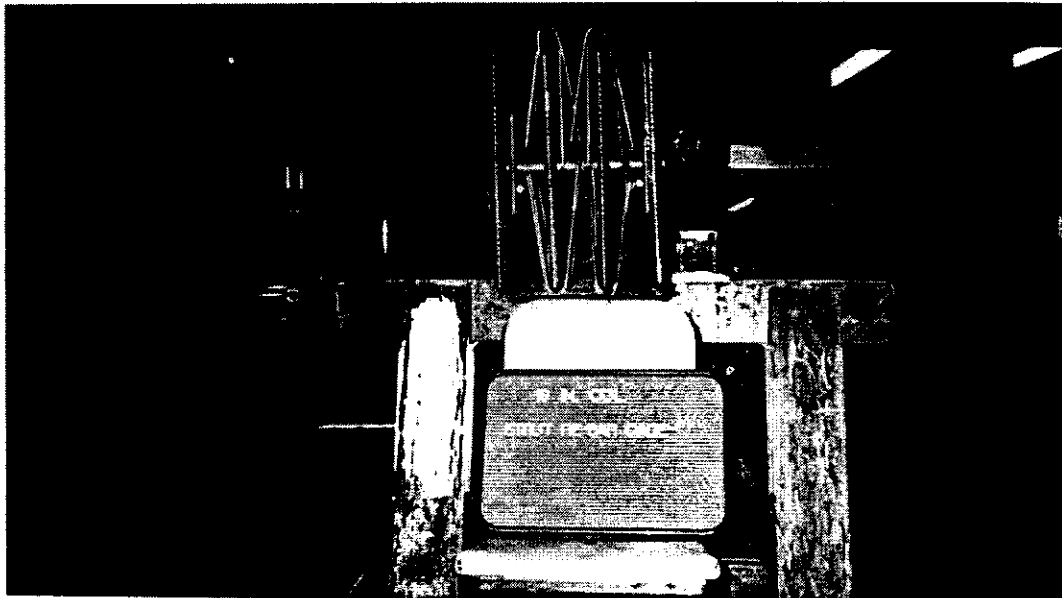


Figure 49 An end-on view of the reinforcing steel cage for the struts of Unit I near the sleeve region.



Figure 50 The reinforcing steel cage for the lower column of Unit I.

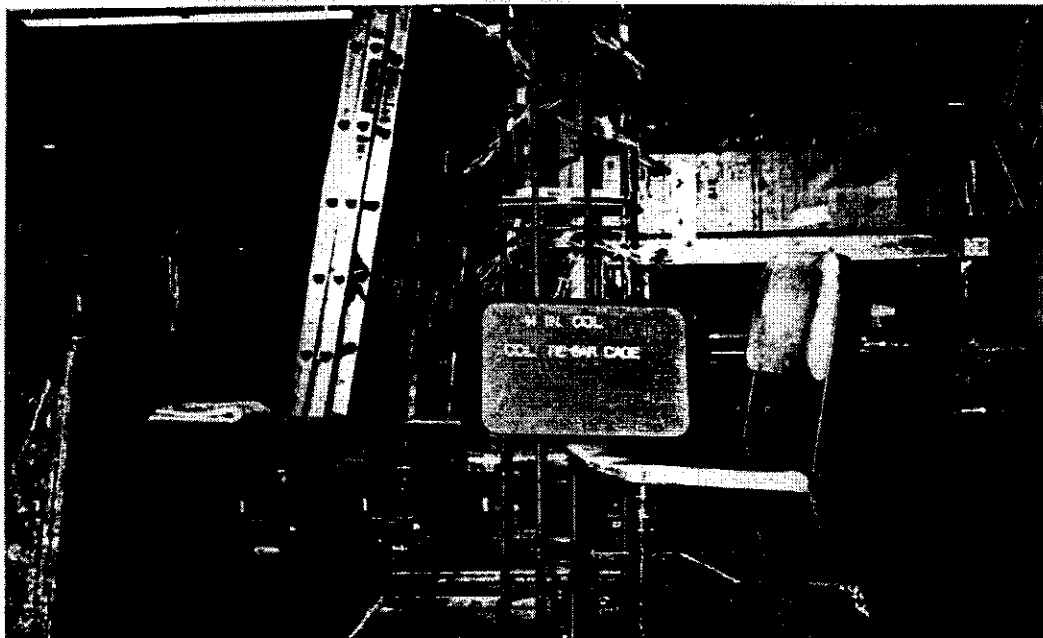


Figure 51 The reinforcing steel cage for the lower column of Unit II.

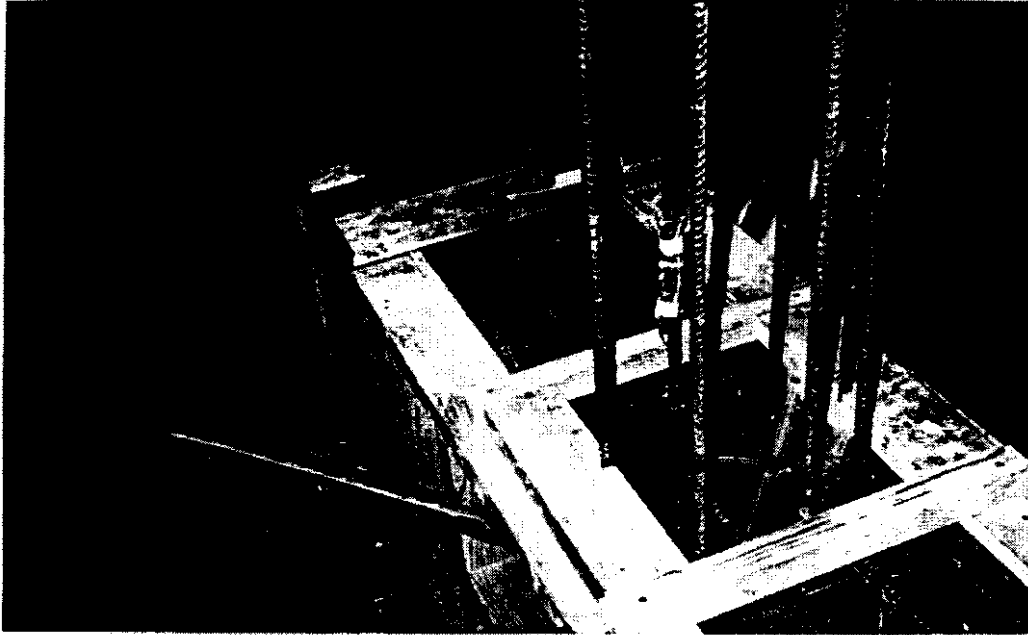


Figure 52 The reinforcing steel cages for the lower column and for the struts in the forms for Unit II.

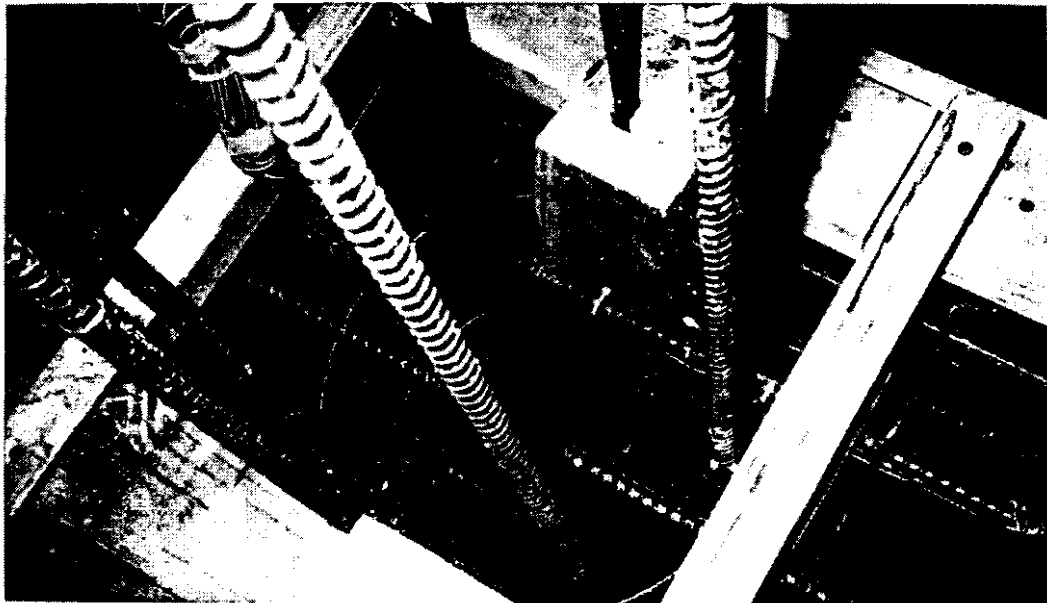


Figure 53 The joint region of the reinforcing steel cages in the forms for Unit II.

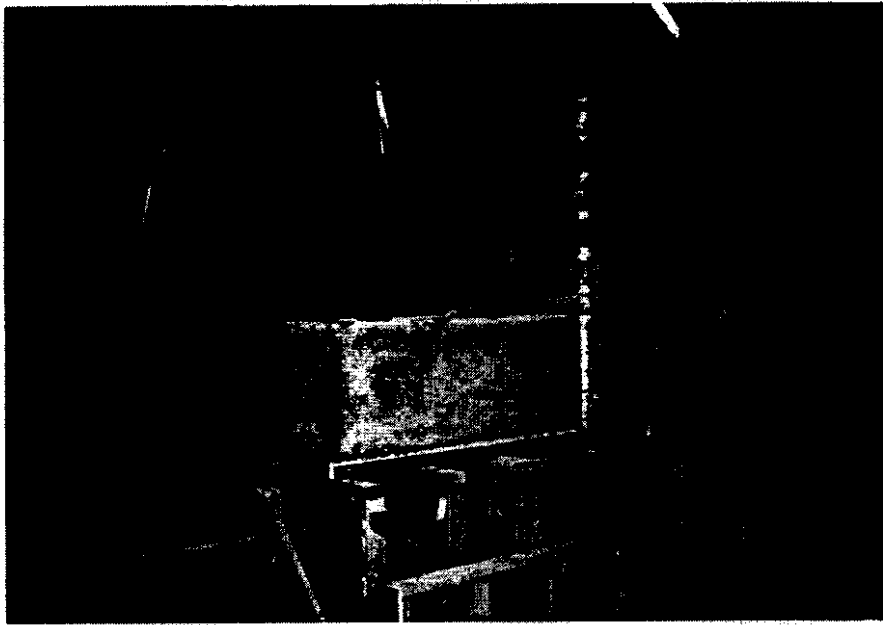


Figure 54 The specimens following removal of all formwork.

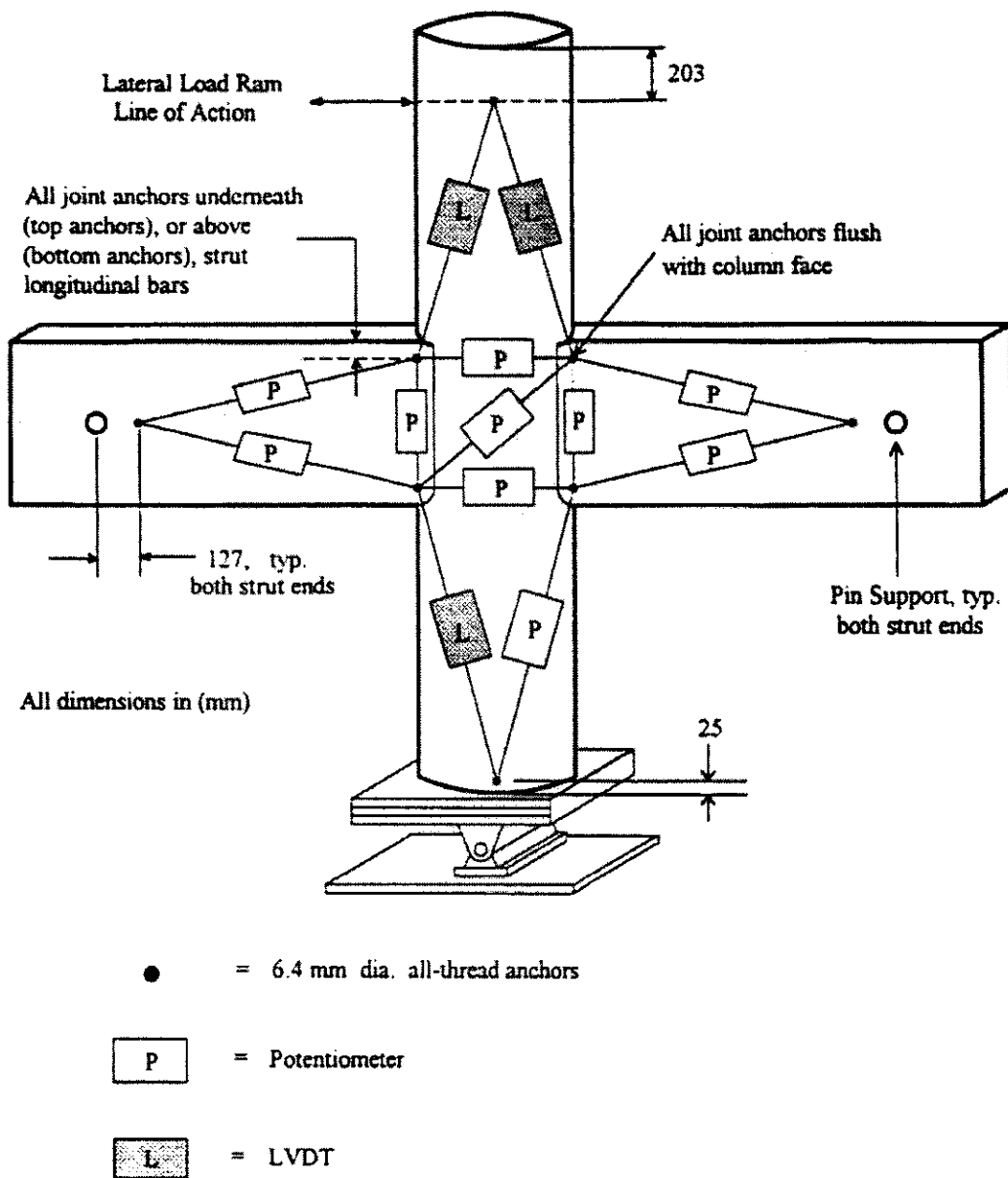


Figure 55 Layout of the instrument array used to measure joint distortion and member rotation (pot.'s and LVDT's).

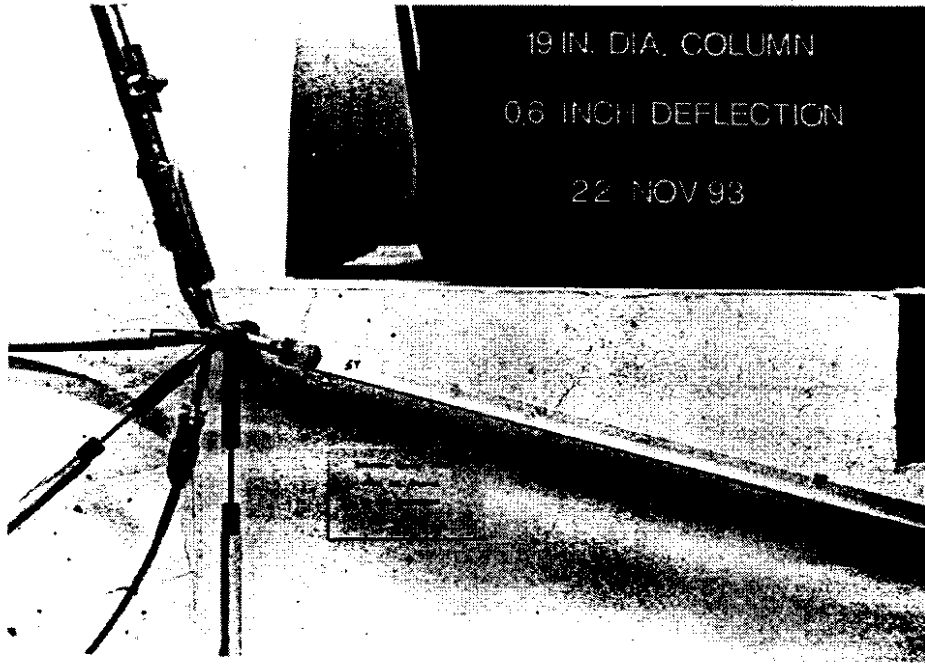
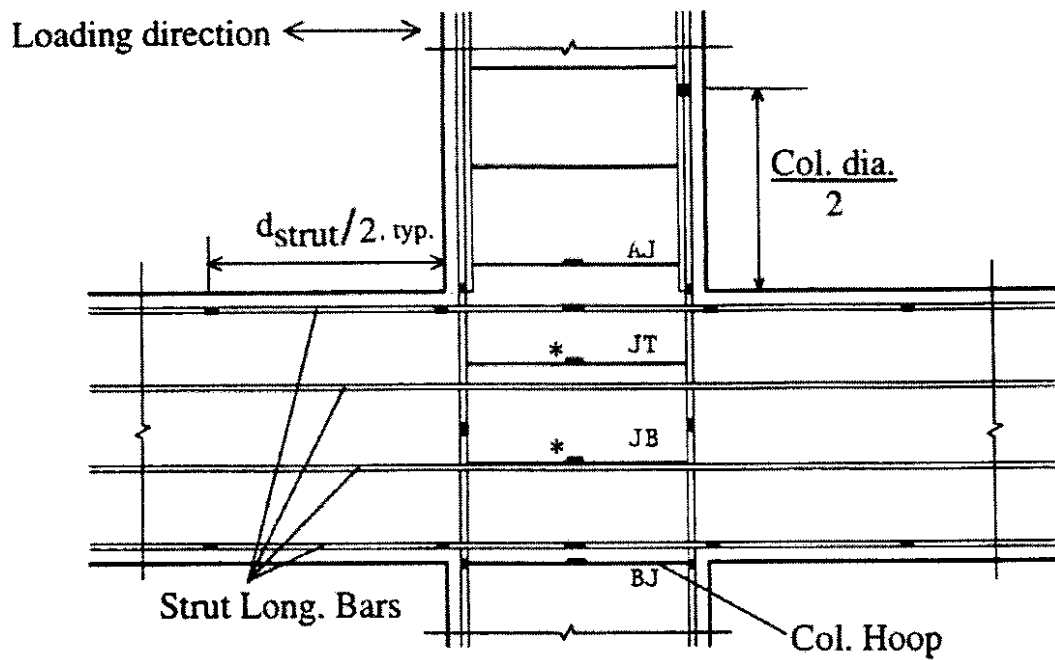
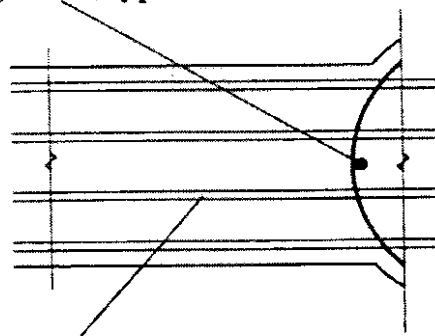


Figure 56 The pot. and the LVDT rigs.



■ = ERSG      \* = 2 gages; 180 deg. apart

a) The locations of the ERSG's  
 Gaged bar, typ. both column sides



Gaged bar, typ. top and bottom  
 b) The locations of the gaged bars

Figure 57      The locations of the ERSG's used in the test specimens.

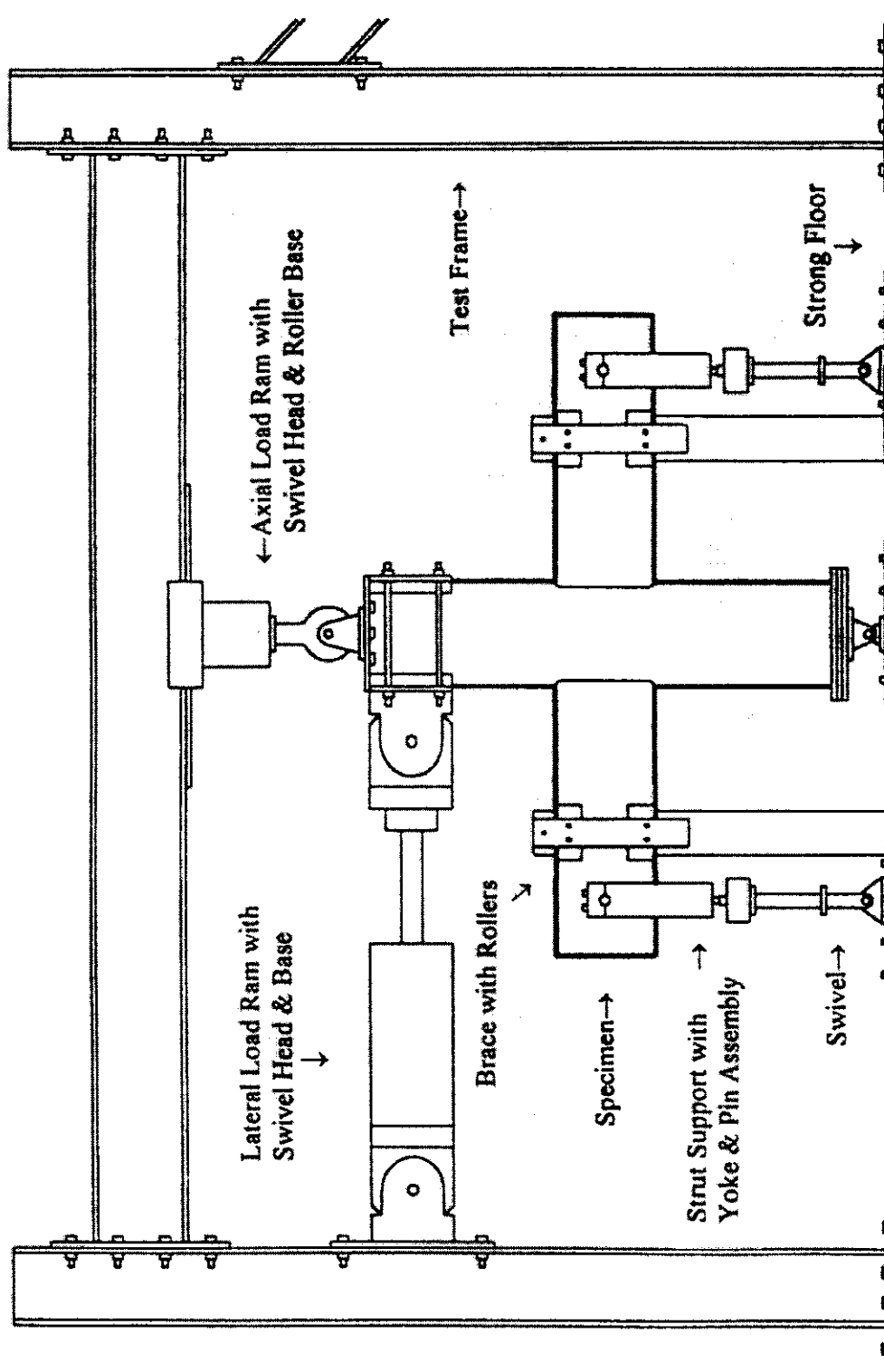


Figure 58 Unit I in the test frame with the load actuators and the fixtures.

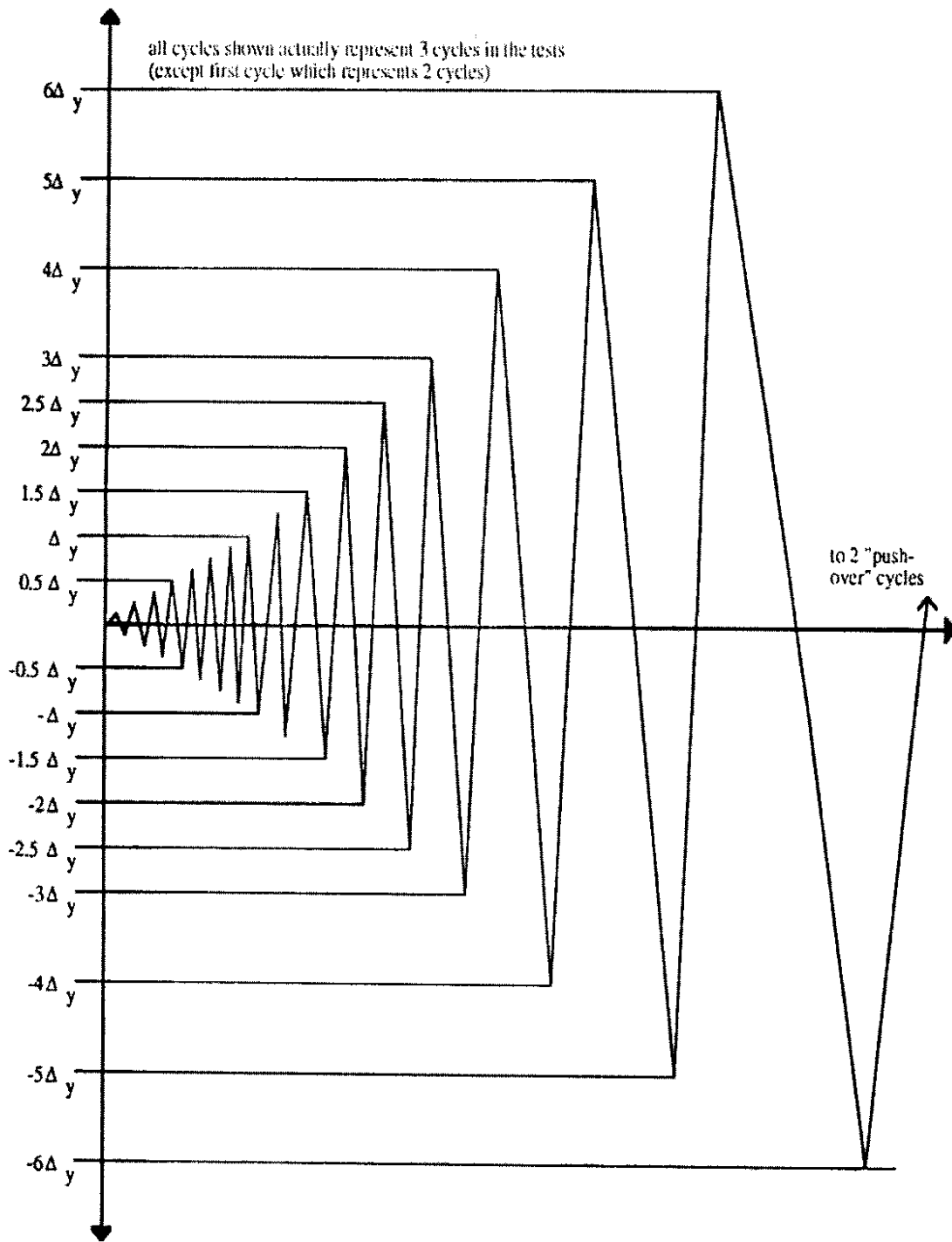


Figure 59 Displacement history used for the test specimens.

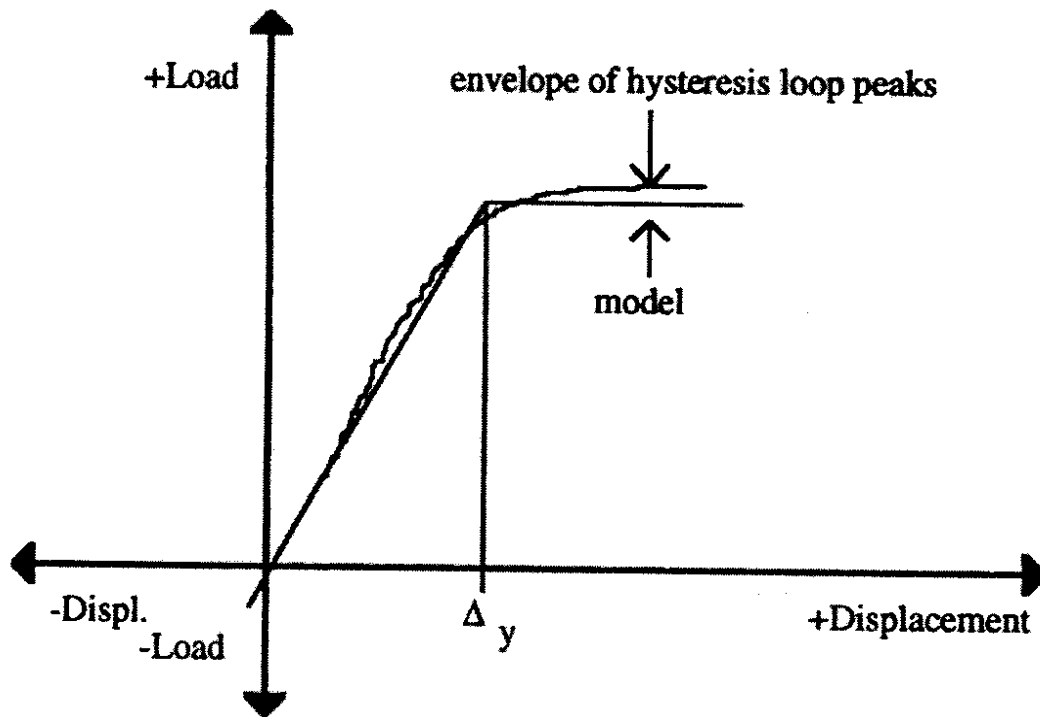


Figure 60 Elastic-perfectly plastic model used to determine  $\Delta_y$  of the test specimens.

## CHAPTER 5

### EXPERIMENTAL FINDINGS

In this chapter the results are presented from the two experimental tests that were conducted. The test results for Unit I are considered first, followed by the results for Unit II. Both specimens suffered severe damage within the B-C joint regions, although they were able to sustain the axial load throughout the tests (which ultimately imparted displacement ductility demands in excess of 9.0). In several instances, the data obtained from the electrical resistance strain gages (ERSG) were used in plots in this chapter to demonstrate certain behaviors that occurred during the tests. However, in neither test did the ERSG's function for the entire test. Thus, the plots described above terminate suddenly, unless otherwise noted.

Prior to presentation of the test results, the displacement convention that was used for "positive" and "negative" displacements is explained. This will provide the frame of reference for the discussion of the results and for the figures and graphs that compliment the discussion.

#### 5.1 The Displacement Convention

In Figure 58 both the ram on the MTS actuator and Unit I are shown in their zero-displacement positions. In the remainder of this chapter, references made to the "retract" direction imply that the ram had pulled the specimen to the left. This direction of displacement represents "positive" displacements. Conversely, references to the "extend" direction imply displacement to the right ("negative" displacements). Figure 61 is a sketch that clarifies this convention. Figure 61a shows a subassembly displaced in the retract direction ("+" displacements), while Figure 61b shows a subassembly displaced in the extend direction ("- displacements). The following is an example of how the convention

is used in the presentation of the test results: For a cycle to 1.0 mm, references made to the retract portion of this cycle are related to behavior/events that occurred at displacements between 0.0 mm and +1.0 mm. On the other hand, references made to the extend portion would refer to behavior/events that occurred at displacements between 0.0 mm and -1.0 mm.

## **5.2 Experimental Test Results From Unit I**

In Unit I the specimen stiffness degraded dramatically as testing progressed. The B-C joint was the site of most of this degradation, since damage was confined primarily to the joint region. While the nominal moment capacity ( $M_{nb}$ ) of the strut was not reached, there was some strut spalling due to large strut fixed-end rotations. Herein, a summary of the findings is given, followed by a full description of the findings in accordance with the following sequence of behavioral milestones: joint shear cracking, specimen yield, and post-specimen-yield. In what follows, the "load" and the "displacement" were obtained from the MTS actuator (Chap. 4, Sec. 4.3.5, "Loading"). The "load" data was corrected for the contribution of the axial load to the lateral load (i.e., the product of the axial load and the corrected MTS displacement, divided by the specimen height from the swivel pin at the base to the line of action of the MTS actuator).

### **5.2.1 Summary of Findings**

The first major event in the test of Unit I was B-C joint shear cracking. The strains in the hoops in and adjacent to the B-C joint indicated that this probably first occurred during the cycles to 7.62 mm. During the cycles beyond those to 7.62 mm, it was noticed that the portions of the strut main bars at the locations adjacent to the B-C joint were increasingly losing the capability to develop compressive strains (when the sense of the

moments dictated that compressive strains were appropriate). The cycles to 17.78 mm brought about yielding in the lower main bars in the struts and in some of the column bars in the lower column. Also, the bond force developed by the strut bars on the bottom of the B-C joint began to deteriorate, and long B-C joint shear cracks appeared.

The next major event was the attainment of yield by Unit I. During the cycles to 20.32 mm, the upper main bars in the strut yielded, and the hysteretic behavior of Unit I indicated that the specimen had yielded. Also, the bond force developed by the upper main bars of the strut began to deteriorate.

There were several major events in the post-yield portion of the test of Unit I. Hysteretic pinching at small displacements became apparent during the cycles to  $1.25\Delta_y$ . Also, the growth of visible cracks concentrated in the B-C joint region, there were relatively large increases in the strains in the hoops in the B-C joint, and the strains in the extreme bars of the lower column at the underside of the B-C joint indicated that these bars were slipping (as a result of bar bond deterioration in the B-C joint, not as a result of deterioration of the lap splice). During the first cycle to  $2\Delta_y$ , the maximum strength of Unit I was reached in the extend direction. At the displacements equal to  $\pm 2\Delta_y$  the cracks along the major diagonals of the B-C joint became the dominant shear cracks. During the first cycle to  $4\Delta_y$ , the maximum strength of Unit I was reached in the retract direction. This strength was not enough for plastic hinges to develop in the members, and it resulted in a relatively small value of B-C joint shear stress ( $v_{jt} = 0.5\sqrt{f'_c}$ ).

During the rest of the test, Unit I was able to develop strength and stiffness at the larger displacement levels when the strut main bars were developed outside of the B-C joint. The largest value of displacement ductility reached by Unit I was approximately 12.5. Based on the data that was obtained and the observations that were made, it is likely that the lap-splice in the lower column performed well throughout the test.

### 5.2.2 B-C Joint Shear Cracking

#### Initial Stiffness

The initial stiffness of Unit I was determined from the hysteresis plots from two cycles to 2.54 mm (Fig. 62). The hysteresis loops indicate that the stiffness of Unit I in the retract direction was approximately 9.7 kN/mm, while in the extend direction it was approximately 9.1 kN/mm (as determined from the data at the respective displacement peaks). The six percent decrease in stiffness from the retract direction to the extend direction diminished as the test progressed (this sec., "B-C Joint Shear Cracking").

#### Initial Cracking

Following the two initial cycles, three cycles were conducted at each subsequent displacement increment (Fig. 59). The first visible cracks occurred during the first cycle to 5.08 mm. These were vertical hairline cracks at intersection of the strut sides and the B-C joint faces in the corners of the B-C joint. During the second cycle, horizontal hairline cracks appeared on the sides of the upper column just above the tops of the struts. The same type of cracking occurred in the lower column as well.

From the cycles to 7.62 mm through the cycles to 12.7 mm, the cracks described above grew (primarily in length). Additionally, hairline flexural cracking was observed in the struts. These flexural cracks occurred between the B-C joint sides and distances of half the strut depth away from the joint (i.e.,  $d_{bm}/2 \approx 230$  mm). While these cracks were initiated in flexure, they propagated as flexure-shear cracks. Figure 63 shows a sketch of Unit I with the typical cracking observed during the test through the cycles to 12.7 mm.

### B-C Joint Shear Cracking

*Visible Cracks versus Hoop Strains.* During the cycles to 15.24 mm, all of the observed cracks grew. In addition, hairline diagonal cracks were noticed on both faces of the B-C joint. These cracks began near the corners of the joint faces and were 50 - 100 mm long.

While cracks in the B-C joint became visible at this point, B-C joint shear cracking probably occurred first during the cycles to 7.62 mm. The reason being that the strains in the hoops in and adjacent to the B-C joint suddenly increased at the displacements equal to  $\pm 7.62$  mm (Chap. 3, Sec. 3.6.4, "The Behavior of Joint Reinforcement"). Two examples of this are shown in Figures 64 and 65. Each figure is a plot of lateral load versus strain in a hoop at each of the displacement peaks reached in the beginning of the test. Figure 64 is for hoop "AJ", which was the hoop just above the B-C joint (ref. Fig. 57). Figure 65 is for hoop "JB", which was the hoop in the lower half of the B-C joint (ref. Fig. 57). It should be noted that hoop "JB" had two ERSG's and Figure 65 is for the ERSG on the front face of the B-C joint. As Figures 64 and 65 show, significant increases in strain occurred at the displacements equal to  $\pm 7.62$  mm, relative to the strains in the previous set of cycles, and in some instances, relative to the strains in a previous cycle to 7.62 mm.

*Shear Stress in the B-C Joint.* Equations 1 and 2 were used to determine the maximum value of the B-C joint shear stress ( $v_{jt}$ ) for the displacements equal to  $\pm 7.62$  mm. The result was:  $v_{jt} = 0.18\sqrt{f'_c}$  ( $f'_c$  in MPa). However, this value is only approximately accurate because Equation 2 is based on a "7/8" factor that is applied to the effective depth of the struts ( $d_{bm}$ ) in the denominator of the equation. The use of this factor presumes that the horizontal forces in the B-C joint are from two layers of bars, one layer in tension and the other in compression, that are separated by a distance of  $7/8d_{bm}$ . As Figure 66 shows, this does not accurately represent the situation in Unit I. The figure shows the strain distributions in the left and right struts at the B-C joint sides at a peak

displacement equal to +7.62 mm. The strains in the main bars were measured (ref. Fig. 57), while the strains in the intermediate bars were interpolated assuming the strain distributions were linear.

The resulting bar forces, the concrete forces required for equilibrium in each cross-section, the shear forces in the columns, and the shear forces in the upper and lower halves of the B-C joint are shown in the figure also. The concrete compressive stress blocks (not shown) are confined to very small regions because most of each of the strut cross-sections are in tension. The resultants from these stress blocks ( $C_c$ ) are actually located much closer to the layers of the main bars than is indicated in the figure. As such, the resultant couple for each of the strut cross-sections are separated by lengths in excess of  $7/8d_{bm}$ . With the value of  $V_{jt}$  obtained from Figure 66 (154.1 kN), Equation 1 gives:  $v_{jt} = 0.12\sqrt{f'_c}$ . An unrealistic value of "1.1" is required in Equation 2 (in lieu of "7/8") in order for the correct value of  $V_{jt}$ , and thus  $v_{jt}$ , to be obtained.

In subassemblages where the columns are much wider than the framing beams, the interaction between the beams and the portions of the joint region that are far from the sides of the beams will be ineffective (Chap. 3, Section 3.6.5, "Member Cross-Sectional Dimensions"). In Unit I, the crests of the joint faces are approximately 89 mm from the sides of the struts, and half of the twelve column bars are located outside of the width of the struts. In the event that Unit I behaved as if the columns were too wide (relative to the beams) for the entire column cross-sectional area to represent the effective B-C joint area ( $A_{jt}$ ), it was decided to study the effect of neglecting the portions of the joint beyond the sides of the struts on the value of  $v_{jt}$ . These portions of the B-C joint represent nearly 25% of the value of  $A_{jt}$  for Unit I. When 75% of the value of  $A_{jt}$  is used in Equation 1, the result is:  $v_{jt} = 0.16\sqrt{f'_c}$ . Therefore, the effect of neglecting the portions of the joint beyond the sides of the struts is a increase of approximately 33% in the value of  $v_{jt}$  (over the value that was calculated with 100% of the value of  $A_{jt}$ ). In all likelihood, the value of  $v_{jt}$  is probably between the two values (i.e.,  $0.12\sqrt{f'_c} \leq v_{jt} \leq 0.16\sqrt{f'_c}$ ).

*Hysteretic Behavior.* The hysteretic behavior of Unit I, through the cycles where B-C joint cracking became visible, is shown in Figure 67. At the points labeled "probable first cracking in B-C joint" the stiffness of Unit I had decreased by approximately ten percent from the initial stiffness (in each direction). The sudden drop in stiffness in the retract (positive displacement) direction during the cycles to 12.7 mm caused the stiffness in both directions to become equal (this sec., "Initial Stiffness"). The B-C joint shear cracking that was underway may have caused decreases in stiffness during the cycles to 12.7 mm because:

- 1.) the cracking in the B-C joint had progressed to where it was visible at that point, and
- 2.) the cracking in the B-C joint had progressed to where the bond force was affected (i.e., the slopes of the curves in Figs. 70 and 73 had changed).

However, these factors would likely have caused decreases in stiffness in both directions. Since the initial stiffness of Unit I in the retract-direction was larger than that of the extend-direction, and since after the decrease in stiffness in the retract direction occurred the stiffness in both directions was nearly identical, the cause was likely a change in the performance of the support fixtures, and/or a change in the interaction between the support fixtures and the specimen. There is reason to suspect the fixtures as the source of this discrepancy since some slippage was noted between the fixture that attached the MTS ram to the column (Fig. 44) and the column at the larger displacement increments (the slippage was arrested by shoring this fixture against the top of one of the struts).

*Strains in the Strut Main Bars.* In the cycles following those to 7.62 mm, at the locations adjacent to the B-C joint, the magnitudes of the compressive (negative) strains in the instrumented strut main bars decreased. An example of this behavior, which was typical for all of the instrumented main bars, is shown in Figure 68. In this figure, the strain history is shown for the location adjacent to the right side of the B-C joint in the strut lower main bar. As the cycling progressed through increasingly larger displacement increments, increasingly larger compressive strain magnitudes should have resulted. To

the contrary, increasingly larger tensile strain magnitudes resulted, beginning with the cycles to 12.7 mm. Figure 69 shows the strain versus displacement history near the edge of the anticipated flexural hinge region for the same bar (approximately 230 mm outward from the B-C joint). The figure is typical for all of the main bars that were instrumented. As the positive displacements increased, the values of compressive strain magnitudes increased.

The reason that tensile strains could occur in all of the bars in the struts at a side of the B-C joint simultaneously was discussed in Chapter 3, Section 3.6.3, "The Effect of Bond on the Shear Transfer Mechanisms". When a beam has equal areas of top and bottom bars and bar slippage occurs, reversing bending moment will not cause separation between a beam and a B-C joint over the full depth of a beam cross-section. The concrete on the compression portion of the beam cross-section will maintain contact with the B-C joint side, and as such it can equilibrate the tension forces in the bars, regardless of how many bars are in tension.

### 5.2.3 Specimen Yield

#### Precursors to Specimen Yield

During cycles to 17.78 mm there were several significant occurrences, besides the growth of previously formed cracks:

- 1.) some of the column bars in the lower column (i.e., the splice region) may have yielded,
- 2.) the lower main bars in the struts yielded,
- 3.) the bond conditions for the strut bars on the bottom of the B-C joint deteriorated, and
- 4.) long shear cracks appeared across the B-C joint faces.

*Bar Yielding in the Lower Column.* The moment in the lower column reached the value corresponding to the theoretical first yield of the extreme tensile bar at the

displacements equal to +17.78 mm. That yield actually occurred in the rightmost column bar at the bottom of the B-C joint was substantiated with strain data at that location (ref. Fig. 57). The strain there exceeded the yield strain at the peak displacements equal to -15.24 mm. However, the strains at the bottom of the B-C joint in the leftmost column bar were well below the yield strain at the displacements equal to +15.24 mm. The strain data from this location were erratic during the cycles to the subsequent displacement increments. However, the trend of the data, through the cycles to 15.24 mm, indicated that the yield strain might have been reached during the retract portion of the cycles to 17.78 mm. The displacements at which yield of the other column bars occurred were not determined because of the difficulty presented by having to extrapolate strain data from the extreme column bars to bars in a circular arrangement.

*Yielding of the Strut Lower Main Bars.* The theoretical yield moment for the lower main bars in the struts was attained during the cycles to 17.78 mm. The strains in the instrumented lower main bar at the sides of the B-C joint exceeded the yield strain at the appropriate displacement peaks (i.e., the portion of this bar at the left side of the joint was beyond yield at a displacement equal to +17.78 mm, and vice-versa). Thus, it is likely that all four main bars yielded because they were all in one layer, and their yield strengths were nearly identical. The upper main bars did not yield because the yield moment for these bars had not been attained (the value of  $f_y$  of the upper main bars was slightly greater than that of the lower main bars). Additionally, none of the strain data indicated that the yield strain had been reached in these bars.

*Bond Deterioration at the Bottom of the B-C Joint.* Typically, bond deterioration is initiated by B-C joint shear cracking and member bar yielding (Chap. 3, Sec. 3.6.3, "Bond in B-C Joints"). Once the displacements had reached  $\pm 17.78$  mm, both B-C joint shear cracking and yield in the strut lower main bars had occurred. Therefore, it was likely that bond deterioration was well underway. To investigate this, the strains at the sides of the B-C joint in the strut lower main bar were used to compute the bar forces. The bar forces

were in turn used to determine the bond force ( $F_b$ , Equation 4) that was transferred through the B-C joint. Figure 70 is graph of the values of  $F_b$  versus displacement for the peak displacements in each cycle. The set of cycles in which the bar yielded in tension are labeled for both displacement directions. The figure shows that the values of  $F_b$  begin to continuously decrease at the displacement peaks equal to +17.78 mm and -15.24 mm.

Figure 70 also has labels for those displacements at which the lower main bar yielded ( $\pm 17.78$  mm). Additionally, the value of  $F_b$  is given for the hypothetical situation where yielding occurs on the tension-side of the B-C joint and there is no contribution from the compression-side of the joint (i.e., "C" = 0.0). Figure 71 explains the terms "tension-side of the B-C joint" and "compression-side of the B-C joint" and shows three different bond-condition scenarios for B-C joints. In Figure 71a shows the scenario where the bond conditions are "optimum", meaning that a bar passing through a B-C joint can yield in tension on one side of the joint and in compression on the other side. Figure 71b is the scenario referred to earlier where the bond conditions are only good enough for a bar to yield on the tension-side of the joint. This scenario represents bond conditions that are less than optimum ("moderate"). Lastly, Figure 71c is the scenario where the bond conditions in a B-C are still favorable enough for the bar to yield on the tension-side of the joint, but there is a significant amount of tension in the bar on the compression-side of the joint. This scenario represents "poor" bond conditions. In the extreme case of "poor" bond conditions there is no bond provided through the B-C joint at all. With no bond in the B-C joint, a bar pulled from the tension-side of the joint can only be developed in the beam on the compression-side of the joint. Yield strains may then be distributed over the entire joint region in such a bar.

For the retract direction in Figure 70, the bond conditions could be described as "moderate to poor", in accordance with Figures 71b and 71c. The reason being the value of  $F_b$  at the first displacement equal to +17.78 mm was less than 46 kN (i.e., approximately 44 kN). This means that the portion of the bar on the compression-side of

the B-C joint was in tension when the portion of the bar on the tension-side of the joint was yielding (i.e.,  $44 \text{ kN} = 46 \text{ kN} - 2 \text{ kN}$ ; "C" = -2 kN). In the extend direction, the situation was worse, as the bond force was decreasing even before the bar on the tension-side of the B-C joint had yielded. Thus, the bond conditions for this bar, for both displacement directions, were clearly on the way to becoming "poor" shortly after yield occurred. Moreover, it is likely that the same bond conditions existed in the B-C joint for the other strut lower main bars during the cycles to 17.78 mm (because all of the bars were in one layer).

*B-C Joint Shear Cracking.* Until cycling to 17.78 mm, all of the visible cracks in the B-C joint were of relatively short length. However, when the displacements equal to  $\pm 17.78$  mm were attained, a long diagonal crack formed in the lower portions of both faces of the B-C joint.

#### Specimen Yield

*Yielding of the Members.* During the cycles to 20.32 mm, the strut attained its yield moment for yielding of the upper main bars. The yielding of these bars was confirmed with the strain data. Therefore, three out of the four members in Unit I (both of the struts and the lower column) had yielded before/during the cycles to 20.32 mm. The hysteretic behavior of Unit I reflected this finding.

*Change in the Hysteretic Behavior.* The hysteretic behavior for Unit I for the cycles through 25.4 mm is shown in Figure 72. By comparing the hysteretic behavior of Unit I through the cycles to 20.32 mm with the subsequent set of cycles, it is clear that a change occurred following the cycles to 20.32 mm that is indicative of yielding (i.e., the strength and the stiffness began to "roll off"), particularly in the extend direction.

Additionally, from the start of testing through the cycles to 20.32 mm, the stiffness of Unit I degraded by about 10% for each 5.08-mm increase in displacement (in each

direction). This trend was maintained for the first displacement equal to +25.4 mm, but was not for the first displacement equal to -25.4 mm, where the stiffness degradation increased in the extend direction. Then, during the second displacement equal to +25.4 mm, the stiffness degradation increased in the retract direction as well.

The occurrence of yielding in most of the members of Unit I and the degradation of its hysteretic behavior lead to the identification of  $\pm 20.32$  mm as  $\pm \Delta_y$ , respectively. There are two other topics relevant to the cycles to 20.32 mm that warrant consideration: the deterioration of the bond conditions in the top of the B-C joint, and the B-C joint shear stress.

*Bond Deterioration in the Top of the B-C Joint.* Figure 73, developed in the same manner as Figure 70, shows that the bond force developed by one of the upper main bars of the strut began to deteriorate at the displacements equal to -20.32 mm (the displacements which caused yielding). However, unlike the lower main bars, when yielding occurred in the upper main bars there was some compressive force at the compression-side of the B-C joint (for the first displacement equal to -20.32 mm). While the values of  $F_b$  at the displacement peaks beyond +20.32 mm did at times exceed 48 kN, Figure 73 shows clearly that these values had begun to "roll off" in the retract direction. Moreover, the higher values of  $F_b$  occurred only sporadically (and still well below the optimum level of 96 kN). Thus, while the bond index (BI) values for both of the layers of the main strut bars (approximately 0.8, Table 9) were well below the adopted limit (i.e., 1.7, Chap. 3, Sec. 3.6.6), bond deterioration was advanced before, or certainly immediately after, these bars yielded.

*Shear Stress in the B-C Joint.* The maximum value of  $v_{jt}$  for the displacements equal to  $\pm 20.32$  mm was determined with Equation 1. A procedure similar to the one outlined in Figure 66 was used to find the value of  $V_{jt}$ , which was then substituted into Equation 1. The result was:  $v_{jt} = 0.26\sqrt{f'_c}$  ( $f'_c$  in MPa). When the areas of the portions

of the joint beyond the width of the struts were subtracted from the value of  $A_{jt}$ , the following result was obtained:  $v_{jt} = 0.35\sqrt{f'_c}$ .

If "1.0" was used in lieu of "7/8" in Equation 2, then the correct value of  $V_{jt}$ , and thus  $v_{jt}$ , was obtained. A check of the accuracy of Equation 2 at the peak displacements from the previous set of cycles (i.e.,  $\pm 17.78$  mm) indicated that the value of the factor that was required to obtain accurate results was "1.04". Therefore, from the first analysis of this equation (i.e., for displacements equal to  $\pm 7.62$  mm the required factor was "1.1") through the next two analyses, the value of "7/8" became more accurate. This finding is important because Equation 2 was used (with the "7/8") to determine the values of  $V_{jt}$  at the peak displacements subsequent to  $\pm \Delta_y$ . This was done because the strain distributions in the strut cross-sections at the B-C joint sides were no longer linear at the peak displacements subsequent to  $\pm \Delta_y$ . In the absence of linear strain distributions, the forces from the intermediate bars could not be determined. Also, within a matter of a few displacement increments beyond  $\pm \Delta_y$  the ERSG's had failed. For these reasons, the methodology depicted in Figure 66 to determine the value of  $V_{jt}$  was no longer a viable alternative to Equation 2.

#### 5.2.4 Post-Specimen-Yield

##### Cycles to $1.25\Delta_y$

There were many significant behavioral changes in Unit I during the first set of cycles following specimen yield. The three cycles to  $1.25\Delta_y$  saw changes in the behavior of:

- 1.) the hysteresis of Unit I,
- 2.) the cracking in Unit I,
- 3.) the hoops in and adjacent to the B-C joint, and
- 4.) the lower column bars at the underside of the B-C joint.

*Hysteretic "Pinching".* Figure 72 shows that the hysteresis loops that developed during the cycles to  $1.25\Delta_y$  began to noticeably pinch at small displacements. Additionally, the strength and the stiffness of Unit I were noticeably less in the second cycle than they were in the first cycle.

To this point, the energy dissipated by Unit I in the second cycle compared to the first was always less by a consistent amount. However, the dissipated energy dropped even more during the cycles to  $1.25\Delta_y$ .

*Concentration of Cracking.* During the cycles to  $1.25\Delta_y$ , most of the growth and the spread of visible cracks was in the B-C joint region, as compared to the previous cycles when cracking randomly occurred throughout much of the subassembly. As was the case earlier, most of the visible cracks in the B-C joint were in the lower portion of the joint.

*Strains in the B-C Joint Hoops.* The strains in the hoops in the B-C joint began to increase at each successive displacement equal to  $\pm 1.25\Delta_y$ . This behavior is evident in Figures 74 and 75. The figures are similar to Figure 65, except that the data for both ERSG's on both B-C joint hoops are presented here: Figure 74 shows the load versus strain plots for the hoop in the upper portion of the joint ("JT"; two ERSG's), and Figure 75 shows the plots for the hoop in the lower portion of the joint ("JB"; two ERSG's). For comparison, Figure 76 shows the plots for the hoops above and below the B-C joint ("AJ" and "BJ"). Increasing strains from cycle to cycle for the displacements equal to  $\pm 1.25\Delta_y$  was common for hoops JT and JB. Also, the strains in these hoops at the first displacements equal to  $\pm 1.25\Delta_y$  increased significantly from the strains in the preceding three cycles to  $\pm \Delta_y$ . Since hoops AJ and BJ were outside of the B-C joint, these trends did not occur until the displacement increments were increased.

*The Lower Column Bars at the Underside of the B-C Joint.* During the cycles to  $1.25\Delta_y$ , the strains in the extreme bars of the lower column at the underside of the B-C joint indicated that these bars were slipping. The reason being that under loading

conditions that had been producing compressive strains, tensile strains occurred. Therefore, it can be concluded that bond had locally deteriorated at the B-C joint for the column extreme bars, and perhaps for the other lower column bars nearby.

*Shear Stress in the B-C Joint.* With the increase in strength of Unit I during the cycles to  $1.25\Delta_y$ , the maximum value of  $v_{jt}$  for these cycles exceeded the maximum value of  $v_{jt}$  for the cycles to  $\Delta_y$ . The new value was:  $v_{jt} = 0.35\sqrt{f'_c}$ . When the areas of the portions of the joint beyond the width of the struts were subtracted from the value of  $A_{jt}$ , the result was:  $v_{jt} = 0.46\sqrt{f'_c}$ .

#### Cycles to $1.5\Delta_y$

During the cycles to  $1.5\Delta_y$ , the hysteretic behavior of Unit I worsened, diagonal cracks appeared in the upper portion of the B-C joint, and the hoop in the upper portion of the B-C joint (JT) yielded.

*Hysteretic Behavior.* Figure 77 is the hysteresis plot for the entire test. As the figure shows, the stiffness of Unit I during the cycles to  $1.5\Delta_y$  decreased, although the strength remained essentially the same relative to the stiffness and strength at  $1.25\Delta_y$ . Also, there continued to be significant decreases in stiffness, strength, and in dissipated energy during the second cycle relative to the first cycle. The hysteretic pinching during each of the cycles at small displacements continued to worsen as well.

*B-C Joint Cracking.* Until the cycles to  $1.5\Delta_y$  began, any large visible cracks in the B-C joint were diagonal cracks in the lower portion of the joint. However, as Figures 78 and 79 attest, long diagonal cracks occurred approximately along the major diagonals of the front and the back faces of the B-C joint, respectively, at the displacements equal to  $\pm 1.5\Delta_y$ .

*B-C Joint Hoop Yielding.* Hoop JT, the hoop in the upper half of the B-C joint, exceeded its yield strain at the first displacements equal to  $\pm 1.5\Delta_y$  (Fig. 74).

### Cycles to $2\Delta_y$ through Cycles in Excess of $6\Delta_y$

*Cycles to  $2\Delta_y$ .* During the first cycle to  $2\Delta_y$ , the maximum strength of Unit I was reached in the extend (negative displacement) direction (Fig. 77). The strength increased in the retract direction as well. The largest value of  $v_{jt}$  that was attained in either direction during this cycle was  $0.36\sqrt{f'_c}$  ( $v_{jt} = 0.48\sqrt{f'_c}$ , without the portions of the joints that extend beyond the sides of the struts).

By the final displacements equal to  $\pm 2\Delta_y$ , the hoops in the B-C joint experienced decreasing strains. Figure 75 shows this behavior for hoop JB.

The cracks along the major diagonals of the B-C joint became the dominant shear cracks at the displacements equal to  $\pm 2\Delta_y$ . Figures 80 and 81 show these cracks in the B-C joint on the front and back faces, respectively. Moreover for the first time, these cracks did not close at small displacements. In other words, both of the major diagonal joint cracks on the faces of the B-C joint remained open at displacements equal to zero.

Yield penetration into the B-C joint from the members was advanced during the cycles to  $2\Delta_y$ . The ERSG's on the member bars mid-way into the B-C joint indicated that these bars had yielded in those locations at the peak displacements.

*Cycles to  $2.5\Delta_y$ .* The strength that Unit I attained during the cycles to  $2\Delta_y$  was maintained in both directions during the cycles to  $2.5\Delta_y$  (Fig. 77). The stiffness of Unit I continued to decrease, while the pinching of the hysteresis loops continued to affect wider ranges of the displacements.

Spalling began to occur during these cycles along the major joint diagonals of the B-C joint, in the column where the upper column met the tops of the struts and where the lower column met the bottoms of the struts. Also, the corners of the struts began to spall, as did the corners of the B-C joint faces where the strut corners met the joint faces. The spalling of the strut corners and of the joint face corners was caused by the large end

rotations of the struts that resulted from the bond deterioration in the B-C joint (Figs. 70 and 73). In some instances this spalling resulted in the exposure of the strut corner bars.

The lap-splice in the lower column showed no signs of distress to this point, except for some small flexural cracks. The strains in the two lap-spliced bars that were instrumented were nearly identical. As such, no loss of bond was evident. Subsequent to the cycles to  $2.5\Delta_y$ , the ERSG's on these bars failed. However, observation indicated that the lap-splice continued to performed well.

*Cycles to  $3\Delta_y$ .* Unit I continued to maintain strength when the displacement was incremented to  $3\Delta_y$ , while degradation of the stiffness of, and the cracking and the spalling in the B-C joint region worsened. These occurrences were to be expected given the behavior indicated by Figures 70 and 73. Figure 70 indicates that the lower main bars in the strut were pulling and pushing through the B-C joint at the displacements equal to  $\pm 3\Delta_y$ , as no bond force was developed in either of the displacement directions. For the upper main bars in the strut, Figure 73 indicates that these bars were pulling and pushing through the B-C joint at the displacements equal to  $-3\Delta_y$ , as no bond force was developed in the extend direction. This lack of bond resulted in an increase in the strut end rotations, which was primarily responsible for the degradation in the stiffness of Unit I, for the spalling of the strut corners and spalling of the corners of the faces of the B-C joint.

From this point on, the displacement ductilities attained by Unit I are not a good measure of its performance. The reason being that the bar bond failures created conditions where little energy was dissipated and the stiffness had deteriorated to the point that very little restoring force was available.

*Cycles to  $4\Delta_y$ .* The maximum strength of Unit I was attained at the first displacement peak equal to  $+4\Delta_y$ , as the strength in the retract direction increased from the level of the previous three displacement peaks to the largest value for the test (Fig. 77). This strength, however, was not sufficient to develop full plastic hinging in any of the members, since the ultimate flexural capacities of the members were never attained. The

value of the demand moment in the lower column exceeded 90% of the calculated value of  $M_{nc}$ , and for the struts, the value of the demand moment was nearly 80% of the calculated value of  $M_{nb}$  (based on extreme fiber strains in the concrete of 0.004). Also, no significant damage was observed in the regions of the columns and the struts that normally would constitute plastic hinge zones.

Figure 77 also shows that the drop in the strength and in the stiffness of Unit I, from the first cycle to  $4\Delta_y$  to the second cycle, is large relative to the decreases that had occurred in the previous sets of cycles. The larger decrease in stiffness is in accordance with what is indicated by Figures 70 and 73, where the implication is that both layers of the main bars in the struts were pulling/pushing through the B-C joint after the second displacement equal to  $+4\Delta_y$ . The pulling/pushing of one of the corner bars through the B-C joint was visually observed (the cover for this bar had spalled near the joint). From this point, there was only one way for Unit I to develop strength and stiffness beyond the levels attained in the pinched regions of the hysteresis loops: the displacements had to be large enough for the strut main bars to be developed in the strut on the opposite side of the B-C joint.

In accordance with the behavior described above, the cracking and the spalling in the B-C joint region at the displacements equal to  $\pm 4\Delta_y$  were significantly worse than had been the case earlier. Figures 82 and 83 show the front and the back faces of the B-C joint, respectively, for peak displacements in each direction during the cycles to  $4\Delta_y$ .

The largest value of  $v_{jt}$  that was attained in either direction for the entire test was  $0.5\sqrt{f'_c}$ . This value was calculated without the portions of the joints that extend beyond the sides of the struts, given the extensive damage that these areas had sustained. Thus, despite the extent of damage in the B-C joint region, the shear stress there was very small compared to values that have been associated with joint shear failures (i.e.,  $0.75\sqrt{f'_c} \leq v_{jt} \leq 1.5\sqrt{f'_c}$ ; Chapter 3, Section 3.6.2, "Limits on Applied Shear Stress").

*Cycles to  $5\Delta_y$  and to  $6\Delta_y$ .* During the cycles to  $5\Delta_y$  and to  $6\Delta_y$ , the decay of the strength and of the stiffness of Unit I increased (Fig. 77). The damage to the B-C joint region increased as well.

*"Push-Over" Cycles.* Having reached the displacements where the strength of Unit I was steadily decreasing, Unit I was subjected to two additional cycles to determine the maximum ductility displacement that it could achieve. Figure 77 shows that the value of the maximum displacement ductility reached by Unit I in the first cycle in the retract direction was approximately 9.0 ( $\approx$  8% drift), while in the extend direction it was approximately 12.5 ( $\approx$  11% drift). In both instances the displacements that Unit I was subjected to were limited by the stroke of the ram. Figure 84 shows Unit I at the displacement ductility of 12.5 in the extend direction. The hysteresis loop for the first cycle remained pinched in-between displacements of -50 mm and +50 mm. Beyond that displacement range, Unit I stiffened and eventually attained strengths in both directions that exceeded that which was achieved during the cycles to  $6\Delta_y$ . The reason that such strength was attained was because of the relatively large increase in the displacement increment. Had the even displacement increments that were used earlier been maintained (e.g.,  $7\Delta_y$ ,  $8\Delta_y$ ,  $9\Delta_y$ , etc.), Unit I would not have shown the strength that it did during the first "push-over" cycle. The deformed shape of the lobe on the extend (negative displacement) portion of the hysteresis loop was caused by a problem with the data acquisition software.

The displacement ductility that was attained in the retract portion of the second cycle was identical to that of the first, while the strength and the stiffness decreased markedly. The extend portion of the second cycle was stopped well-short of the displacement ductility that was achieved in this direction in the first cycle because it was clear that Unit I was not resisting load. Figures 85 and 86 show the front and the back of Unit I at the peak displacement in the extend portion of the second cycle. A third cycle was begun in which the displacement ductility of Unit I in the retract direction reached a value of 9.0 again,

albeit with less strength and stiffness than before. This cycle was not completed because Unit I did not resist any load in the extend direction during the second cycle.

Figure 85 also shows that the entire lengths of the struts participated in bending action. Thus, because the potentiometers and LVDT's were attached to all-thread anchors that were mounted in the sides of the struts (Fig. 55), the data obtained from these instruments could not be used (i.e., the bending and B-C joint shear deformation data was convoluted).

Following the "push-over" cycles, all of the loose concrete was removed from the faces of the B-C joint in order to determine whether or not the depths of the major diagonal cracks were limited to the curved portions of the joint faces. Figures 87 and 88 show the results of this procedure. The crack in the B-C joint in Figure 87 is on the front face of the joint; this is the same crack shown in Figure 85. The depth of this crack extended into the core of the joint. Figure 88 shows the back face of the joint. So much of this face was removed that no single crack was prominent. This is consistent with what is shown in Figure 86. The two large cracks shown in that figure caused the entire face of the joint to become loose. However, upon closer inspection of the joint, it was obvious that these cracks had penetrated the joint core.

### 5.3 Experimental Test Results From Unit II

In Unit II the B-C joint was severely damaged also. However, the lower column strength exceeded the value of  $M_{nc}$ , and while full plastic hinging did not develop there, the damage was extensive due to large end rotations. After the value of  $M_{nc}$  was reached in the lower column, the strength of Unit II continued to increase, although its stiffness continued to decrease. The probable cause of the decay of the stiffness of Unit II was the degradation of the B-C joint. Herein, a summary of the findings is given, followed by a full description of the findings in accordance with the following sequence of behavioral

milestones: joint shear cracking, first specimen yield, and post-specimen-yield. Figure 89 shows Unit II prior to the start of testing. In what follows, the "load" and the "displacement" were obtained from the MTS actuator (Chap. 4, Sec. 4.3.5, "Loading"). These data, as well as all of the other data, were corrected in the same manner as for Unit I.

### 5.3.1 Summary of Findings

The first major event in the test of Unit II was B-C joint shear cracking. This probably first occurred during the cycles to 5.08 mm (based on the data from the ERSG's on the B-C joint hoops). During the cycles beyond those to 5.08 mm, it was noticed that the portions of the strut main bars at the locations adjacent to the B-C joint were increasingly losing the capability to develop compressive strains (when the sense of the moments dictated that compressive strains were appropriate). During the cycles to 15.24 mm the lower column probably reached first yield. At the displacements equal to  $\pm 17.78$  mm the deterioration of the bond force developed by the strut bars in the B-C joint, and the diagonal cracking in the B-C joint, was pronounced.

The next major event was the attainment of yield by Unit II. While the displacements equal to  $\pm 20.32$  mm were taken as  $\pm \Delta_y$ , respectively, neither the data nor the visual observations clearly indicated that Unit II actually yielded at these displacements because, to this point, the behavior of Unit II was governed primarily by the lower column (only the lower column had yielded and its circular bar arrangement caused a gradual rounding of the hysteresis loop peaks).

There were several major events in the post-yield portion of the test of Unit II. During the cycles to  $1.25\Delta_y$ , the theoretical value of  $M_{nc}$  was attained in the lower column (plastic hinging never occurred in the lower column), the cracking in the B-C joint worsened, and the specimen began to exhibit pinched hysteretic behavior at the smaller displacements. During the cycles to  $1.5\Delta_y$ , the moment in the upper column exceeded the

theoretical first yield moment, and the upper main bars in the struts yielded in one displacement direction. During the first cycle to  $2\Delta_y$ , the strut upper main bars yielded at the locations adjacent to the B-C joint in both displacement directions. Also, the lower main bars in the right-hand strut yielded as they were pulled from across the B-C joint by the left-hand strut (i.e., there was no bond in the B-C joint). During the extend portion of the first cycle to  $2.5\Delta_y$ , the lower main bars in the left strut yielded at the locations adjacent to the B-C joint as these bars were pulled from across the joint. Unit II reached its maximum strength in the extend direction at the first displacement equal to  $-2.5\Delta_y$ . At the first displacement equal to  $+4\Delta_y$  the maximum strength that Unit II had attained at the first displacement equal to  $+2\Delta_y$  was reached again. The maximum strength of Unit II produced a relatively small value of B-C joint shear stress ( $v_{jt} = 0.48\sqrt{f'_c}$ ).

During the rest of the test, the strength and the stiffness of Unit II degraded more rapidly than was the case with Unit I. However, as with Unit I, the strength and stiffness that Unit II was able to develop at the larger displacement increments were the result of the strut bars being developed outside of the B-C joint. The largest value of displacement ductility reached by Unit II was approximately 11. Based on the recorded data and the observations, it appears that the lap-splice in the lower column performed well throughout the test.

### 5.3.2 B-C Joint Shear Cracking

#### Initial Stiffness

The initial stiffness of the Unit II was determined from the hysteresis plots from two cycles to 2.54 mm. Figure 90 shows these hysteresis loops. The hysteresis loops indicate that the stiffness of Unit II in the retract direction was approximately 5.6 kN/mm,

while in the extend direction it was approximately 8.3 kN/mm (as determined from the data at the respective displacement peaks).

The stiffness behavior of Unit II in each displacement direction early in the test differed from Unit I. In Section 5.2.2, the performance of the fixtures were cited as the probable cause of the difference in stiffness between the retract and the extend directions in Unit I. If the behavior of the fixtures differed from one displacement direction to the other at the smaller displacement increments, then this should have had a greater effect on Unit II because of its smaller diameter columns (i.e., Unit II was less stiff than Unit I). Also, the 8.27-kN/mm initial stiffness of Unit II in the extend-direction was about 91% of the initial stiffness of Unit I in that direction. Such a high percentage must have been a result of the behavior of the fixtures, given the differences in the column diameters of the two specimens. Finally, just as was the case with Unit I, the stiffness of Unit II in each direction eventually became nearly identical.

### Initial Cracking

The first visible cracks occurred during the first cycle to 5.08 mm. All of the cracks were very thin, and most of them were horizontal cracks where the upper and the lower column transition into the faces of the B-C joint. There was a vertical crack at one of the B-C joint corners where the strut side intersected the joint. Also, there was a flexural crack in one of the struts at approximately 230 mm from the B-C joint.

From cycles to 7.62 mm through cycles to 12.16 mm, in addition to the growth and the spread of the cracks noted earlier, hairline flexural cracks formed in the struts in-between the B-C joint and a distance of 230 mm away. There was also a small flexural crack in the lower column at a distance of approximately 140 mm (i.e.,  $\approx d_c/2$  = approximately one-half of the effective column depth) below the strut. Figure 91 is a

sketch of Unit II with the typical cracking observed during the test through the cycles to 12.7 mm.

### B-C Joint Shear Cracking

*Visible Cracks versus Hoop Strains.* In addition to the cracks already considered, the first visible B-C joint cracks occurred at the displacements equal to  $\pm 12.7$  mm. A short diagonal crack formed in the center of the B-C joint, along with horizontal cracks that were perpendicular extensions from earlier vertical cracks (i.e., the cracks shown in Fig. 91 at the intersections of the strut sides and the B-C joint faces).

While cracks in the B-C joint became visible at this point, B-C joint shear cracking probably occurred earlier during the cycles to 5.08 mm. The reason being that the strains in the hoops in the B-C joint (JT and JB) suddenly increased at the displacements equal to  $\pm 5.08$  mm (i.e., similar behavior to that shown in Figs. 65).

*Shear Stress in the B-C Joint.* The maximum value of  $v_{jt}$  at first cracking in the B-C joint (for the displacements equal to  $\pm 5.08$  mm) was determined with a procedure that was similar to the one shown in Figure 66. The calculations yielded the following result:  $v_{jt} = 0.17\sqrt{f'_c}$  ( $f'_c$  in MPa).

In Unit II, the crests of the joint faces were 25.4 mm outward from the sides of the struts and the portions of the joint beyond the sides of the struts represented just 7% of  $A_{jt}$ . Additionally, only two of the eight column bars were located outside of the width of the struts. Thus, it was decided that the columns were not wide relative to the struts and the portions of the joint beyond the sides of the struts were included in all calculations of the value of  $v_{jt}$ .

*Hysteretic Behavior.* The hysteretic behavior of Unit II, including the cycles where B-C joint cracking became visible, is shown in Figure 92. The stiffness of Unit II at the peak displacements equal to +5.08 mm was over 10% larger than it was initially.

However, at the displacements equal to +7.62 mm the stiffness of Unit II was nearly equal to the initial stiffness. In the extend direction, the stiffness of Unit II at the displacements equal to -5.08 mm was approximately 10% smaller than it was initially. However, at the displacements equal to -7.62 mm the stiffness of Unit II was approximately 25% smaller than it was initially. As mentioned earlier in this section ("Initial Stiffness"), the erratic behavior of the stiffness of Unit II in the two displacement directions early in the test was likely a result of the behavior of the fixtures.

*Strains in the Strut Bars.* For the cycles subsequent to those to 5.08 mm, the strains at the locations adjacent to the B-C joint in the strut main bars exhibited behavior similar to that shown in Figure 68 for Unit I. However, unlike Unit I, where the bars adjacent to the B-C joint were in compression (when the sense of the moments so dictated) until displacements of 12.7 mm, the bars in Unit II showed increasing values of tensile strains at the start of cycling to 7.62 mm. Thus, the main bars adjacent to the B-C joint were in tension, regardless of the sense of the moments, from the start of cycling to 7.62 mm throughout the rest of the test. To the contrary, at the locations near the edge of the anticipated flexural hinge regions, the compressive strains in the strut bars increased as the displacements increased, when the sense of the moments was such that the respective locations were in compression. (as was the case in Unit I; Fig. 69).

### 5.3.3 Specimen Yield

#### Precursors to Specimen Yield

*Cycles to 15.24 mm.* During the cycles to 15.24 mm, the lower column probably yielded and bond deteriorated in the bottom of the B-C joint.

The calculated first yield moment for the lower column was reached at the displacements equal to  $\pm 15.24$  mm. At these displacements, the strains in the column

extreme bars at the underside of the B-C joint were beyond the yield strain. Hence, it is probable that some of the other bars were at/beyond the yield strain as well. Also, new flexural cracks appeared on both sides of the lower column at a distance of approximately  $d/2$  below strut. These cracks extended around the column to the front and the back faces.

Unlike Unit I, the bond deterioration in the bottom of the B-C joint in Unit II was advanced without the occurrence of strut bar yielding. Figure 93, a plot of the values of  $F_b$  at the displacement peaks versus displacement for the instrumented strut lower main bar, substantiates this. The figure shows that the values of  $F_b$  began to "roll off" at the displacements equal to  $\pm 15.24$  mm; this happened without the occurrence of yielding of the bar at the tension-sides of the joint (Fig. 71; the tension-side of the B-C joint for retract direction displacements is the left side, and vice-versa for extend direction displacements). As a matter of fact, this bar never yielded at the tension-sides of the B-C joint. The bond deterioration in the bottom of the B-C joint became so severe at the larger displacements that this bar yielded only on the compression-sides of the B-C joint. This occurred during the retract portion of the first cycle to  $2\Delta_y$ , and in the extend portion of the first cycle to  $2.5\Delta_y$  (Fig. 93). Thus, the peaks of the curve in Figure 93 are not near the value of  $F_b$  (45 kN) that would have occurred had this bar yielded on the tension-sides of the joint, without any contribution from the bar at the compression-sides of the joint. Based on the bond conditions for this bar, it is likely that the bond conditions were poor for all of the strut lower main bars in the B-C joint for the majority of the test.

*Cycles to 17.78 mm.* At the displacements equal to  $\pm 17.78$  mm, bond deterioration in the top of the B-C joint was advanced, and the diagonal cracks in the B-C joint spanned the faces of the joint.

Figure 94 shows that the values of  $F_b$  for the instrumented strut upper main bar began to "roll off" at the displacements equal to  $\pm 17.78$  mm. This occurred before the upper main bar yielded. However, unlike the lower main bar, the upper main bar did eventually yield at the tension-sides of the B-C joint during the cycles that are labeled in

Figure 94 (i.e., during the first cycle to  $2\Delta_y$  in the retract direction, and during the cycles to  $1.5\Delta_y$  in the extend direction), but this occurred after significant tensile forces were in this bar on the compression-sides of the B-C joint. In the extend direction for example, the values of  $F_b$  during the cycles to  $1.5\Delta_y$  are approximately 10 - 12 kN. The value of  $F_b$  required for bar yielding with no compression force is shown in Figure 94 to be equal to 48 kN. Therefore, the part of the upper main bar on the compression-side of the B-C joint was experiencing 36 to 38 kN of tensile force when the part of the bar at the tension-side of the joint yielded. As mentioned earlier, this type of behavior represents significant bond deterioration in the B-C joint.

The diagonal cracks on the faces of the B-C joint lengthened at the displacements equal to  $\pm 17.78$  mm. These cracks extended across the faces of the B-C joint and then continued into the sides of the struts. The cracks were "anchored" in the sides of the struts at the projections of the apexes of the columns (this behavior is clearly depicted in Figs. 101 and 102, which are photographs that were taken at a larger displacement increment). In other words, the cracks in the B-C joint were behaving as if the joint were part of a 356-mm square column, rather than a 356-mm diameter column.

### Specimen Yield

While the displacements equal to  $\pm 20.32$  mm were taken as  $\pm \Delta_y$ , respectively, neither the data nor the visual observations clearly indicated that Unit II actually yielded at these displacements. The difficulty that was encountered in clearly identifying the yield displacement is explained by the hysteretic behavior of Unit II prior to and just following the cycles to 20.32 mm.

*Hysteretic Behavior.* Figure 95 is the hysteresis plot for Unit II through the cycles to  $1.25\Delta_y$ . The peaks of the three cycles at which Unit II was considered to have yielded

are labeled for each displacement direction ( $\pm\Delta_y$ ). Figure 95 does not indicate that there was as sudden a change in the strength or in the stiffness of Unit II, from the cycles to  $\Delta_y$  to the cycles to  $1.25\Delta_y$ , as was the case with Unit I (Fig. 72). The fact that the shape of the envelope of the hysteresis loop peaks in Figure 95 forms a smooth curve is not coincidental. From the start of the test through the cycles to  $\Delta_y$ , only the lower column of Unit II had yielded. Thus, the shape of the envelope was defined by the circular arrangement of the column bars and the associated differences in the occurrence of bar yield. It should be noted that the difference that existed early in the test between the retract direction stiffness and the extend direction stiffness was nearly gone during the cycles to  $\Delta_y$ .

*Shear Stress in the B-C Joint.* For purposes of comparison with Unit I, the maximum value of  $v_{jt}$  was determined for the displacements equal to  $\pm\Delta_y$  for Unit II. Using a procedure similar to the one outlined in Figure 66, the value of  $V_{jt}$  was determined and used with Equation 1. The result was as follows:  $v_{jt} = 0.31\sqrt{f'_c}$ .

#### 5.3.4 Post-Specimen-Yield

##### Cycles to $1.25\Delta_y$

There were several significant behavioral changes in Unit II that occurred in the first set of post-yield cycles. The three cycles to  $1.25\Delta_y$  brought about changes in the behavior of:

- 1.) the lower column,
- 2.) the cracking in the B-C joint, and
- 2.) the hysteresis of the specimen.

*The Lower Column.* The theoretical value of  $M_{nc}$  in the lower column was attained during the cycles to  $1.25\Delta_y$ . However, there were no visible signs of plastic hinge

formation when the displacements equaled  $\pm 1.25\Delta_y$ . Therefore, the capacity of the column may have been larger than the theoretical capacity. Figure 96 shows the extent of the flexural cracking in the anticipated plastic hinge region on the back face of the lower column at a displacement equal to  $-1.25\Delta_y$ .

*Cracking in the B-C Joint.* Several new B-C joint cracks appeared during cycling to  $1.25\Delta_y$ , and several of the old cracks grew. Many of the new cracks were concentrated in the upper portion of the back face of the B-C joint. Figure 97 shows some of the new cracks at a displacement equal to  $-1.25\Delta_y$ . Figure 98 shows the extent of cracking on the front face of the joint at a displacement equal to  $+1.25\Delta_y$ . The "anchoring" of the B-C joint cracks in the struts is also shown in this figure. The older cracks in the lower portion of the B-C joint also grew.

*Hysteretic Behavior.* As is shown in the hysteresis plot in Figure 95, during the cycles to  $1.25\Delta_y$  the pinching in the hysteresis loops began to become more pronounced at the smaller displacements. However, this was more difficult to detect in Unit II than it was in Unit I (Fig. 72). The reason being that in Unit II the change in the shape of the hysteresis loops from the preferred "spindle"-shape to the pinched-shape is much more gradual than was the case with Unit I. This difference in the onset of "pinching" between Units I and II is due to the fact that bond deterioration progressed in Unit II in the B-C joint for the strut main bars without the occurrence of yield in these bars (Figs. 93 and 94). In Unit I, bond deterioration did not progress until after the main bars in the struts had yielded (Figs. 70 and 73). Thus, in Unit II, the loss of bond, and the occurrence of the pinched-shape of the hysteresis loops, was gradual. Conversely, in Unit I the loss of bond and the occurrence of "pinching" was more sudden.

The decrease in the energy dissipated by the Units in the second cycles versus the first seemed to be independent of the way that bond deterioration progressed. Both Units

experienced consistent decreases in the amount of energy dissipated in the second cycles compared to the first until the cycles to  $1.25\Delta_y$ , at which point the trend became worse.

#### Cycles to $1.5\Delta_y$

During the cycles to  $1.5\Delta_y$ , the following significant events occurred:

- 1.) the moment in the upper column exceeded the calculated yield moment,
- 2.) the upper main bars in the struts yielded in one displacement direction only,
- 3.) the hysteresis plot indicated that there was a relatively large decrease in the strength and in the stiffness of Unit II from the first cycle to the second cycle.

*The Upper Column.* While the calculated yield moment for the upper column was exceeded at the displacements equal to  $\pm 1.5\Delta_y$ , the bar strains above the B-C joint in the column extreme bars did not indicate that yield occurred. As cycling progressed to larger displacement increments, the ERSG on the column left extreme bar never indicated that the yield strain was attained at that location above the B-C joint. As for the ERSG on the column right extreme bar, no information was obtained at the larger displacement increments as the instrument failed during the cycles to  $2\Delta_y$ .

*The Struts.* The strut upper main bars yielded during the extend portion of the cycles to  $1.5\Delta_y$  (on the left side of the B-C joint only; Figure 94), as indicated by the instrumented upper main bar of the struts.

*Hysteretic Behavior.* Figure 99 shows the hysteretic behavior of Unit II for the entire test. The hysteresis loops that correspond to the cycles at  $1.5\Delta_y$  showed a strength gain in the first cycle, relative to the strength attained during the cycles to  $1.25\Delta_y$ . However, the significant drop in the strength and the stiffness of Unit II, and in the energy dissipated by Unit II, in the second cycle to  $1.5\Delta_y$  was the start of a trend that continued for the duration of the test.

*B-C Joint Shear Stress.* Since some of the ERSG's on the strut bars failed after the cycles to  $1.5\Delta_y$  were concluded, the maximum value of  $v_{jt}$  was determined from the bar strains (Fig. 66) for the final time. The value of  $v_{jt}$  was  $0.41\sqrt{f'_c}$ . However, as was the case in Unit I, as the bending moments in the struts at the B-C joint in Unit II increased, Equation 2 became more accurate in predicting the value of  $V_{jt}$ . Therefore, the results from Equation 2 were used for all of the subsequent calculations of  $v_{jt}$ .

#### Cycles to $2\Delta_y$ through Cycles in Excess of $6\Delta_y$

*Cycles to  $2\Delta_y$ .* The calculated first yield moment for the struts was attained at the displacements equal to  $\pm 2\Delta_y$ . During the first cycle to  $2\Delta_y$ , the strut upper main bars at the locations adjacent to the right side of the B-C joint (Fig. 94) actually yielded. At approximately the same point, the lower main bars in the right strut also yielded as they were pulled from across the B-C joint by the left strut (Fig. 93). It should be noted that after the displacement equal to  $+2\Delta_y$  was reached for the first time there was no longer any bond force transferred through the bottom of the B-C joint in the retract direction.

Unit II reached its maximum strength in the retract (positive displacement) direction at the first displacement equal to  $+2\Delta_y$  (Fig. 99; note that the same peak strength is reached later on in the first displacement equal to  $+4\Delta_y$ ).

The load versus strain plots for the hoops in and adjacent to the B-C joint indicated that the strains in these hoops grew suddenly at the displacements equal to  $\pm 2\Delta_y$ . Figure 100 shows the plots for the hoop JT. JT1 and JT2 clearly indicate significant increases in:

- 1.) the strain at the first displacements equal to  $\pm 2\Delta_y$ , relative to the strain at the last displacements equal to  $\pm 1.5\Delta_y$ , and
- 2.) the strain at the second and third displacements equal to  $\pm 2\Delta_y$ , relative to the first displacement equal to  $\pm 2\Delta_y$ .

At the displacements equal to  $\pm 2\Delta_y$ , the ERSG's in the lap splice indicated that the bar in the lap splice extending through the B-C joint (starter bar) yielded in tension, while the splice bar was at about 85% of its yield strain. The magnitudes of the compressive strains in these bars at this location (approximately half of the column depth below the bottom of the strut) were significantly larger relative to the magnitudes experienced by the bar locations in and adjacent to B-C joint. The spliced bar was consistently able to develop 85% of the compressive strain developed by the starter bar (the value of which was in excess of 75% of the yield strain). Additionally, no distress was seen in the splice at this point, or for the duration of the test.

*Cycles to  $2.5 \Delta_y$ .* During the extend portion of the first cycle to  $2.5\Delta_y$ , the lower main bars in the left strut yielded at the locations adjacent to the B-C joint as these bars were pulled from across the joint (Fig. 93). It should be noted that once a displacement equal to  $-2.5\Delta_y$  was achieved there was no longer any bond force through the bottom of the B-C joint in either direction. The upper main bars in the left strut were beyond yield at this point. From this point on, the displacement ductilitys attained by Unit II are not a good measure of its performance (Sec. 5.2.4, "Cycles to  $2\Delta_y$  through Cycles in Excess of  $6\Delta_y$ ").

Unit II reached its maximum strength in the extend (negative displacement) direction at the first displacement equal to  $-2.5\Delta_y$  (Fig. 99). This strength was nearly identical to that attained in the retract direction at the first displacement equal to  $+2.5\Delta_y$ . Once the maximum strength of Unit II was attained in the extend direction, Unit II experienced consistent strength and stiffness decay in each of the subsequent displacement increments, particularly in the second and third cycles at each increment.

The strength attained by Unit II was barely adequate to develop first yield in the struts (approximately 60% of the value of  $M_{nb}$  was developed). While the strength attained by Unit II was more than enough to cause yield in the upper column, whether or

not yielding actually occurred could not be verified (this sec., "Cycles to  $1.5\Delta_y$ "). However, the maximum strength of Unit II was sufficient to develop approximately 90% of the value of  $M_{nc}$  in the upper column. The lower column did yield, and Unit II attained enough strength to exceed the value of  $M_{nc}$  by over 10%, although there were no visible signs of plastic hinging (i.e., there was no significant damage to the concrete).

Finally, the strength that Unit II was able to attain resulted in a maximum value of  $v_{jt}$  of  $0.48\sqrt{f'_c}$  ( $f'_c$  in MPa). This is similar to the value that was determined for Unit I (Sec. 5.2.4, "Cycles to  $2\Delta_y$  through Cycles in Excess of  $6\Delta_y$ "). Such B-C joint shear stress values are relatively small considering the amount of damage that was sustained by the B-C joints in Units I and II.

Figures 101 and 102 show the condition of the front and back, respectively, of Unit II at the last displacement equal to  $-2.5\Delta_y$ . By this point in the test:

- 1.) Unit II had attained its maximum strength in both directions,
- 2.) the lower column was beyond the value of  $M_{nc}$ ,
- 3.) the upper column was beyond the first yield moment,
- 4.) the lower main bars of the struts were slipping through the B-C joint, and
- 5.) the hoops in and adjacent to the B-C joint had experienced large increases in strain (the hoop in the upper portion of the joint was beyond yield).

Note that in each figure there is one large B-C joint shear crack that is closely aligned with the major joint diagonal. Additionally, during the cycles to  $2.5\Delta_y$  these cracks did not close when the displacements were zero. There is no indication in either Figure 101 or 102 of plastic hinge formation in the lower column.

*Cycles to  $3\Delta_y$ .* The column extreme bar on the right side of the B-C joint yielded at the mid-height of the joint at the displacements equal to  $-3\Delta_y$ . At the same point, the ERSG in the B-C joint on the left extreme bar was reporting questionable data. However, from the trend seen in the earlier data from this ERSG it was possible that yielding occurred on the left extreme bar in the B-C joint.

Figure 103 shows the spalling that began to occur in the lower column at the cycles to  $3\Delta_y$ . Just as the large end rotations of the struts in Unit I were responsible for most of the spalling in that specimen, the large end rotations of the lower column were responsible for the majority of the spalling in Unit II. In both instances, the end rotations resulted from bond deterioration of the member bars in the B-C joint. Figure 103 does not give any indication that a plastic hinge had formed in the lower column.

Figure 100 indicates that at the displacements equal to  $\pm 3\Delta_y$  the strains in hoop JT began to decrease. By this point in the test the ERSG's on the other hoops (AJ, JB, and BJ) had failed.

*Cycles to  $4\Delta_y$ .* At the first displacement equal to  $+4\Delta_y$  the strength that Unit II had attained during the first displacement equal to  $+2\Delta_y$  was reached again (Fig. 99). This coincided with a considerable increase in the damage in the B-C joint. Figure 104 shows the back face of B-C joint at the first displacement equal to  $+4\Delta_y$ . The cracks with the slopes up and to the right were open because of the forces imposed by the displacement in the retract direction. Spalling began in the crack with the slope up and to the left (the crack closely aligned with the major joint diagonal) as the compression parallel to that crack became large.

Also in Figure 104, the concrete on the compression-side (left) of the lower column is pushing away from the column. This is probably a continuation of the spalling that had begun during the previous sets of cycles, since the rotation of the lower column had become quite large.

Figure 99 shows that for the remainder of the cycles to  $4\Delta_y$  the specimen exhibited both decreased strength and stiffness, particularly in the case of the last two cycles, where these quantities reached new lows.

*Cycles to  $5\Delta_y$  and to  $6\Delta_y$ .* During the cycles to  $5\Delta_y$  and to  $6\Delta_y$ , the decay of the strength and the stiffness of Unit II continued to occur (Fig. 99). Also, the range of displacements over which the hysteresis loops were pinched became larger. The damage to

the B-C joint region increased, and it became evident that the curved regions of the joints were being pushed away from the joint core by the sides of the struts. On the back face of the B-C joint, the curved portion eventually spalled off. Figure 105 shows sketches of a cross-section through the B-C joint of Unit II before and after the curved portions of the joint were pushed away from the joint core.

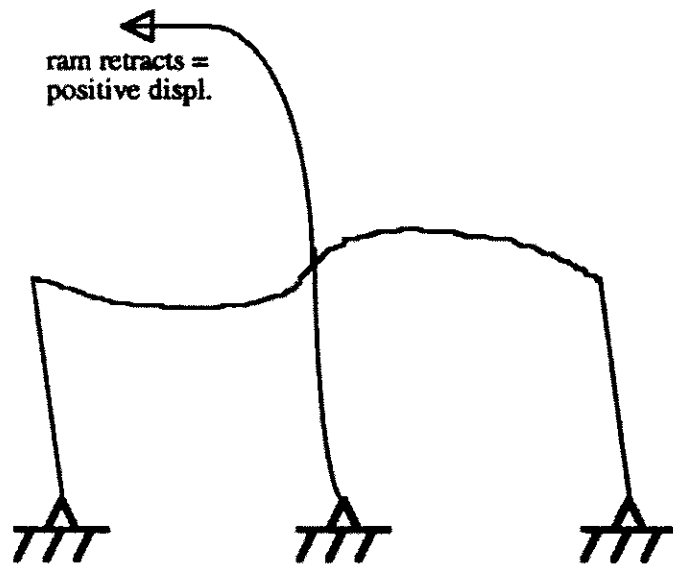
*"Push-Over" Cycles.* Having reached the displacements where the strength of Unit II was steadily decreasing, the specimen was subjected to two additional cycles to determine the maximum displacement ductility that it could endure. Figure 99 shows that the value of the maximum displacement ductility reached by Unit II in the first cycle in the retract direction was approximately 10 ( $\approx$  9% drift), while in the extend direction it was approximately 11 ( $\approx$  10% drift). In both instances the displacements that Unit II was subjected to were limited by the stroke of the ram. Figure 106 shows Unit II at its maximum displacement ductility in the extend direction. The hysteresis loop for the first cycle remained pinched over the range of most of the displacements that were previously attained. Then, Unit II noticeably stiffened and showed levels of strength in both directions that approached the strengths attained in the cycles to  $6\Delta_y$  (note that this "apparent strength" is a result of the relatively large increase in the displacement increment).

The displacement ductility applied in the retract portion of the second cycle was less than 70% of that attained in the first cycle, and the strength and the stiffness of Unit II decreased markedly. The reason that the displacement ductility in the retract direction was decreased was because a true hinge had formed in the lower column. As Figure 107 shows, the hinge in the lower column resulted in the concentration of all of the subassembly deformation at the "hinge". As a result, the brace fixture on the right side of the Unit II interfered with the travel of strut "roller" support fixture. A "hinge" also formed in the lower column in the extend portion of the second cycle but this did not

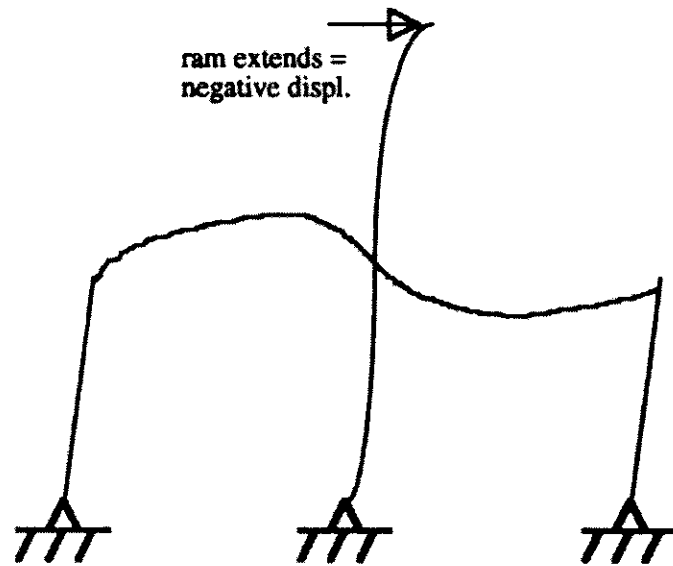
prevent Unit II from reaching the same displacement ductility that was achieved in this direction in the first cycle.

Figure 106 shows that the all-thread anchors located near the B-C joint region in Unit II were too far from the joint for the potentiometer and LVDT data to be useful, just as was the case with Unit I (Sec. 5.2.4, "Cycles to  $2\Delta_y$  through Cycles in Excess of  $6\Delta_y$ ").

After the conclusion of the "push-over" cycles, all of the loose concrete was removed from the faces of the B-C joint region in order to determine whether or not the depth of the major diagonal cracks were limited to the curved portions of the joint faces. Figures 108 and 109 show the results of this procedure. The crack in the upper portion of the B-C joint in Figure 108 is on the front face of the joint. This crack is the same crack shown in Figure 101 and the depth of this crack extended into the core of the joint. Figure 109 shows the back face of the joint after the loose material had been removed. The large crack in this figure is the same crack shown in Figure 104 (i.e., the crack with the negative slope). This crack penetrated the joint core as well.



a) Specimen undergoing positive displacement



b) Specimen undergoing negative displacement

Figure 61 The displacement convention used in the tests.

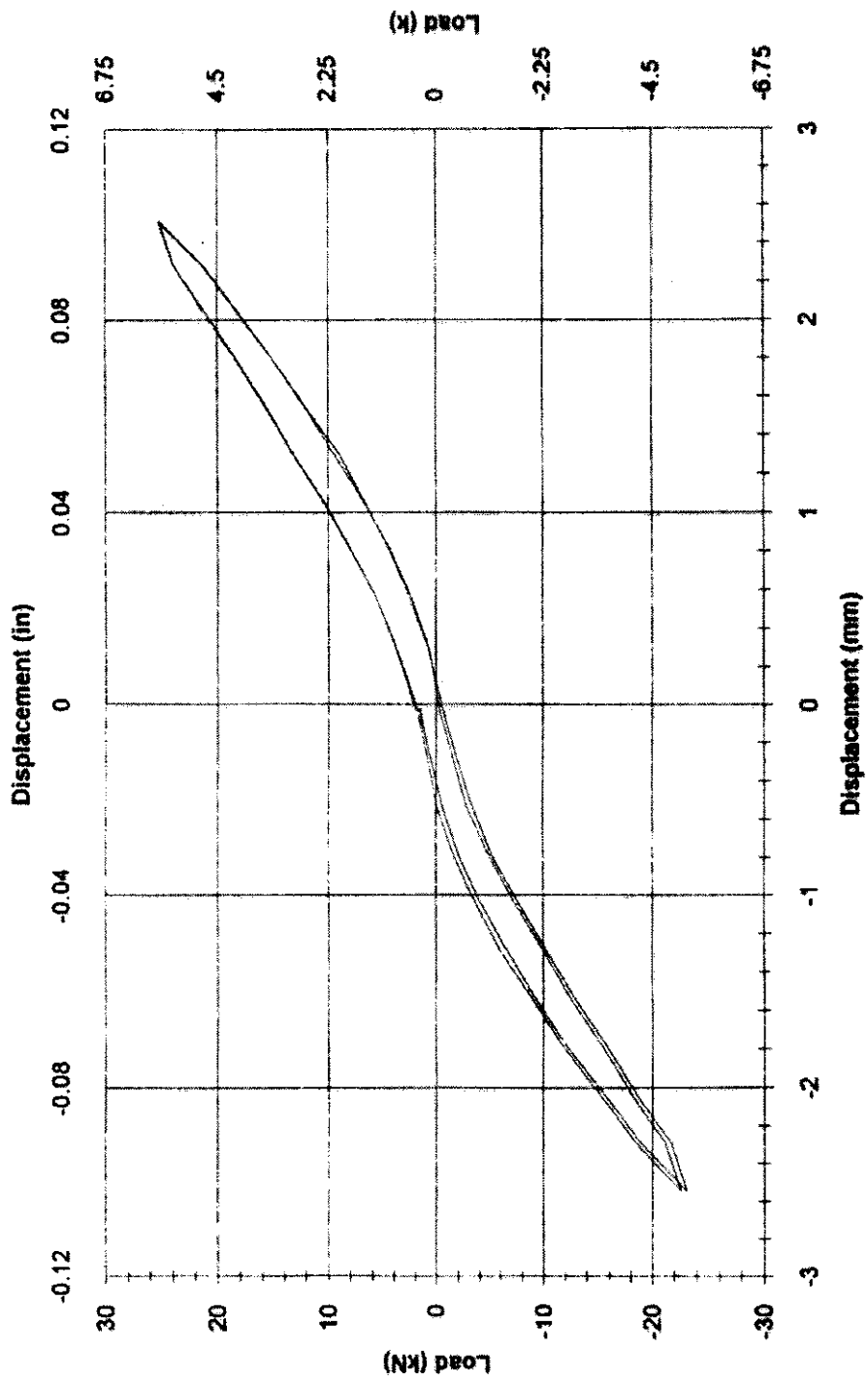


Figure 62 Hysteresis loops for Unit I (two cycles to 2.54 mm).

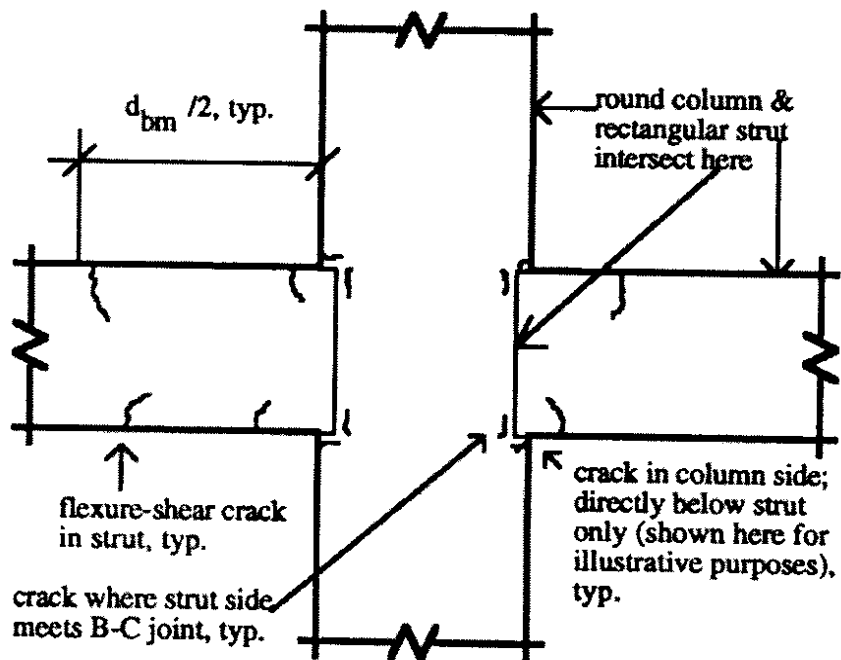


Figure 63 Cracking typically observed in Unit I through the cycles to 12.7 mm.

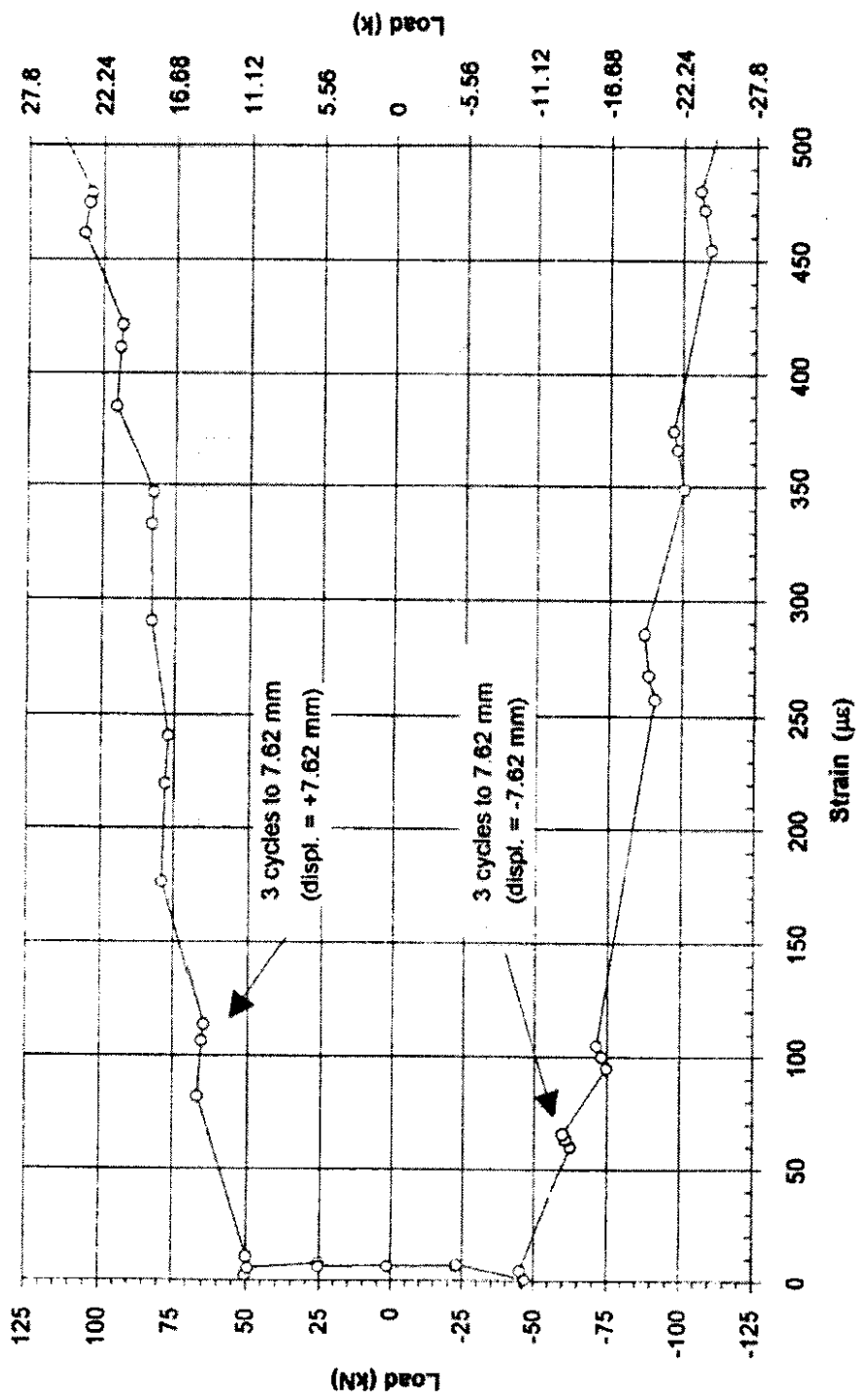


Figure 64 Load versus strain for hoop AJ in Unit I (at the displacement peaks early in the test).

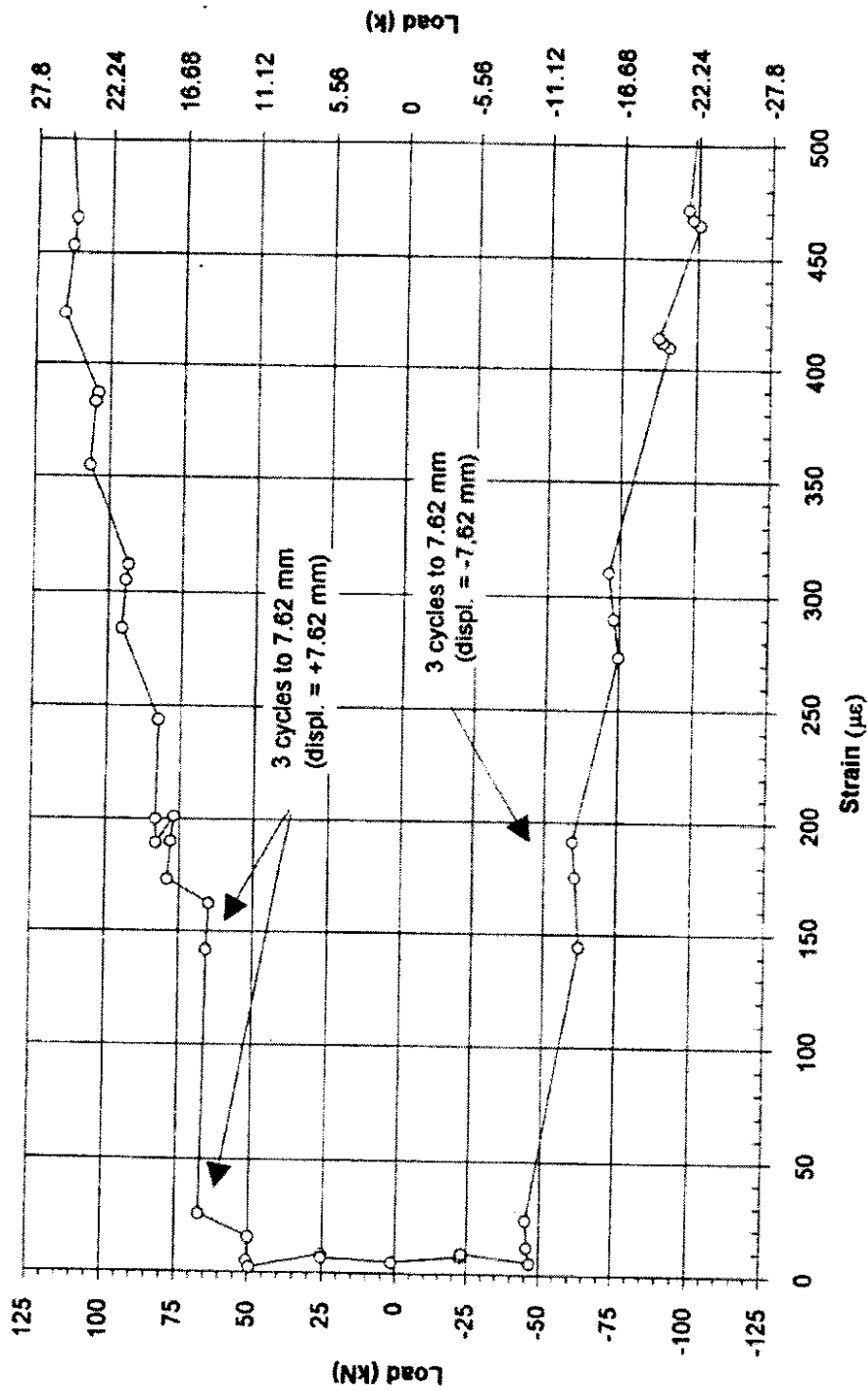


Figure 65 Load versus strain for hoop JB -- front face of B-C joint in Unit I (at the displacement peaks early in the test).

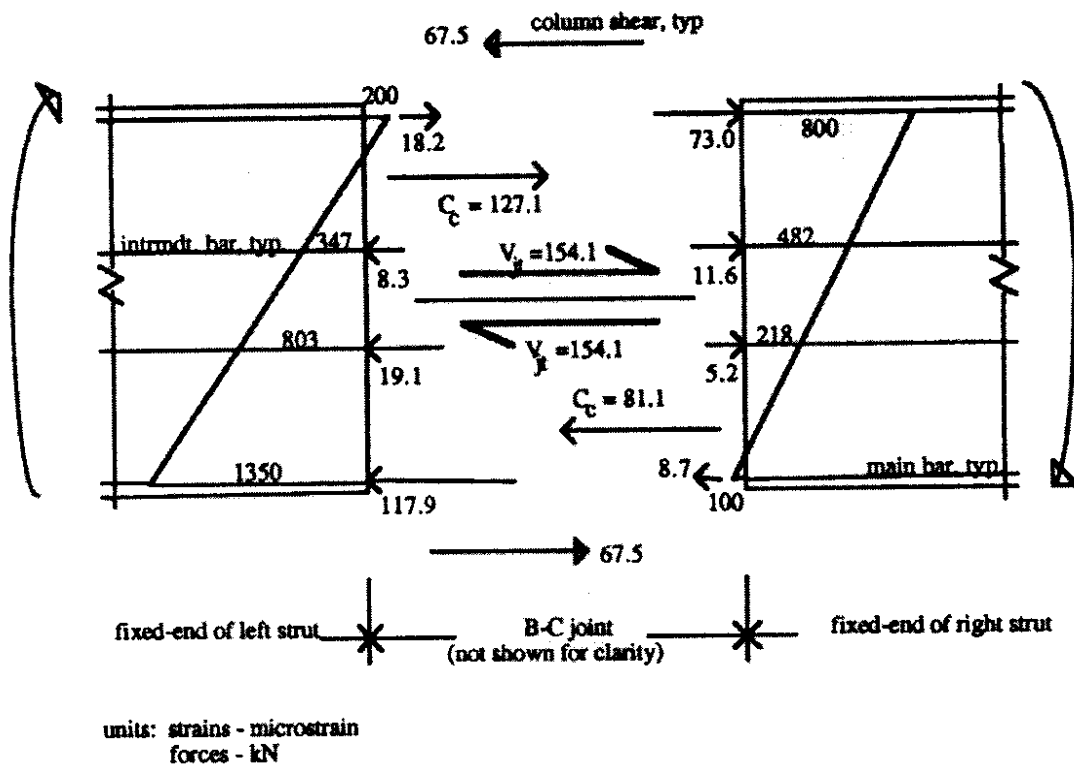


Figure 66 Determination of the value of the horizontal shear force at the mid-depth of the B-C joint in Unit I at a peak displacements equal to +7.62 mm.

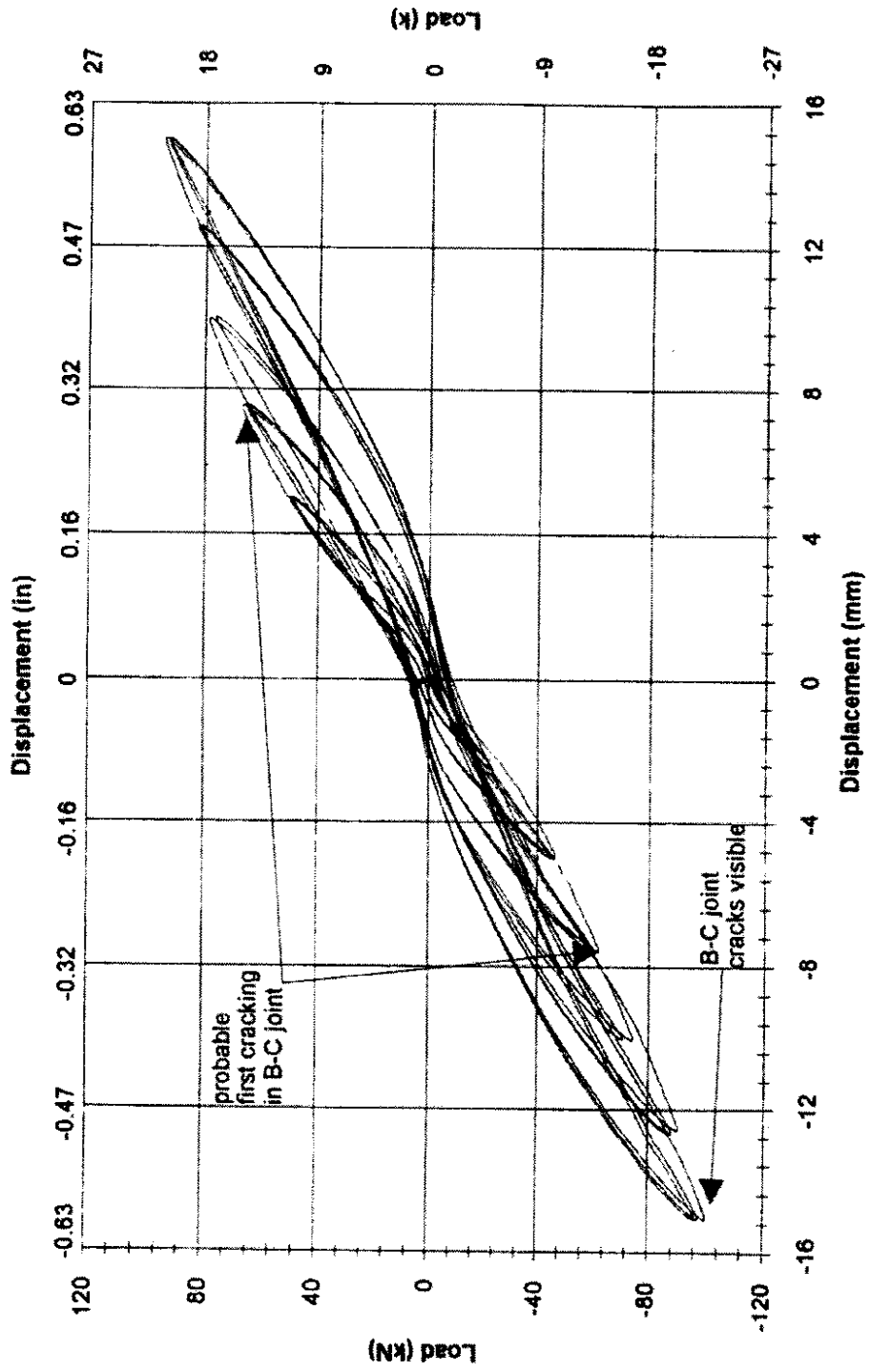


Figure 67 Hysteresis loops for Unit I (cycles through 15.24 mm).

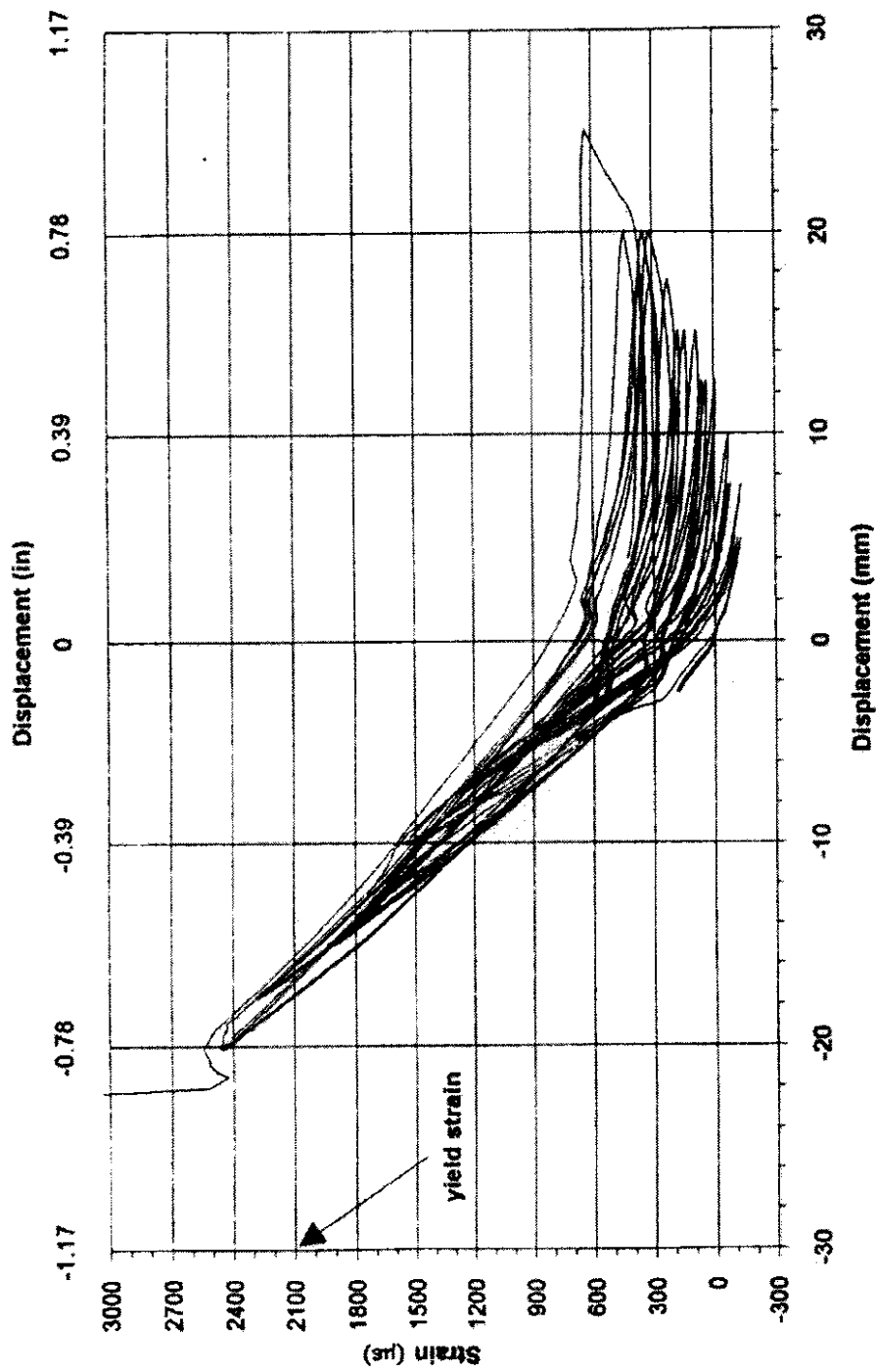


Figure 68 Typical strain history at the locations adjacent to the B-C joint for the main bars in the struts in Unit I (at the fixed-end of the right strut in one of the lower main bars).

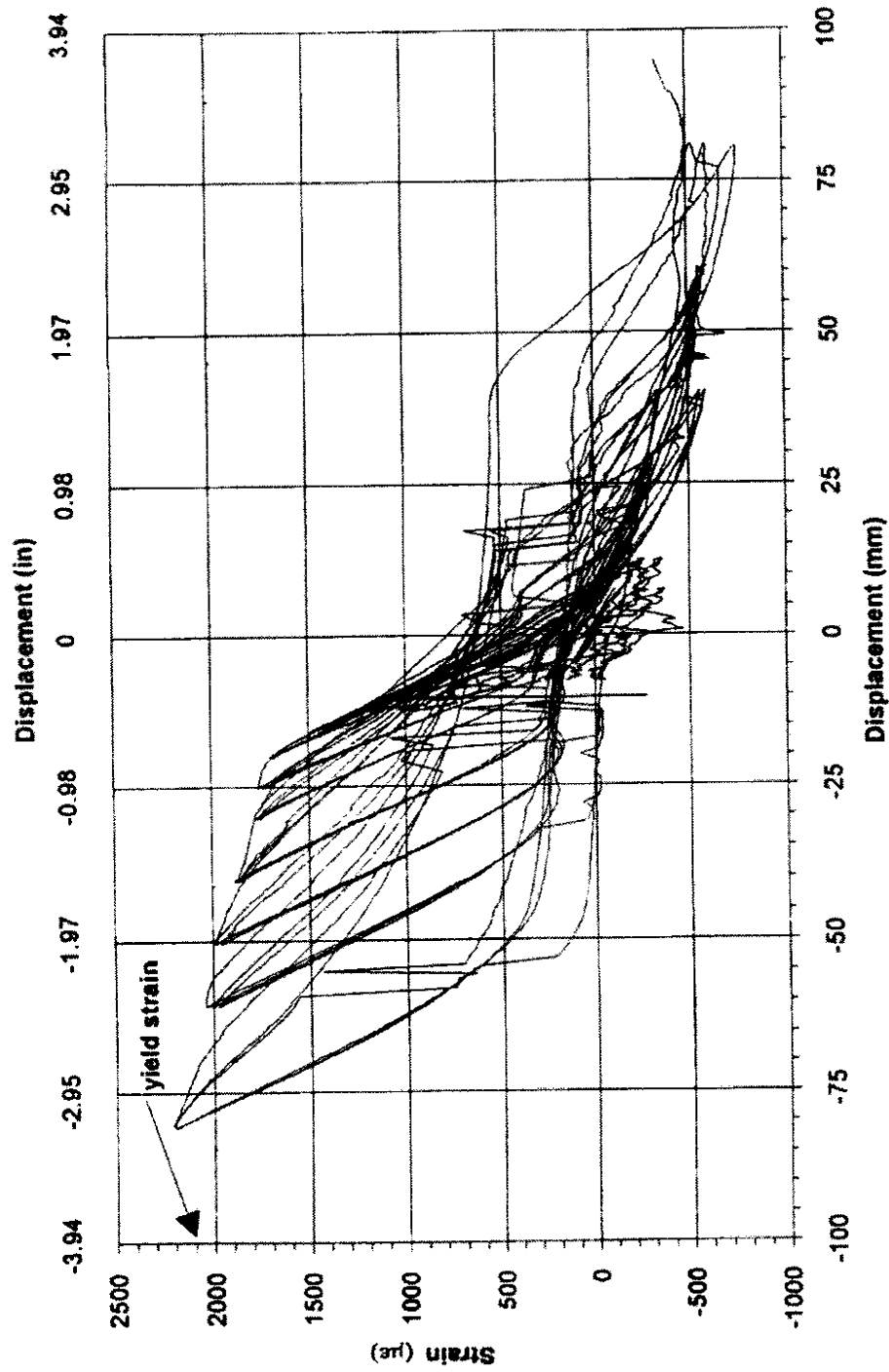


Figure 69 Typical strain history at the locations near the expected plastic hinge regions for the main bars in the struts in Unit I (near the fixed-end of the right strut in the lower main bar).

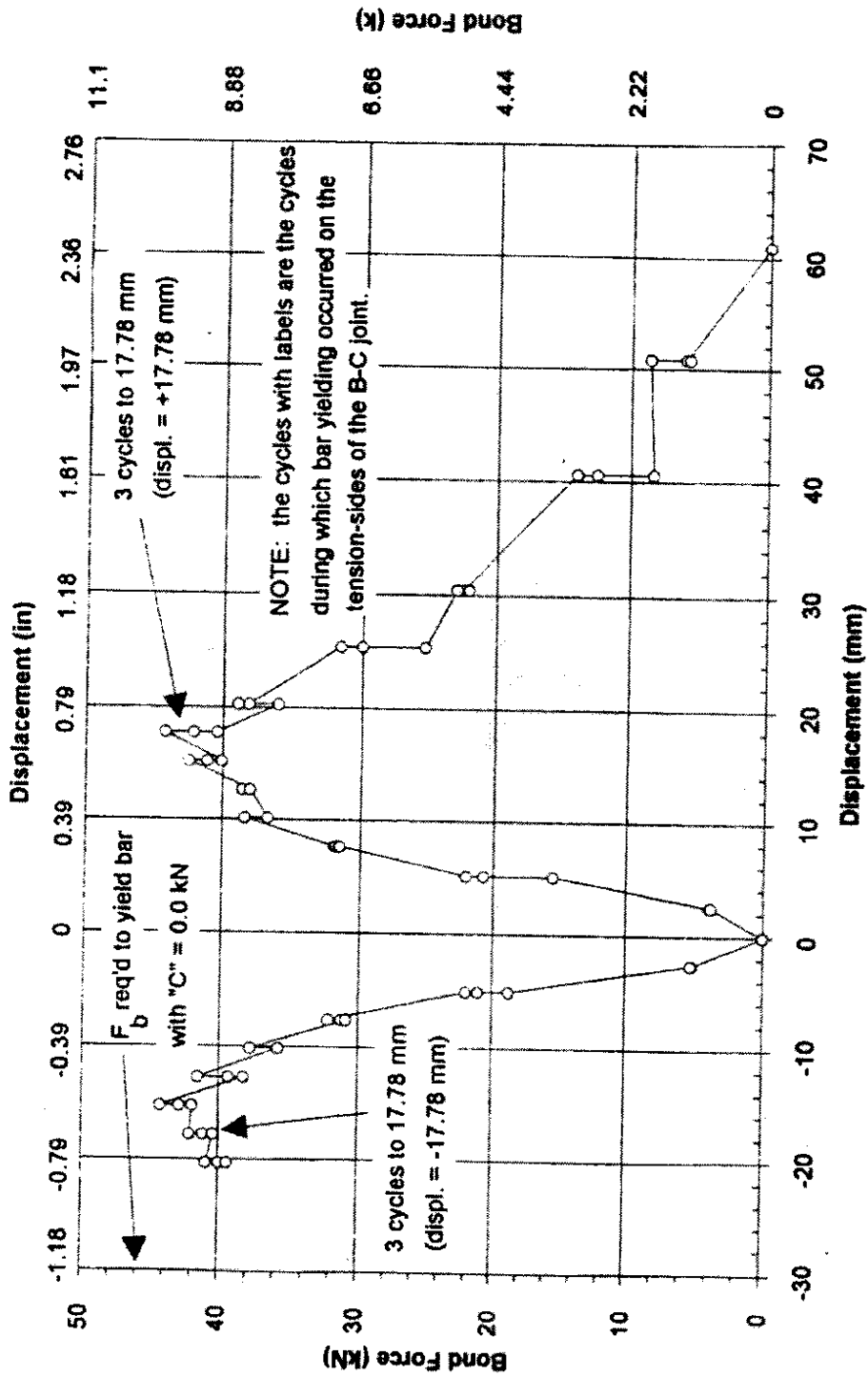
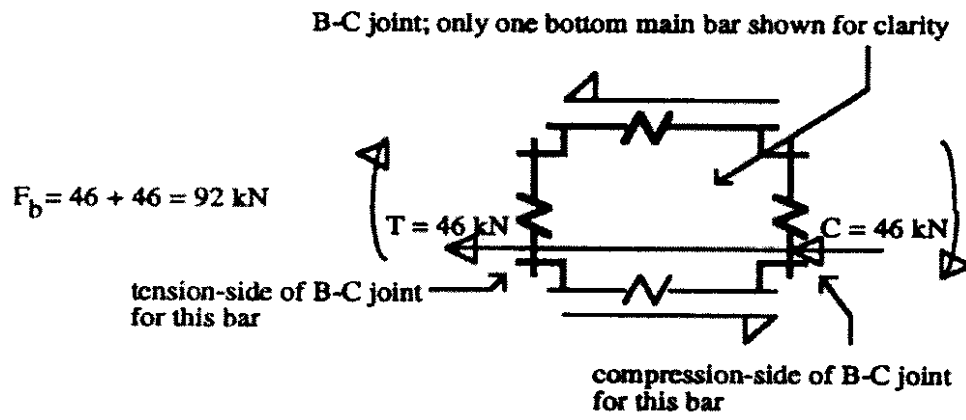
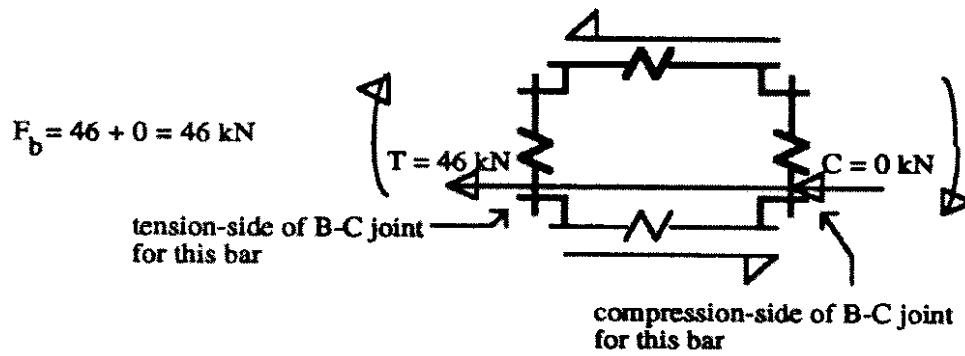


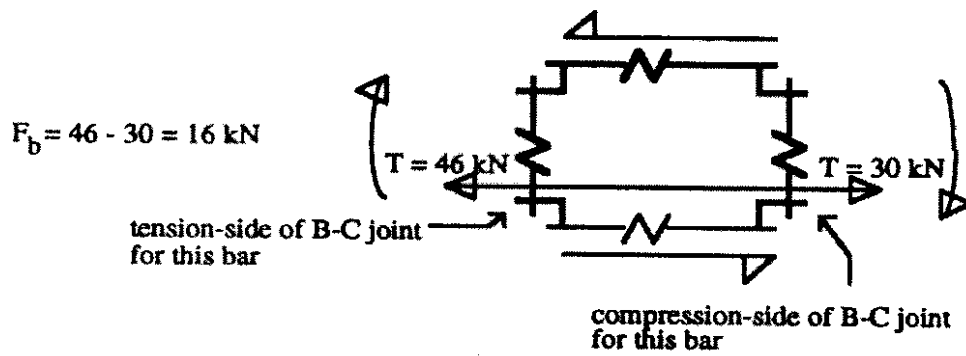
Figure 70 Bond force in a strut lower main bar versus displacement for Unit I (at the displacement peaks).



a) Optimum bond conditions



b) Moderate bond conditions



c) Poor bond conditions

Figure 71 Three B-C joint bond-condition scenarios; retract-direction displacement, yield force for bar = 46 kN.

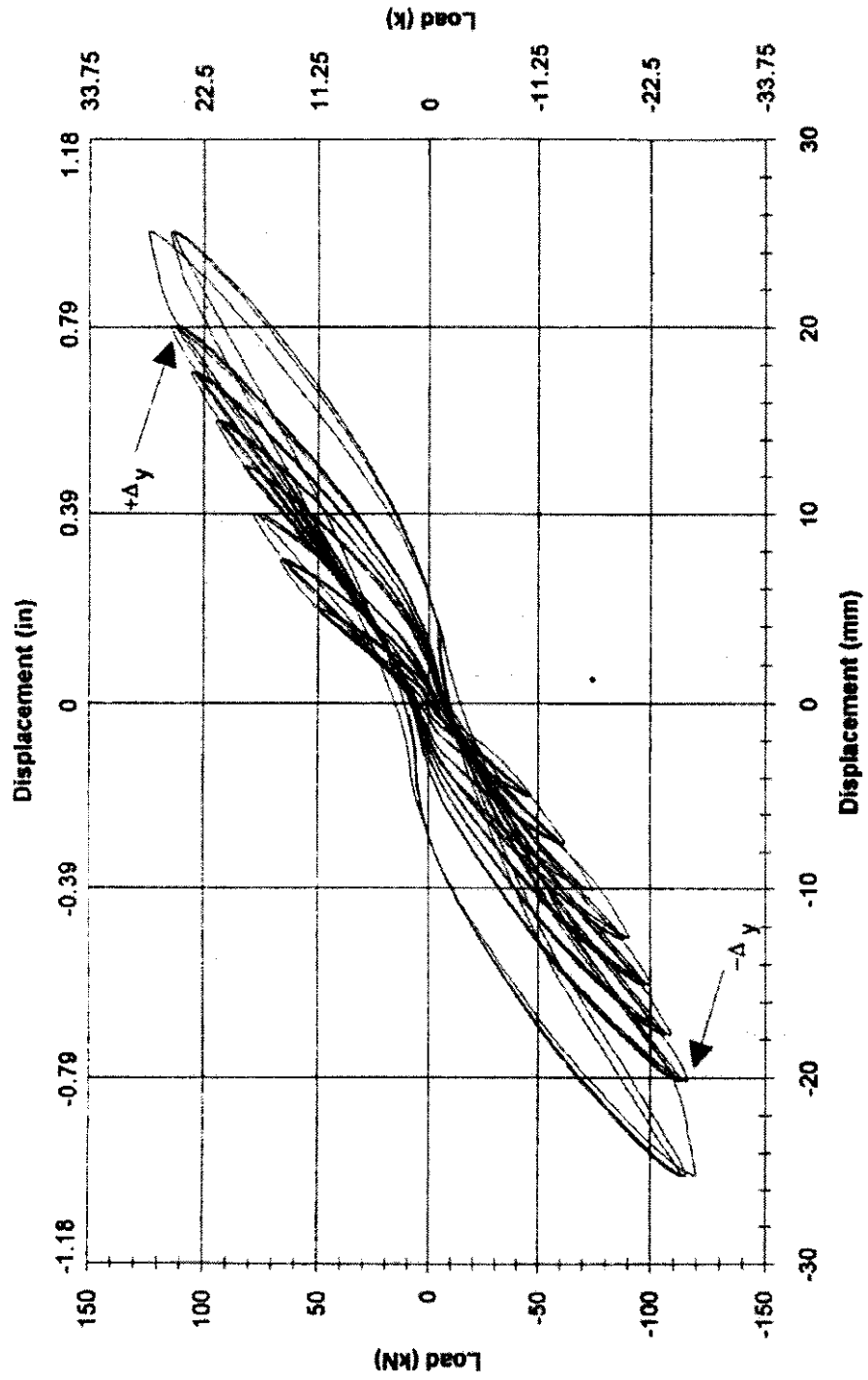


Figure 72 Hysteresis loops for Unit I (cycles through 25.4 mm).

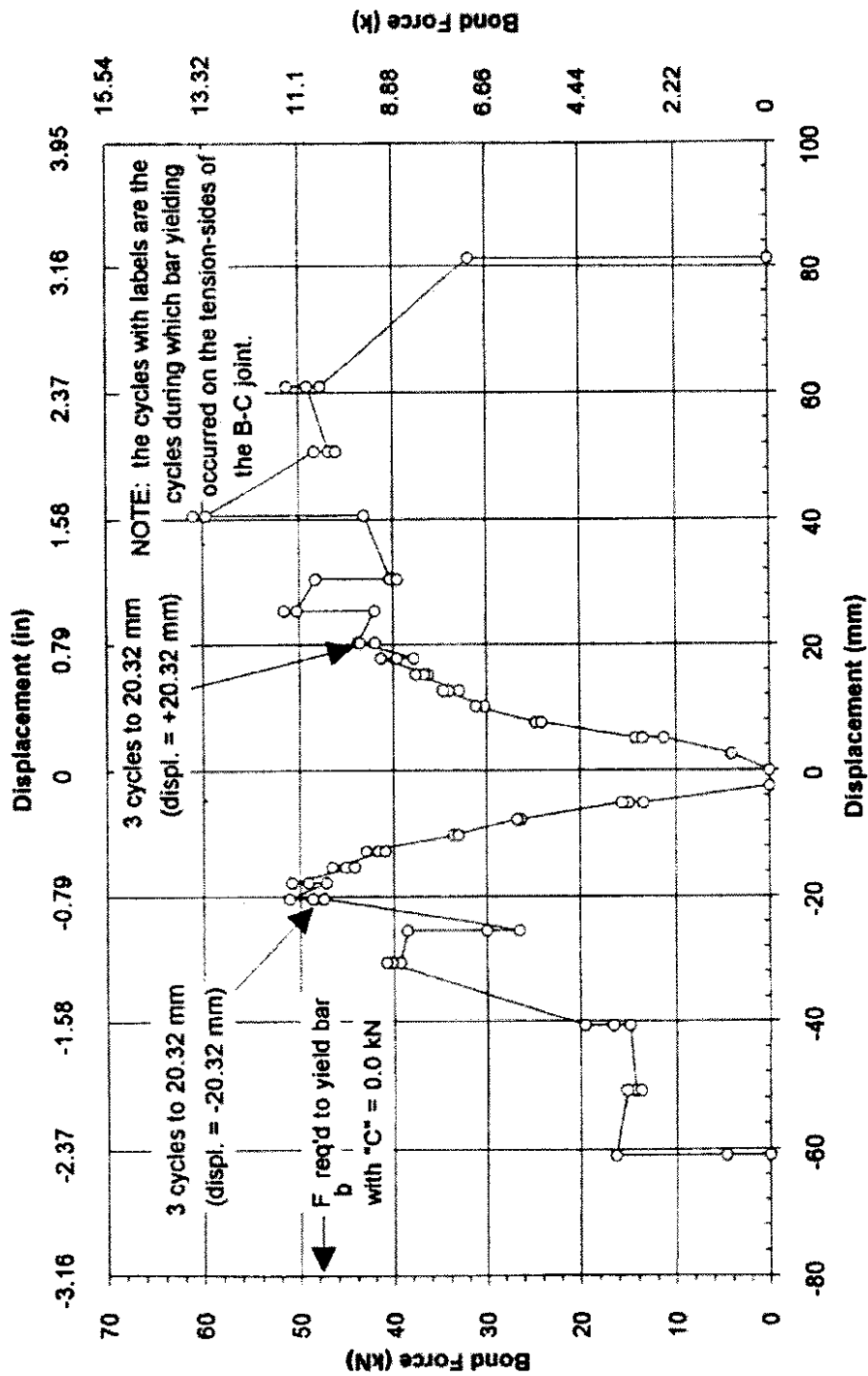


Figure 73 Bond force in a strut upper main bar versus displacement for Unit I (at the displacement peaks).

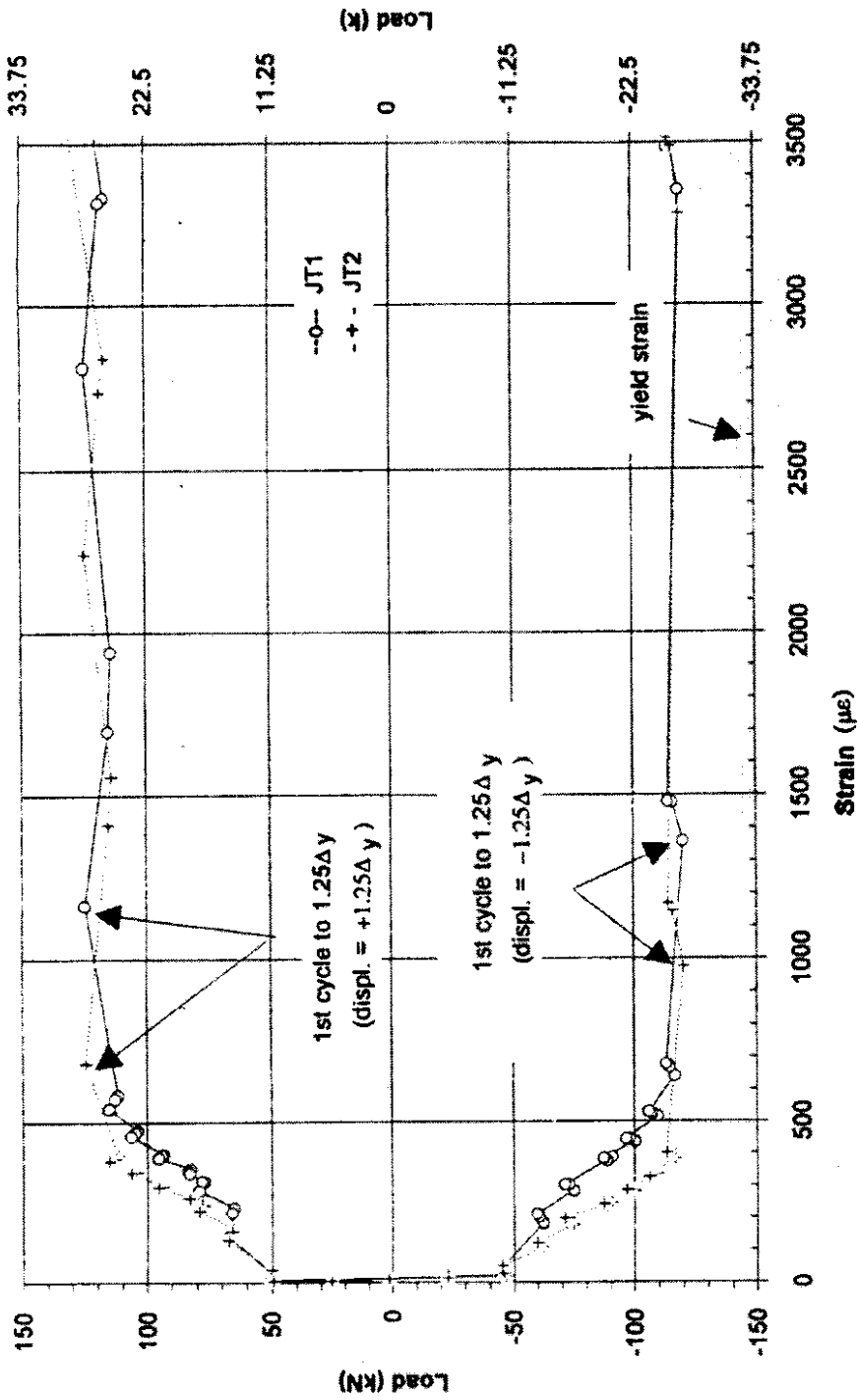


Figure 74 Load versus strain for hoop JT in Unit I (at the displacement peaks).

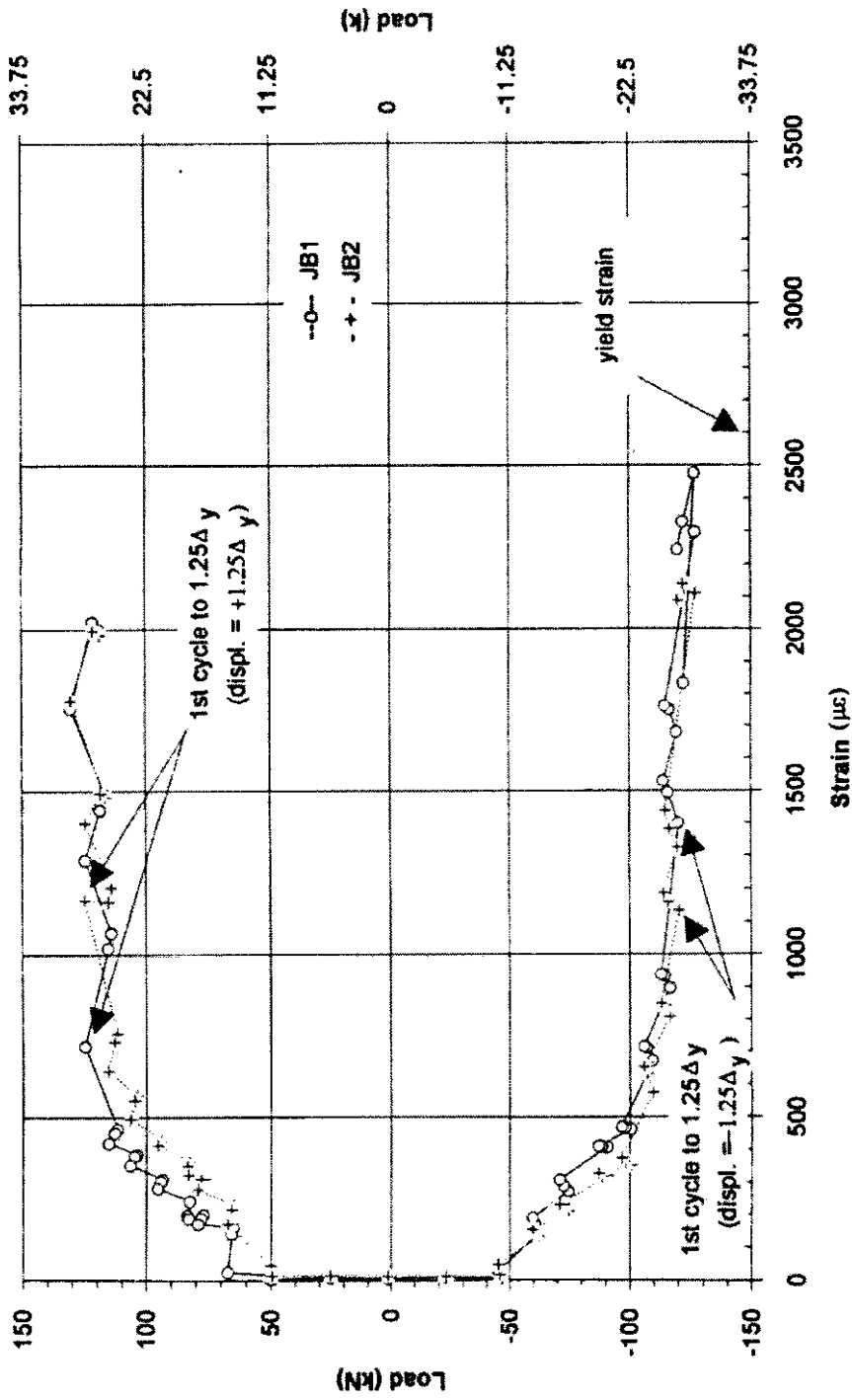


Figure 75 Load versus strain for hoop JB in Unit I (at the displacement peaks).

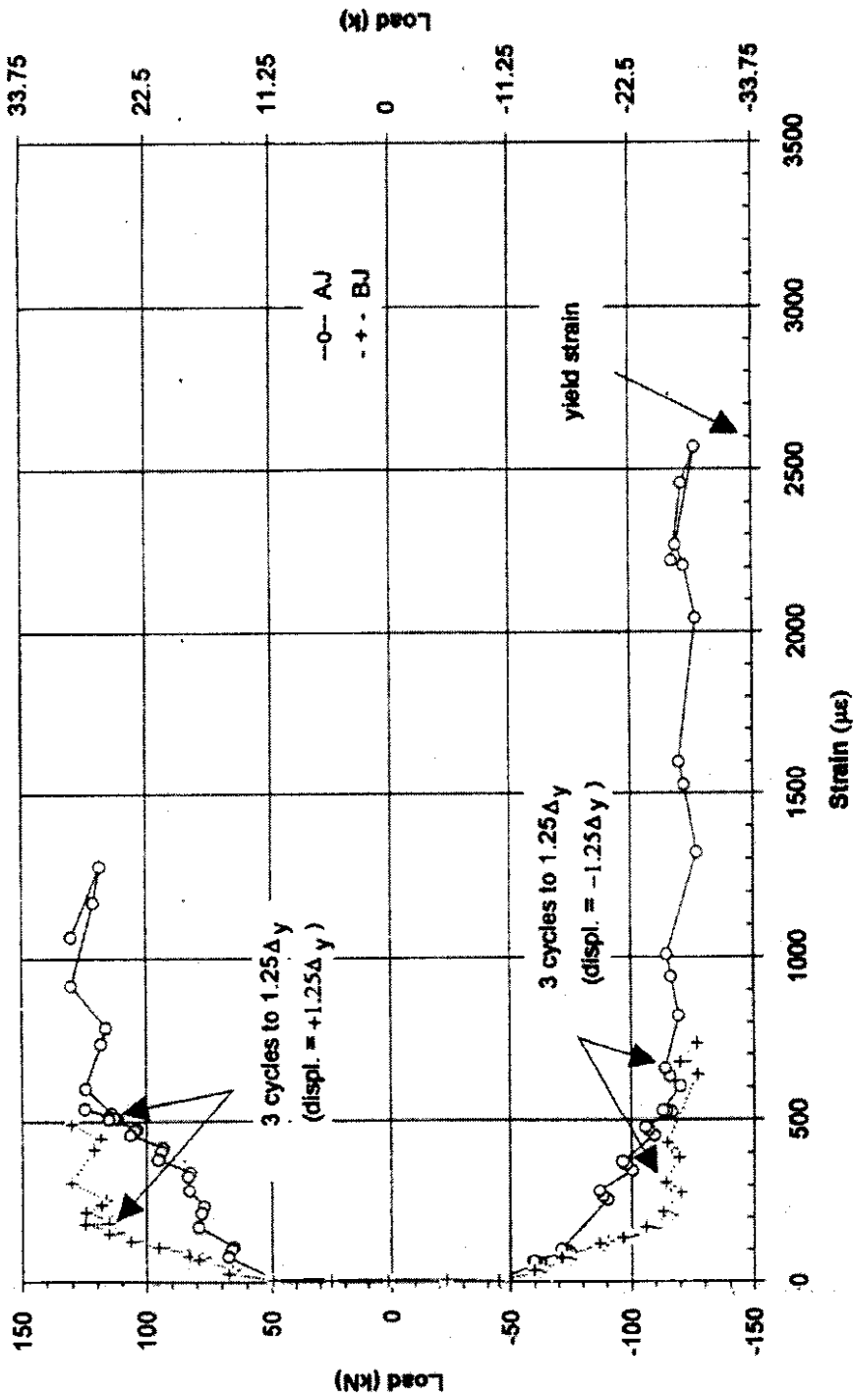


Figure 76 Load versus strain for hoops AJ and BJ in Unit I (at the displacement peaks).

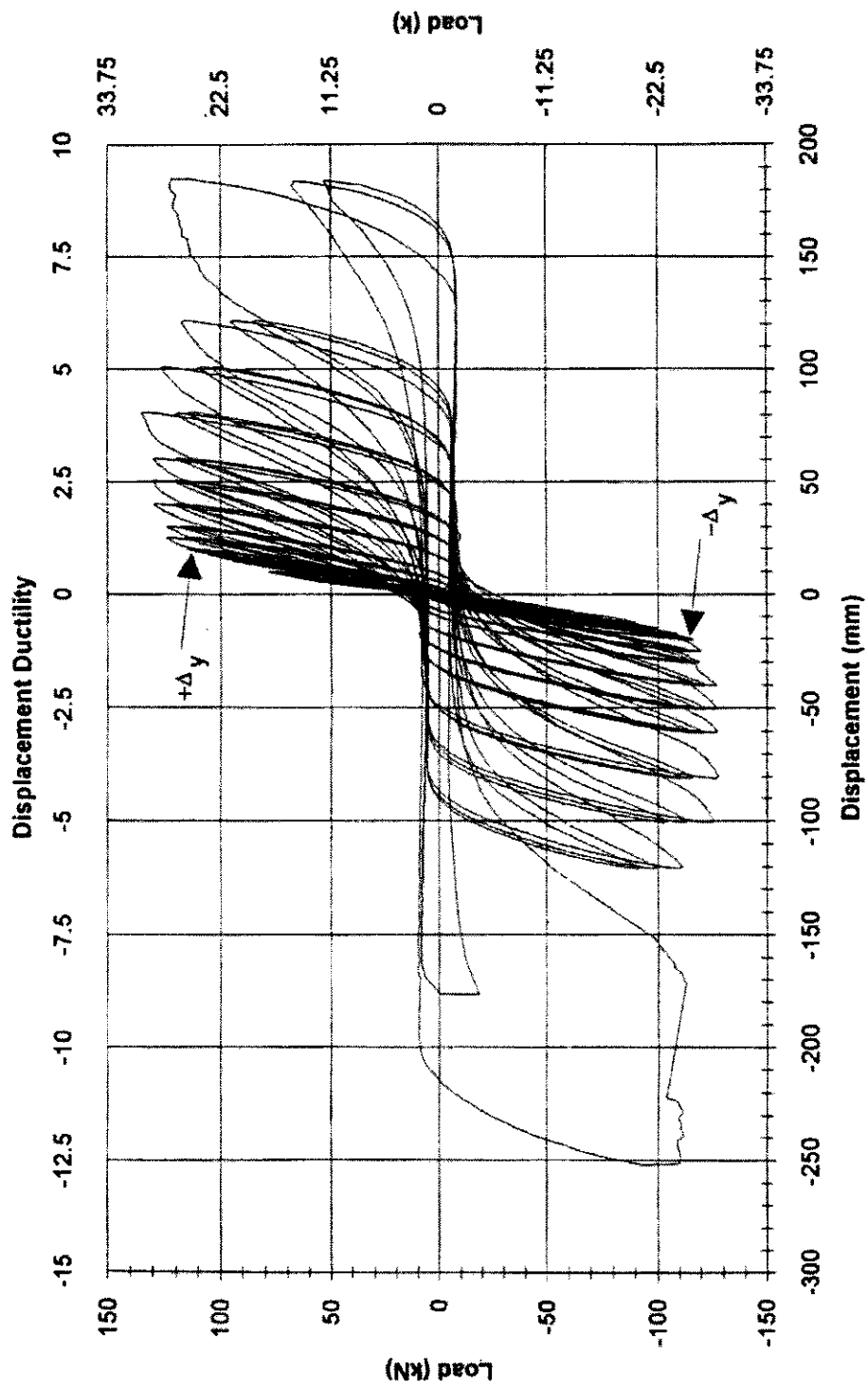


Figure 77 Hysteresis loops for Unit I (all cycles).

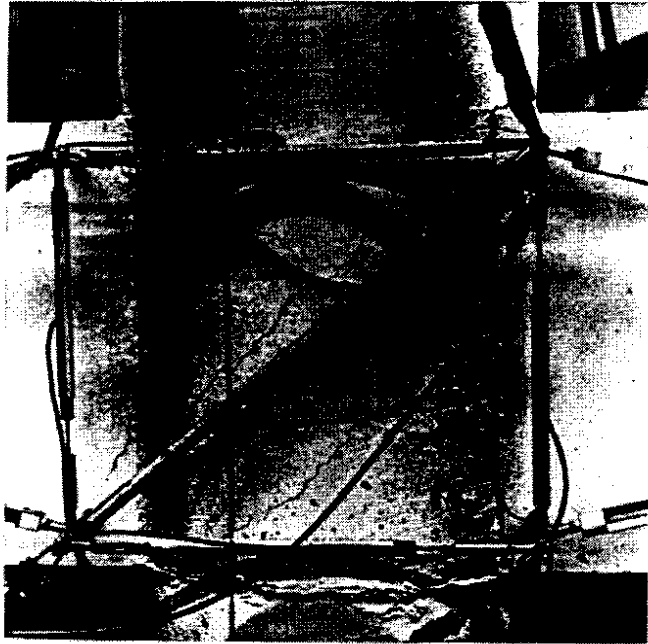


Figure 78 Cracking along the major joint diagonal of the front face of the B-C joint at the displacements equal to  $-1.5\Delta_y$  for Unit I.

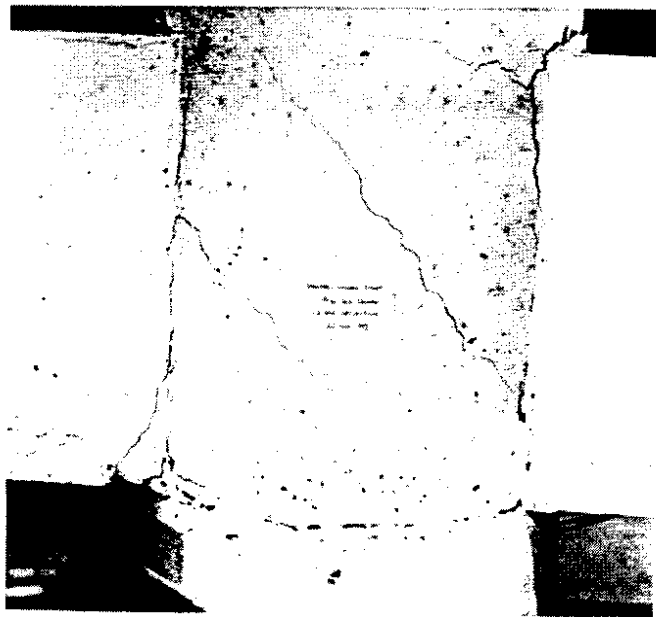


Figure 79 Cracking along the major joint diagonal of the back face of the B-C joint at the displacements equal to  $-1.5\Delta_y$  for Unit I.

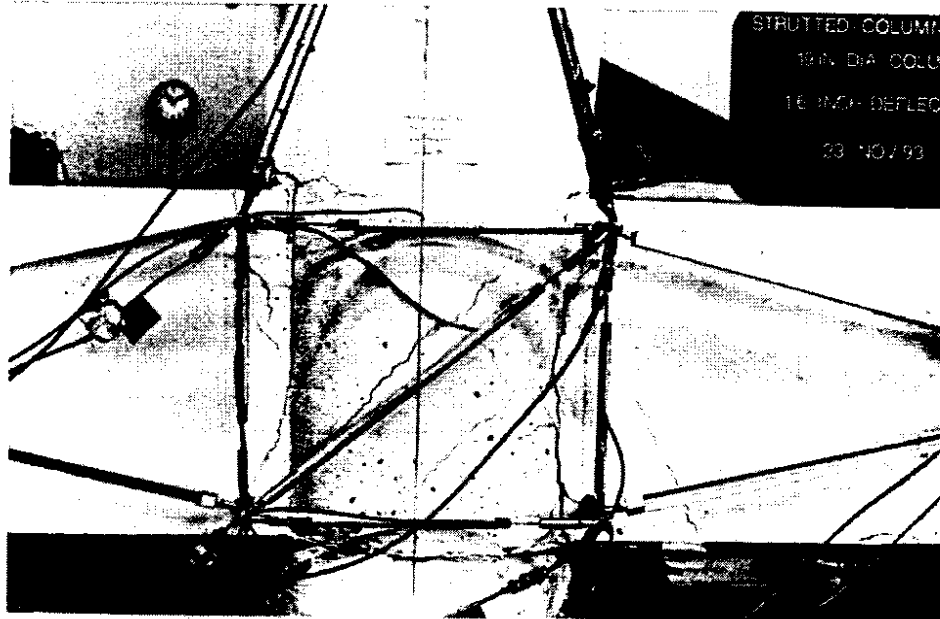


Figure 80 Cracking along the major joint diagonal in the B-C joint during the cycles to  $2\Delta_y$  for Unit I (front face of the B-C joint).

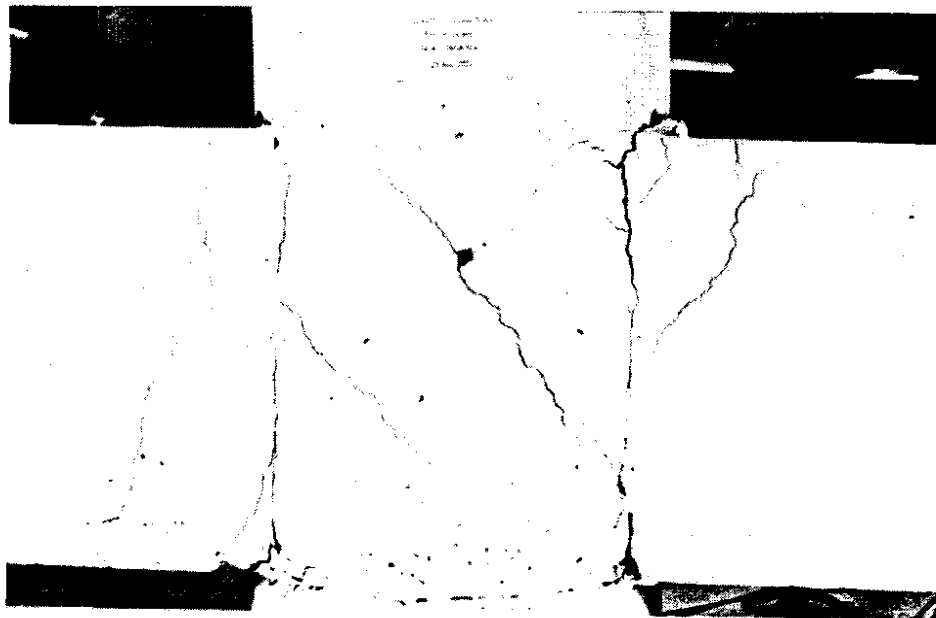


Figure 81 Cracking along the major joint diagonal in the B-C joint during the cycles to  $2\Delta_y$  for Unit I (back face of the B-C joint).

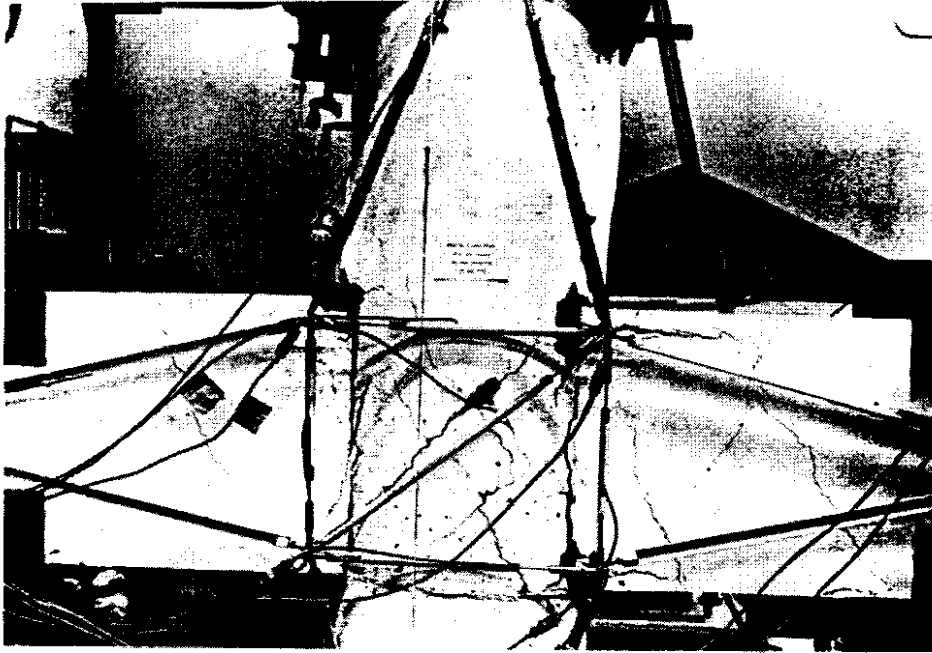


Figure 82 Spalling in the B-C joint region at a displacement equal to  $-4\Delta_y$  for Unit I (front face).

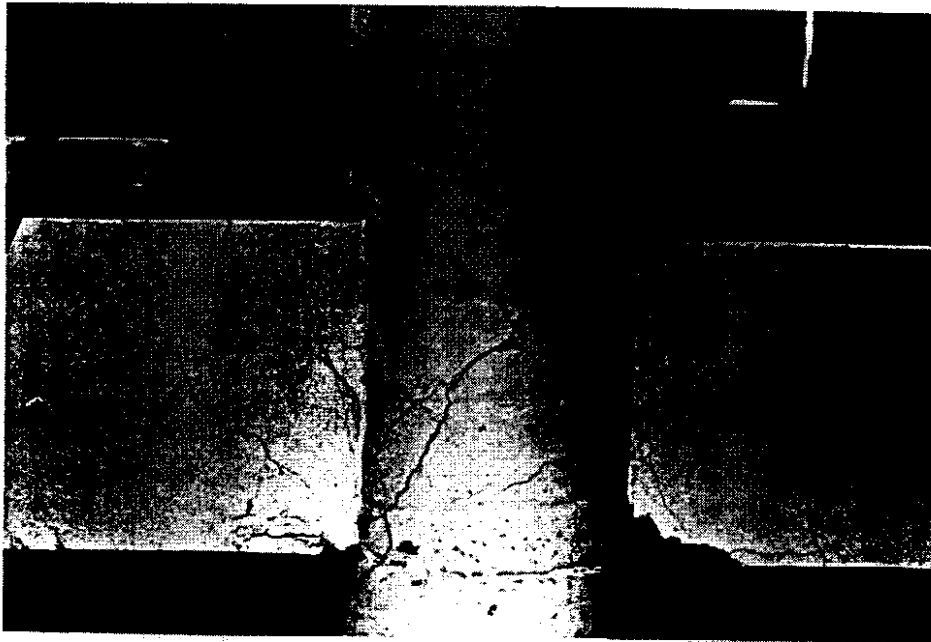


Figure 83 Spalling in the B-C joint region at a displacement equal to  $+4\Delta_y$  for Unit I (back face).

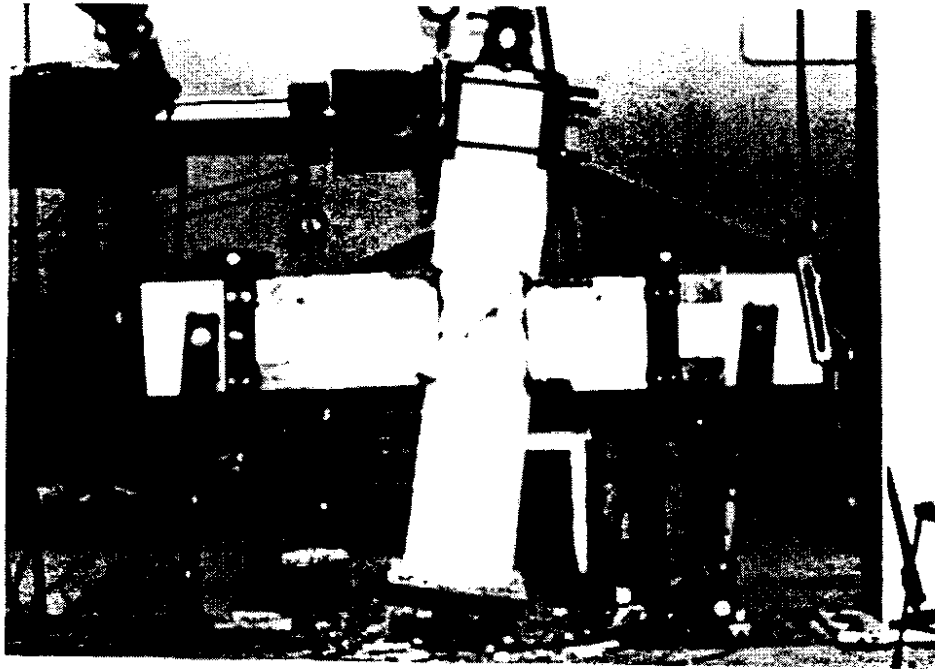


Figure 84 Unit I at the peak displacement reached in the extend portion of the first "push-over" cycle.

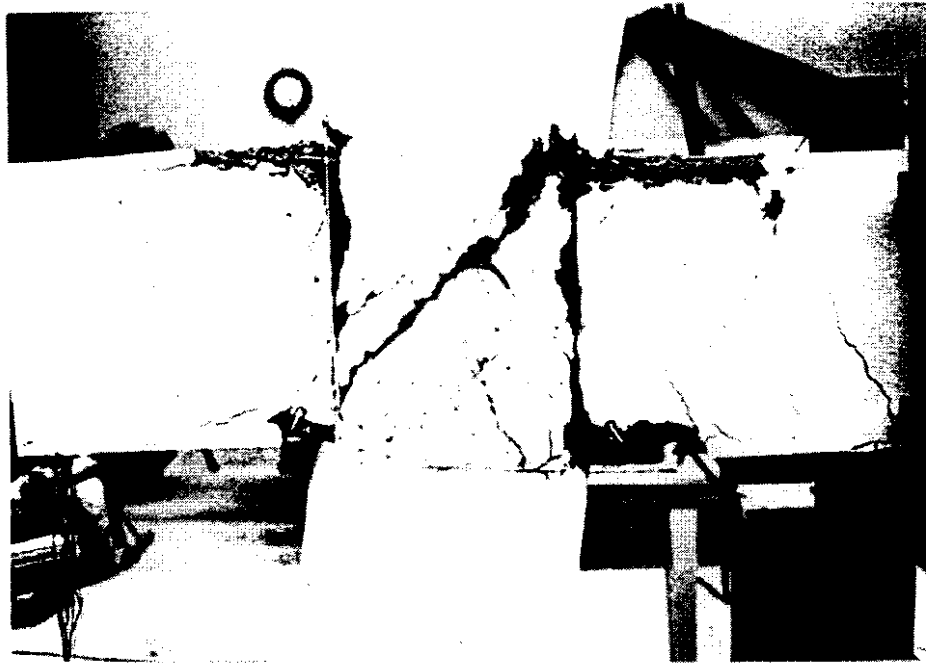


Figure 85 The front face of the B-C joint of Unit I at the peak displacement reached in the extend portion of the second "push-over" cycle.



Figure 86 The back face of the B-C joint of Unit I at the peak displacement reached in the extend portion of the second "push-over" cycle.



Figure 87 The front face of the B-C joint of Unit I following the removal of loose concrete.

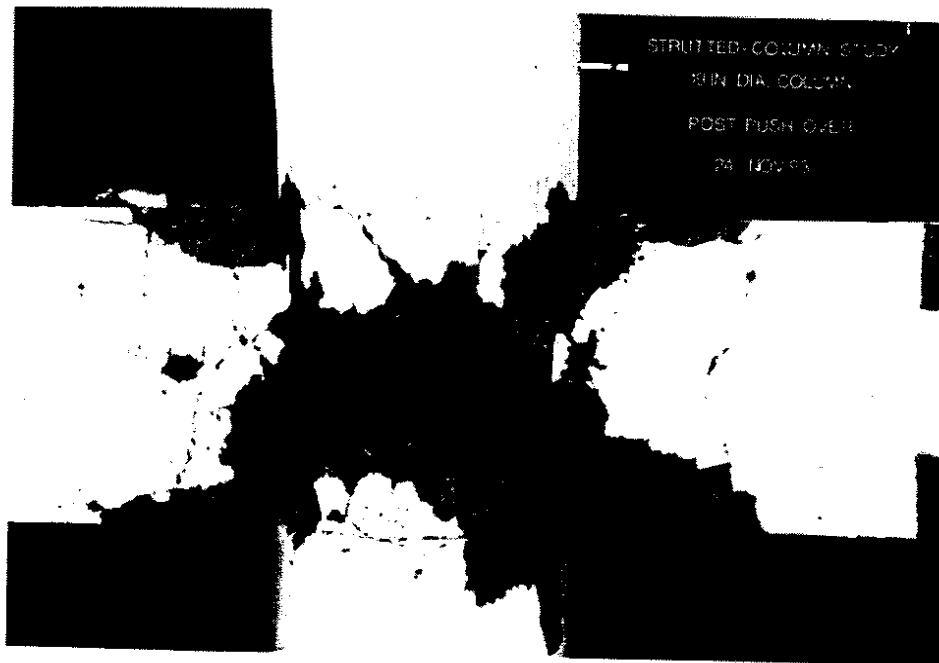


Figure 88 The back face of the B-C joint of Unit I following the removal of loose concrete.

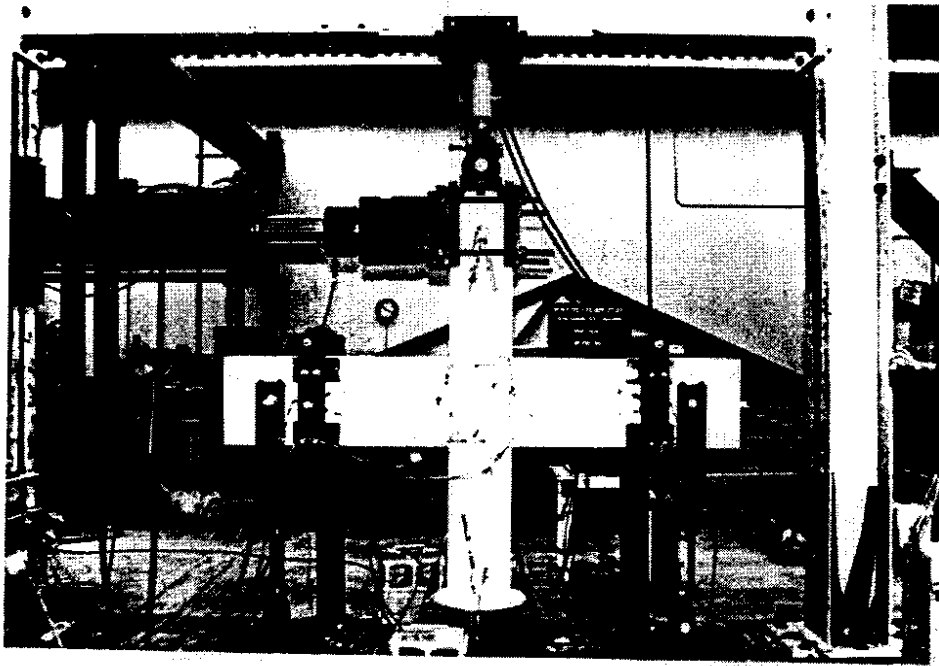


Figure 89 Unit II prior to the start of testing.

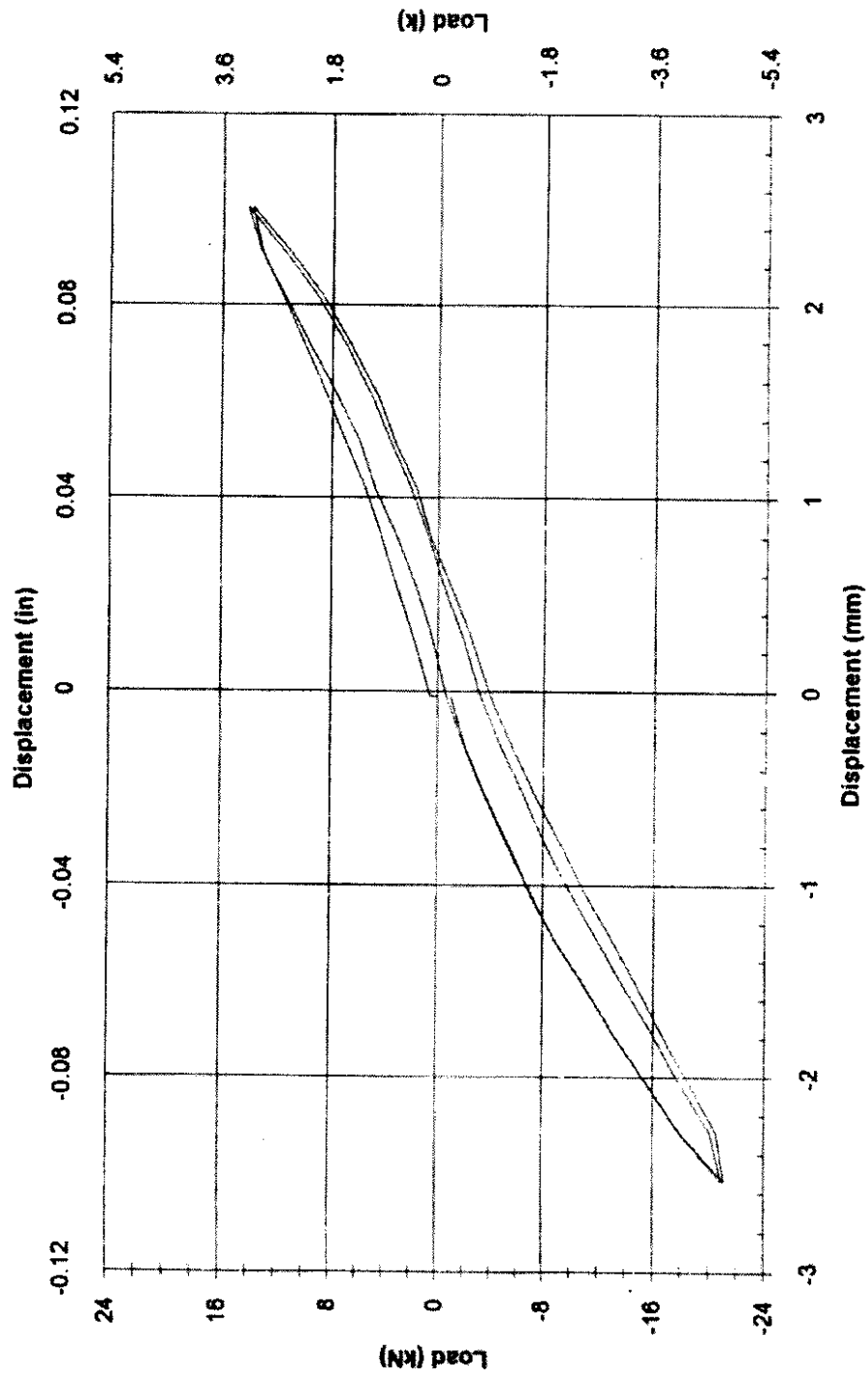


Figure 90 Hysteresis loops for Unit II (two cycles to 2.54 mm).

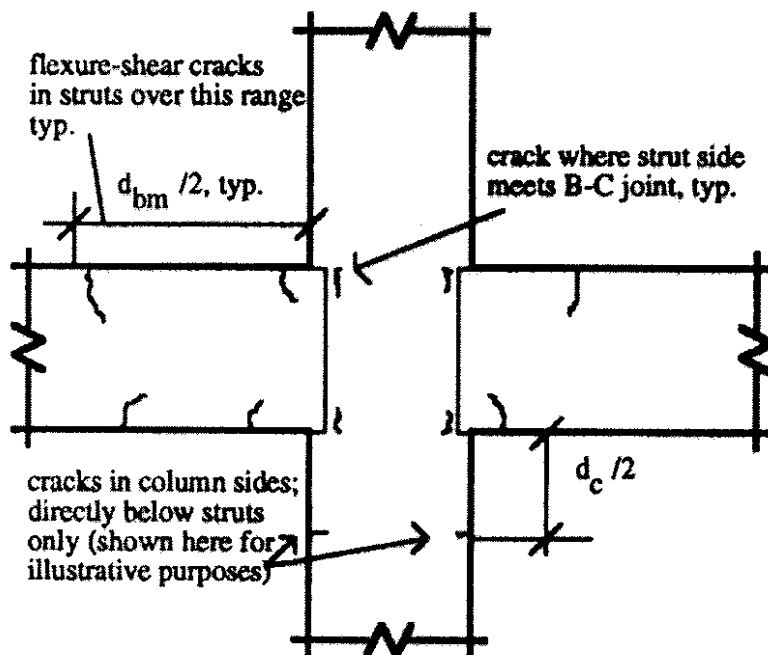


Figure 91 Cracking typically observed in Unit II through the cycles to 12.7 mm.

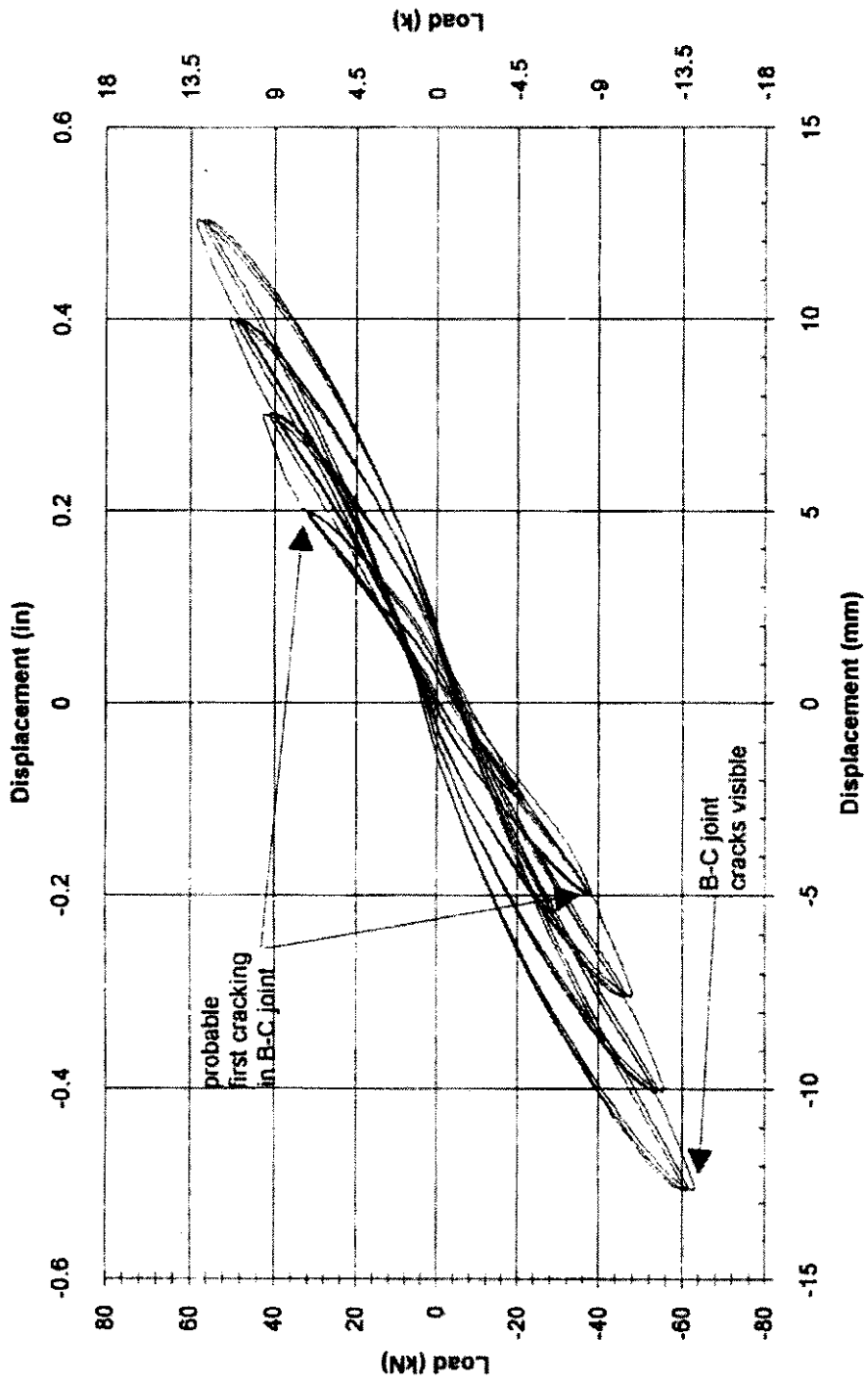


Figure 92 Hysteresis loops for Unit II (cycles through 12.7 mm).

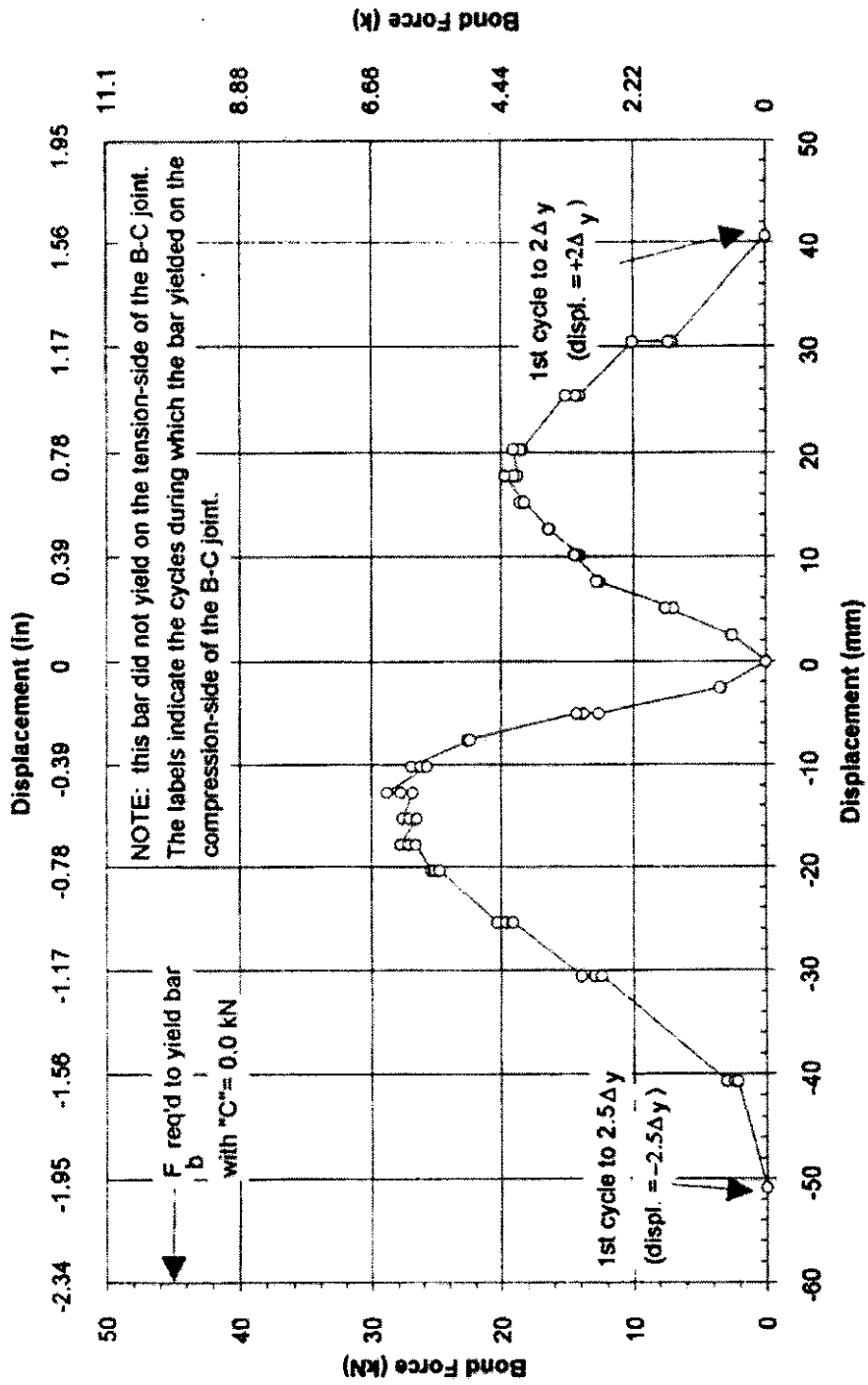


Figure 93 Bond force in a strut lower main bars versus displacement for Unit II (peak values).

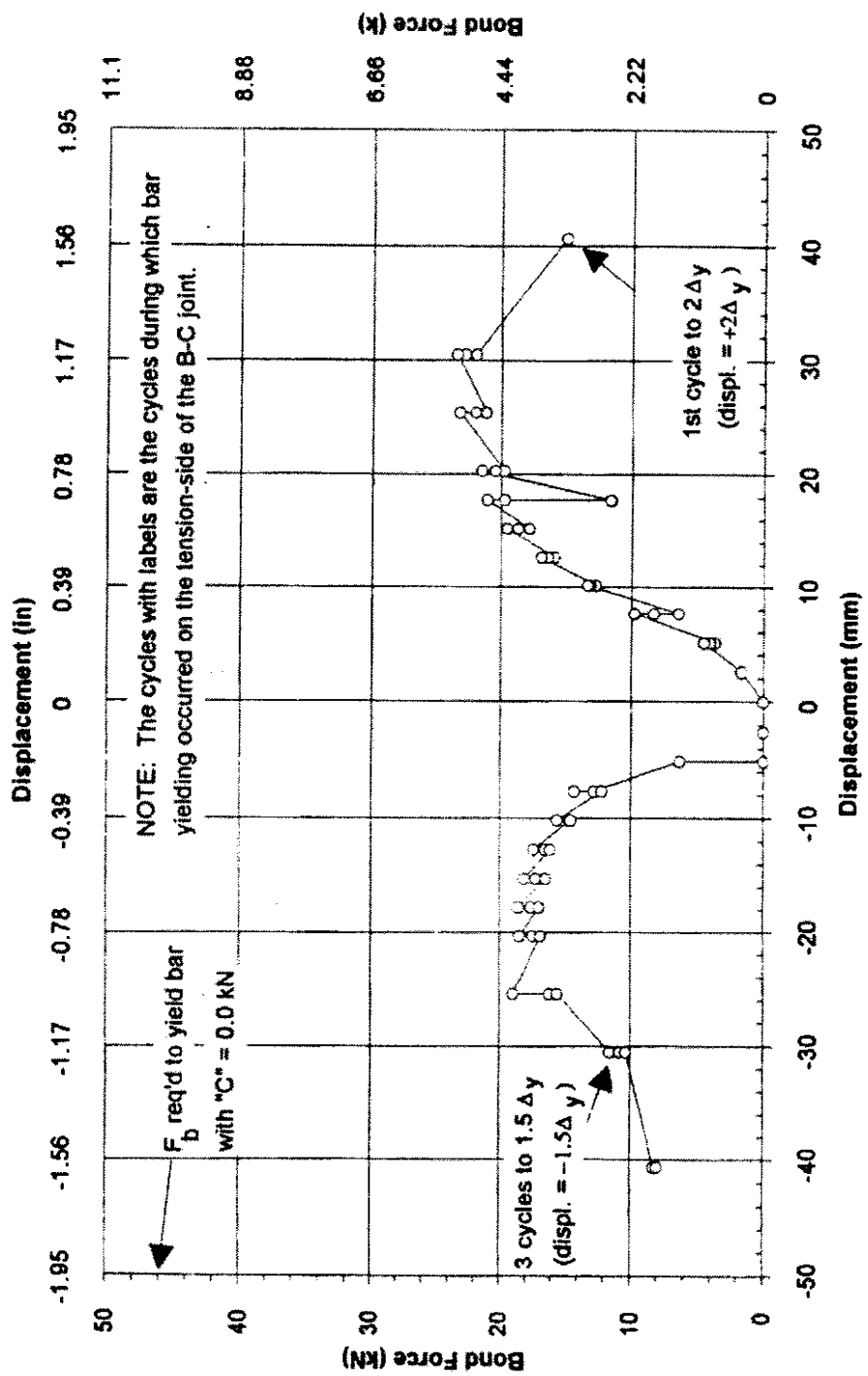


Figure 94 Bond force in a strut upper main bar versus displacement for Unit II (peak values).

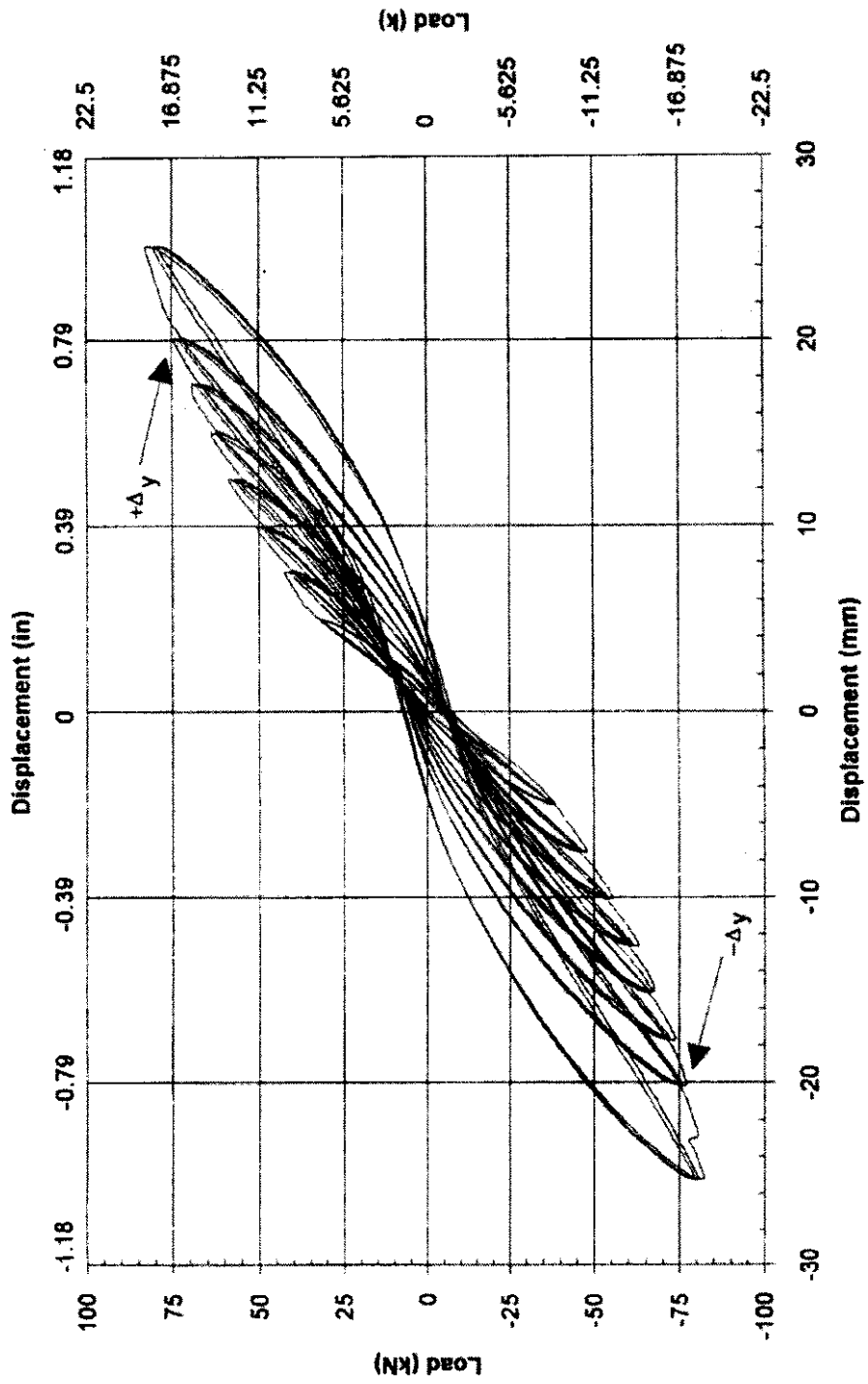


Figure 95 Hysteresis loops for Unit II (cycles through  $1.25\Delta y$ ).

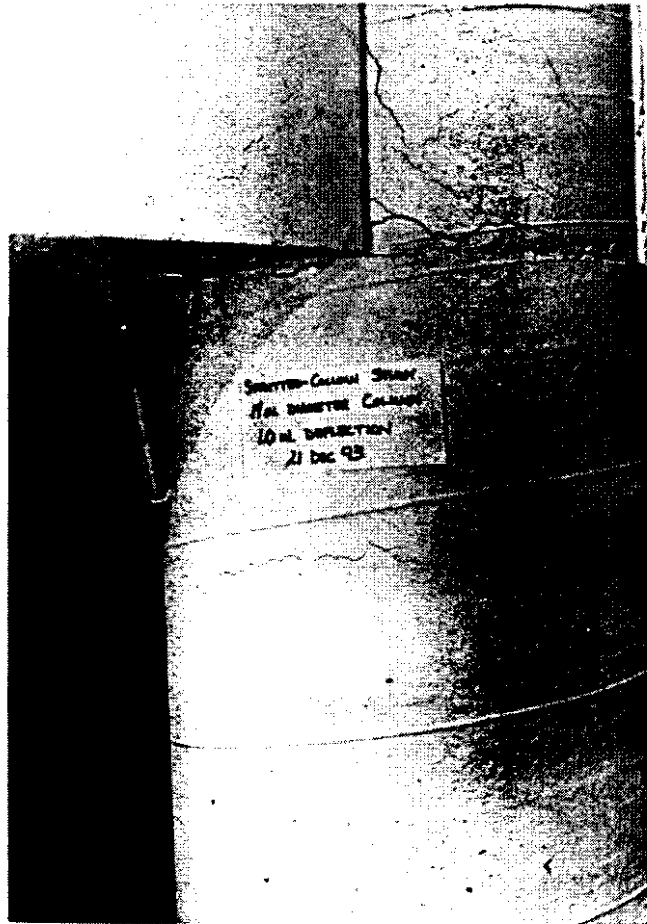


Figure 96 The extent of flexural cracking in the anticipated plastic hinge region of the lower column at a displacement of  $-1.25\Delta_y$  in Unit II.

STRUTTED-COLUMN STUDY  
1/4 IN. DIAMETER COLUMN  
1.0 IN. DEFLECTION  
21 DEC 93

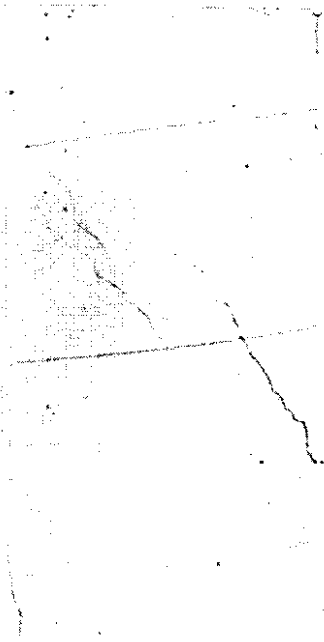


Figure 97 Shear cracks on the back face of the B-C joint that occurred at the displacements equal to  $-1.25\Delta_y$  in Unit II.

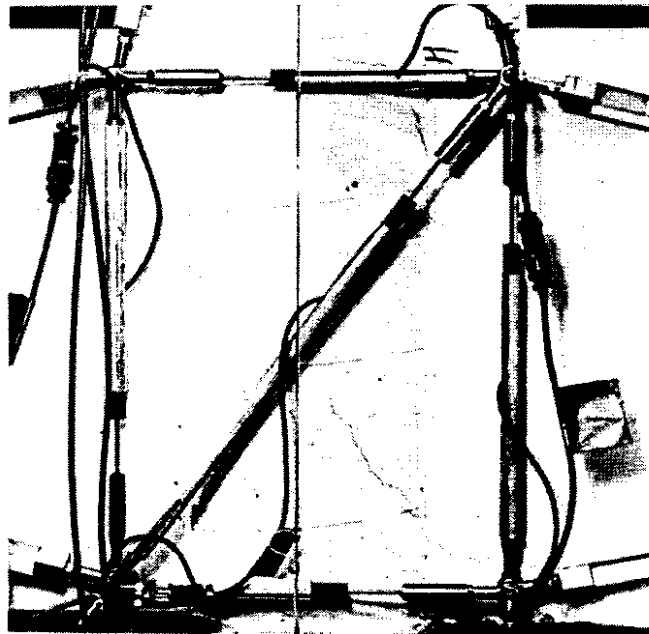


Figure 98 Shear cracks on the front face of the B-C joint that occurred at the displacements equal to  $+1.25\Delta_y$  in Unit II.

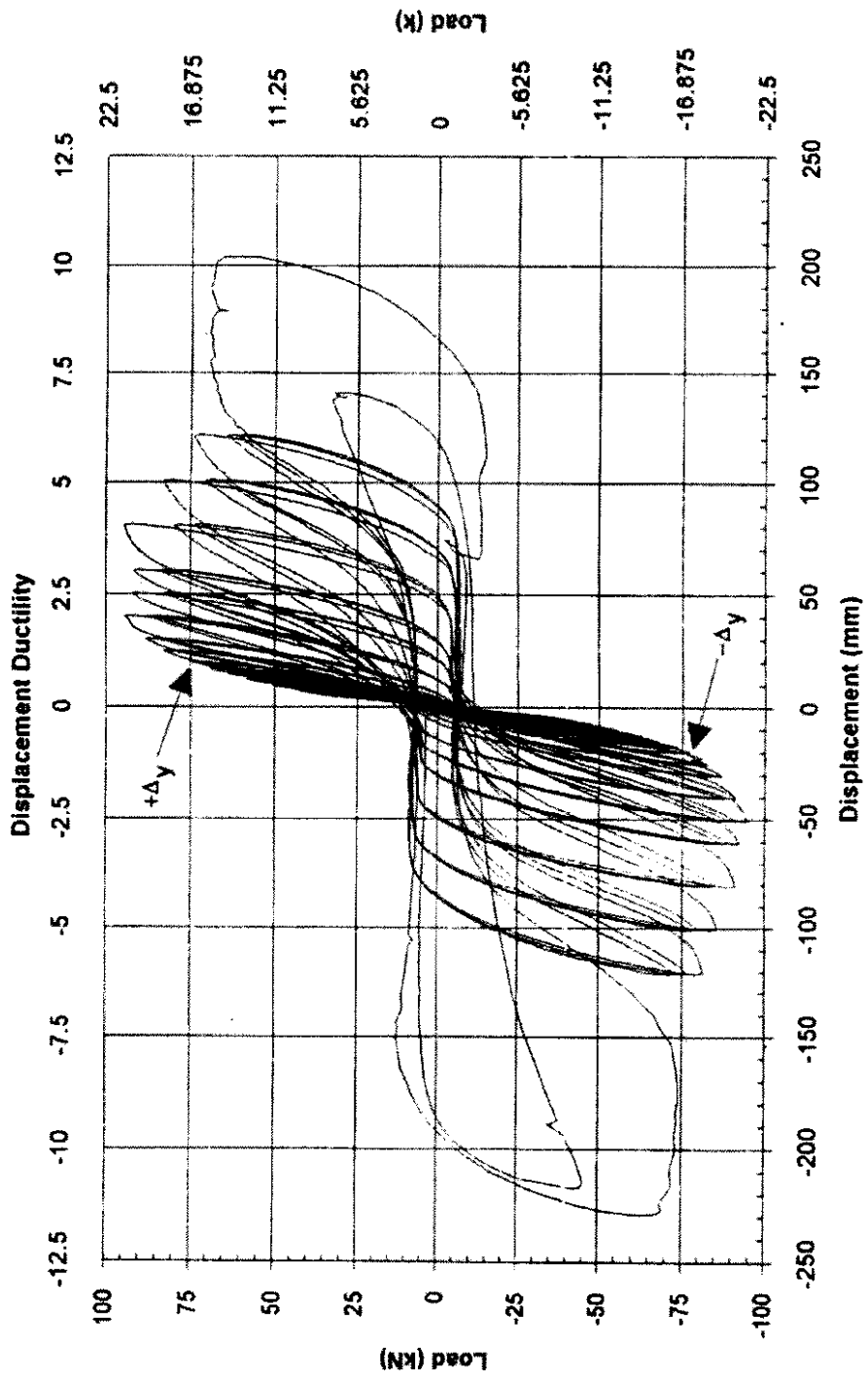


Figure 99 Hysteresis loops for Unit II (all cycles).

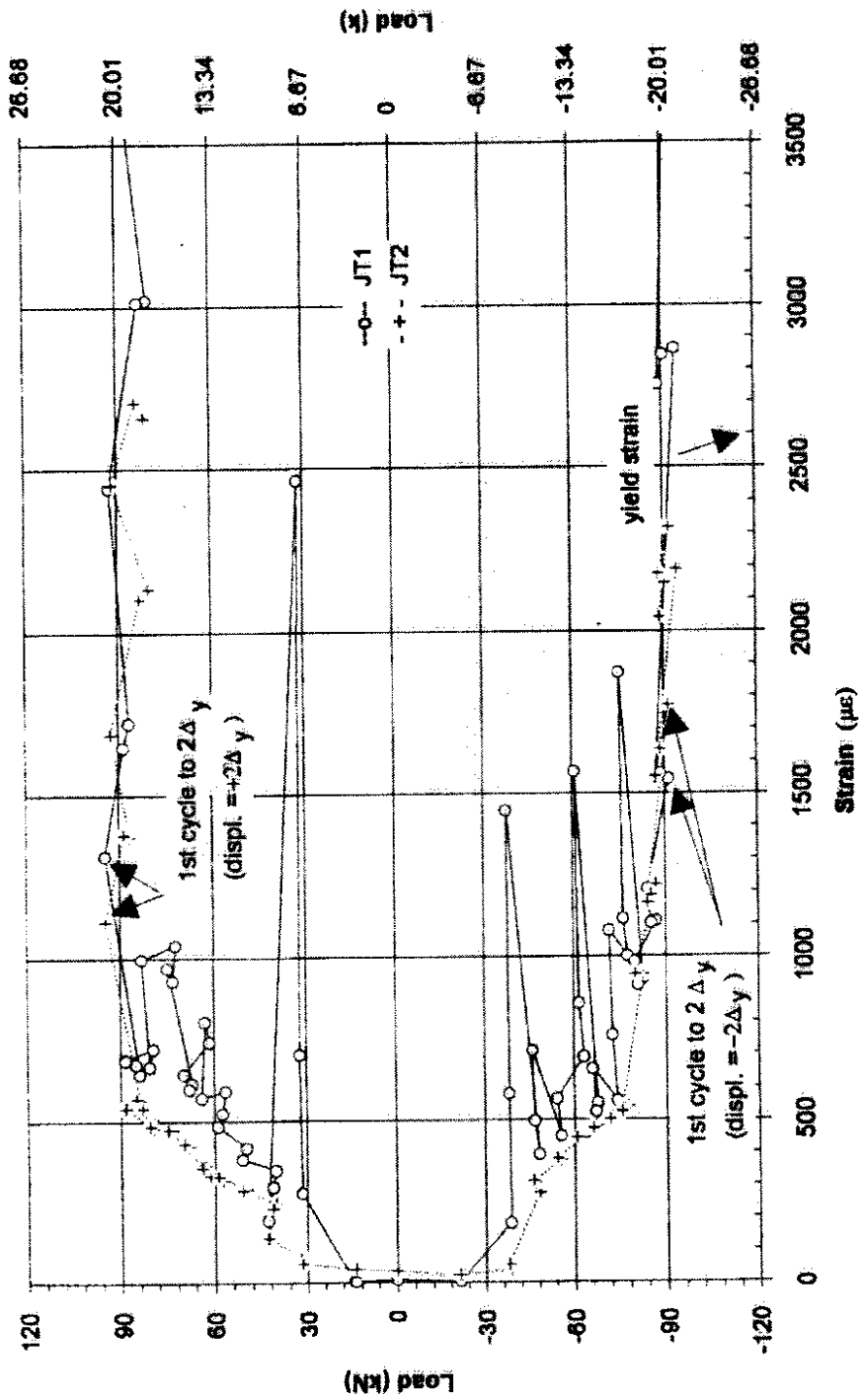


Figure 100. Load versus strain for hoop JT in Unit II (at the displacement peaks).

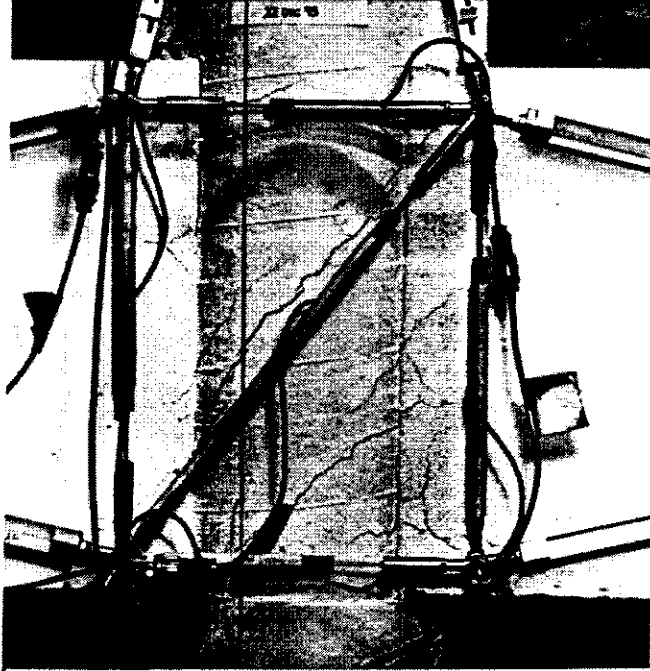


Figure 101 The front face of Unit II at the last displacement equal to  $-2.5\Delta_y$ .

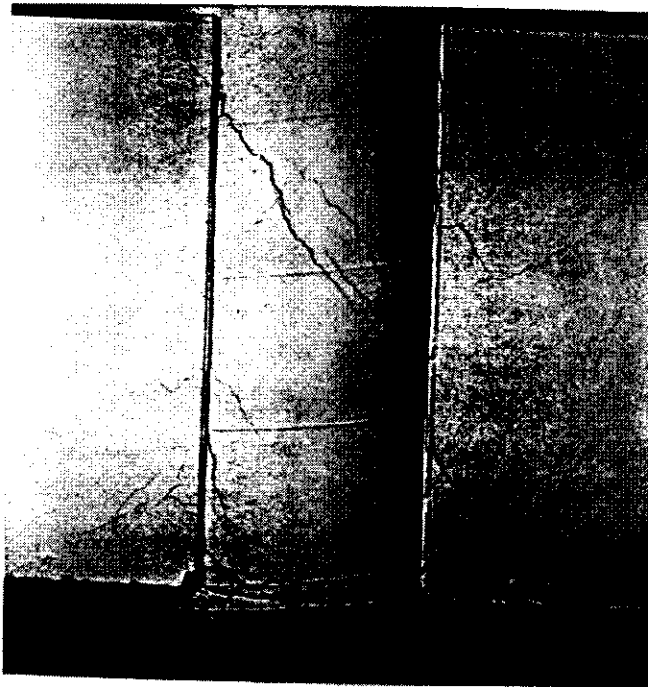


Figure 102 The back face of Unit II at the last displacement equal to  $-2.5\Delta_y$ .

Figure 104 Damage on the back face of the B-C joint and in the lower column of Unit II at the first displacement equal to  $+4\Delta_y$

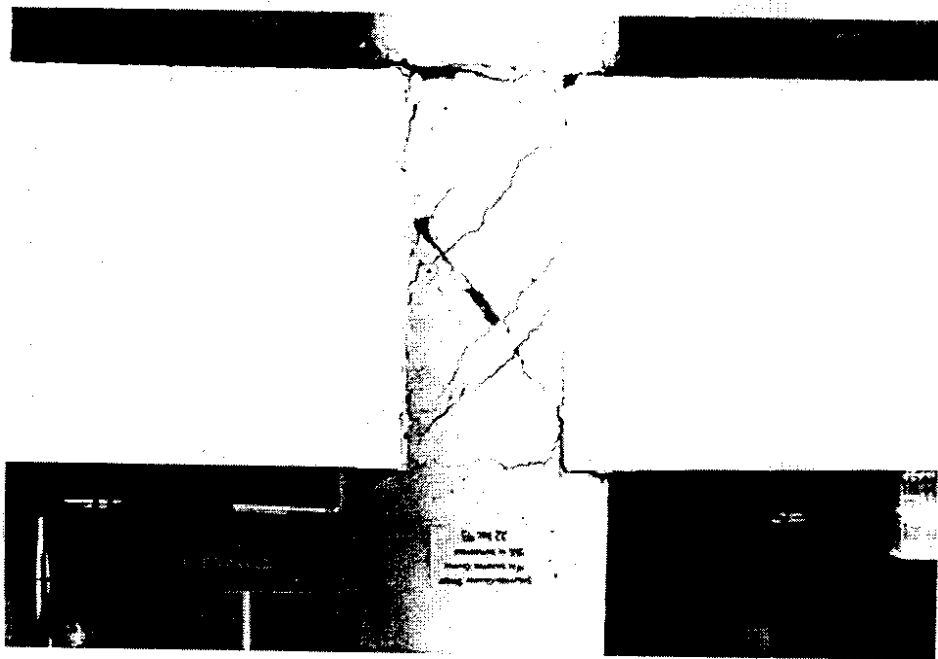
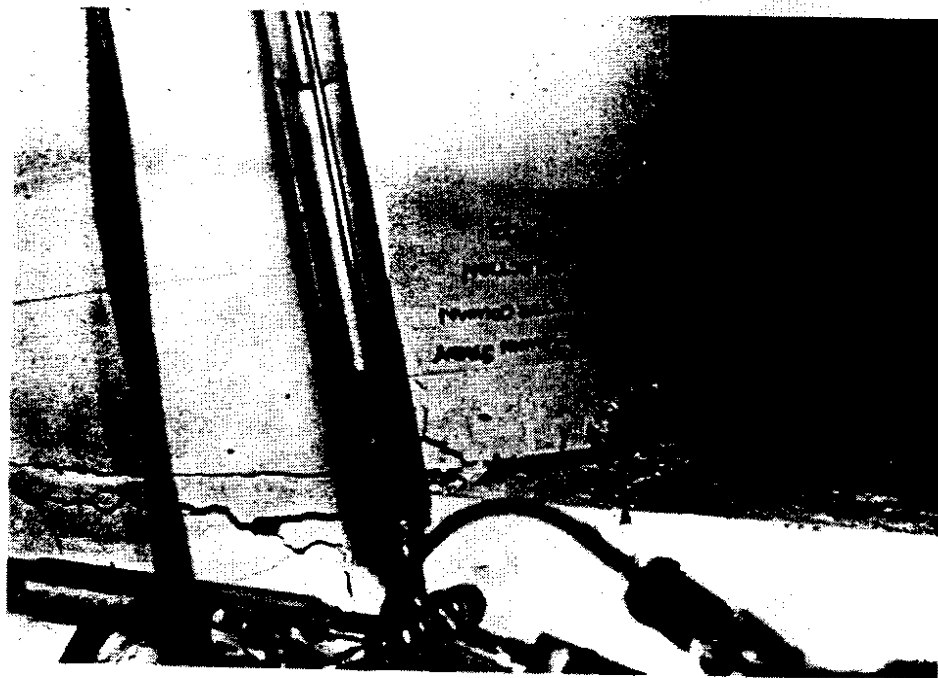
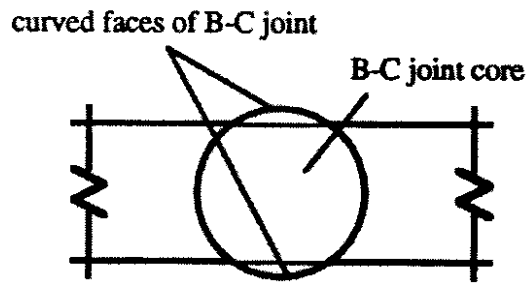
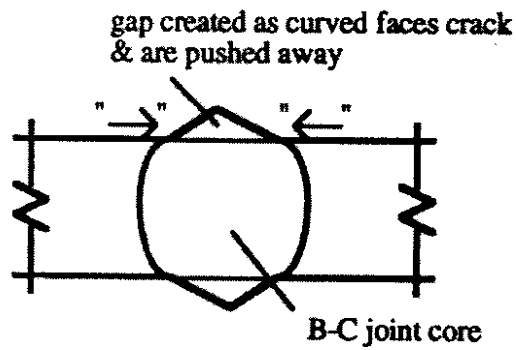


Figure 103 Typical spalling in the front of the lower column of Unit II (displacements equal to  $\pm 3\Delta_y$ )





a) B-C joint with curved faces in-tact



b) B-C joint with curved faces pushed away

Figure 105 Sketches of the B-C joint of Unit II before and after the joint faces are pushed away from the core.

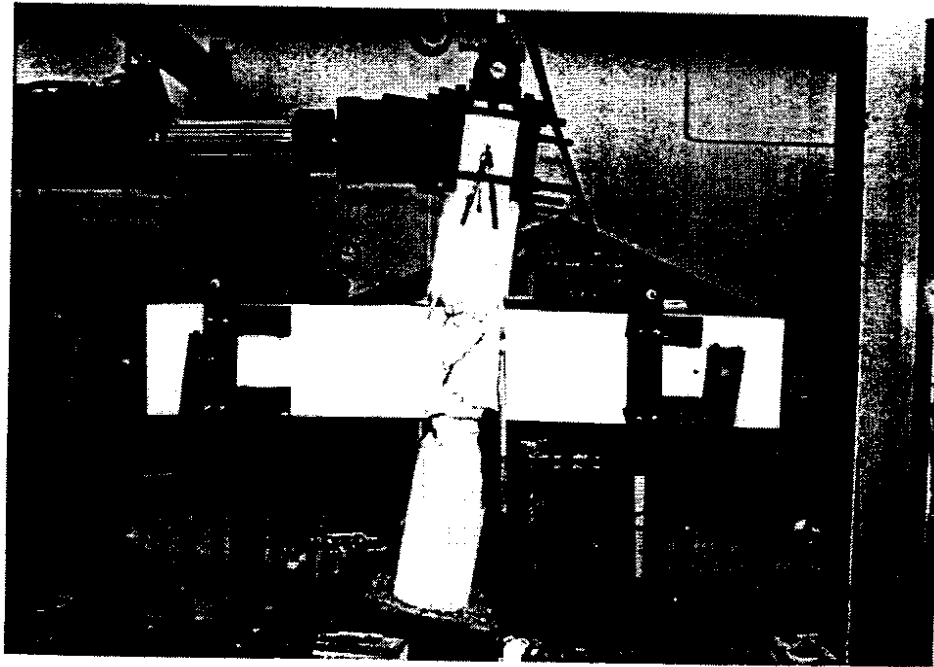


Figure 106 Unit II at the peak displacement reached in the extend portion of the first "push-over" cycle.

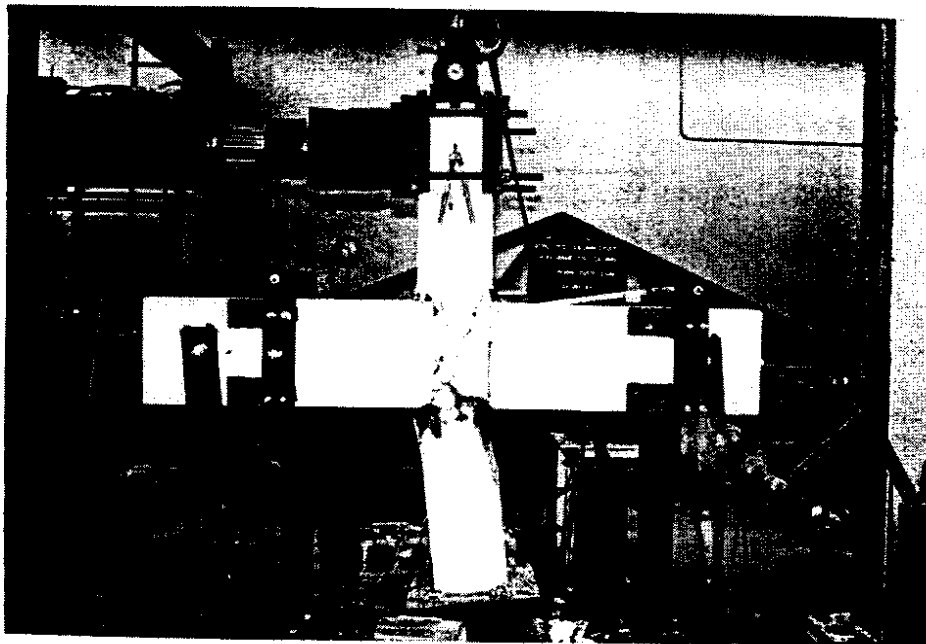


Figure 107 Unit II at the peak displacement reached in the retract portion of the second "push-over" cycle.

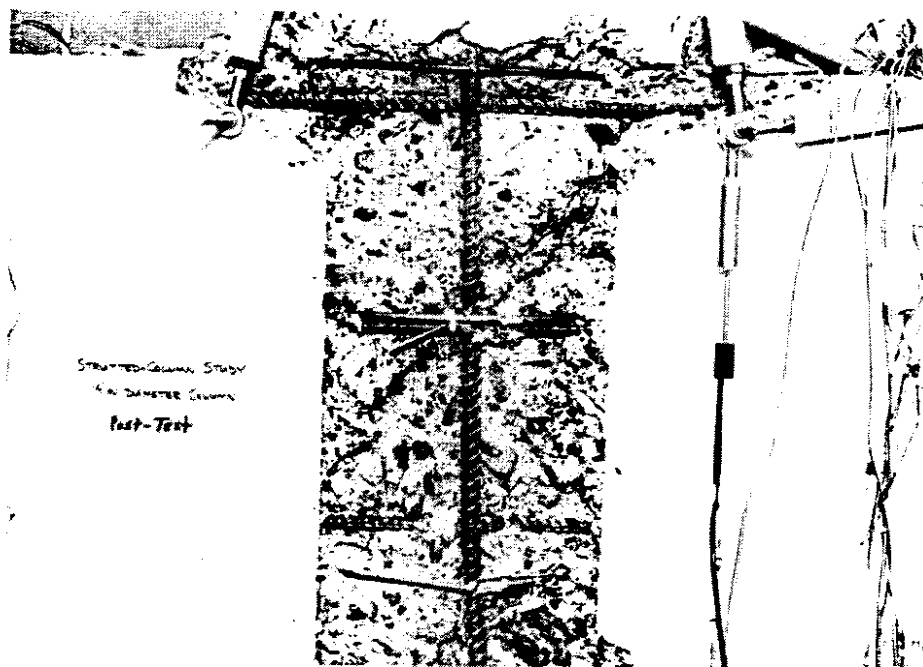


Figure 108 The front face of the B-C joint of Unit II following the removal of loose concrete.

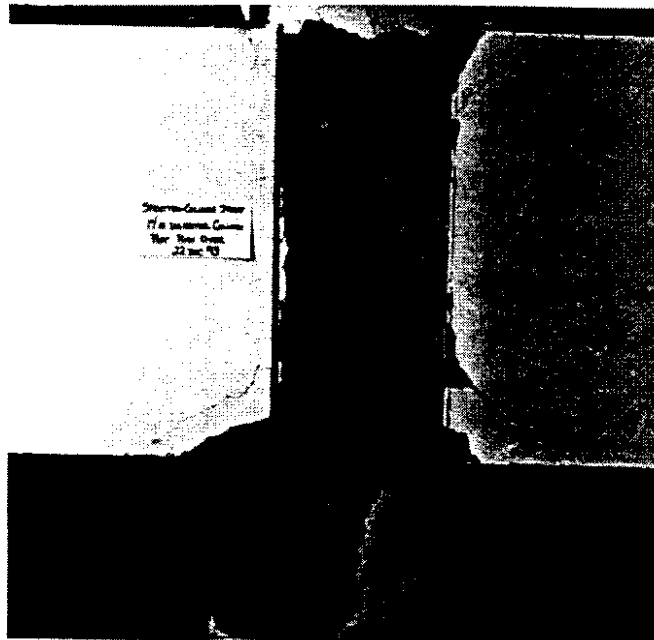


Figure 109 The back face of the B-C joint of Unit II following the removal of loose concrete.

## **CHAPTER 6**

### **INTERPRETATION, APPRAISAL AND APPLICATION**

To this point, this work has transitioned from assessing the seismic performance potential of an inventory of bridges with a unique type of substructure to the experimental testing of two subassemblages. Thus, the primary goal of this chapter is to interpret the findings from the experimental tests such that an appraisal can be made with regard to the seismic performance potential of the substructures in the inventory and of the bridges of which the substructures are an important component. First, the experimental findings are interpreted. Then, the empirical model presented in Chapter 3 (Fig. 22) is calibrated with the results from the experimental tests. Finally, an appraisal is given of the seismic performance potential of the substructures and the bridges.

#### **6.1 Interpretation of the Experimental Findings From Unit I**

Herein, an interpretation is given of the experimental findings from Unit I. The format that will be used is identical to the one used in the presentation of the findings in Chapter 5: B-C joint shear cracking, specimen yield, and post-specimen-yield.

##### **6.1.1 B-C Joint Shear Cracking**

###### **B-C Joint Shear Cracking**

The occurrence of first B-C joint shear cracking is an important milestone because of the detrimental effects of joint cracking on bar bond (Chap. 3, Sec. 3.6.3, "Bond in B-C Joints"). For a B-C joint that is as lightly confined as the one in Unit I (i.e., two hoops),

the repercussions on bar bond from cracking in the joint may be very severe. Accordingly, this topic received much attention in Chapter 5.

*Visible Cracks versus Hoop Strains.* The sudden increase in the strains in the B-C joint hoops at the displacement peaks in the cycles to 7.62 mm identified first joint cracking. A reason that B-C joint cracks were not visible until the cycles to 15.24 mm might be that the interaction between the regions of the joints beyond the width of the struts and the struts was less effective than the interaction between the joint core and the struts (Chap. 3, Sec. 3.6.5, "Member Cross-Sectional Dimensions").

*Strains in the Strut Main Bars.* A pattern of decreasing compressive strains at the locations adjacent to the B-C joint in the strut main bars were noted in the cycles subsequent to those to 7.62 mm (Fig. 68). The reason that this occurred must have been the onset of bond deterioration in the B-C joint (Fig. 69 versus Fig. 68). Bond in the B-C joint began to deteriorate soon after the first shear cracks occurred because the two hoops in the joint were unable to prevent the spread and the growth of these cracks. Once the main bars yielded the deterioration of bond in the B-C joint became worse. This is not surprising given the actual volumetric hoop ratio,  $\rho_s$ , was 0.1% rather than the 0.5% recommended based on Figure 22.

### 6.1.2 Specimen Yield

#### Precursors to Specimen Yield

Three of the significant occurrences during the cycles to 17.78 mm were related: the yielding of the strut lower main bars, the start of the deterioration of the values of  $F_b$  (Fig. 70), and the long shear cracks that appeared across the B-C joint faces. The relationship among these occurrences is clear: once the bars yielded, the bond deterioration in the B-C joint increased to the point where the concrete began to assume a larger role in

shear transfer in the bottom of the B-C joint (Chap. 3, Sec. 3.6.3, "The Effect of Bond on the Shear Transfer Mechanisms"). It follows that long shear cracks occurred (Chap. 3, Sec. 3.6.3, "The Effect of Bond on the Shear Transfer Mechanisms").

### Specimen Yield

*Bond Deterioration in the Top of the B-C Joint.* Once the specimen had reached displacements equal to  $\pm\Delta_y$ , the bond conditions in the top of the B-C joint had begun to rapidly deteriorate (Fig. 73). Thus, while the bond index (BI) value for the strut main bars (i.e., approximately 0.8) was low relative to the standard adopted from Fig. 22 (i.e.,  $BI \leq 1.7$ ), the bond conditions in the B-C joint in Unit I became poor as soon as the bars yielded. With poor bond conditions in the top and the bottom of the B-C joint, the strut mechanism began to play a larger role than the truss mechanism in the transfer of joint shear stress. The result was the strut mechanism of joint shear stress transfer dominated the post-specimen-yield stage for Unit I.

### 6.1.3 Post-Specimen Yield

#### Cycles to $1.25\Delta_y$

The four "significant behavioral changes" noted at this point in Chapter 5 (the hysteretic pinching, the concentration of cracking in the B-C joint, the large increase in the strains of the hoops in the B-C joint, and the slippage of the lower column bars) were all induced by the effects of the strut mechanism and by the effects of the deteriorated bond conditions in the B-C joint

*Hysteretic "Pinching".* Figure 72 showed that the hysteresis loops during the cycles to  $1.25\Delta_y$  ( $\approx 1\%$  drift) began to noticeably pinch at small displacements. This was

to be expected given the increases in both the cracking in the B-C joint (see below) and in the increased bond deterioration in the B-C joint that had occurred during these cycles (Chap. 3, Sec. 3.6.3, "The Effect of Deterioration of Bond on Seismic Response").

Also, a trend where the stiffness and the strength of Unit I in the second cycle were noticeably less than those quantities in the first cycle had begun. This behavior is also largely attributable to the increases in the B-C joint cracking and the deteriorating bond conditions in the B-C joint. For the cycles to  $1.25\Delta_y$  through the next several displacement increments, its strength increased slightly or remained the same, and its stiffness incrementally decreased, when Unit I was pulled/pushed to a new positive/negative displacement peak. However, upon returning to the peak for the second time, the bond deterioration sustained in displacing to the peak for the first time softened the subassembly. The response of Unit I during the third cycles did not degrade from the response in the second cycles because Unit I had not attained its maximum strength. Once Unit I was pushed/pulled to displacements that caused its maximum strength to be exceeded, then each of the three cycles caused damage that softened the specimen more than the preceding cycle.

The trends in the hysteretic response with respect to the strength and to the stiffness of Unit I generally apply to the energy dissipated by Unit I. While the energy dissipated by Unit I was noticeably less in the second cycles compared to the first cycles throughout the test, the trend seemed to worsen in each set of cycles starting with the cycles to  $1.25\Delta_y$ . Early on, the decrease is attributable to the typical degrading-type behavior exhibited by cyclically-loaded, lightly-confined reinforced concrete structures. During the cycles to  $1.25\Delta_y$  and beyond however, the B-C joint cracking and the bond deterioration in the B-C joint were the cause of most of the degradation in the response of Unit I. Thus, it is also the likely cause of the change in the trend of the energy dissipated between the first and the second cycles.

*Concentration of Cracking.* Since the strut mechanism became prominent as bar bond deteriorated, the B-C joint became the "weak link" in the subassembly. Crack activity (opening and closing) outside of the B-C joint virtually ceased, and it intensified in the joint.

*Strains in the B-C Joint Hoops.* As noted in Chapter 3 (Sec. 3.6.4, "The Functions of Joint Reinforcement"), when the strut mechanism becomes the predominant means of shear transfer through a B-C joint, the role of the hoops becomes one of confinement. In Unit I, the increase in cracking in the B-C joint was evidence that the joint was trying to dilate. Thus, the large increases in the strains in the B-C joint hoops (Figs. 74 and 75) were a result of these hoops acting to confine the dilating B-C joint. The onset of this behavior probably marked the complete transition from the truss mechanism to the strut mechanism.

*Slippage of the Lower Column Bars.* With damage done to the bottom of the B-C joint by cracking, both from joint shear and the process of bond deterioration for the strut lower main bars, the slippage of the column extreme bars that was noted in Chapter 5 is essentially assured. The slippage of these bars is all the more likely since they had yielded prior to the cycles to  $1.25\Delta_y$ . Additionally, it is reasonable to assume that some of the neighboring bars in the lower column were beyond yield at this point and were also slipping.

#### Cycles to $1.5\Delta_y$

At the peak displacements to  $\pm 1.5\Delta_y$ , the repercussions of having the strut mechanism transfer all of the B-C joint shear in a lightly-confined joint became evident, as cracking along the major joint diagonals and yielding of the hoop in the upper portion of the B-C joint occurred. The fact that the hoop in the lower portion of the joint did not yield was unexpected.

Given that the first large diagonal cracks occurred near the bottom of the joint, it was reasonable to expect that the hoop in the lower portion of the joint should have yielded before the hoop in the upper portion. A reason that the hoop in the lower portion of the B-C joint did not yield is a lack of adequate bond. At displacements near the peak displacements, it is possible that the dilation of the B-C joint and the lack of ribs on the hoop did not allow for enough bond to be developed for the hoop to yield (i.e., the lap-splice of the ends of the hoop failed).

#### Cycles to $2\Delta_y$ through Cycles in Excess of $6\Delta_y$

*Cycles to  $2\Delta_y$ .* The fact that the strains in the hoops in the B-C joint began to decrease at the second and the third peak displacements equal to  $\pm 2\Delta_y$  agrees with the fact that new strength levels were attained by Unit I at the first peak displacements equal to  $\pm 2\Delta_y$ . Because the B-C joint was the "weak link" in Unit I, any gains in specimen strength resulted in damage occurring in the joint. Decreasing strains in joint hoops at peak displacements are a result of concrete crushing (Chap. 3, Sec. 3.6.4, "Behavior of Joint Reinforcement"). It should be noted that because the yield strength of the hoops used in Unit I were high compared to the "as-built" yield strengths (i.e., 538 MPa = 78 ksi versus Gr 40), crushing of concrete in the B-C joint was probably delayed (Chap. 3, Sec. 3.6.4, "Behavior of Joint Reinforcement").

The penetration of yield of the member bars mid-way into the B-C joint was part of the advanced stage of inelastic behavior that the B-C joint was experiencing during the cycles to  $2\Delta_y$  (Chap. 3, Sec. 3.6.3, "Factors that Influence Bond").

*Cycles to  $2.5\Delta_y$  through Cycles to  $4\Delta_y$ .* In this range of cycles Unit I was able to maintain its strength at the first peak displacements in each cycle, with the exception of the first peak displacement equal to  $+4\Delta_y$ , where the strength attained was the largest for the

test. However, these cycles caused continued deterioration of the B-C joint that lead to worsening hysteretic behavior.

The B-C joint in Unit I can be considered to have failed at the first displacements equal to  $\pm 4\Delta_y$  ( $\approx 3.6\%$  drift) for two reasons (Fig 10d and 10e):

- 1.) There was no bond of the strut main bars in the B-C joint at all. This was evident in the data (Figs. 70 and 73), and was observed visually in one instance.
- 2.) The B-C joint had failed in shear. This was visually evident from the extent of the cracking in the B-C joint (Figs. 82 and 83), and the continued decrease in the strength of Unit I in the subsequent cycles supports this assertion as well.

Due to the bond and the shear failures in the B-C joint, no attempt was made to either repair this specimen and continue testing, or construct and test a retrofitted version of Unit I. Repair and retrofit schemes that might have improved conditions in the B-C joint region would probably have been quite elaborate, expensive and time consuming (e.g., encasing the region with a specially fabricated assembly of steel plates, or with a reinforced concrete "jacket"). Moreover, the improvement that would have been provided by such schemes was questioned since they might not have been able to provide the confinement to the B-C joint required to prevent the deterioration of bar bond. Finally, by testing Unit I to failure, the performance of the unrepaired specimen during large inelastic displacements was determined

## **6.2 Interpretation of the Experimental Findings From Unit II**

Given the poor performance of the B-C joint in Unit I, and given that Unit II was identical to Unit I with the exception of a smaller diameter column, the interpretation of the test results for Unit II closely follows that of Unit I. As such, only the differences that existed between the test results for the two specimens are discussed in what follows.

### 6.2.1 Bond Deterioration in the B-C Joint

In Unit II bond deterioration in the B-C began earlier than was the case in Unit I (i.e., cycles to 5.08 mm versus cycles to 7.62 mm), and the complete loss of bond occurred earlier too (e.g. cycles to  $2.5\Delta_y$  versus cycles to  $4\Delta_y$ ). There were two reasons for this:

- 1.) The effective B-C joint area of Unit II was nearly fifty percent smaller than that of Unit I (nearly 30% smaller if the portions of the B-C joint beyond the width of the struts in Unit I are neglected).
- 2.) The BI value of Unit II was 37.5% larger than that of Unit I (e.g. 1.1 versus 0.8).

Thus, with both specimens having similar small amounts of B-C joint confinement (i.e.,  $\rho_s = 0.1\%$ ), the faster deterioration and loss of bond in Unit II should be expected.

### 6.2.2 The Role of the Strut Mechanism

Despite the fact that bond deteriorated faster in Unit II, the detrimental effects of the strut mechanism did not occur as quickly as they did in Unit I. In Unit I the strut mechanism had caused the strains in the hoops to increase significantly at the peak displacements equal to  $\pm 1.25\Delta_y$ , and cracking along the major joint diagonals became prominent at the peak displacements equal to  $\pm 1.5\Delta_y$ . In Unit II these events occurred at the peak displacements equal to  $\pm 2\Delta_y$ , and  $\pm 2.5\Delta_y$ , respectively (Figs. 100, 101 and 102).

The reason that the effects of the strut mechanism were delayed in Unit II relative to Unit I was that in Unit II the lower column yielded (i.e., cycles to 15.24 mm) prior to the increase in the role of the strut mechanism. This occurrence limited the amount of horizontal shear applied to the B-C joint of Unit II at each set of peak displacements. However, once the effects of the strut mechanism became apparent in Unit II, the

degradation of both the B-C joint in Unit II and the response of Unit II progressed more rapidly than was the case in Unit I.

### 6.2.3 B-C Joint Failure

The B-C joint in Unit II failed at the first peak displacements to  $+2\Delta_y$  ( $\approx 1.8\%$  drift) and to  $-2.5\Delta_y$  ( $\approx 2.3\%$  drift). The failure referred to here is loss of bar bond in the B-C joint (Fig. 10d). Were it not for the fact that the strength attained at  $+2\Delta_y$  was matched at the first peak displacement equal to  $+4\Delta_y$ , then the joint shear failure mode (Fig 10e) would have applied as well (at  $+2\Delta_y$  and at  $-2.5\Delta_y$ ). The reason being that with the exception the first displacement peak equal to  $+4\Delta_y$ , the strengths attained by Unit II at the peak displacements in the retract direction clearly degraded in each of the cycles subsequent to the first cycle to  $2\Delta_y$ . As for the extend direction, the strength of Unit II degraded subsequent to the first peak at  $-2.5\Delta_y$ .

As was mentioned in Chapter 5, over-strength prevented the formation of a plastic hinge in the lower column of Unit II. Had a plastic hinge formed in the lower column in accordance with the theoretical calculations (i.e., during the cycles to  $1.25\Delta_y$ ), then the degradation of the response of Unit II would likely have been different. The poor confinement detailing in the plastic hinge region of the lower column probably would have allowed for failure there (Fig. 10b) before the B-C joint failed. Regardless, any of the possible failure modes for Unit II (10b, and/or 10d and 10e) are all undesirable (Chap. 3, Sec. 3.4). Finally, the lap splice in this region did not deteriorate despite the high moment demands there. The reason was probably the length of the lap splice ( $48d_b$ ). This length is long relative to the lap splices used in most of the bents in the inventory. A shorter lap splice length would likely not have fared as well.

Due to the bond and the shear failures in the B-C joint, no attempt was made to either repair this specimen and continue testing, or construct a retrofitted version of Unit II (ref. Sec. 6.1, "Cycles to  $2\Delta_y$  through Cycles in Excess of  $6\Delta_y$ ").

### 6.3 The Test Results Versus the Proposed Empirical Method

In Chapter 3 (Sec. 3.4.6) an empirical method was proposed for the prediction of B-C joint performance in B-C joint subassemblages. The method consisted of determining the type of failure that a B-C joint subassemblage would experience based on whether or not the following limits were met:  $\rho_s \geq 0.5\%$ , and  $BI \leq 1.7$ . It was found that if a subassemblage met these limits that it could be expected to develop flexural hinges in the beams (Fig 22). Exceptions occurred in a few subassemblages that were cycled to drifts in excess of 4%. Figure 110 is a version of Figure 22 that has been updated to include the results from the tests of Units I and II. The figure indicates that Unit I adds an additional data point to the "S. F., A. F."-category, while Unit II adds a new category of failures to the legend - - "A. F., S. F.". The reason that Unit I does not appear in this new category, in accordance with the experimental findings, is that "S. F." in the figure corresponds to a B-C joint shear failure indicated by yielding of the hoops in the B-C joint (Chap. 3, Sec. 3.4.6). Despite the fact that the B-C joint in Unit I was determined to have failed in shear after anchorage of the strut bars in the B-C joint was lost, yielding of the hoops in Unit I occurred first.

Regardless of how a shear failure in the B-C joint is defined, these results suggest that regardless of how low the value of  $BI$  is, if the value of  $\rho_s$  in the subassemblage is too small then a bond/anchorage failure is possible. Thus, this performance prediction method is probably not useful for the inventory studied in this work. In order for a B-C joint with #4 hoops spaced at 305 mm to have a value of  $\rho_s \geq 0.5\%$ , Equations 6 and 7 reveal that the diameter of the column (or the length of a column side in a square column) would have to be less than approximately 230 mm (the height of the strut and the number of hoops used

are related by the 305-mm hoop spacing). The column dimensions and the hoop spacings shown in Tables 2 and 4 reveal that the values of  $\rho_s$  in the interior B-C joints in the inventory are far less than 0.5%. Thus, the performance prediction method would indicate that the interior B-C joints in the inventory all have the potential for loss of bar bond.

#### 6.4 Appraisal of the Seismic Performance Potential of the Inventory

The transition from the findings that were obtained from the experimental tests of the two subassemblages to the appraisal of the seismic performance potential of the bridges in the inventory will be done in three increments: 1.) appraisal of the seismic performance potential of multiple column bents with circular columns (MCC category), 2.) appraisal of the seismic performance of the three other types of bents (i.e., DRC, MRC, and DCC categories), and 3.) appraisal of the seismic performance of the bridges in the inventory. Items 1.) and 2.) will be performed by comparing the experimental findings with the results of the evaluation of the various categories of bents (Chap. 4, Sec. 4.1.2).

The various appraisals were developed based on the following perspectives concerning the experimental findings:

1.) While the B-C joints in Units I and II experienced shear failures, the flexural strength ratios ( $\Sigma M_{nc}/\Sigma M_{nb}$ ) were approximately equal to one and less than one, respectively. Most research has proven that larger ratios (e.g.,  $\Sigma M_{nc}/\Sigma M_{nb} \geq 1.8$ ) increase the likelihood of good joint performance (Leon et al. 1986). Additionally, the relative sizes of the members in Unit I were proportional, and in Unit II the columns were substantially smaller than the struts. Research on subassemblages that did not have significant amounts of joint hoops indicated that large effective joint areas are important in ensuring good joint performance (Chap. 3, Sec. 3.6.4, "The Functions of Joint Reinforcement"). Note that the research findings related to the flexural strength ratios are not necessarily related to the research findings related to the effective joint sizes. For example, a column and a beam of

similar size might have a large flexural strength ratio, if the reinforcement index of the column relative to those of the beam is large enough.

2.) As mentioned in Chapter 3 (Secs. 3.5.1 and 3.5.2), post-earthquake reconnaissance has shown that B-C joints are often not the weak links in structures typically suggested by experimental studies. Also, B-C joint subassemblages tested in experimental studies do not account for the redistribution of forces that may occur in actual indeterminate frames.

#### **6.4.1 Appraisal of the Seismic Performance Potential of the MCC Category**

The comments that follow are made with reference to Chapter 4, Sec. 4.1.2, "MCC Category". Conclusions "1.)" through "5.)" are addressed.

"1.)" The interior B-C joints in these bents are susceptible to bond deterioration, perhaps at member displacement ductilitys ( $\mu$ ) not much greater than 1.0, as a result of the poor joint confinement. The weak column-strong strut bents are susceptible to B-C joint shear failures, although it is not likely that the values of  $\mu$  will become large enough (i.e., four or more) for these failures to occur (given the redundancy in these bents and the redistribution of forces that may result from this redundancy).

"2.)" The weak column-strong strut bents will probably not have large inelastic demands on plastic hinges in the struts. B-C joint anchorage and shear failures may occur prior to the formation of plastic hinges in the struts of these bents.

"3.)" Since the struts in the bents in this category have the shear capacities required for plastic hinges to form, and since plastic hinges will likely form only in the struts of the strong column-weak strut bents, strut shear failures probably would be limited to the strong column-weak strut bents.

"4.)" Failures of the column lap-splice regions for those bents/portions of bents with single struts that are located near grade are possible if the flexural ductility demands become large in the portions of the columns just above the struts. Also, the likelihood of

having small amounts of axial column loads on the poorly confined lap splice regions adds to the potential for such failures.

"5.)" These bents should respond as "flexible" structures (i.e., the spectral demands will cause increased response and decreased force demands) because period elongation seems likely, regardless of whether or not there is degradation of column lap splices or of strut plastic hinges. The reason being that bond will likely deteriorate in the B-C joints (relatively early on in the case of the weak column-strong strut bents).

Additionally, it is not likely that the weak-column-strong-strut bents will be able to form a full mechanism because:

- 1.) B-C joint failures may occur: loss of bond at  $\mu = 1.25$ , and shear at  $\mu = 4.0$ .
- 2.) the formation of enough plastic hinges at the ends of the struts is not likely, and
- 3.) the plastic hinges that form early on will not have the ductility required to remain viable while the other hinges are forming.

#### **6.4.2 Appraisal of the Seismic Performance Potential of the Other Categories**

##### **DRC Category**

The comments that follow are made with reference to Chapter 4, Sec. 4.1.2, "DRC Category". Conclusions "1.)" through "4.)" are addressed.

"1.)" Because the B-C joints in the test specimens performed so poorly with such small shear stress demands, there is cause for concern regarding the exterior joints as well (these joints were originally dismissed from consideration because the demands were even smaller than the demands on the interior joints). With just one framing strut, exterior joints are afforded less confinement than interior joints and as such they could fare worse. However, with a couple of exceptions, the columns in most of these bents are much

stronger and larger relative to the struts. Thus, most of these B-C joints are probably not susceptible to shear failures. Deterioration or the loss of strut bar bond in the B-C joints in these bents is far more likely to occur, since the B-C joints lack adequate confinement and the strut bars do not terminate properly in the columns.

"2.)" If large ductility demands occur at the ends of the struts, then it is possible that plastic hinges may fail in those locations, provided that bar bond is not lost in the B-C joints first.

"3.)" If strut shear failures occur they will probably be limited to those bents where plastic hinges form in the struts, since most of the bents in this category have an adequate shear stress capacity required for plastic hinges to form.

"4.)" The response of these bents will likely increase and the force demands on them will likely decrease from the deterioration of bar bond, whether or not damage occurs elsewhere.

Additionally, it does not seem likely that these bents will attain a full mechanism because of the limited ductility of the plastic hinge zones and because enough plastic hinges might not form in the struts due to bond deterioration in the B-C joints.

#### MRC Category

The comments that follow are made with reference to Chapter 4, Sec. 4.1.2, "MRC Category". Conclusions "1.)" through "5.)" are addressed.

"1.)" The typically small expected B-C joint shear stress demands in these bents does not preclude shear failures. Some of these bents feature weak-column-strong-strut construction, which has been shown in this work to be susceptible to B-C joint shear failures. Even in the bents with strong-column-weak-strut construction, the narrow dimension of the columns may serve as the column depth. Thus, the effective B-C joint area may be small if the portions of these joints beyond the widths of the struts are not effective in resisting

shear. Also, it is possible that B-C joint bar bond failures may occur due to the consistently poor joint confinement. Bond failures may occur at small values of  $\mu$  in those cases where square bars are used.

"2.)" Strut hinge failures at the exterior joints of most of these bents are not likely since the exterior B-C joints may not withstand enough inelastic cycles. Moreover, the possibility of bond deterioration may prevent plastic hinging from occurring.

"3.)" Strut shear failures are possible in those struts where the shear capacity is less than the demand associated with the formation of plastic hinges. However, in many of the other cases, the possible degradation of the B-C joints may preclude the formation of strut plastic hinges, thereby decreasing the likelihood of shear failures.

"4.)" In the cases where the struts are located near grade column lap splices may degrade if the flexural ductility demands become large in the portions of the columns just above the struts (Chap. 3, Secs. 3.7.1 and 3.7.2). Also, the likelihood of having small amounts of axial column loads on the poorly confined lap splice regions adds to potential for failure.

"5.)" With or without damage in the members, the response of these bents will likely increase and the force demands will likely decrease due to the probability of bond deterioration in the B-C joints.

Additionally, the formation of a full mechanism in these bents does not seem probable for reasons similar to those given for the other bent categories.

#### DCC Category

The comments that follow are made with reference to Chapter 4, Sec. 4.1.2, "DCC Category". Conclusions "1.)" through "5.)" are addressed.

"1.)" While the expected B-C joint shear stress demands for these bents are small, the members are of similar proportion and the flexural strength ratios are smaller than that

preferred. As such, joint shear failures are a possibility at large values of  $\mu$ . Also, bond deterioration at small values of  $\mu$  is possible given the lack of adequate confinement of the B-C joints (with respect to having just one framing strut and only a few hoops).

"2.)" Development of full plastic hinges in the struts are not likely because of the poor confinement of the B-C joints.

"3.)" Strut shear failures are not anticipated since the shear capacities are adequate and since strut plastic hinges may not develop.

"4.)" Failure in the column lap-splice regions above the struts near grade are possible at large values of  $\mu$  for the reasons given for the MCC and the MRC categories.

"5.)" These bents will more than likely respond as "flexible" structures given that bond deterioration in the B-C joints is likely.

Additionally, the formation of a full mechanism in these bents does not seem probable for the same reasons given for the other bent categories.

#### Other Considerations

To this point, the appraisal of the seismic performance potential of each of the four categories of bents has been based on the conclusions that were drawn in the evaluation of the bents in the inventory (Chap. 4, Sec. 4.1.2) and on the modifications of those conclusions based on the lateral testing performance of two subassemblages. What follows are considerations that affect the appraisals but could not be taken into account in either the experimental tests. These considerations are: vertical acceleration and vibration, both of which are effects that the bents will experience in an earthquake.

*Vertical Acceleration.* The recent Northridge earthquake demonstrated the vulnerability of bridges to the loads induced from vertical accelerations. The bents considered in this work are typically very lightly loaded vertically, relative to the axial capacities of the columns. Thus, these bents may have enough reserve capacity to

withstand the loads from vertical accelerations. However, the poor detailing of the bents in the inventory may negate any excesses in capacity and render the bents vulnerable to failure (as was typically the case in the bridges that failed in the Northridge earthquake). Moreover, the performances of the B-C joints could possibly be affected if the column axial loads were to become large (Chap. 3, Sec. 3.6.5, "Column Axial Load"), .

*Vibration.* As mentioned in Chapter 5, loose concrete was removed from the B-C joints of Units I and II in order to determine the extent of damage to the joint cores. This material was removed quite readily because of the scarcity of hoops. Thus, if the B-C joints in bents in the inventory are damaged in an earthquake it is possible that the vibrations from the earthquake may cause the joints to perform worse than the B-C joints in Units I and II did. The vibrations in an earthquake might be strong enough to dislodge fractured concrete. This effect could be detrimental to the B-C joints in the bents if vertical accelerations are substantial. Such conditions could conceivably result in the column-crushing failure mode (Fig. 10c).

#### **6.4.3 Appraisal of the Seismic Performance Potential of the Bridges**

Based on the appraisals for the different bent categories, it is logical to conclude that the seismic performance potential of the bridges in the inventory should be satisfactory for small values of  $\mu$  (e.g., less than four) and suspect for large values of  $\mu$  (e.g., four or more). However, there are several factors that this work has not addressed that need to be considered in order for the expected performance of the bridges to be appraised: the intensity and the duration of ground motion, the interaction between the soil and a bridge, the way that seismically-generated loads are distributed throughout a bridge, and the locations of strutted-column bents in a bridge. Herein, the seismic performance potential of the bridges will be appraised in light of these factors.

*Intensity and Duration of Ground Motion.* Two of the most important pieces of information required to determine how a structure will perform in an earthquake are the intensity and the duration of ground motion. Each of the bridges in the inventory is old enough to have experienced several earthquakes and yet they all remain serviceable. Thus, these bridges have not been exposed to levels of intensity or duration of ground motion sufficient to bring about significant damage. However, the inference that can be made from this work is that if the intensity and the duration of ground motion cause inelastic behavior in these bridges, namely in the strutted-column bents, particularly in the B-C joint regions therein, there is the potential for poor performance in many cases. It can also be inferred from this work that in some cases it is likely that the bridges will become more "flexible" at small ductility demands due to bond deterioration in the B-C joints in the strutted-column bents. If the intensity and the duration of ground motions do cause the stiffness of a bridge to decrease then it is likely that the response of the bridge will increase, while the force demands on the bridge will decrease. This effect may be beneficial to the performance of the applicable bridges.

*Soil-Structure Interaction.* Another issue that is very important in determining how a bridge will perform in an earthquake is the interaction between the soil and the structure. The degree of fixity of the foundations in the soil is a critical link between the ground motions that occur and the forces that a bridge experiences. In longer bridges this topic is complex since the spatial variation of ground motions may be a factor. In other words, in each of the longer bridges, it is likely that the ground motions that the foundations in one location within a bridge will experience may differ from the ground motions that the other foundations may experience. Thus, not only will the energy input into the longer bridges from the foundations vary, but the force distribution over the length of these bridges will likely be affected as well. While research on the effects of soil-structure interaction on the response of structures continues, the results from the early studies generally indicate that structures that are flexible relative to the soil that they are founded on experience relatively

small effects from soil-structure interaction (Derecho et al. 1991). Therefore, the increased flexibility that the bridges in the inventory may experience as they respond to earthquakes (as inferred from this work) could lessen or increase the effects of soil-structure interaction.

*Distribution of Loads.* Under earthquake excitation, the manner in which forces are distributed throughout the bridges affects the performance. The construction of the superstructures (e.g., their stiffness relative to that of the bents and their continuity) will largely dictate the damage sustained by each of the strutted-column bents. For example, it is possible that much of the damage done to a bridge from an earthquake could be concentrated in the superstructure if the superstructure is relatively flexible. Conversely, for bridges with relatively stiff superstructures the damage will either be concentrated in the bents or in the abutments. As far as the continuity of a superstructure is concerned, it is possible that the damage sustained by a given bent will decrease as the continuity of the superstructure increases. The reason being the damage will be distributed over more bents, unless all of the bents are subjected to the same loading. The more that damage is diverted from or distributed among the strutted-column bents, the more likely it will be that their potential deficiencies will be suppressed.

*Inconsistency in the Use of the Bents.* As mentioned in Chapter 3, rarely do the bridges in the inventory have substructures consisting solely of strutted-column bents. Typically, only the shorter bridges are supported entirely by this type bent. In these cases, the abutments will probably attract much of the force from ground motions. For the longer bridges, the inconsistency in the use of strutted-column bents and the change in the bent heights that typically occurs when the bent-types change may act to limit the response of, and the force demands on, the strutted-column bents.

In conclusion, the interaction of several factors will determine how the bridges in the inventory will perform in an earthquake. The nature of these factors is such that their effects on the seismic performance of the bridges will likely vary from bridge to bridge. Thus, the extent of an appraisal of the seismic performance potential of the bridges that can

be made based on this work is limited to the following: the strutted-column bents in these bridges have many potential deficiencies that may prove beneficial or detrimental to the performance of the bridges, depending on the ductility demands imposed by a seismic event. The deterioration of bar bond in the B-C joints of the bents may occur at small displacement ductilities (i.e., less than four). This may result in increased response and decreased force demands in the bents, both of which could be beneficial. On the other hand, larger displacement ductilities could cause the loss of bar bond in the B-C joints of the bents (thereby presenting the possibility of B-C joint shear failures), and/or the failure of plastic hinge zones (particularly those in the portions of columns where lap splices occur). Such behavior could jeopardize the ability of the bents to support the superstructure.



## **CHAPTER 7**

### **CONCLUSIONS, RECOMMENDATIONS AND IMPLEMENTATION**

At the outset of this work, concerns were raised about the inelastic behavior of strutted-column bents. An inventory of bridges with these types of bents was identified. The bents in the inventory were then reviewed concerning characteristics and construction details, and evaluated with respect to inelastic demands and seismic performance criteria. Experimental test prototypes were selected from the bents that were considered to have the greatest potential for poor seismic performance and that were considered to have the most importance (i.e., multiple-column bents with circular columns). The prototypes were designed to be representative of "as-built" portions of these bents (i.e. B-C joint subassemblages). Test specimens were designed and built according to scaled-down versions of the prototypes. These specimens were tested using cyclic, quasi-static loading. The support fixtures were designed to account for the surrounding portions of the bents and thus to produce the correct boundary conditions. Finally, the information that was obtained from each of the steps outlined above was synthesized and appraisals were given of the seismic performance potential of the various types of strutted-column bents, and of the bridges, in the inventory. What follows are the important results that were obtained from each of the "steps," as well as the highlights of the appraisals. Also, some recommendations are provided for implementing the results of this work.

#### **7.1 Review of the Characteristics and the Construction Details of the Bents**

- The bent members are not confined adequately for ductile performance.
- The struts have small longitudinal reinforcement indices.

- The positions of the struts in a given bent may vary from grade to above the mid-height of the clear height of the columns.
- The columns typically have lap-spliced longitudinal bars above the B-C joints.
- The columns have small axial dead loads.
- The strutted-column bents are typically not the sole type of substructure used along the length of a bridge.

## **7.2 Review of the Evaluation of the Bents**

- The steel detailing in the bent members is inadequate for ductile performance.
- The columns are typically, although not always, stronger than the struts.
- The B-C joint shear stress demands associated with flexural hinging of the struts are small relative to current limits.
- The strut shear-stress demands associated with flexural hinging of the struts typically are nearly equal to or exceed the expected capacity.
- The inelastic demands in the column lap-splice regions may be large to produce degradation when the struts are located near grade.
- The inelastic demands in the struts will be large when the struts are located near mid-height.
- Each of the bents, with their tributary portions of the superstructures, will probably experience spectral demands normally associated with more flexible structures.

## **7.3 Review of the Findings/Interpretation of the Findings From the Tests**

Unit I, which had members of similar size and nominal flexural strength, failed in B-C joint shear and had suffered substantial loss of strut bar bond in the B-C joint at a

displacement ductility ( $\mu$ ) of approximately 4.0. These failures occurred prior to the development of the nominal flexural strengths of the members. The hysteresis loops began to "pinch" at the smaller displacements soon after the specimen yielded due to the deterioration of strut bar bond in the B-C joint. As the displacement increments increased, this pinching worsened. After the bar bond was lost, the specimen developed strength and stiffness during a given cycle only after the displacement was large enough for the strut bars to become anchored at locations outside of the B-C joint. The axial load was sustained throughout the entire test (i.e., values of  $\mu$  greater than 9.0) and there were no signs of deterioration in the column splice zone.

Unit II, which had struts that were much larger and stronger than the columns, performed worse than Unit I. Unit II suffered almost complete loss of strut bar bond in the B-C joint by a value of  $\mu \approx 2.5$ . This specimen then failed in B-C joint shear at a value of  $\mu \approx 4.0$ . The theoretical nominal flexural strength of the column splice zone was attained prior to the occurrence of the failures. The hysteretic behavior of this specimen was similar to that of Unit I with the exception that the pinching phenomenon occurred sooner (as indicated by the earlier loss of strut bar bond in Unit II). The axial load was sustained throughout the entire test (i.e., values of  $\mu$  greater than 10.0) and there were no signs of deterioration in the column splice zone.

#### **7.4 Review of the Appraisals of the Bents and of the Bridges**

The seismic performance potential of the strutted-column bents is limited by the poor confinement and the poor detailing found in these bents. In most cases, the effects of the poor confinement and detailing will probably result in bond deterioration of the member bars in the B-C joints at small values of member displacement ductilities ( $\mu$ ). If the severity of the ground motion is such that only small values of  $\mu$  (e.g., less than four) are required, then the bents may perform satisfactorily. Under such conditions the extent of damage to a

bent will probably be limited to bond deterioration, which may cause increased response of the bent but decreased force demands. However if large values of  $\mu$  (e.g., four or more) are required, the performance of the bents will likely be poor. The bond deterioration will probably: inhibit the development of the member flexural strengths, cause the B-C joints to behave inelastically, and limit the energy dissipation capacities of the bents. Large values of  $\mu$  in those bents where bond deterioration does not play a large role may also cause poor bent performance due to the poor confinement and detailing in these bents probably producing brittle failure modes (e.g., member shear failures) or inadequate plastic hinge ductility in the members.

The seismic performance potential of the bridges can not be fully assessed from this work because factors such as earthquake intensity and duration, soil-structure interaction effects, the way that loads are distributed throughout the bridges, and the sporadic use of strutted-column bents in the bridges must be addressed on a case-by-case basis. The conclusion that can be drawn from this work is that the strutted-column bents in these bridges have many potential deficiencies that may prove beneficial or detrimental to the performance of the bridges, depending on the magnitude of the displacement ductility demands in the B-C joint regions imposed by a seismic event. The deterioration of bar bond in the B-C joints of the bents may occur at small values of the displacement ductility demands in the B-C joint regions. This might result in increased response and decreased force demands in the bents, both of which could be beneficial. On the other hand, larger values of the displacement ductility demands in the B-C joint regions could cause the loss of bar bond in the B-C joints of the bents (thereby presenting the possibility of B-C joint shear failures), and/or the failure of plastic hinge zones (particularly those in the portions of columns where lap splices occur). Such behavior could jeopardize the ability of the bents to support the superstructure.

## **7.5 Recommendations and Implementation**

As a result of this research the following actions are recommended:

### Determine the expected response of some of the bridges

Since the indication from this work is that the bridges in the inventory will perform satisfactorily when the displacement ductility demands in the B-C joint regions of the strutted-column bents are small, analyses should be conducted on the bridges in order to determine if these demands are indeed expected to be small. It is recommended that preliminary "push-over" analyses be used to "screen" the bridges of similar construction and layout. The inelastic demands predicted by these analyses should be compared with the inelastic deformation capacities of the subassemblages experimentally tested in this work. When conducting these analyses it is important that consideration is given to the following factors:

- 1.) the analyses may over-predict the stiffness of the strutted-column bents unless some account is taken of shear cracking and deterioration of bar bond in the B-C joints, and
- 2.) the analyses will not account for the potential "impact" loads that the bridges may experience in an earthquake when the direction of motion reverses. In other words, the hysteretic pinching that may occur at small displacements of the bents could create a situation where the bents have little restoring force until the end of each half-cycle of displacement.

When the results of these "push-over" analyses do not clearly indicate whether the values of the displacement ductility demands in the B-C joint regions in the bents of given bridges will be large or small, more extensive analyses of these bridges may be required. Such analyses could be non-linear finite element analyses, where appropriate hysteretic models could be used to account for the deterioration of bar bond in the B-C joints.

Determine whether or not to remove or replace the struts

In those instances where the bridge response analyses indicate that large values of the displacement ductility demands in the B-C joint regions are anticipated in the members of the strutted-column bents, the bridges should be analyzed again without the struts to determine if the response is improved or worsened. In the bridges where the response without the struts is improved, consideration should be given to removal of the struts in the field. The reasons for removing the struts are:

- 1.) the struts are typically the source of the problems of the strutted-column bents (i.e., the problems associated with the additional B-C joints and column lap-splices), and
- 2.) whether the struts are removed or not, large values of the displacement ductility demands in the B-C joint regions in these bents will probably necessitate retrofits in the columns at the superstructure soffits and at the foundations. If the struts are removed, then the prospect of having to retrofit the B-C joints are eliminated. If the struts are not removed, then it is likely that the B-C joints will have to be retrofitted, since retrofits made in other areas of the bents will likely cause the inelastic capacities of the B-C joints to be exceeded.

In the bridges where the response without the struts is worsened, consideration should be given to replacing the struts in the field with an alternative strut. For instance, steel sections could be used instead of the existing struts. These sections would be connected to the columns with partial-moment connections. The connections would be strong enough to afford the bents with some lateral stiffness at the smaller displacements. At the larger displacements the connections would be designed to fail so as to not damage the B-C joints. The magnitudes of these "small" and "large" displacements would be defined by the bridge analyses.

**Perform additional research in the following areas:**

- a) Conduct an experimental test on an interior B-C joint subassembly from the MCC category that has columns that are larger and flexurally stronger than the struts. Since this type of subassembly was not considered in the experimental portion of this work, no information regarding the inelastic deformation capacity of this type of B-C joint region was obtained. Such information may prove useful in the bridge response analyses for the bridges with bents from the MCC category.
  
- b) Conduct experimental tests on exterior B-C joint subassemblies from the MCC category. These tests are recommended for the same reason as that given for the test suggested in "a)".
  
- c) Conduct experimental tests on B-C joint subassemblies from the DRC, MRC, and the DCC categories. The B-C joint regions in the bents from these categories have several potential vulnerabilities that were not pursued in the experimental portion of this work. Information from experimental tests regarding the inelastic deformation capacities of the B-C joint regions from the bents in these categories would be useful in the respective bridge response analyses.

## REFERENCES

1. AASHTO (1991). *Standard Specifications for Highway Bridges, 1989, with Interim Specifications, 1991*, American Association of State Highway and Transportation Officials, Washington, D.C.
2. ACI Committee 318 (1989). *Building Code Requirements for Reinforced Concrete (ACI 318M-89)*, American Concrete Institute, Detroit, MI.
3. ACI Committee 408 (1991). "Abstract of: State-of-the-Art-Report: Bond Under Cyclic Loads." *ACI Materials Journal*, 88(6), 669-673.
4. ACI-ASCE Committee 352 (1985). "Recommendations for Design of Beam-Column Joints in Monolithic Reinforced Concrete Structures (ACI 352 R-85)." *ACI Structural Journal*, 82(3), 266-283.
5. Architectural Institute of Japan (AIJ 1975). *Standard for Structural Calculation of Steel Reinforced Concrete Structures*.
6. American Society for Testing and Materials (ASTM 1985). *Standard Specification for Steel Wire, Deformed, for Concrete Reinforcement (A 496-85)*.
7. Bonnaci, J., and S. Pantazopoulou (1993). "Parametric Investigation of Joint Mechanics." *ACI Structural Journal*, 90(1), 61-70.
8. Cheung, P. C., T. Paulay, R. Park (1991). "New Zealand Tests on Full-Scale Reinforced Concrete Beam-Column-Slab Subassemblages Designed for Earthquake Resistance." *Design of Beam-Column Joints for Seismic Resistance (SP-123)*, American Concrete Institute, Detroit, MI, 1-37.
9. Chung, L., and S. P. Shah (1989). "Effect of Loading Rate on Anchorage Bond and Beam-Column Joints." *ACI Structural Journal*, 86(2), 132-142.
10. *New Zealand Standard Code of Practice for the Design of Concrete Structures (NZS 3101 1982)*, Standard Association of New Zealand, Wellington, NZ.

11. Dai, R., and R. Park (1987). "A Comparison of the Behavior of Reinforced Concrete Beam-Column Joints Design for Ductility and Limited Ductility." *Research Report 87-4*, Dept. of Civil Engrg., University of Canterbury, Christchurch, NZ.
12. Darwin, D., S. L. McCabe, E. K. Idun, and S. P. Schoenekase (1992). "Development Length Criteria: Bars Not Confined by Transverse Reinforcement." *ACI Structural Journal*, 89(6), 709-720.
13. Ehsani, M. R., and J. K. Wight (1985). "Effect of Transverse Beams and Slab on Behavior of Reinforced Concrete Beam-to-Column Connections." *ACI Journal*, 82(4), 188-195.
14. Ehsani, M. R., and J. K. Wight (1990). "Confinement Steel Requirements for Connections in Ductile Frames." *Journal of Structural Engineering*, ASCE, 116(3), 751-767.
15. Ferguson, P. M. (1979). "Shear in Beams and One-Way Slabs." *Reinforced Concrete Fundamentals*, John Wiley & Sons, New York, NY, 140.
16. Filippou, F. C., E. P. Popov, and V. V. Bertero (1986). "Analytical Studies of Hysteretic Behavior of R/C Joints," *Journal of Structural Engineering*, ASCE, 112(7), 1605-1622.
17. Fujii, S., and S. Morita (1991). "Comparison Between Interior and Exterior RC Beam-Column Joint Behavior." *Design of Beam-Column Joints for Seismic Resistance (SP-123)*, American Concrete Institute, Detroit, MI, 145-165.
18. George, O. R. (1991). "Bridge Seismic Retrofit Program Recommendations." Washington State Department of Transportation, Olympia, WA.
19. Ghee, A. B., M. J. N. Priestley, and T. Paulay (1989). "Seismic Shear Strength of Circular Reinforced Concrete Columns." *ACI Structural Journal*, 86(1), 45-59.

20. Hanson, N. W., and H. W. Connor (1967). "Seismic Resistance of Reinforced Concrete Beam-Column Joints." *Journal of Structural Engineering*, ASCE, 93(5), 533-560.
21. Hanson, N. W., and H. W. Connor (1972). "Tests of Reinforced Concrete Beam-Column Joints Under Simulated Seismic Loading." *Portland Cement Association Research and Development Bulletin (RD012.01D)*, Skokie, Ill.
22. Hayashi, S., T. Morimoto, and S. Kokusho (1985). "The Bond Behavior of Reinforcing Bars through the interior of the Beam-Column Joint." Transactions of the Architectural Institute of Japan, *Journal of Structural and Construction Engrg.*, 357, 101-111.
23. Ichinose, T. (1991). "Interaction Between Bond at Beam Bars and Shear Reinforcement in RC Interior Joints." *Design of Beam-Column Joints for Seismic Resistance (SP-123)*, American Concrete Institute, Detroit, MI, 379-399.
24. Jirsa, J. O., D. F. Meinheit, and J. W. Woollen (1975). "Factors Influencing the Shear Strength of Beam-Column Joints," *Proc., US. National Conference on Earthquake Engineering*, Ann Arbor, MI, 297-305.
25. Joh, O., Y. Goto, and T. Shibata (1991a). "Influence of Transverse Joint and Beam Reinforcement and Relocation of Plastic Hinge Region on Beam-Column Joint Stiffness Deterioration." *Design of Beam-Column Joints for Seismic Resistance (SP-123)*, American Concrete Institute, Detroit, MI, 187-223.
26. Joh, O., Y. Goto, T. Shibata (1991b). "Behavior of Reinforced Concrete Beam-Column Joints with Eccentricity." *Design of Beam-Column Joints for Seismic Resistance (SP-123)*, American Concrete Institute, Detroit, MI, 317-357.
27. Kaku, T., and H. Asakusa (1991). "Bond and Anchorage of Bars in Reinforced Concrete Beam-Column Joints." *Design of Beam-Column Joints for Seismic Resistance (SP-123)*, American Concrete Institute, Detroit, MI, 401-423.

28. Kitayama, K., S. Otani, and H. Aoyama (1991). "Development of Design Criteria for RC Interior Beam-Column Joints." *Design of Beam-Column Joints for Seismic Resistance (SP-123)*, American Concrete Institute, Detroit, MI, 97-123.
29. Kurose, Y., G. N. Guimaraes, L. Zuhua, M. E. Kreger, and J. O. Jirsa (1991). "Evaluation of Slab-Beam-Column Connections Subjected to Bidirectional Loading." *Design of Beam-Column Joints for Seismic Resistance (SP-123)*, American Concrete Institute, Detroit, MI, 39-67.
30. Leon, R. T., and J. O. Jirsa (1986). "Bidirectional Loading of R. C. Beam-Column Joints." *Earthquake Spectra*, EERI, 2(3), 537-564.
31. Leon, R. T. (1990). "Shear Strength and Hysteretic Behavior of Interior Beam-Column Joints." *ACI Structural Journal*, 87(1), 3-11.
32. Leon, R. T. (1991). "Towards New Bond and Anchorage Provisions for Interior Joints." *Design of Beam-Column Joints for Seismic Resistance (SP-123)*, American Concrete Institute, Detroit, MI, 425-442.
33. Lukose, K., P. Gergely, and R. N. White (1982). "Behavior of Reinforced Concrete Lapped Splices for Inelastic Cyclic Loading." *ACI Structural Journal*, 79(5), 355-365.
34. Meinheit, D. F., J. O. Jirsa (1981). "Shear Strength of R/C Beam-Column Connections." *Journal of Structural Engineering*, ASCE, 107(11), 2227-2244.
35. Otani, S. (1991). "The Architectural Institute of Japan (AIJ) Proposal of Ultimate Strength Design Requirements for RC Buildings With Emphasis on Beam-Column Joints." *Design of Beam-Column Joints for Seismic Resistance (SP-123)*, American Concrete Institute, Detroit, MI, 125-144.
36. Pantazopoulou, S., and J. Bonnaci (1992). "Consideration of Questions about Beam-Column Joints." *ACI Structural Journal*, 89(1), 27-36.

37. Park, R., and T. Paulay (1975a). "Strength of Members with Flexure and Axial Load." *Reinforced Concrete Structures*, John Wiley & Sons, New York, NY, 118-122.
38. Park, R., and T. Paulay (1975b). "The Art of Detailing." *Reinforced Concrete Structures*, John Wiley & Sons, New York, NY, 675-676.
39. Park, R., and T. Paulay (1975c). "The Art of Detailing." *Reinforced Concrete Structures*, John Wiley & Sons, New York, NY, 746-747.
40. Paulay, T. (1982). "Lapped Splices in Earthquake-Resisting Columns." *ACI Journal*, 79(6), 458-469.
41. Paulay, T., and R. Park (1984). "Joints in Reinforced Concrete Frames Designed for Earthquake Resistance." *Research Report 84-9*, Dept. of Civil Engrg., University of Canterbury, Christchurch, NZ.
42. Paulay, T. (1986). "A Critique of the Special Provisions for Seismic Design of the Building Code Requirements for Reinforced Concrete (ACI 318-83)." *ACI Journal*, 83(2), 274-283.
43. Paulay, T. (1989). "Equilibrium Criteria for Reinforced Concrete Beam-Column Joints." *ACI Structural Journal*, 86(6), 635-643.
44. Priestley, M. J. N., and R. Park (1984). "Strength and Ductility of Bridge Substructures." *Research Report 84-20*, Dept. of Civil Engrg., University of Canterbury, Christchurch, NZ.
45. Priestley, M. J. N. (1991). "Seismic Assessment of Existing Concrete Bridges." *Seismic Assessment and Retrofit of Bridges (SSRP 91/03)*, 84-149.
46. Soleimani, D., E. P. Popov, and V. V. Bertero (1979). "Hysteretic Behavior of Reinforced Concrete Beam-Column Subassemblages." *ACI Journal*, 76(11), 1179-1195.

47. Soroushian, P., and K. Choi (1989). "Local Bond of Deformed Bars with Different Diameters in Confined Concrete." *ACI Structural Journal*, 86(2), 217-222.
48. Stevens, N. J., S. M. Uzumeri, and M. P. Collins (1991). "Reinforced Concrete Subjected to Reversed Cyclic Shear - Experiments and Constitutive Model." *ACI Structural Journal*, 88(2), 135-145.
49. Sugano, S., T. Nagashima, H. Kimura, and A. Ichikawa (1991). "Behavior of Beam-Column Joints Using High-Strength Materials." *Design of Beam-Column Joints for Seismic Resistance (SP-123)*, American Concrete Institute, Detroit, MI, 359-377.
50. Tada, T., and T. Takeda (1991). "Analysis of Bond Deterioration Process in Reinforced Concrete Beam-Column Joints Subjected to Seismic Loading." *Design of Beam-Column Joints for Seismic Resistance (SP-123)*, American Concrete Institute, Detroit, MI, 443-464.
51. Washington Standard Specifications (1963). *State of Washington Standard Specifications for Road and Bridge Construction, 1963, and, Amendments 1 and 2*, Washington State Highway Commission, Department of Highways, Olympia, WA.
52. Wong, P. K. C., M. J. N. Priestley, and R. Park (1990). "Seismic Resistance of Frames with Vertically Distributed Longitudinal Reinforcement in Beams." *ACI Structural Journal*, 87(4), 488-498.
53. Yankelevsky, D. Z., M. A. Adin, and D. N. Farhey (1992). "Mathematical Model for Bond-Slip Behavior Under Cyclic Loading." *ACI Structural Journal*, 89(6), 692-698.

## APPENDIX A

### ADDITIONAL INFORMATION ON B-C JOINTS

Contained in this chapter is additional information from the literature review on B-C joints that was not included in Chapter 3. As before, emphasis is placed on planar, reverse-cyclically loaded, interior B-C joints (i.e., no floor slabs, transverse beams, or bi-directional loading). This description applies to the B-C joints referred to herein unless noted otherwise. Additionally, the beams and columns that frame into a joint are referred to as "members", the longitudinal reinforcing steel in the members is referred to as "bars", and the horizontal transverse reinforcement in both columns and joints is referred to as "hoops". Finally, this chapter is organized in the same manner as Chapter 3. Therefore, information that is listed under a given heading herein can be referenced directly to Chapter 3 under the identical heading, unless otherwise noted.

#### A.1 Seismic Shear Transfer in B-C Joints

##### A.1.1 Seismic Shear Transfer Mechanisms

As mentioned in Chapter 3, Section 3.6.1 there does not seem to be a consensus on either the make-up of the strut and the truss mechanisms, or the relative contributions of the two mechanisms to the transfer of joint shear at any given point in time. In this section, an alternative description of the mechanisms is given, as well as an alternative opinion on the relative contributions of the mechanisms in the transfer of shear at selected points in time.

#### The Mechanisms

Figure 11 depicts the commonly accepted versions of the mechanisms. Figure A.1 shows the versions of Wong et al. (1990). Figure A.1 indicates that the composition of the

two mechanisms is not as extreme as indicated in Figure 11. Figure A.1a shows the forces acting on the joint that must be transferred through the joint core, as well as the resulting crack pattern in the joint core. Wong et al. surmise that the forces acting on the joint are transferred through the joint core:

- 1.) partly by a version of the strut mechanism that transfers the concrete forces and some of the bond forces from the member bars (Fig. A.1b), and
- 2.) partly by a version of the truss mechanism that carries the remainder of the bond forces from the member bars (Fig. A.1c).

Both types of joint reinforcement (hoops and vertical bars) are considered necessary to maintain the equilibrium of the compression struts of the truss mechanism

#### The Relative Contributions of the Mechanisms

*"Strut" Versus "Truss" - After First Yield.* Figure 12b showed the scenario where bond conditions were good and the "truss" was predominant. However, the stipulation was made that for the "truss" mechanism to be predominant, the faces of the beams had to be fully separated from the faces of the joint. This can be expected to occur only when the areas of steel at the top ( $A_S'$ ) and at the bottom ( $A_S$ ) of the beams are not equal, as is typically the case in building frames. However, the B-C joints in this work had  $A_S' = A_S$ . Thus, when the issue was explored further (Section 3.6.3, "The Effect of Bond on the Shear Transfer Mechanisms", "*Joint Shear Transfer with Good Bond Conditions*"), a full explanation was given as to why the "strut" and "truss" contributions would likely be similar in cases where  $A_S' = A_S$ , while it was only mentioned that under conditions with  $A_S' \neq A_S$ , the "truss" will probably be predominant. Attention will now be focused on this latter case.

According to Leon (1990), with good bond conditions most bar yielding takes place at the joint boundaries, hence there is little or no slip nor any yield penetration into the joint.

Under these conditions, Leon and Paulay et al. (1984) claim that as beams undergo flexure, the flexural cracks in the regions with larger areas of bars will probably not close when sense of the moments forces these bars to go into compression. The reason being that these bars must yield in compression in order for the cracks to close. Equilibrium of a beam cross-section near the face of a joint will usually dictate that the compressive force that these bars must develop will be less than the force required to yield the bars. The open cracks and the lack of bar slip will prevent the beam concrete compression blocks in these regions from confining the joint. Moreover, the cracks in the regions with smaller areas of bars will only close after these bars yield. Thus, during the majority of the loading history, all compression forces will be transferred through the joint by bond stresses. Hence, the "truss" plays a much larger role than the "strut" in the transfer of joint shear in typical building frames.

The bond forces that the "strut" is assumed to carry (Fig. A.1b) have implications in the relative contribution of the mechanisms when "*Joint Shear Transfer with Deteriorated Bond Conditions*" (Section 3.6.3, "The Effect of Bond on the Shear Transfer Mechanisms") is in effect. According to Paulay et al. (1984), if bond conditions are still good enough such that there is no slip yet, the role of the "strut" can diminish because of the increased yield penetration that can be expected with increased inelastic cycling. Not only are the compression blocks in the beam unable to react at the joint corners, but now the possibility of bond transfer in the corners of the joint is taken away. Thus, the "truss" will become more effective than was the case when bond conditions were good.

#### A.1.2 Quantifying the Shear Stress

This section begins with the presentation of material that provides detail for a point that was made in developing the equation for the applied shear stress ( $v_{jt}$ ) in Chapter 3. Then, material is presented that supplements the point that was made in Chapter 3 regarding

the different philosophies used in determining the shear stress capacity ( $v_{njt}$ ) in the building codes of the countries most concerned with seismic design.

### Applied Shear Stress

In Chapter 3, the equation for determining  $v_{jt}$  was presented (Equation 1). One of the variables in the equation was the effective area of the joint ( $A_{jt}$ ). It was said that in non-code-related experimental work, the value of  $A_{jt}$  is typically taken as the gross cross-sectional area of the column ( $A_g$ ). However, when the goals of the experimental research are to validate or advance code provisions, then the methods for calculation of  $A_{jt}$  are in accordance with those of the respective code, for instance:

$$A_{jt} = d_c \frac{b_b + b_c}{2} \quad \text{(Equation A.1)}$$

where:

$d_c$  = the column depth (the dimension parallel to the applied load)

$b_b$  = the beam width

$b_c$  = the column width

or:

$$A_{jt} = j_c \frac{b_b + b_c}{2} \quad \text{(Equation A.2)}$$

where:

$j_c$  =  $0.875d_c$ , where  $d_c$  is the column effective depth

and the other terms are as previously defined.

Equations A.1 and A.2 come from ACI-ASCE Committee 352 (ACI 352 R-1985) and from the Architectural Institute of Japan (AIJ 1975), respectively.

### Shear Stress Capacity

In Chapter 3, the different philosophies used in determining the value of  $v_{njt}$  in the design codes from the United States (US), New Zealand (NZ) and Japan were reviewed. In B-C joint subassemblage tests done by Kurose et al. (1991), the  $v_{njt}$  values from the various codes were compared with the maximum values of  $v_{jt}$  ( $v_{jt}^*$ ). The test results showed that values of  $v_{jt}^*$  were under-predicted by 10 to 35% with ACI 318M-89, and by 40 to 80% with NZS-3101. Kurose et al. proposed that the reason for the discrepancies produced in the use of the two codes was the increased relative emphasis placed on the role of the hoops in NZS-3101. While the AIJ expression for  $v_{njt}$  contains a joint reinforcement term, the emphasis on the role of the hoops, relative to that of the concrete, is not as substantial as in the case of NZS-3101. Therefore, the results obtained from the use of the AIJ-SRC expression tended to be similar to those obtained from the ACI 318M-89 expression.

#### **A.1.3 The Effect of Member Bar Bond on Shear Transfer**

This section begins with the presentation of material that supplements the material found in Chapter 3 under "Bond in B-C Joints". Then, material is presented that supplements the material found in Chapter 3 regarding shear transfer with deteriorated bond conditions. Also, some details behind a point made in Chapter 3 concerning the factors that influence bond is presented, along with some supplementary material on the same topic. Finally, material is presented that gives the detail behind a point made in Chapter 3 that

dealt with the amount of bond that is required for structural performance, along with material that supplements the discussion on specific bond criteria.

### The Mechanics of Bar Bond

Herein, "bond" and "anchorage" will imply "bar bond" and "bar anchorage", respectively. According to Soroushian et al. (1989), when reinforced concrete is subjected to reversed cycling, cracks are initiated in the concrete as bar lugs mechanically bear on the concrete in front of them, and the cracked concrete in-between lugs takes the form of "keys". As cycling progresses the concrete keys are crushed and sheared. Eventually, increasingly larger portions of these keys shear off, until finally entire keys shear off. Without keys for the bar lugs to bear on, the only thing preventing pull-out of a bar is friction. Friction decreases with cycling so it is unreliable for force transfer. As the effectiveness of force transfer between bars and the surrounding concrete decreases, bond is lost locally and the bars slip (local-type of bond failure). If deterioration in the effectiveness of force transfer continues, bars can slip along their lengths (global-type of bond failure signifying loss of anchorage where bars will pull/push through a joint).

### The Effect of Bond on the Shear Transfer Mechanisms

*Joint Shear Transfer with Deteriorated Bond Conditions.* Research done by Joh et al. (1991a), on five bonded-beam-bar specimens (one of which was specimen MH) and on one unbonded-beam-bar specimen (MHUB), had results that seemingly conflict with the idea that the truss mechanism is preferable to the strut mechanism. The "M" in "MH" corresponds to medium amounts of joint hoops and "H" corresponds to high amounts of closed stirrups in the beam ends; both amounts were relative to amounts used in the rest of the specimens tested. During construction of the MHUB specimen vinyl chloride pipes

were placed around the portion of the beam bars in the joint. This ensured that joint shear transfer could only be accomplished via the strut mechanism.

At the conclusion of testing the MHUB specimen exhibited no joint cracking (compared to a bonded-beam-bar specimen, MH; Fig. A.2). However, it is important to note that the MHUB specimen had the poorest hysteretic behavior of all of the specimens and it was the only specimen in which the beam bars did not strain-harden (the other specimens failed in beam flexure at strengths greater than the  $M_{nb}$  values). The reason that the MHUB specimen did not exhibit any damage or ultimate strength enhancement was probably because the bar strains did not exceed the yield strain by much, even at large specimen deflections. After the beam bars in specimen MHUB yielded, the deformable length of these bars was at least as large as the column depth, and therefore the tension stresses in these bars occurred uniformly across this length. Also, specimen MHUB showed low stiffness, even in the elastic range. The authors mention that, in general, because bonded-beam-bar specimens may have excessive damage in the joint, the joint shear capacities may be less than those in unbonded-bar specimens. It is important to note that the purpose of these tests was to investigate the influence of joint hoops on B-C joint stiffness deterioration. Therefore, conclusions made about the performances of specimens MH and MHUB must be viewed in accordance with the specific amounts of hoops used in these specimens (Chapter 3, Sec. 3.6.4, "Specific Amounts of Joint Reinforcement", discusses the effects of specific amounts of hoops on structural performance in more detail).

*Other Considerations Regarding the Relationship Between Bond and Joint Shear.*

Joh et al. (1991a) developed a link between bond and the joint shear stress ( $v_{jt}$ ) at first cracking. The  $v_{jt}$  for first cracking were calculated from principal stresses using:

$$v_{jt} = f'_t \sqrt{1 + \frac{\sigma_0}{f'_t}} \quad (\text{Equation A.3})$$

where:

- $f'_t$  =  $\beta\sqrt{f'_c}$ , the tensile strength of the concrete
- $\beta$  = 0.3 - 0.6, a coefficient which relates  $f'_t$  &  $f'_c$
- $\sigma_0$  =  $P/A_g$ , the column axial load divided by the gross cross-sectional area of the column (note that the value of "P" is negative when the column axial load is tensile, indicating the detrimental effect of this type of load).

Joh et al. found that Equation A.3 accurately predicted the value of  $v_{jt}$  at first cracking for each of the specimens (the maximum shear stress in specimen MHUB = the first cracking stress). The conclusion reached was that perhaps the diagonal tensile stress in a joint is dependent on the bond stress along the beam bars within the joint.

### Factors that Influence Bond

*The Effect of Joint Design Details on Bond.* One factor, discussed in the related area of Chapter 3, Sec. 3.6.3, involved in the design of a specimen that affects bond is the bar anchorage length ( $l_d$ ). Herein, some additional comments are made that supplement those of Chapter 3. Additionally, the ratio  $A'_s/A_g$  in the beams is a design-related feature that also effects bond. This was not covered in Chapter 3 but it will be here.

In Chapter 3, research by Leon's (1991) was reviewed that lead him to conclude that the values of  $l_d$  and  $v_{jt}$  had an influence on bond. It was mentioned that of the

specimens he tested, only those that had values of  $l_d = 24$ , or  $28d_b$  were able to develop enough bond for the beams to reach their ultimate moment capacities. Although,  $v_{jt}$  values at the time of beam yield were all about equal, regardless of  $l_d$ . Therefore, Leon concluded that some account should be taken of the value of  $v_{jt}$  in the determination of the value of the sustained bond strength. He defined the sustained bond strength,  $u_{bu}$ , as the minimum value of  $u_b$  available after a bar has undergone at least four full cycles of loading beyond yield. Leon derived an expression for the minimum desirable column depth ( $d_c$ ), based on the development of  $u_{bu}$ , with a factor in it to account for the effect of  $v_{jt}$ :

$$d_c^2 = \frac{2580d_b^2}{\sqrt{f'_c C_v}} \quad (\text{Equation A.4})$$

where,

$$C_v = 2 - (\gamma/1.28)$$

$$\gamma = \text{a constant} = V_{jt}/(A_{jt}\sqrt{f'_c}); f'_c \text{ in MPa}$$

and other terms are as previously defined.

Equation A.4 was derived under the assumption that beam bars yield at one joint face and there is bar stress at the other (a condition that is reasonable for design purposes). The equation is used by Leon in two hypothetical examples to illustrate the effects of the values of  $l_d$  and  $v_{jt}$  on bar bond deterioration. In the first example,  $l_d = 20d_b$  and  $v_{jt} = 1.67\sqrt{f'_c}$ , the maximum change in bar stresses from one side of the joint to the other side would be only 70% of the value of  $f_y$  after four inelastic cycles. In the second example,  $l_d = 28d_b$  and  $v_{jt} = 1.33\sqrt{f'_c}$ , 194% of the value of  $f_y$  would be obtained (implying that the bars would yield in tension and in compression even after four inelastic cycles).

Dai et al. (1987) showed that the ratio  $A_s/A'_s$  can influence bar bond. Use of larger  $d_b$  values in the top of a beam is permissible when  $A_s$  is less than  $A'_s$  (Fig. A.3). With  $A_s = A'_s$ , and good bond, increased reversed cyclic loading will produce full-depth flexural

cracks at the beam-joint interface, and yielding in all bars at the interface. Under this scenario, and increased levels of loading, deterioration of bond can be expected. However, when  $A_S < A'_S$  the flexure crack will not be full-depth on the side of the joint where the loading produces compression in the bottom of the beam. In order to maintain equilibrium at the beam cross-section at the interface with negative bending moment, the bottom of the beam will have a concrete compressive force in addition to the steel compressive forces. The presence of the concrete compressive force provides a better bond environment for the bottom bars, as opposed to the situation described earlier (i.e.,  $A_S = A'_S$ ; no concrete compressive force). On the positive-moment side of the joint there may well be a full-depth crack, however, equilibrium dictates a compressive force in the top bars that is below yield. In this way, the bond environment for the top bars is also enhanced, versus the case where  $A_S = A'_S$ .

#### Criteria for Bond for Seismic Performance

*The Amount of Bond Required for Structural Performance.* Kitayama et al. (1991) claimed that some beam bar slip could be allowed and they quantified how much, based on consideration of the energy dissipation capacity of beam ends and on the influence of the energy dissipation capacity of beam ends on the seismic response of frames. The smaller of two criteria, a beam ductility factor ( $\mu$ ) of four or a story drift of 2%, were arbitrarily determined to be acceptable levels of structural deformation prior to the occurrence of joint shear failure and/or significant beam bar slippage.

Several multi-story frames, designed in accordance with Japanese Building Standard Law, were subjected to earthquake response analyses. A portion of each of the frames, consisting of a single column and the beams that framed into the column, was taken from the prototype. The beams were cut at mid-span (the assumed inflection points).

The members in each of the "fish-bone" portions of the prototypes were represented by one-component models. The B-C joints were assumed to be rigid and the inelastic deformations in the members were assumed to be concentrated in a nonlinear spring. Several hysteresis models were selected to simulate the pinching behavior caused by bond deterioration (one of the models simulated no pinching, implying good bond). The additional deformation caused by the pull-out of the beam bars from a joint was neglected. Input ground motions were scaled to provide maximum values of  $\mu \approx 4$  at the beam plastic hinge zones. Kitayama et al. found that the effect of the hysteretic energy dissipated on the response amplitudes was relatively small when the equivalent viscous damping ratio ( $h_{eq}$ ) was in-between 0.1 and 0.25 at  $\mu = 4$ , where,

$h_{eq}$  = the ratio of the dissipated energy in half of a cycle from the actual system to  $2\pi$  times the strain energy from an equivalent linearly elastic system (for identical peak values of displacement).

Thus, Kitayama et al. concluded that some bond deterioration within a joint may be permissible.

Based upon the results from the earthquake response analyses, Kitayama et al. determined an allowable value of the bond index (BI) by comparing the BI and  $h_{eq}$  values at 2% story drifts. Values for damping were seen to decrease as BI increased (less energy was dissipated with increasing bar slip). It was determined that, for an allowable deformation level equal to a story drift of 2%, BI should be  $\leq 1.4$  in order to ensure that  $h_{eq} \geq 0.1$ .

*Additional Research Results and Criteria.* ACI 352 R-85 recommends that  $l_d \geq 20d_b$  be used in well-confined concrete (ACI Committee 408 1991). According to ACI Committee 408, if critical member sections and joints are confined to levels two to three times those required by current codes, and  $l_d$  values are increased by 1.5 times over provisions, then bond deterioration under conditions where  $u_b$  is large relative to the

ultimate bond strength (i.e.,  $u_b > 50\%$  of  $1.25u_b$ ) can be prevented. However, bond damage near the most highly stressed regions may still occur.

Darwin et al. (1992) state that ACI Committee 318 is currently considering revising the provisions related to the development of deformed bars for those instances where development of bars not confined by hoops occur.

Paulay (1986) and Sugano et al. (1991), based on their experimental research, claim that consequences of bond deterioration during inelastic seismic response are tolerable if  $d_c/d_b > f_y/11$ . Bonnaci et al. (1993) conclude that for specimens with Gr 60 beam bars and BI values  $> 1.7$ , bond failures occurred.

Ichinose's (1991) criterion for bond for seismic performance is based upon his description of the ways that shear can be transferred through a joint under a "weak beam-strong column" scenario. His description is based on several idealized models that he developed ("strut actions A, C, and D", "quasi-strut action A", "truss actions A and C"). The three "strut actions" are composed of different portions of the strut mechanism. The two "truss actions" are composed of different portions of the truss mechanism. The "quasi-strut action A" is composed of those portions of the strut and truss mechanisms that were not used in the "strut actions" or the "truss actions". The local bond strength of the beam bars in a joint and the amount of joint confinement determine the contributions of each of the "actions" in transferring shear through a joint. Ichinose proposed that the local bond strength of the bars plays a major role in the performance of a joint because of the effect of the local bond strength of the bars on the participation of the hoops in the transfer of joint shear. Ichinose claims that when more than twice the over-strength of beam bars can be developed through bond in a joint, as the local bond strength gets larger the demand on the hoops decreases ("strut actions" are predominant). Conversely, he claims that when bond can only be developed up to twice the over-strength of the beam bars, as the local bond strength gets larger the demand on the hoops increases ("truss actions" are

predominant). Finally, Ichinose contends that when the bond that can be developed gets too small, as the local bond strength gets larger the demand on the hoops becomes excessive. As a result of these excessive demands on the hoops, joint core dilation takes place. A decrease in the effective compression strength of the concrete will result from joint core dilation, which, in turn, can lead to joint shear failures.

Leon et al. (1986), based upon experimental research results, stated that for joints to remain "essentially elastic", and for frames to exhibit stable-hysteretic performance,  $l_d$  values should be  $30 - 35d_b$  (for beams with Gr 60 bars). In later work, Leon (1990) conducted experimental tests on subassemblages with lightly-reinforced joints in order to study the performance of the strut mechanism (Leon was trying to validate ACI 318-83 provisions, which he claims emphasize the "strut"). Leon's research indicated that beam bar  $l_d$ 's of  $20d_b$  do not ensure that beams can develop any post-yield strength. The only specimen that he tested that was able to achieve the ultimate flexural strength of the beams (based on confined material properties) had  $l_d = 28d_b$ . This specimen showed no post-yield strength deterioration through drifts in excess of 3.5%. Applied to today's standard (ACI 318M-89), the research also showed that cyclic loading to the code-allowable shear stress ( $1.25 \sqrt{f'_c}$ ) does not produce substantial damage if  $l_d$  values are large. Finally, Leon argued for bars with at least  $24d_b$  anchorage through a joint, only the minimum amount of hoops required for column confinement are required in the joint (because he believed that most of the joint shear in his subassemblages was transferred by the strut mechanism).

Sugano et al. (1991), based on their experimental test results, proposed the criterion  $BI \leq 1.7$ , for beam bar bond performance in higher strength concretes ( $f'_c \geq 35$  MPa). Additionally, for joints with normal strength concretes ( $21 \leq f'_c \leq 35$ ),  $BI \leq 2$  was suggested by Sugano et al.

#### **A.1.4 The Effect of Joint Reinforcement on Shear Transfer**

In this section, background material is presented concerning the points made in Chapter 3 regarding the roles of the joint hoops in the transfer of shear. Also, additional details are provided concerning the shear and the confinement functions of hoops. Finally, details and supplementary information is given about specific amounts of joint reinforcement that are required to perform the shear and confinement functions.

##### The Roles of Hoops in the Joint Shear Transfer Mechanisms

Bonnaci et al. (1993) propose that there are two theories describing the roles of hoops in the B-C joint shear transfer mechanisms.

- 1.) The first theory focuses on interpretation of the stress state of joints subjected to lateral forces. The hoops act as horizontal components of a truss equilibrium model (Fig. A.1c). As a part of the "truss", the hoops carry a large portion of the shear applied to the joint. The remaining portion of the shear is carried by a diagonal compression strut (similar to the compression strut formed by the major joint diagonal in the strut mechanism; Fig. A.1b) in the concrete core.
- 2.) The second theory centers around the flexural behavior of the column. The joint is viewed as a segment of a column that has a steep moment gradient caused by the changes in direction of bending that take place within the height of the joint. This viewpoint, with the aid of arguments similar to those used in the theory of column flexure, leads to the conclusion that shear in the joint is predominantly carried by the strut mechanism and by the column bars. The role of the hoops is to provide confinement to the joint concrete; this both increases the capacity of the "strut" and maintains the integrity of the joint core.

Figure 17 in Chapter 3 was constructed in pursuit of determining the predominance of one theory over the other, given certain amounts of hoops.

### The Functions of Joint Reinforcement

*Shear Transfer.* As a basis for Otani's (1991) claim that increases in the amount of hoops will not contribute as much to shear transfer as believed by some (e.g., researchers from NZ), he presents a plot of the average value of  $v_{jt}$  (at shear failure) divided by  $f'_c$  versus the product of the hoop reinforcement ratio and the yield stress of the hoops (Fig. A.4). The data for the plot is from experimental tests, conducted by others, on subassemblages that failed in joint shear prior to beam flexural hinging. Points in Figure A.4 connected by lines represent results from specimens tested as a series by the same researcher(s). The figure shows marginal strength gains for increasing amounts of hoops. Fujii et al. (1991) report their subassemblage test results showed that an increase in the amount of hoops gave a very minor increase in joint shear strength. Pantazopoulou et al. (1992) claim that joint shear capacity is improved with more hoops to a point, and then there is no further effect because once the joint shear capacity reaches a certain level it will exceed the flexural capacity of the members (the majority of the actions that cause joint shear comes from flexure from the members). Joh et al. (1991b) believe that more research is required on the roles of joint hoops in the shear strength of joints.

### Specific Amounts of Joint Reinforcement

Experimental studies were conducted by Kitayama et al. (1991) on three test specimens with varying joint reinforcement layouts (Fig. A.5), hoop volumetric ratios ( $\rho_s$ ; Chapter 3, Equation 6), and BI values. The purpose was to determine the  $\rho_s$  values required to transfer shear, and to confine the core concrete, after bond deterioration of the beam bars occurs at high joint shear levels. Specimens B1 and B2 were designed with  $\rho_s = 0.44\%$ , and  $BI = 1.6$ , while specimen B3 had  $\rho_s = 0.95\%$ , and  $BI = 1.0$ . The specimens were designed to develop joint shear stresses of  $1.49\sqrt{f'_c}$  ( $f'_c$  in MPa); B1 and

B2 achieved  $1.53\sqrt{f'_c}$  and B3 achieved  $1.39\sqrt{f'_c}$ . Damage was concentrated in the panel regions of all of the specimens at drifts (R) of 1/25 radians (= 4%).

Hysteresis plots for specimens B1 and B3 are shown in Figure A.6. Figure A.7 shows the bond forces along the beam bars within the joints of B1 and B3 versus the story drifts. The bond forces for all three specimens began to drop off at drifts of 1/100 radians, although the beam bars had not yet yielded.

Figure A.5 depicts the detailing for the joint reinforcement in the three specimens; two schemes were used in the three specimens. B1 and B3 had cross ties in the two orthogonal directions, while B2 had hoops. Figure A.8 represents the performance of the "parallel" ties. Kitayama et al. claim that the ties parallel to the loading direction transferred joint shear and confined the joint core concrete through a story drift angle of 1/100 radians. The claim was also made that, through story drifts of 1/100 radians, the "parallel" ties were performing as portions of the truss mechanism. As the drifts increased from 1/100 radians to 1/50 radians, the strains in the "parallel" ties did not change much, perhaps indicating a change from the "truss" to the "strut". Even though B3 had a much higher  $\rho_s$  value than did B1, the magnitudes and distributions of the strains in the ties were similar.

The ties perpendicular to the loading direction confined the joint core concrete normal to the loading direction, according to Kitayama et al. Figure A.9 shows that the strains in these ties increased markedly with drift, implying lateral expansion of the joint core concrete. Figure A.10 shows the sum of the forces in the "parallel" ( $\sum F_L$ ) and "perpendicular" ( $\sum F_O$ ) ties versus the joint shear distortion angles for the indicated direction of loading. For drifts larger than 1/100 radians, the point at which bond deterioration begins, the contribution by the "parallel" ties toward the transfer of joint shear decayed, indicating the decay of the truss mechanism. Kitayama et al. argue that once the truss mechanism decayed the principal role of the lateral reinforcement became confinement of the cracked core concrete. The confinement function was fulfilled by the specimens until

yield of the lateral reinforcement normal to the loading direction occurred (approximately 0.1% strain at a story drift of 1/50 radians).

The conclusion drawn by Kitayama et al. from their tests was that values of  $\rho_s < 0.44\%$  may provide sufficient confinement to the core concrete. However, a minimum value of  $\rho_s = 0.5\%$  is recommended. Lowering  $\rho_s$  below 0.5% is considered acceptable if  $v_{jt} \ll 1.25\sqrt{f'_c}$  ( $f'_c$  in MPa).

Bonnaci et al. (1993) recommended that the joint hoop "potential", as defined below, should be at least as much as the "potential" of the beams, in order to prevent failure by joint shear.

"joint hoop potential" =  $V_p$  = the total yield force that can be developed by joint hoops parallel to the direction of the applied load, divided by  $A_{jt}$ , and normalized with respect to  $\sqrt{f'_c}$ .

"potential of the beams" =  $V_y$  = to the joint shear stress required to develop nominal flexural yielding of bars in the adjacent beams, normalized with respect to  $\sqrt{f'_c}$ .

Figure A.11 shows that for the battery of subassemblage test results considered, when  $V_p/V_y$  exceeds unity the mode of specimen failure was predominantly one of beam hinging, versus the joint-shear mode of specimen failure for ratio values less than unity.

#### A.1.5 Other Factors That Affect Shear Transfer

In this section, supplementary information and details that support points made in Chapter 3 are provided regarding the effect of: the strength of the concrete used in the joint, the joint shear distortion, the cross-sectional dimensions of the members, the deformation of the members, and the amount of column axial load on B-C joint shear transfer.

### Joint Concrete Compressive Strength

According to many researchers, a most important parameter in determining the performance of seismically loaded B-C joints, is the strength of the concrete used in a joint ( $f'_c$ ).

Otani's experimental research (1991), as well as his review of the experimental research done by others, revealed that when B-C subassemblages experienced joint shear failures the joint shear strength was heavily dependent on the value of  $f'_c$ , and not to a great extent on the value of  $\rho_s$ . Sugano et al. (1991) developed a graph (Fig. A.12) that relates values of  $v_{jt}$  to values of  $f'_c$ . The values of  $v_{jt}$  and  $f'_c$  that are used in the graph are from experimental subassemblage tests done by others. Each data point represents the test result for one subassemblage. With the use of the plotted points and knowledge of the mode of failure of each subassemblage, Sugano et al. created boundaries on the graph that separate the joint shear failure modes prior to and after flexural yielding of the beams. The "lower bound" boundary indicates that for  $v_{jt} < 2\sqrt{f'_c}$  joint shear failures occurred only after the beams had yielded (the specimens that met this criterion performed in a ductile manner to story drifts in excess of 2%).

Sugano et al. (1991) saw increasing joint shear distortion as  $f'_c$  decreased from high-strength (60+ MPa) values down to normal strength (30 MPa) values. Joint shear distortion has been established as a measure of joint and structure performance.

### Joint Shear Distortion

Joh et al. (1991b) state that more research is required concerning the correlation between frame deformability and joint shear strength. However, from the research that has been conducted, some believe that the deformations experienced by B-C joints (exclusive

of bar bond deterioration and of bar slippage), relative to the total deformation of the frame/subassemblage, is related to the performance of joints.

Leon's (1990) experimental tests revealed that joint shear failures can be expected when the joint shear strain contributes 17 to 25% of the total frame/subassemblage deformation.

In two of the specimens tested by Sugano et al. (1991), J6-O and J4-O, relationships were noted between  $f'_c$  values, the amounts of relative joint shear deformation, and joint shear failure. Specimen J6-O was designed with  $f'_c = 61$  MPa and  $BI = 1.3$ , while specimen J4-O had  $f'_c = 30$  MPa and  $BI = 1.6$ . Both specimens were provided with  $\rho_s = 1.1\%$ . Flexural hinges were expected to form at the beam ends of the specimens. Specimen J4-O exhibited a contribution in excess of 50% from joint shear distortion, at a story drift of 2%. At the same drift, specimen J6-O had a contribution of 30% from joint shear distortion. Both of the specimens subsequently failed in joint shear at story drifts in excess of 4%. However, J4-O failed prior to flexural yielding of beams, while J6-O failed after plastic hinges had formed in beams.

In experimental tests on B-C joints by Cheung et al. (1991), in which the joints were detailed in accordance with the NZ code, the subassemblages did not suffer joint shear failures despite having relatively large joint deformation contributions (20 - 25%). Cheung et al. concluded that the use of relatively large  $\rho_s$  values, along with beam bars with small  $d_b$  values, enabled the joints in their subassemblages to perform satisfactorily.

Pantazopoulou et al. (1992) argue that the smaller the joint deformation contribution is to the total structure deformation, the better overall structural response will be.

#### Member Cross-Sectional Dimensions

Otani (1991), based on his study of experimental research done by others, noted that when the depth of the intersecting beam,  $h_b$ , exceeds twice the column depth,  $d_c$ , that

the shear resistance of the joint decreases. However, this scenario also produces the undesirable "strong beam-weak column" behavior.

Meinheit et al. (1981) found no trend related to the variation of the joint aspect ratio (for  $0.72 \leq d_c/h_b \leq 1$ ) in their experimental tests. However, when beams were deeper than the columns the diagonal cracks in the joint were oriented at angles exceeding  $45^\circ$ . This implies that shear cracks propagated along lines parallel to the main joint diagonal regardless of the joint dimensions.

Paulay (1989) claims that the width of the beam relative to that of the column is an irrelevant parameter, as long as most of the beam bars pass through the column, because beams dilate joint cores. In other words, as a beam undergoes flexure the effect on a B-C joint is to allow the joint to expand, regardless of the width of the beam. Perhaps, the typically small axial loads on beams is the reason. On the other hand, Paulay (1984) noted that when the width of the column is too large, relative to the width of the beam, the interaction of the beam with the column will not be effective (i.e., neither the concrete areas nor the bars that are far from the vertical faces of the beam will participate efficiently in resisting the beam moments).

Conversely, in experimental research by Leon et al. (1986), the widths of beams relative to the column widths affected the behavior of test specimens. Two subassemblages (BCJ11 and BCJ12) that had vastly different beam widths exhibited behavior that was dissimilar. The widths of the framing beams in BCJ12 were 20% larger than the column width, and the flexural strength ratio of the columns and beams ( $\sum M_{nc}/\sum M_{nb}$ ) was 1.13 (Leon does not indicate the locations of the beam bars relative to the column width). BCJ11 had beam widths that were one-half of that of the column, and  $\sum M_{nc}/\sum M_{nb} = 1.25$ . In comparing the resulting performance of the two specimens, Leon found that in BCJ11 the relatively early failure was due to spalled joint corners, along with the resulting loss of section and bond of the beam corner bars. Because the strength of the beam could not be mobilized, BCJ11 had flexural hinging in the column above and below the joint, and

it had relatively low values of  $v_{jt}$ . In BCJ12, while the beams did not reach yield and the hinging was in the column, there was no extensive joint damage, despite relatively high values of  $v_{jt}$ . In BCJ12 the increased joint size permitted a large diagonal compression strut to be maintained, thereby enabling more shear stress to be carried than was the case with BCJ11.

### Member Deformation

Experimental work done by Joh et al. (1991b) suggests that the degree of deformation of the members, after plastic hinges have formed in them, influences the joint shear strength. Figure A.13 qualitatively models the relationship between the total applied horizontal shear force through the joints (" $V_{jh}$ ") and the story drift angles (" $R$ ") for three test specimens (B1, B2, and B6) that were designed to have flexural hinges form in the beams prior to flexural yielding in the columns or to shear failure in the beams, columns, or the joints. Details of the three test specimens are shown in Figure A.14, where all dimensions are in mm. B1 was designed as the control specimen and it had beams with widths that were 50% of the column width. B2 had beams that were equal in width to the columns. B6 had beams that were 50% as wide as the columns, and the beams framed into the column eccentrically. All three specimens had  $\rho_s = 0.3\%$ .

The three specimens had identical values of the joint shear force required to develop the flexural strengths of the beams (" $V_{bf}$ "). While all three specimens were able to form plastic hinges in the beams at the joint faces, only B2 failed due to beam flexure (at drift angle " $R_{B2}$ "). Specimens B1 and B6 failed in joint shear (at the respective drift angles of " $R_{B1}$ " and " $R_{B6}$ ") due to the inability of the joints in these specimens to sustain the plastic hinges in the beams through increasing inelastic deformations and increasing load reversals. The  $R_{B1}$ ,  $R_{B2}$ , and  $R_{B6}$  values were selected in accordance with the following

criterion: the ultimate/limit story drift angle was the angle at the time the strength of a specimen degraded such that the value of  $V_{jh}$  decreased to  $V_{bf}$ .

The curves in Figure A.13 model the relationship found between the specimen ductilities ( $\mu = R/R_y$ ) and the increments of the potential joint shear strength (" $V_{js-B1}$ ", " $V_{js-B2}$ ", and " $V_{js-B6}$ "; each calculated using an empirical equation) above the  $V_{bf}$  values. The three falling branches (dashed lines), assumed by Joh et al. to be parallel to one another, models the respective responses of the specimens after they reached their respective values of  $V_{js}$ . The actual respective R-values (those reached by the specimens in the tests) are indicated by the model at the intersection of the respective falling branches and the solid horizontal line (at  $V_{bf}$ ).

#### Column Axial Load

Currently there seems to be little consensus regarding the effects of column axial compressive load on B-C joint shear transfer. The lack of agreement stems from the fact that column axial compressive load may interact with other aspects of joint shear transfer (e.g., joint shear stress demand, bar bond, joint reinforcement, etc.). With one exception (Pantazopoulou et al. 1992), none of the work reviewed indicates that column axial compressive load is detrimental to B-C joint shear transfer. Opinion seems to be split between those who believe that axial load enhances joint shear performance and those that feel it has little effect on joint performance.

*Column Axial Compressive Load Is Beneficial.* It is well established that "weak beam-strong column"-frames generally provide better seismic performance. "Weak beam-strong column"-behavior is ensured by requiring that the ratio of column and beam flexural strengths ( $\Sigma M_{nc}/\Sigma M_{nb}$ ) exceeds some value that is greater than unity (different codes specify different values). Many researchers agree that larger values of  $\Sigma M_{nc}/\Sigma M_{nb}$  (e.g., 1.8 - 2.5; Leon et al. 1986) are beneficial for ensuring elastic joint performance, and stable-

hysteretic frame/subassemblage performance. Therefore, an extension of the logic would be that increasing the column axial compressive load is beneficial. For a given set of members at a B-C joint, increasing the axial compressive load will increase the value of  $\Sigma M_{nc}/\Sigma M_{nb}$  until the column "balanced-failure-point" is reached.

The NZ code requires more joint reinforcement when column axial compressive loads are small. The research, on which the code provisions are based, shows that when column axial compressive loads are small the shear resistance provided by the strut mechanism diminishes, while that provided by the truss mechanism increases (Cheung et al. 1991).

Through theoretical considerations based on first principles, Paulay (1986) claims that, all else being equal, axial compression on a member reduces the need for hoops. Also, from experimental work he observes that the contribution of the joint core concrete to the shear strength of interior joints, with plastic hinges in adjacent beams, deteriorates rapidly when there is little or no axial compressive load on the column. The result is that the value of  $\rho_s$  must be increased. Paulay (1989) also demonstrated analytically that the column axial compressive load will beneficially decrease internal vertical tensile forces at the joint centerline.

Experimental tests by Jirsa et al. (1975) included column axial compressive loads from  $0.03-0.35f'_cA_g$ . In these, the hysteretic behavior of all the specimens was nearly identical. Increasing in the column axial compressive load from "0.03" to "0.35" had the effect of increasing joint stiffness and had little effect on the joint shear capacity. However, shear at first cracking for the " $0.35f'_cA_g$ " specimen was over double that of the most lightly loaded specimen. This was attributed to the higher axial stress increasing the shear at which principal diagonal stresses reached the tensile capacity of the concrete. It was also observed that the specimens with higher axial compressive loads had steeper diagonal joint cracks than did the other specimens. This was the result of the maximum principal tensile stresses becoming more vertical as the axial load increased. In the case of the " $0.03f'_cA_g$ "

specimen, extensive joint cracking and spalling was noted at large deformations, along with reduced joint shear stiffness and slippage of bars in the joint.

The experimental work of Fujii et al. (1991) and Meinheit et al. (1981) also observed that increases in column axial load give an increase in joint shear corresponding to first cracking, and had no influence on ultimate joint shear strengths.

Fujii et al. (1991) also found that specimens with higher column axial compressive load ( $0.25f_cA_g$ ) had much lower hoop strains at lower specimen load levels ( $0.083f_cA_g$ ). They concluded that column axial compressive load is beneficial in that it can reduce the amount of hoops required in a joint. However, for the conclusion to be applicable, joint shear failure must be designed against and column axial load must be kept constant during the response.

Ichinose (1991) analytically argues that larger column axial compressive load will increase the width of the column flexural compressive stress blocks above and below the joint, thereby providing better bar bond conditions and lowering the stresses in the hoops.

Bonnaci et al. (1993) conducted a review of 86 experimental tests and found that the effect of column axial load on joint shear transfer was inconclusive. Whether or not joint shear transfer is helped or hindered by the presence of column axial compressive load, Bonnaci et al. state that it seems clear that increased column axial load increases joint stiffness, increases the joint shear corresponding to first cracking, and decreases cracking and hoop strains. All of these effects are beneficial.

*Column Axial Compressive Load Is Negligible.* Tests by Leon et al. (1986) showed that the difference between subassemblages with columns with zero axial load and one subassemblage with a column loaded to the "balanced-failure-point" axial compressive load was negligible, in so far as joint behavior was concerned. The "zero-axial-load" specimen showed less joint shear strain, more column rotation, and identical elastic deformations and beam rotations.

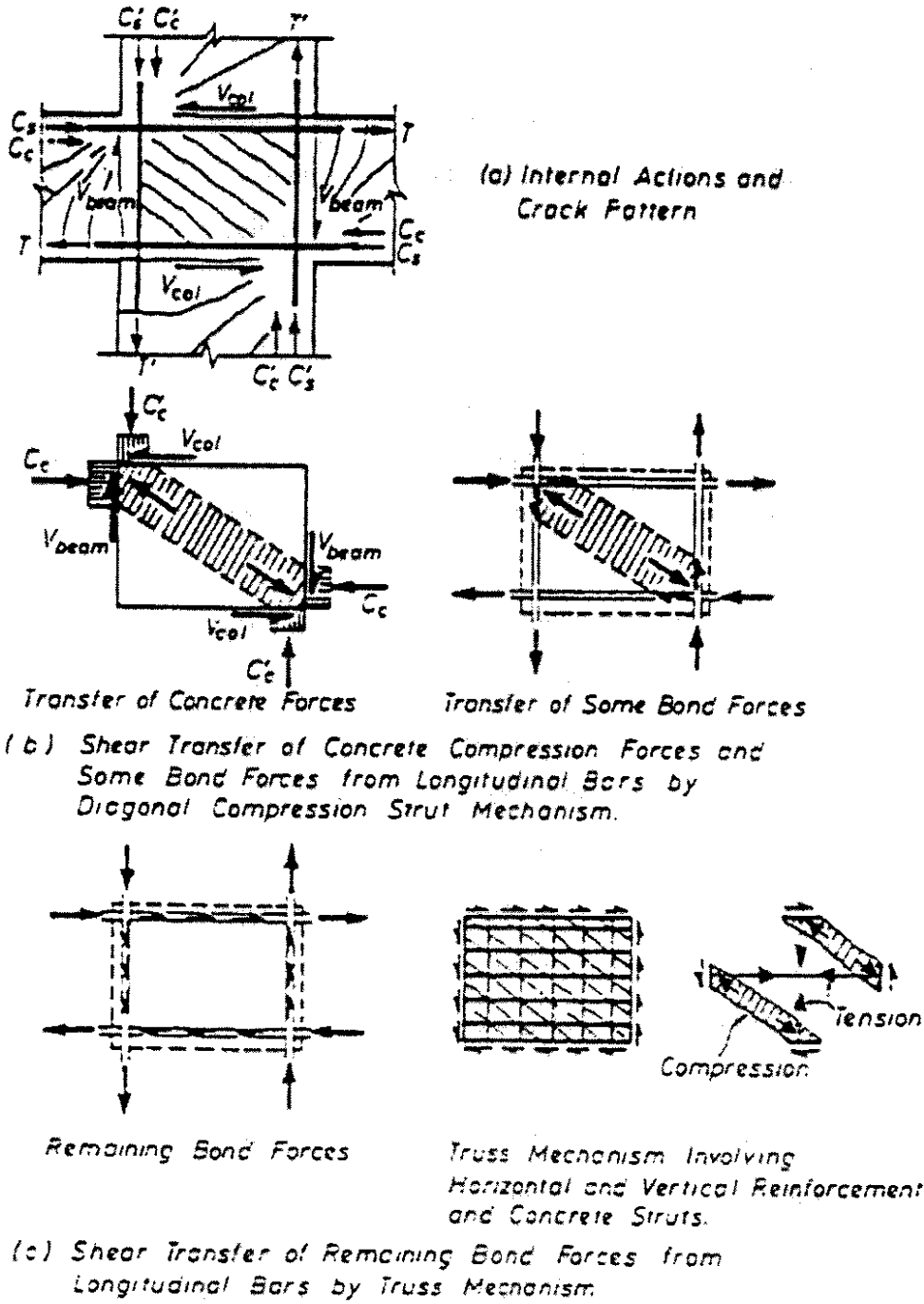


Figure A.1 Mechanisms of seismic shear transfer in B-C joints (from Wong et al. 1990).

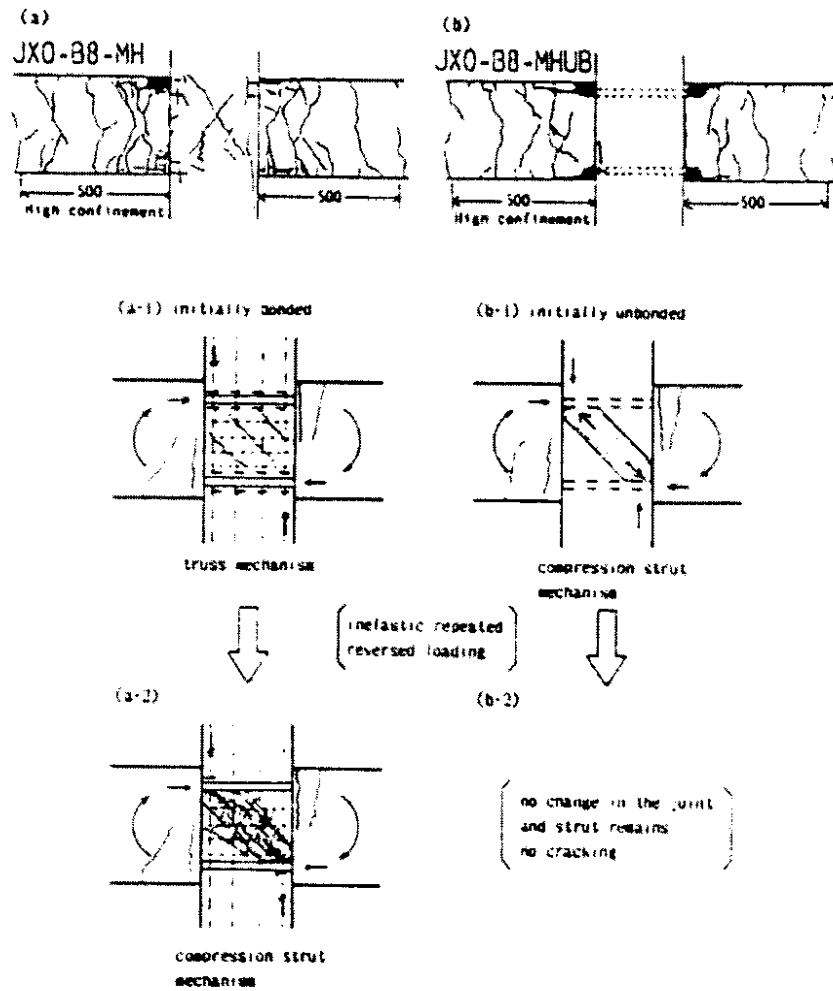


Figure A.2 Post-test crack patterns of a specimen with bonded bars and of a specimen with unbonded bars (from Kaku et al. 1991).

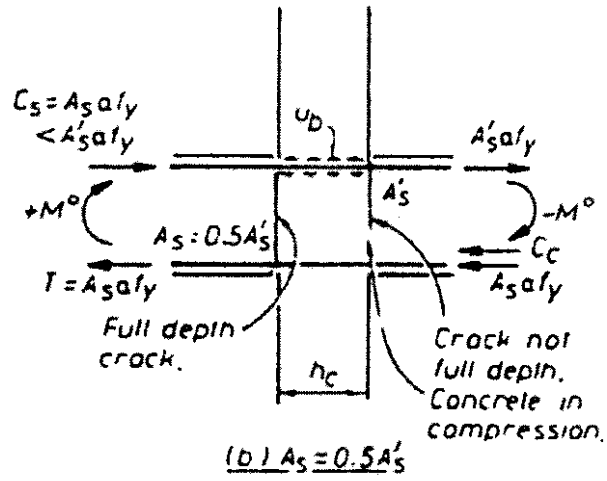
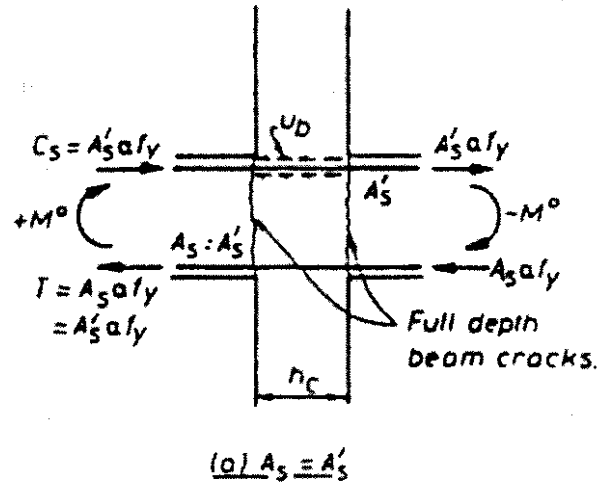
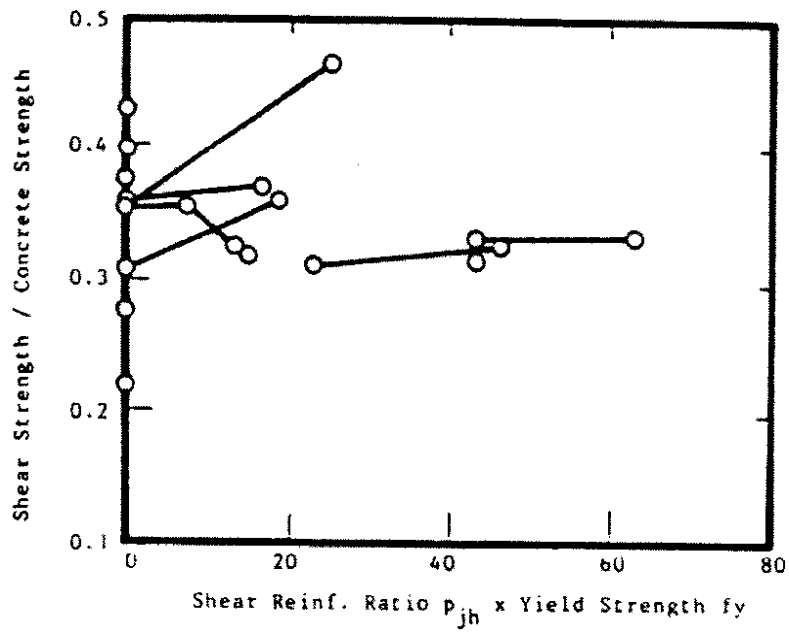


Figure A.3 "Forces acting on beam bars across a joint core" (from Kaku et al. 1991).



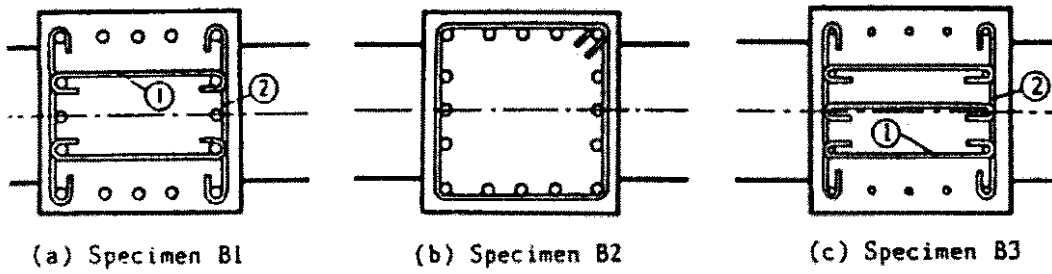


Figure A.5 Detail of B-C joint lateral reinforcement schemes (from Kitayama et al. 1991).

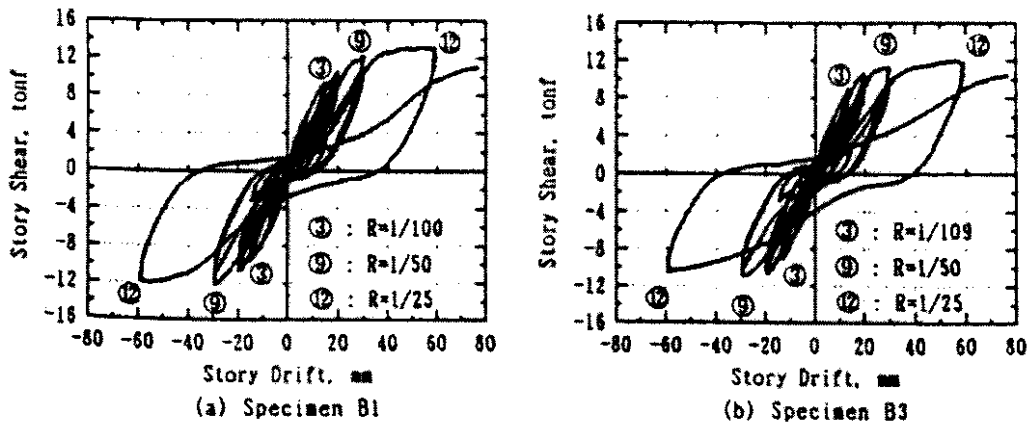


Figure A.6 "Story shear -- story drift relations" (from Kitayama et al. 1991).

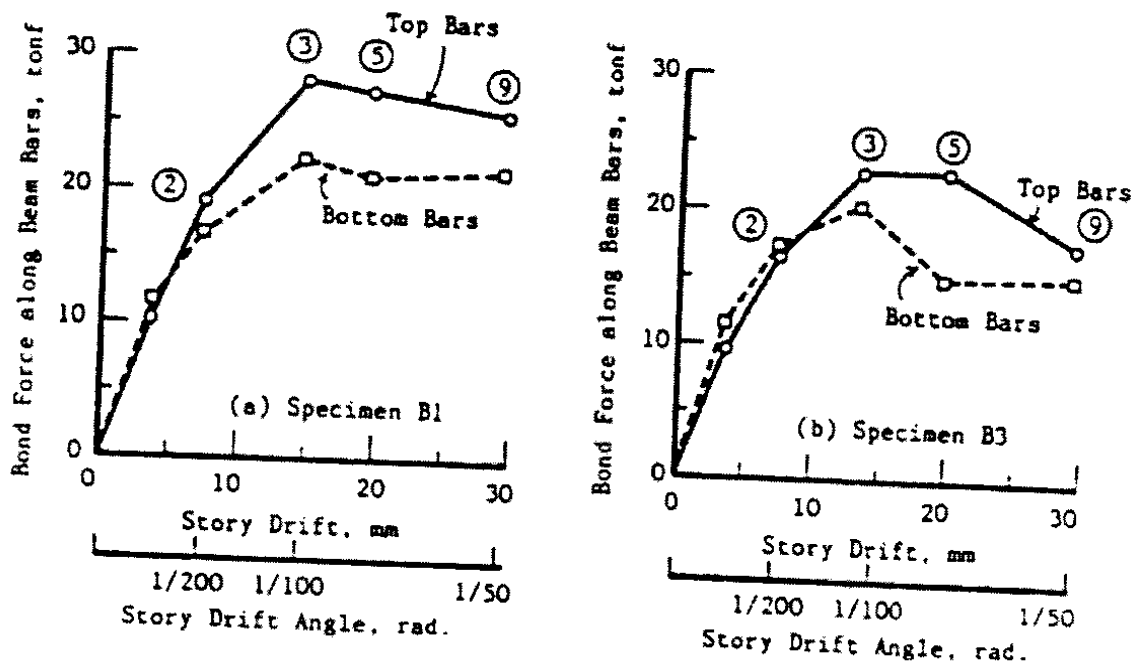


Figure A.7 Bond forces along beam bars within B-C joints (from Kitayama et al. 1991).

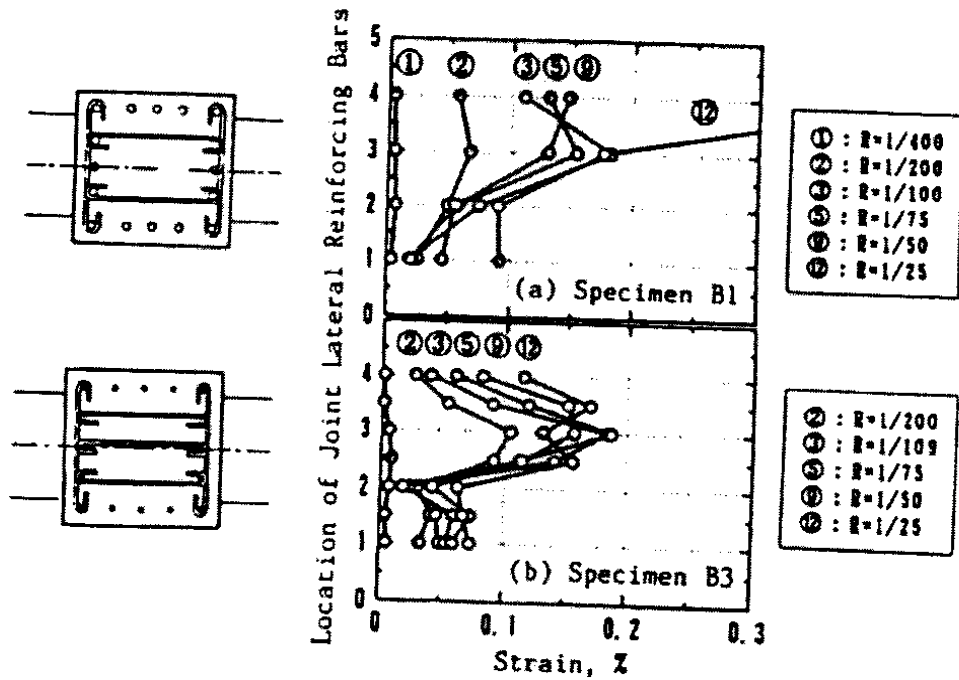


Figure A.8 "Strains in joint ties parallel to loading direction" (from Kitayama et al. 1991).

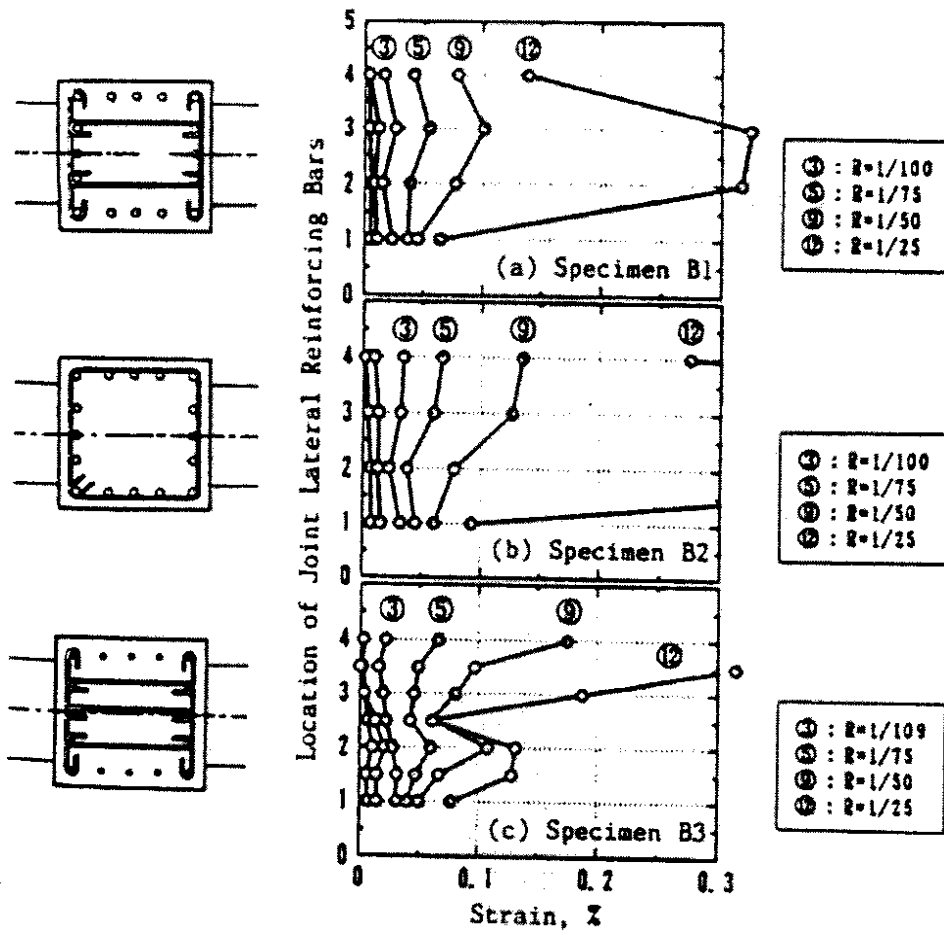
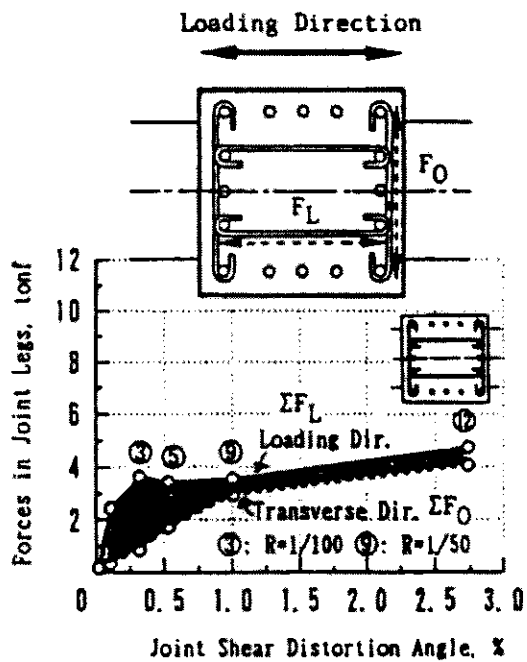
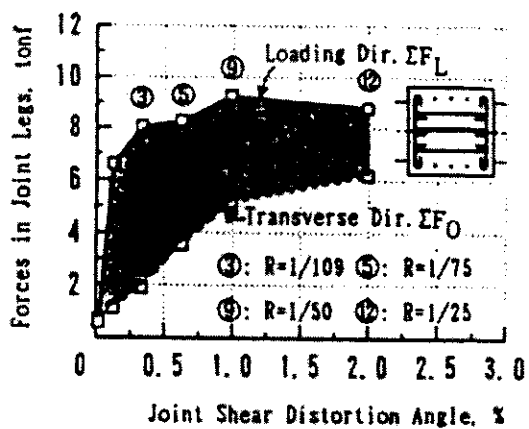


Figure A.9 "Strains in joint ties orthogonal to loading direction" (from Kitayama et al. 1991).



a) Specimen B1



b) Specimen B3

Figure A.10 "Total tensile force in joint ties" (from Kitayama et al. 1991).

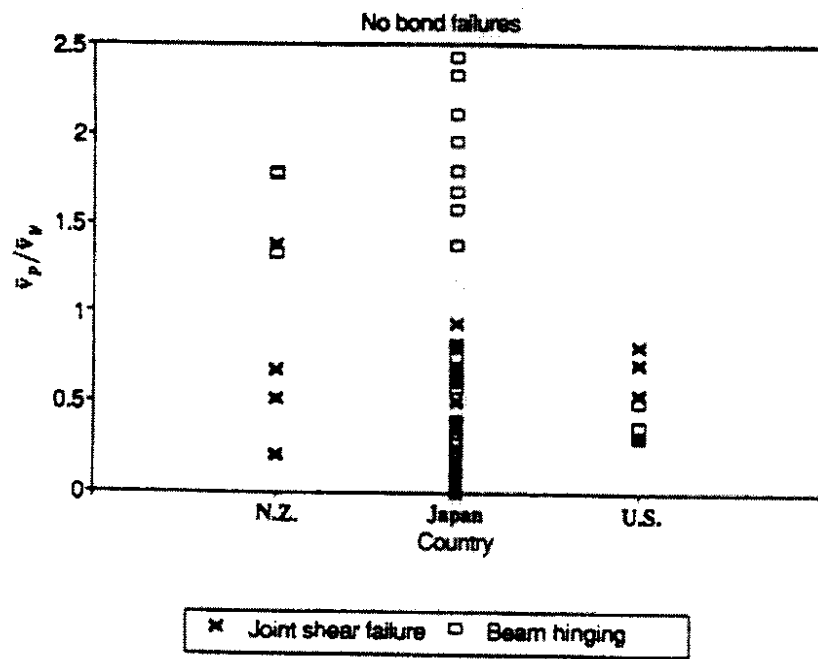
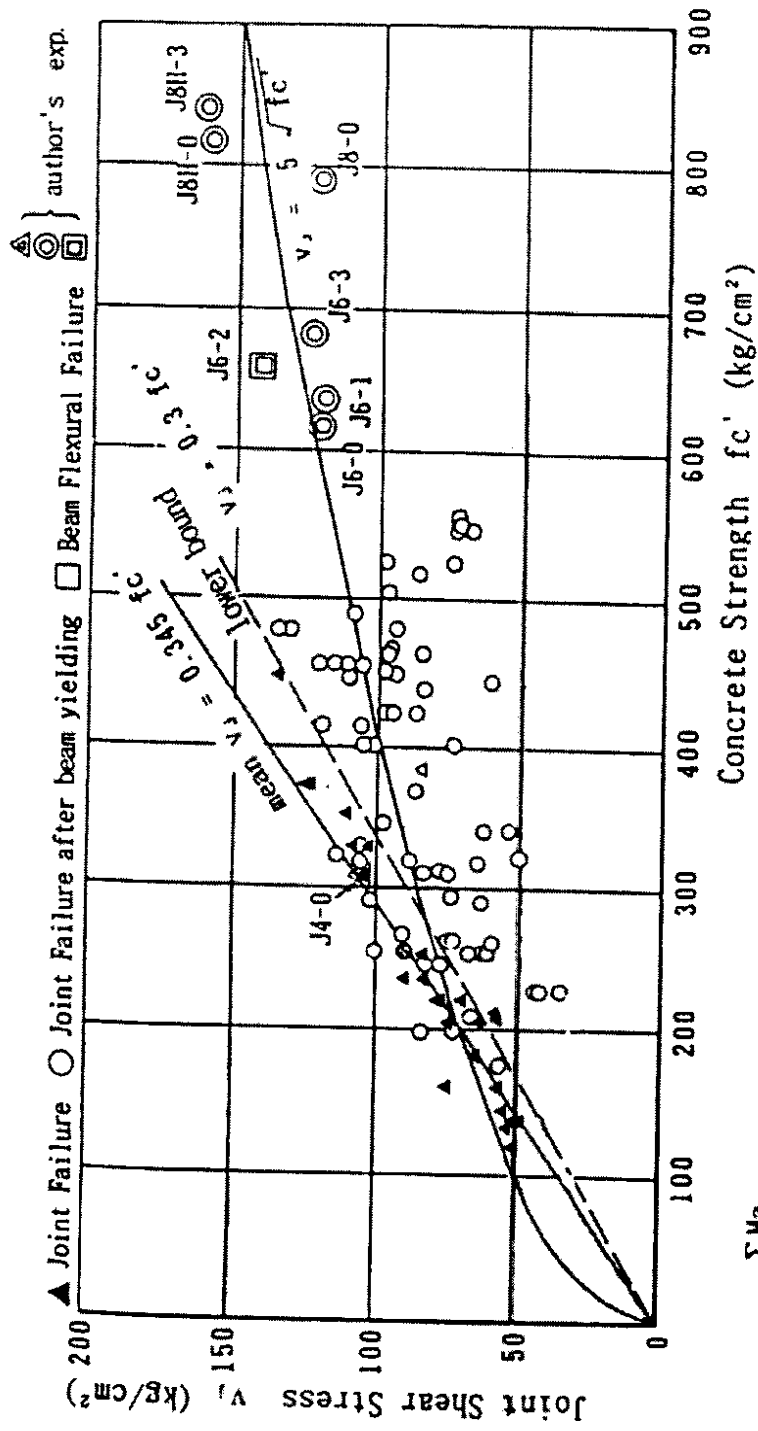


Figure A.11 The relationship between specimen failure modes and a shear stress ratio (from Bonacci et al. 1993).



$$v_j = \frac{\sum M a}{(1 + \xi) \cdot t_p \cdot j_m \cdot D_c} \quad (\text{kg/cm}^2)$$

- $M_a$  : Maximum moment in the beam or column adjacent to the joint (kg·cm)
- $\xi$  : Ratio of beam depth to column clear span
- $t_p$  : Average of column depth and beam depth (cm)
- $j_m$  : 7/8 of effective beam depth (cm)
- $D_c$  : Column depth (cm)

Figure A.12 "Maximum joint shear stress versus compressive strength of concrete" (from Sugano et al. 1991).

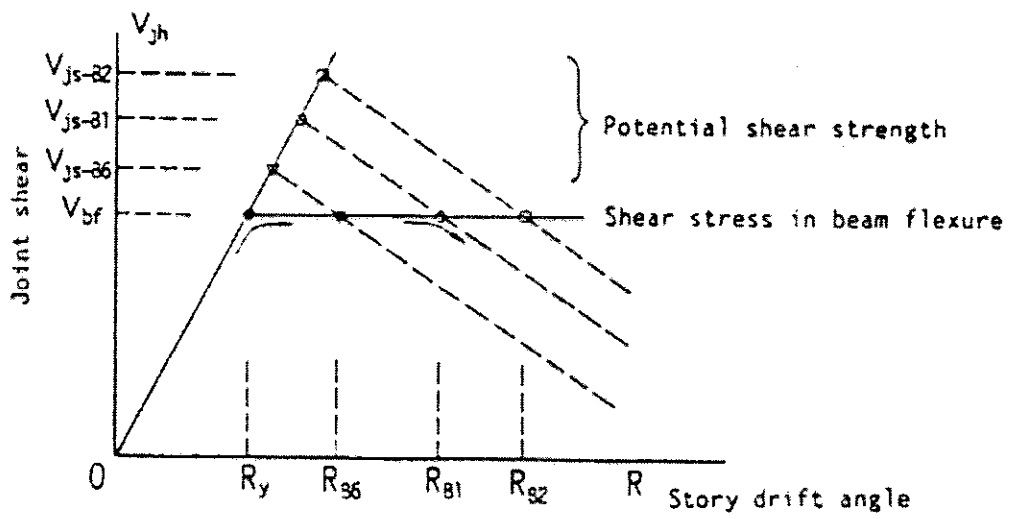


Figure A.13 "Relation of joint shear strength and ductility factor" (from Joh et al. 1991b).

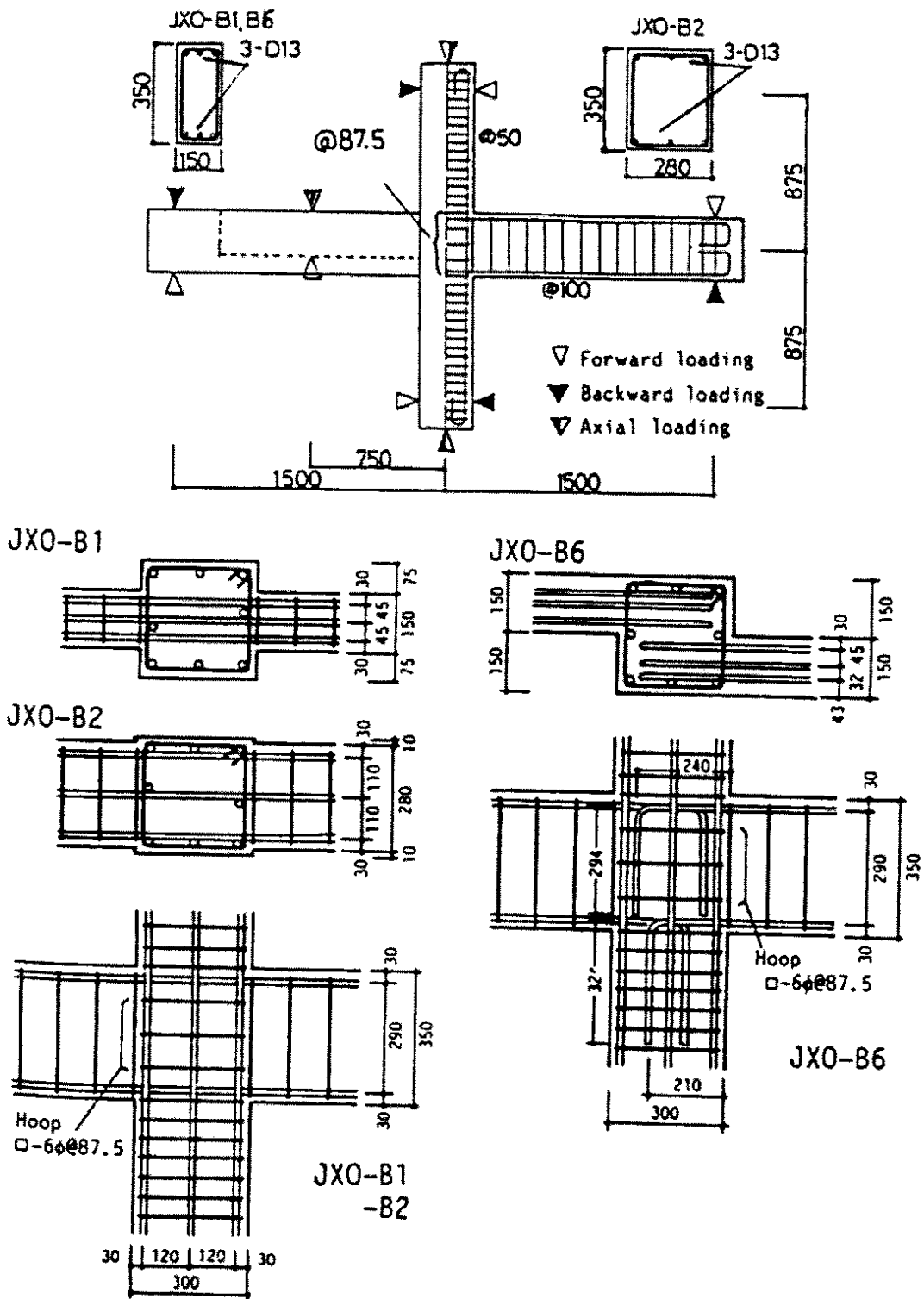


Figure A.14 Details of the specimens tested by Joh et al. (from Joh et al. 1991b).